colorants

MDPI

Review

5′-Substituted Indoline Spiropyrans: Synthesis and Applications

Andrey A. Khodonov [1,*], Nikolay E. Belikov [1], Alexey Yu. Lukin [2], Alexey V. Laptev [1], Valery A. Barachevsky [3,†], Sergey D. Varfolomeev [1] and Olga V. Demina [1]

1 Institute of Biochemical Physics, Russian Academy of Sciences, 119334 Moscow, Russia
2 Department of Biotechnology and Industrial Pharmacy, MIREA—Russian Technological University, 119571 Moscow, Russia
3 Photochemistry Center, Federal Scientific Research Center "Crystallography and Photonics", Russian Academy of Sciences, 119421 Moscow, Russia
* Correspondence: khodonov@gmail.com
† Dedicated to the memory of prof. Valery A. Barachevsky, who passed away after COVID-19 attack at the end of 2021.

Abstract: Methods for preparation of 5′-substituted spiropyrans, their chemical properties, and the effects of various factors on the relative stabilities of the spiropyrans and their isomeric merocyanine forms are examined, reviewed, and discussed.

Keywords: 5′-substituted spiropyrans; photochromism; photochromic labels and probes

check for updates

Citation: Khodonov, A.A.; Belikov, N.E.; Lukin, A.Y.; Laptev, A.V.; Barachevsky, V.A.; Varfolomeev, S.D.; Demina, O.V. 5′-Substituted Indoline Spiropyrans: Synthesis and Applications. *Colorants* **2023**, *2*, 264–404. https://doi.org/10.3390/colorants2020017

Academic Editors: Anthony Harriman and Julien Massue

Received: 4 April 2023
Revised: 20 May 2023
Accepted: 24 May 2023
Published: 5 June 2023

1. Introduction

Among the large number of various phenomena occurring in the matter under the action of light, the phenomenon of "photochromism" is of particular interest. "The photochromism phenomenon" is understood as a reversible transformation of a substance from one state to another, occurring at least in one direction under the action of light with a definite wavelength and accompanied by a change in the structure of the molecule and in its optical characteristics [1–3]. At present, significant progress has been made in synthesis and study of the polyfunctional properties of photochromic organic compounds of the following classes of spiropyrans, spirooxazines, chromenes, diarylethylenes, fulgides, indigoids, etc. [2–19]. Since the discovery of the spiropyran photochromism in the 1950s by Hirshberg [20] and in the course of more than 70 years of subsequent development, the photoactive materials with photoswitchable fragments have found their applications in various scientific research fields, ranging from chemistry, physics, and materials science, to biology and nanotechnology, but not in industry.

By now, more than several thousand spiropyrans were synthesized and their photochromic parameters were thoroughly studied. Taking into consideration the limited scope of this review, we deliberately restricted the structural diversity of the target scaffold of the spiropyran molecule according to the following criteria:

1. Aza- and thioheterocyclic spiropyran analogs, having benzothiazoline, benzoxazoline, thiazolidine, thiazine, oxazoline, oxazine, pyrrolidine, and piperidine moieties in the indoline fragment, except substituted indoline ring; and heteroanalogs with benzoselenazole, benzoxazole, benzothiazole rings and related spirobenzoxazine, spironaphthoxazine, spirobenzothiopyran derivatives in the benzopyran part; all were excluded from the discussion and analysis.
2. Spiropyrans with hetero- and aryl-fused indoline and benzopyrane fragment also were excluded.
3. Restrictions were also introduced on the structure of the substituents $R_{1'}$ at N1′-atom and $R_{3'}$ at C3′-atom, except for the methyl group.

To create photochromic labels with the desired spectral and photochemical parameters it is necessary to introduce an additional electron-acceptor substituent (EWG), e.g., a nitro group, to position C6 of the molecule. The structure of potential targets governs the nature of reactive anchor groups. Today, the design and development of effective methods for the preparation of new hybrid molecular structures and systems, containing photochrome fragments as active working elements, whose characteristics significantly change under the influence of light, are of special interest for bionanophotonics and nanomedicine.

Spiropyrans of the indoline series are in focus as the most promising and the most studied representatives of multi-sensitive spirocyclic compounds, which can be switched by a number of external stimuli, including light, temperature, pH, presence of metal ions, mechanical stress, and other compounds. The spectral properties and parameters of their phototransformations strongly depend on the substituents present in the molecule; therefore, a directed change in their nature enables the search for new photochromes with desired properties and various stimulus-responsive structural elements [4,5,17,21–28].

Photochromic labels and probes have particular prospects as a safer replacement of still widely used radioactive radiotracers. The most promising approach toward design and development of these hybrid photoactive and photo-controlled systems and materials consists of binding the photochromic labels by covalent immobilization onto the surface or into the active binding site of the targets, e.g., various substrates, polymers, DNA, lipids, proteins, cations, and quantum dots. To perform this procedure, it is necessary to develop a new generation of photochromic labels and probes containing substituents with the respective types of functional groups [16].

Particular attention will be paid to the structural features of molecules, their influence on photochromic properties, and the reactions taking place during isomerization, as the understanding of the structure–property relationships will rationalize the synthesis of compounds with predetermined characteristics.

For spiropyrans, works on modification of the prepared initial precursor have been described, but structural diversity of the molecules was limited and was created mainly by introducing the respective amphiphilic linker at N1′-atom of the indoline fragment by its quaternization with a halogen derivative. As a rule, significant decrease in the yields of target products was observed with an increase in complexity of the alkylating agent structure [21,23,24].

We proposed 5′-substituted spiropyran derivatives as promising precursors scaffold for synthesis of photochromic labels and probes for different types of targets. It was necessary to modify their molecules to provide them the ability to form a covalent or non-covalent (ligand specific) interaction with different types of targets by introducing diverse reactive terminal groups or "molecular addresses" into a distinct position of the label molecules.

Additional advantages of photochromic spiropyran-based photo-controlled systems and materials are that:

1. They possess a binary set of two different types of analytical signals (photo-induced light absorption in the range 560–600 nm and fluorescence induction in the colored merocyanine form);
2. The functional linker fragment is located at the C5′-atom while the EWG group is at C6-postion pyran fragment along one axis (uniaxial orientation).

The results of comprehensive investigation of the structure and characteristics of 5′-substituted spiropyrans largely up to year 2000 already have been discussed and analyzed in a number of reviews and monographs [21–23,25], and they have been supplemented by more recent results from our lab at IBCP as well as other research groups [4,9–11,16,24,26].

In this review the principal methods for the production of 5′-substituted spiropyrans (359 examples) and specific novel aspects of their molecule modification as well as their unusual chemical and photochromic applications are examined in detail.

2. Structure and Spectral Properties of Spiropyrans

Spiropyrans (**SP**) are a well-studied class of photochromic compounds. These compounds are usually named in conformity with the IUPAC rules for nomenclature of heterocyclic spirocompounds, as derivatives of 1′,3′,3′-trimethyl-6-nitrospiro[2*H*-1-benzopyran-2,2′-indoline] or 1′,3′-dihydro-1′,3′,3′-trimethyl-6-nitrospiro[2*H*-1-benzopyran-2,2′-indole] (Figure 1). However, other naming variations of these compounds, such as 2*H*-chromene derivatives, were often used in early works.

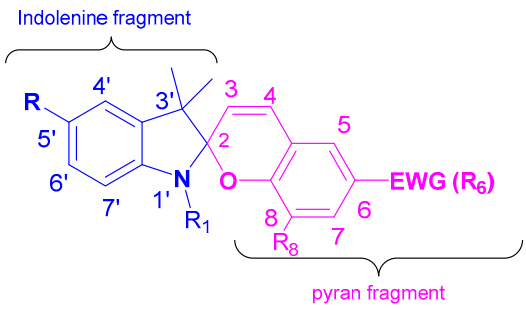

Figure 1. Spiropyran structure.

Spiropyrans typically can exist in an equilibrium mixture between spiroform (**A**) and colored forms of merocyanines (**MC, B**) which themselves can comprise mixtures of geometric isomers with a range of relative stabilities and reactivities. In darkness, spiroform (**A**) spiropyran molecule consists of two heterocyclic fragments in orthogonal orientation, that have a common central sp3-hybridized carbon atom, which is connected to the C2-position of 2*H*-pyran ring without conjugation between two parts of molecule. Photochromism of spiropyrans involves photodissociation of the C-O-bond in the initial cyclic spiroform (**A**) by action of UV light and subsequent thermal *cis*→*trans* isomerization into the deep colored merocyanine isomers (**B**, **MC**) with zwitterionic and/or quinoid structures. The reason for the UV-light-induced color change in this system is formation of a conjugation chain during the transition from spiroform (**A**) (colorless or pale yellow) to **MC** with the appearance of a deep color. Then it is transformed back into the initial spiroform (**A**) by the action of visible light absorbed by the photoinduced form **B** or spontaneously in the dark. Despite suffering from thermoinstability and low fatigue resistance, spiropyrans still offer a unique feature of significantly increased dipole moment after photoisomerization from spiroform (**A**) into **MC** charge-separated zwitterionic form. The open **MC** form has a larger dipole moment (14–20 D) than the closed spiroform (**A**) (4–6 D), and therefore the stability of the **MC** form strongly depends on the electronic effects of substituent(s) in indoline and 2H-pyran moieties, solvent polarity, and presence of metal complexation.

In most cases, the **MC** (**B**) form absorbs at longer wavelengths than spiroform (**A**) (positive photochromism), but the alternative case is also possible (negative or inverse photochromism). Negative photochromism is very much less common than the normal or positive variant and is exhibited by only a few spiropyran derivatives, especially those bearing free hydroxy, carboxy, or amino groups [12,29].

Under external action, spiropyrans, as a rule, undergo isomerization as a result of which the spiroform (**A**) is transformed into the merocyanine (**MC**) isomers (Figure 2). The **MC** form is characterized by the presence of a number of structural isomers of the quinoid and betaine types. This interconversion between two states is accompanied by change of color, but additional changes in refractive index, dielectric constant, redox potentials, solubility, viscosity, surface wettability, magnetism, luminescence, or mechanical effects are also possible.

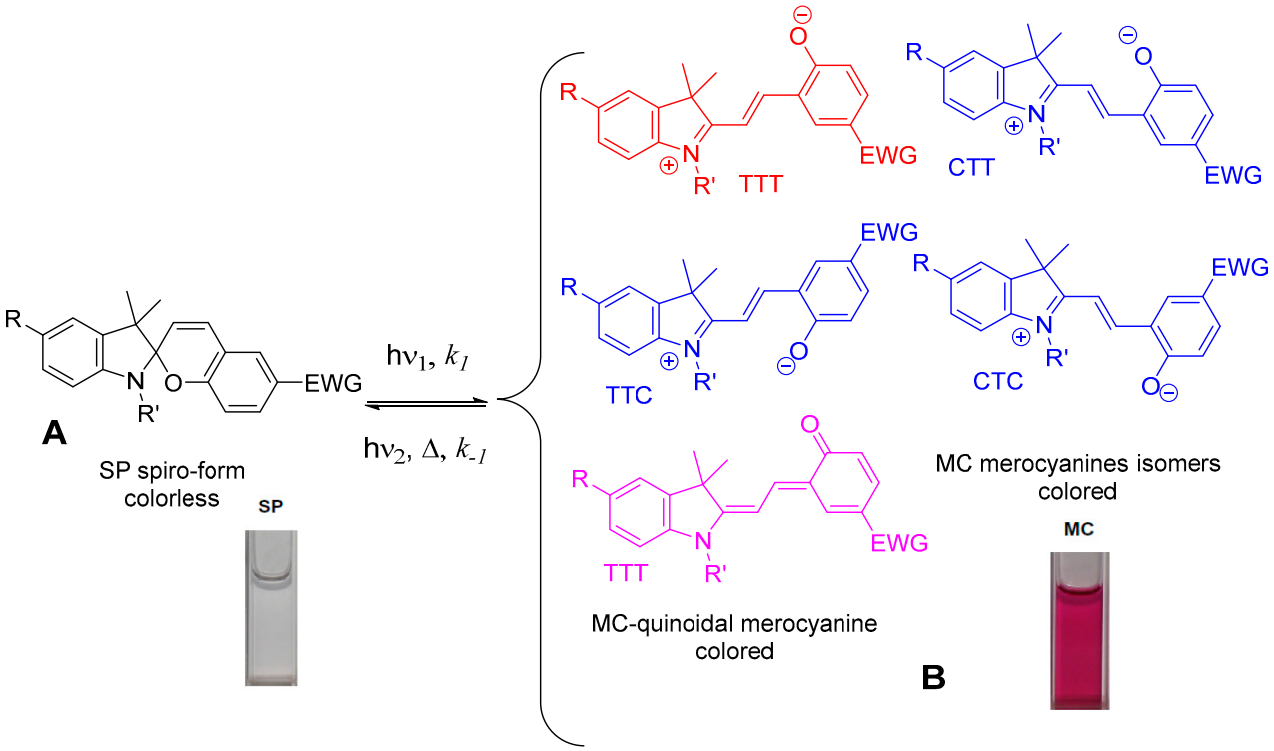

Figure 2. Phototransformations of the spiropyran molecule.

One of the unique features of spiropyrans is that the **MC** form is able to coordinate with metal ions and that the spiroform form (**A**) does not show such a property [6,8,11,13–15,30–40].

The structures of colorless (**A**) and colored **MC** forms of spiropyran molecule were approved unambiguously by modern spectral methods.

IR spectra of the spiroform (**A**) contain characteristic stretching vibrations of a spiro-C-O bond, an intense band at 940–960 cm^{-1}, and a band of the double bond of the pyran ring at 1640 cm^{-1}, which is not found in the IR spectra of the colored **MC** isomers [21,23].

2.1. UV-VIS-Spectra and Fluorescence Spectra of the 5′-Substituted Spiropyran Derivatives

Since the lifetime of a colored **MC** form often ranges from fractions of a second to several seconds, study of composition and structure of its photostationary mixture intermediates is greatly complicated. To solve this complex problem, modern spectral-kinetic methods were proposed, which make it possible to record spectral changes in time range from femtoseconds to minutes in UV- and visible spectral regions by pulsed absorption spectroscopy and laser flash photolysis. The UV-VIS spectra of spiropyran derivatives were discussed in many experimental and theoretical works devoted to study of photochromic compounds [5,9,10,26,30,31,41–43].

To determine the degree of influence of the nature and position of substituents in the photochromic molecule on its spectral parameters and optical characteristics, at first the properties of two reference compounds, unsubstituted spiropyran and its 6-nitroderivative, were studied.

According to these studies (see Table 1) [5,32], the main absorption band of original spiroform (**A**) of the unsubstituted spiropyran **SP1** in ethanol has an λ^{A}_{max} at 295 nm. Under UV irradiation, formation of photoinduced **MC** form was recorded, which manifests itself in appearance of an absorption band in the visible region of the spectrum (λ^{B}_{max} = 550 nm, ε_{550} = 35.0 10^3 M^{-1} cm^{-1}), which immediately spontaneously disappears after turning off the light ($k_{BA}{}^{db}$ = 0.48 s^{-1}) with regeneration of the original **SP1** cyclic form. However, in the dark, an equilibrium occurs between two forms, and the solution acquires a deep violet color, due to a small amount of the **MC** form is present in it. The

reverse reaction that produces the colorless spiroform (**A**) is induced by visible light or heat or even occurs spontaneously. The rate of these reactions depends on the reaction media (i.e., solvent polarity causing stabilization/destabilization of the zwitterionic **MC** form in polar/nonpolar solvents). Stabilization of the zwitterionic **MC** form in polar solvents leads to a larger energy activation and a slower **MC**→**A** transition compared to non-polar solvents.

The results of a complete standard study set are presented for the podand **SP288** as an example, (see Figures 3–7 [44]). Figure 3 shows the photochemical properties of the podand **SP288** in ethanol (A) and in toluene (B). This compound can be observed to exhibit photochromic properties which are typical for 6-nitro-substituted spiropyrans with various substitutients at the 5′-position (see data in Tables 1–5). After UV irradiation, a structured absorption band of the **MC** form appears in the visible region of the spectrum (Figure 3A,B, crv. 2). After turning off the activating irradiation, it spontaneously disappears (Figure 3A,B, crv. 3, 4) accompanied by restoration of the absorption spectrum of the initial cyclic spiroform **A** (Figure 3A,B, crv. 1). Similar photoinduced spectral changes were observed for this compound in acetonitrile and in toluene.

Figure 4A shows fluorescence spectra of photoinduced **MC** form of the podand **SP288** in ethanol (1), acetonitrile (2), and toluene (3). The emission band maxima are at λ 636 nm (in ethanol), at λ 666 nm (in toluene), and at λ 650 nm (in acetonitrile). Therefore, substituted spiroforms of 5′-substituted spiropyran derivatives were demonstrated to not exhibit pronounced fluorescence; however, they are able to reversibly switch from a nonfluorescent spiroform **A** to highly fluorescent **MC** form. These structures form the basis for creation of chemical sensors, when coupled with a suitable ionophore (e.g., iminodiacetate fragment in podand **SP288**). Switching is reversed on exposure to visible light or heat. Importantly, two isomers have a high switching reliability and fatigue resistance, which maximizes the number of switching cycles. Photochromic podand **SP288** is characterized by rather high count of photochromic transformation cycles (Figure 4B). As it can be seen from Figure 4B, upon successive alternation of irradiation of the sample with visible and UV light, the intensity of the absorption band of the **MC** form in ethanol changes insignificantly.

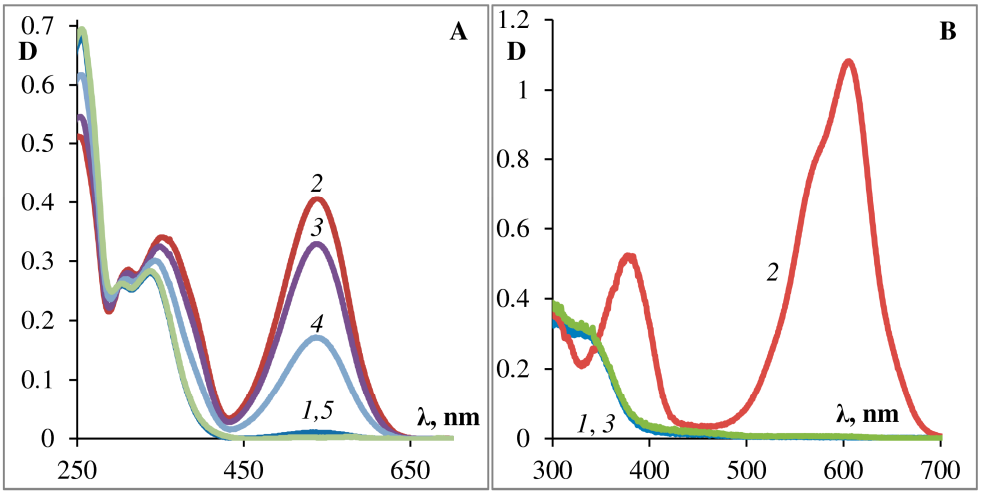

Figure 3. Photochemical properties of podand **SP288** in ethanol (**A**) and in toluene (**B**). The curves on (**A**): 1—before illumination; 2—after 30 s of illumination with UFS-2 filter, 3, 4—after 10, 45 min in the dark, respectively, 5—after 30 s of illumination with visible light. The curves on (**B**): 1—before illumination; 2—after 10 s of illumination with UFS-2 filter, 3—after 30 s in the dark.

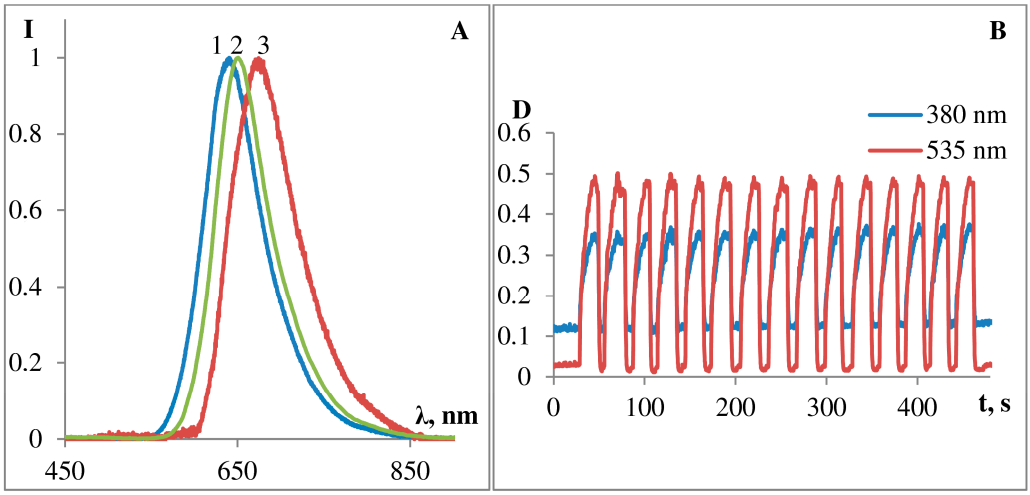

Figure 4. (**A**): Fluorescence spectra of photoinduced **MC** form of podand **SP288** in ethanol (1), acetonitrile (2) and toluene (3) under light excitation with λ_{ex} = 280–370 nm. (**B**): Reproductibility of photocoloring/photobleaching kinetics of podand **SP288** in ethanol, 15 cycles, 25 °C.

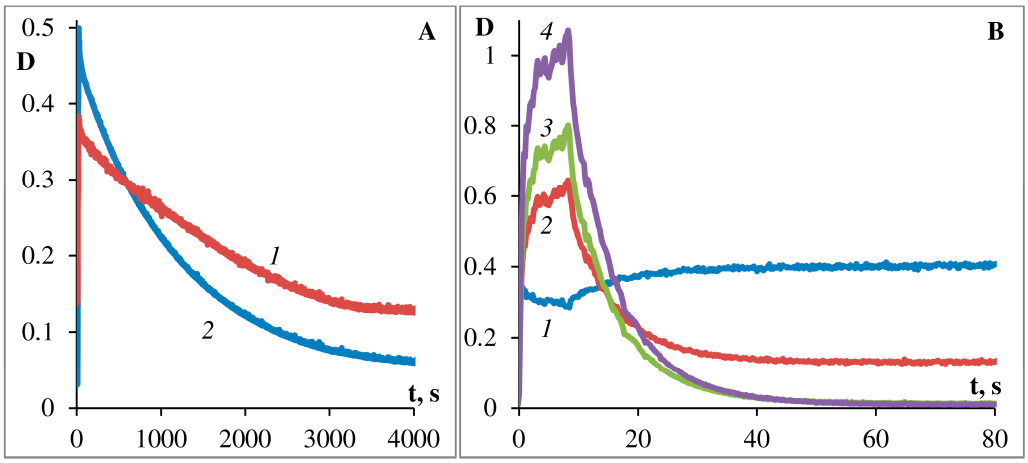

Figure 5. Kinetics of dark bleaching of podand **SP288** in ethanol (**A**) and in toluene (**B**). The curves for (**A**): 1—at 380 nm, 2—at 535 nm. The curves for (**B**): 1—at 330 nm, 2—at 377 nm, 3—at 572 nm, 4—at 605 nm.

Comparison of the data obtained for solutions of photochromic compound shows that upon going from ethanol to toluene, the photostability significantly decreases and the process of dark photobleaching significantly accelerates (Figures 3A,B, 5A,B and 6A,B). Figures 5 and 6 show the kinetics of photocoloring/photobleaching/photo-degradation processes of podand **SP288** samples in ethanol (A) and toluene (B) solutions. The photo-degradation parameter was characterized by how long the irradiation took to decrease photoinduced optical density for the photostationary state at the absorption maximum of the **MC** form by one half ($\tau_{1/2}$, s).

The bands of the photoinduced **MC** form of photochromic podand **SP288** (538 nm ethanol, 605 nm toluene) spontaneously slowly disappear when the sample is kept in the dark or quickly when irradiated with visible light, and in toluene the process of bleaching of the photoinduced merocyanine form occurs 100 times faster than in ethanol. Moreover, comparison of the data obtained for solutions of **SP288** in ethanol and in toluene shows that their fatigue light resistance is sharply increased when changing toluene to ethanol. Table 4 shows that the absorption band maximum of the photoinduced **MC** form undergoes a hypsochromic shift when polarity of the solvent increases, which is consistent with the behavior of spiropyrans in solvents of different polarity. In this case, the rate of spontaneous

dark discoloration of the **MC** form slows down (Figure 5A,B) and the resistance of the compound to irreversible photoconversion increases (Figure 6A,B). The smallest value of the dark relaxation rate constant and high resistance to photodegradation of podand **SP288** in ethanol can be explained by formation of a hydrogen bond between the phenolate oxygen of **MC** forms of spiropyran podand and solvent molecules.

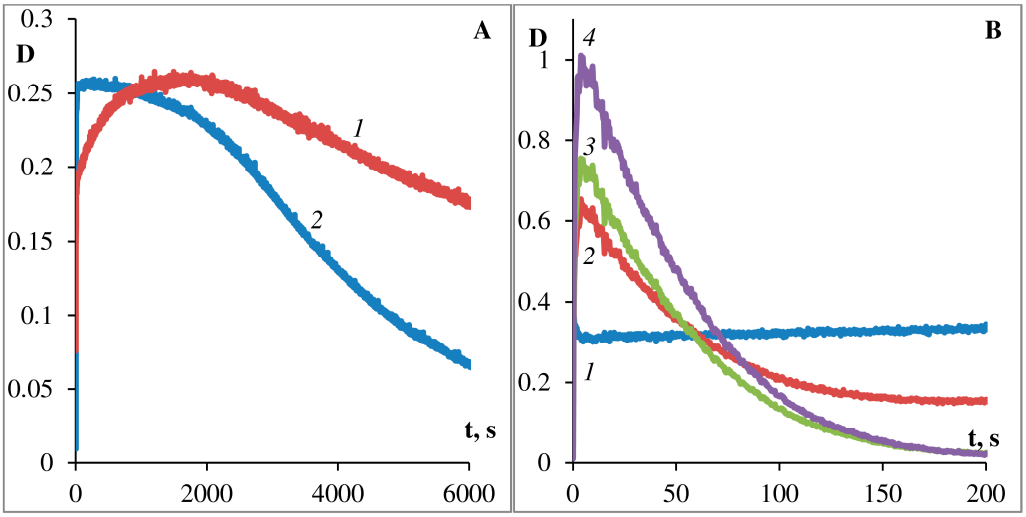

Figure 6. Kinetics of photodegradation of podand **SP288** in ethanol (**A**) and in toluene (**B**). Sample was examined by exposure to unfiltered light illumination of Hamamatsu-LC8 lamp. The curves for (**A**): 1—at 380 nm, 2—at 535 nm. The curves for (**B**): 1—at 330 nm, 2—at 377 nm, 3—at 572 nm, 4—at 605 nm.

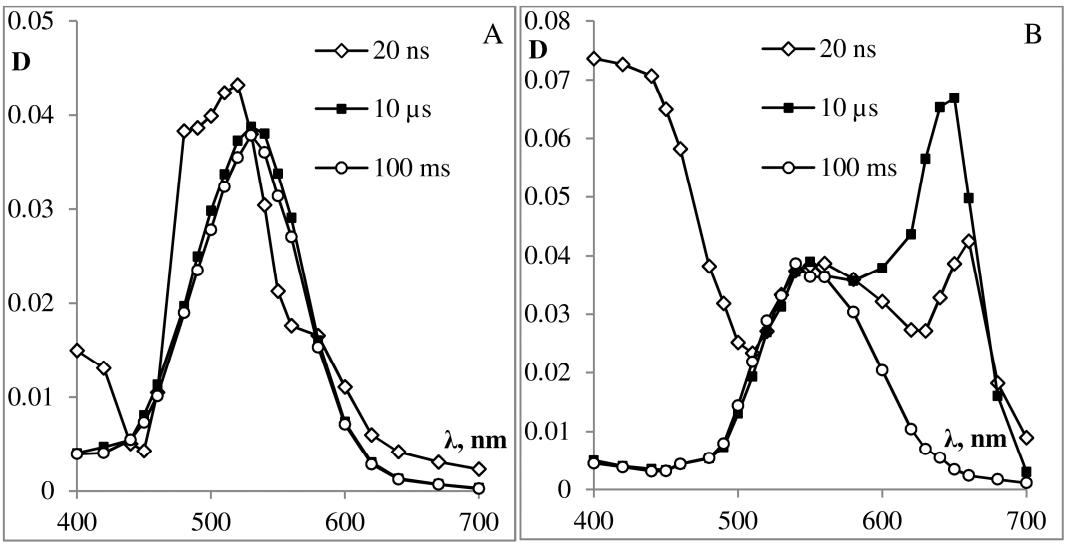

Figure 7. Absorption spectra of laser flash photolysis intermediates of photochromic podand **SP288** in solution of ethanol (**A**) and toluene (**B**) (the value of the optical absorption density at 337 nm is 0.4) after 20 ns, 10 µs, 100 ms after the laser pulse.

Laser excitation of spiropyran **SP288** solution in ethanol (A) or in toluene (B) leads to the formation of a triplet state (^{3}**MC**) of the **MC** form (see Figure 7), similar to what was well-documented for the 6-nitro-substituted derivatives without substituents in the indoline ring [30,31,43,45,46].

In 1982, Krysanov and Alfimov were the first to examine the transient absorption spectra in the photocoloration and photobleaching of the 6-nitro-spiropyran derivatives, which have been investigated with transient picosecond spectroscopy. Their results demonstrated

cleavage of the C-O bond between the spiro carbon and oxygen, which is believed to occur in picosecond to subpicosecond time region, and is assumed to lead to the formation of a primary photoproduct (nonplanar *cis*-cisoid intermediate X at 440 nm) with an orthogonal parent geometry, which is produced in less than 10 ps, followed by a geometrical change to the planar **MC** forms [42].

This data suggest that for 6-nitro-substituted spiropyrans, **MCs** are formed via both singlet and triplet routes. In contrast to 6-nitro-substituted derivatives, unsubstituted indolino spiropyrans demonstrate photochromism only through the excited singlet intermediate, which was confirmed by analyzing the oxygen effect on transient absorption [26,47–49].

Photochromic parameters and spectral properties data for 5′-substituted spiropyrans and their photointermediates were determined by spectral-kinetic methods (stationary and pulsed absorption spectroscopy and laser flash photolysis in the UV- and visible spectral regions) and are presented in the relevant sections of Tables 1–5. For the series of substituted dyads (**SP263**–**SP265**, **SP270**, **SP271**, **SP273**) containing a fragment of the stilbene fluorophore at the 5′-position of the indoline part of the photochromic molecule, the nature of the substituents in the aryl ring of the fluorophore was found to have the strongest influence mainly on the spectra of the spiroform (**A**): λ^{A}_{max} 335–409 nm ($\Delta\lambda^{A}_{max}$ 74 nm) in ethanol and λ^{A}_{max} 325–407 nm ($\Delta\lambda^{A}_{max}$ 82 nm) in toluene solutions. The difference in the λ_{max} for the *Z*- and *E*-isomers in the series of these derivatives, containing a substituted aryl ring in the stilbene fluorophore fragment for spiroform (**A**) was small ($\Delta\lambda^{A}_{max}$ 7–9 nm) and it was almost absent for the **MC** form [16,50].

2.2. NMR Spectroscopy

Since the lifetime of a colored **MC** form often ranges from fractions of a second, several seconds to minute time scale, it greatly complicates the study of composition and structure of its photostationary mixture intermediates. As in the case of study of absorption spectra, the problem of a short lifetime of a colored **MC** form arose, and was not completely solved; therefore, the use of the NMR method was limited only to recording the spectra of a stable spiroforms **A**, and wide application of the NMR spectroscopy in study of photochromic compounds' properties is limited due to the short lifetime of photointermediates of the spiropyran **MC** form. However this problem is solvable with the help of novel equipment for NMR spectroscopy, in which NMR spectra are recorded simultaneously with irradiation of a sample with light of given wavelength [51]. The difference in the spectra of **A** and **B** isomers makes it possible to identify them when both are present. An alternative decision to this problem lies in the development of new approaches to the stabilization of the spiropyran **MC** form lifetime by using more viscous or polar solvents [52], as well as introducing additional functional substituents or fragments of heterocycles into the pyran part of the photochrome molecule. At the same time, a novel way was proposed to stabilize the **MC** form lifetime by complexation with certain cations. We proposed the method of stabilizing the short-lived **MC** form of unsubstituted indoline spiropyran **SP1** by forming stable complexes between the molecules of this compound and aluminum salts [32,53]. Below we present a good illustration of this option to obtain important information about the structure of spiro and **MC** forms of unsubstituted indoline spiropyran **SP1** using ^{1}H- and ^{13}C-NMR spectroscopy.

In case of cyclic form **A** of **SP1**, the upfield initial signals of protons and carbons of two nonequivalent 3′,3′-methyl groups in the form of 2 singlets at δ 1.18 ppm/1.31 ppm (20.8/26.6 ppm) become equivalent due to the quasiplanar structure of complex of **MC** form **SP1**/$Al(NO_3)_3$ and transform with a downfield shift into a single singlet (6H) at δ 1.87 ppm/(27.2 ppm). Similarly, the signal N-1′−CH_3 in the **SP1** cyclic form at δ 2.74 ppm/(29.5 ppm) and in the complex of **MC** form **SP1**/$Al(NO_3)_3$ has downfield shift at δ 4.16 ppm/(34.8 ppm) due to the presence of a positively charged N-atom.

In cyclic form **SP1**, the signals of the AB nuclei in the C3−C4 position of the pyran ring in the form of 2 doublets at δ 5.77 ppm/6.96 ppm with *J* 10.2 Hz are also shifted downfield in the spectrum of complex of **MC** form **SP1**/$Al(NO_3)_3$ (δ 8.72 ppm/7.77 ppm,

J 16.4 Hz), which makes it possible to unambiguously attribute the C=C bond configuration in complex **MC** form **SP1**/$Al(NO_3)_3$ as the *trans*-isomer (TTT) (see Figure 8).

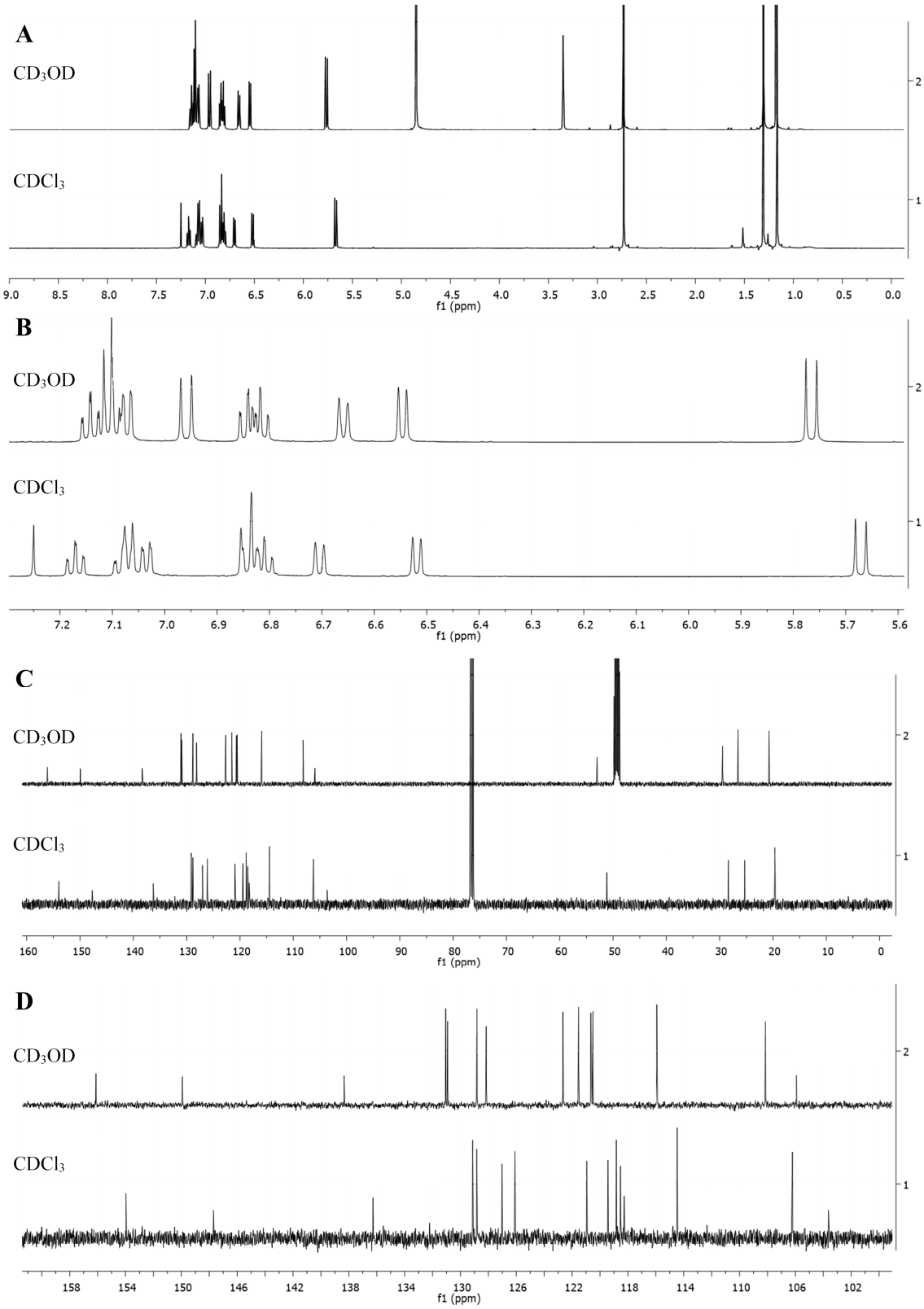

Figure 8. ^{1}H (**A**,**B**) and ^{13}C (**C**,**D**) NMR spectra of the spiroform **SP1** in CD_3OD and in $CDCl_3$, where (**A**,**C**)—spectra of the full range of chemical shifts of signals, (**B**,**D**)—spectra fragments of signals from nuclei of aromatic rings (indoline and benzopyran), Bruker Avance III-500 NMR spectrometer.

2.3. Solvatochromism

Most of the spiropyrans known today in spiroform (**A**) are colorless or slightly colored crystalline substances that are essentially insoluble in water, only slightly soluble in alcohols and aliphatic hydrocarbons, and quite soluble in aromatic hydrocarbons and haloalkanes.

UV irradiation of solutions containing spiropyran results in the formation of colored **MC** form, which is a highly polar isomer and hence the nature of the microenvironment influences the properties of spiropyrans. This causes hypsochromic (blue shift; decrease in λ_{max}) or bathochromic (red shift; increase in λ_{max}) shifts in their absorption spectra depending on the solvent polarities. The effect of solvent polarity and hydrogen bonding on λ_{max} of **MC** form has been investigated. Their solutions in nonpolar solvents are usually colorless, whereas in polar solvents they may be more or less intensely colored, depending on the structure and the nature of the substituents because of thermal equilibrium between **A** and **MC** isomers.

It was found that by dissolving the spiropyran dye in different solvents, a mixture of spiroform (**A**) and **MC** form may be observed due to the occurrence of different interactions between the solvents and the solute, and subsequent effects on ground state and excited state energy levels of the conjugated π electrons in **MC**. The **MC** form is occasionally further stabilized under certain conditions, such as hydrogen bonding, combination with crown ether or β-cyclodextrin and complexation with metal cations.

It can be seen from data in Figure 9A,B and Tables 1–5, that like other merocyanines, the open **MC** form of 5′-substituted spiropyrans is a negative solvatochromic dye, i.e., with increasing solvent polarity, the absorption band undergoes a hypsochromic (or blue) shift. Comparing the presented data, we can draw the following conclusions: as the polarity of the solvent increases, the **MC** in 5′-substituted spiropyrans is obviously characterized by a hypsochromic shift, while the spiroform does not have such a clear dependence.

However, the electronic structure of the **MC**s derivatives was found to be extremely sensitive to influence of substituents in both indoline and pyran rings in these photochromes. By varying the acceptor or donor properties, steric hidrances and positions of the substituents, it is possible to polarize the π-system of the **MC** form sufficiently to reach a zwitterionic-like structure and observe negative solvatochromism in the push-pull-type dyes, containing electron-donating groups in the indoline and electron-withdrawing ones in the pyran moieties [4,5,10,14,23,26,27,54–56].

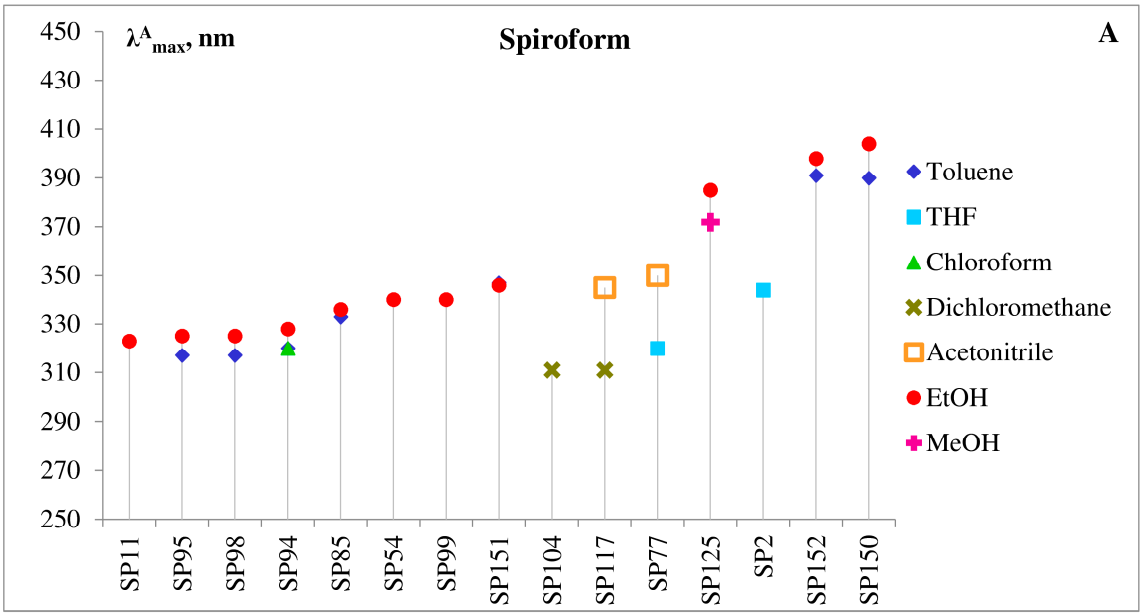

Figure 9. *Cont.*

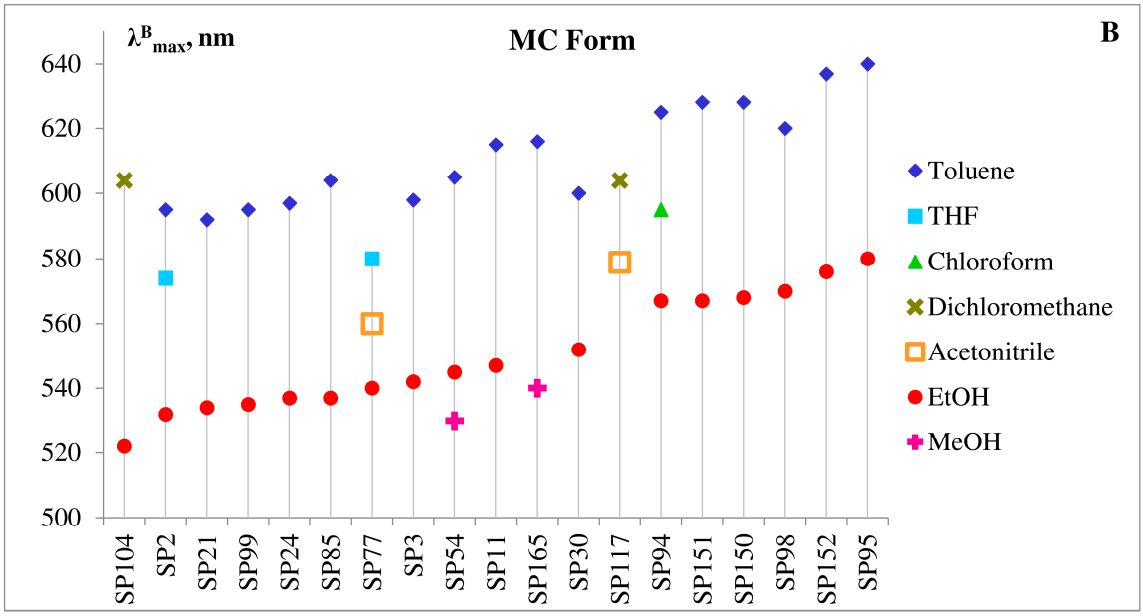

Figure 9. Correlation of molecular structure and absorption maxima for the selected 5′-substituted spiropyrans in various solvents. (**A**)—Absorption maxima of spiroform (**A**,**B**)—absorption maxima of **MC** form. Legends list solvents in order of increasing their relative polarity.

Series of works on spiropyran derivatives demonstrate the possibility of a hydrolytic decomposition of **MC** isomer in aqueous media. **MC** form was also shown to become more stable than spiroform (**A**), and a reverse (negative) photochromic behavior is detected in aqueous solvents.

In recent years, increased interest has been observed in the theoretical and experimental study of isomerization processes of organic photochromes in solid state. Many spiropyran derivatives exhibit photochromic properties in powders or even in single crystals [57].

2.4. Acidochromism

Transformation of spiropyran molecules from the cyclic spiroform (**A**) to the opened **MC** form can be initiated by light and other reasons: changes in temperature, pH, redox potential, polarity of a medium, and even by mechanical stress. For these dyes, the effect on the spectral properties caused by changes in temperature (thermochromism), pH (acidochromism), solvent polarity (solvatochromism), redox potential (electrochromism), interactions with metal ions (ionochromism), and mechanical stress (mechanochromism) has been well studied. Moreover, presence of many metal cations, several nucleophilic anions, and some organic species can also induce their isomerization. Thus, spiropyran-like systems meet the basic requirements for multi-functionality and sensitivity that make them promising building blocks for creation of various dynamic stimulus-responsive materials and systems [4,10,15,16,50].

The two isomeric states of spiropyran have different properties. The **MC** isomer is significantly more basic than spiroform (**A**) (upon the transformation of closed spiroform to **MC**, pK_a value changes by more than six units).

The action of acids on spiropyrans' solutions may be accompanied by: (1) cleavage of the [2H]-pyran ring, (2) protonation the phenolate anion of the **MC** form [24]. The protonation causes a significant shift of the absorption band maximum toward the shorter wavelength compared to that of the **MC** form. In case of **SP2**, two salts with HCl have been isolated, differing in physical characteristics. In toluene at −78 °C a yellowish salt is formed, and it is converted completely into the **MCH⁺** upon boiling sample in alcohol for 10 min (see Figures 10 and 11).

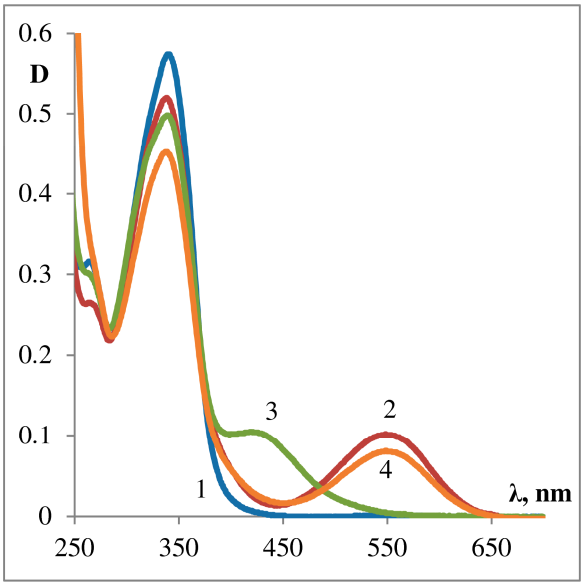

Figure 10. Protonation and deprotonation of **MC** form of **SP263** in ethanol. 1—Spiroform (**A**); 2—**MC** form, after 2 min of sample illumination with UFS-2 filter; 3—**MCH⁺** form protonated with CF_3COOH; 4—**MCH⁺** form deprotonated with Et_3N.

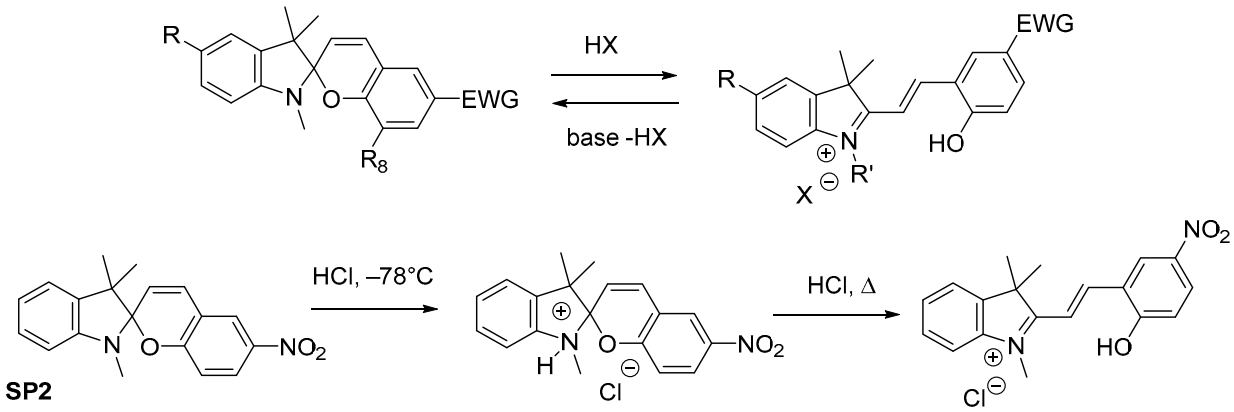

Figure 11. Protonation and deprotonation of the spiropyran molecule by acids.

Protonation and deprotonation of **MC** form of the dyad **SP263** (see λ_{max}**MCH⁺** of **SP263** 426 nm, Table 4) in ethanol is shown on Figure 10. It should also be noted that dyads of this series (**SP263**–**SP273**) have a very low threshold of sensitivity to the traces of acids of various strengths, which allows us to consider their possible use as pH sensitive elements of sensors [15,50].

3. Chemistry of Spiropyrans

The possibility of directional and reversible change of the structure of spiropyrans and their unique properties generate continuously growing interest in the delopment of novel synthetic methods for producing photochromes of this class and study of their properties. The fine tunability of photochromes' chemical structure and their optical properties provides opportunities for designing and developing smart materials for multidisciplinary applications. To make these tasks possible, simple and reliable synthesis methods for both well-known and recently developed photochrome series were needed.

Below, both already well-established methods and the latest approaches for 5′-substituted spiropyran derivatives synthesis are reviewed and critically analyzed.

Synthesis of the 5′-Substituted Spiropyran Derivatives. Side Reactions in the Synthesis

Synthetic approaches and methods to the 5′-substituted spiropyrans synthesis can be conventionally sorted into following groups:

(**A**) "Complete" synthesis of target derivatives by the condensation of two or more key intermediates: X + Y = **SP**;

(**B**) One-step direct modification of a precursor with gived structure: **SP**-precursor → **SP**;

(**C**) Production of a target molecule in several stages by progressive elaboration of the anchor group by introduction of the necessary fragments with a given set of functional groups: **SP**-precursor$_1$ → **SP**-precursor$_2$ → **SP**-precursor$_n$ → **SP**;

(**D**) Modification of the final targets by the photoactive ligands with reactive terminal functions by doping or by immobilization methods.

We labeled them as pathways (**A**–**D**). The functional linker fragment and anchor group at the C5′-atom indoline part are located along the same axis as the EWG group at C6-postion pyran fragment (uniaxially).

The honorable first place in its popularity among known methods for synthesis of indoline spiropyrans is deservedly occupied by a group of condensations of two key components shown in Figure 12A–C (pathway **A**). Most often indolinospiropyrans are synthesized by condensation of Fischer's base (2-methylene-1,3,3-trimethylindoline) and its analogs or their salts with salicylaldehyde derivatives at reflux (see Figure 12A,B). Organic solvents such as methanol, isopropyl alcohol, toluene, DMF are often used. Synthesis simply involves condensation of two key components through reflux in ethanol, then isolation of the precipitated spiropyran dye by filtration from the mother liquor after cooling. The yields of indolinospiropyrans tend to be good: typically at least 70% and sometimes being near quantitative. To improve quality and yield, the following are recommended: (1) Vacuum distillation of these starting materials prior to use; or (2) replacement of unstable free bases with solid hydrohalides or perchlorate salts of Fisher's base, which are much more stable and easier to handle than liquid free bases. Rather than converting them back to free base form immediately before use, the salts may be employed directly (Figure 12B) [5]. The synthesis of spiropyrans using a wide range of organic or inorganic bases such as Et_3N, piperidine, pyridine, and NaOH is reported. To reduce the yield of the "bis-condensed" by-product, it is recommended to use the corresponding quaternary indolenyl salts instead of the free methylene bases in a mixture with an equimolar amount of an organic base (most often piperidine) or to use a slight excess of the aldehyde component [21–24,58].

The first 5′-substituted indoline spiropyrans were prepared by Wizinger [59] in high yields by condensation of 5-methoxy derivatives of 1,3,3-trimethyl-2-methyleneindoline (the Fischer base) with salicylaldehyde and 2-hydroxynaphthaldehyde by heating in methanol. The condensation of acyl- or formyl- Fischer's base derivatives with substituted phenols was used much less frequently (Figure 12C).

A series of 5′-acetyl-substituted **SP99**–**SP102** (see Table 1) was synthesized by condensation of 5-acetyl-substituted Fischer base with 3-substituted-5-nitro-salicylaldehyde. The introduction of an acetyl group does not change the spectral characteristics of the merocyanine form but leads to a decrease in the efficiency of photocoloration [60].

Diversely halogenated, hydroxyl-, and triflat spiropyran derivatives series **SP55**, **SP56**, **SP60**, **SP61**, **SP63**, **SP64**, **SP66**, **SP67**, **SP73**–**SP75**, **SP162**–**SP164**, were synthesized from respectively 5-substituted indolium salts and salicylaldehydes, using a versatile piperidine promoted procedure in ethanol as the solvent. The base was required to induce the *in situ* formation of 2-methyleneindolines (Fischer's bases) as reactive species from indolium salts. The starting 5-substituted indole species were prepared as indolium iodide salts, starting from 1,4-substituted phenylhydrazines. Overall yields: 5R = Br 73%; 5R = I 73%; 5R = OH 56%.

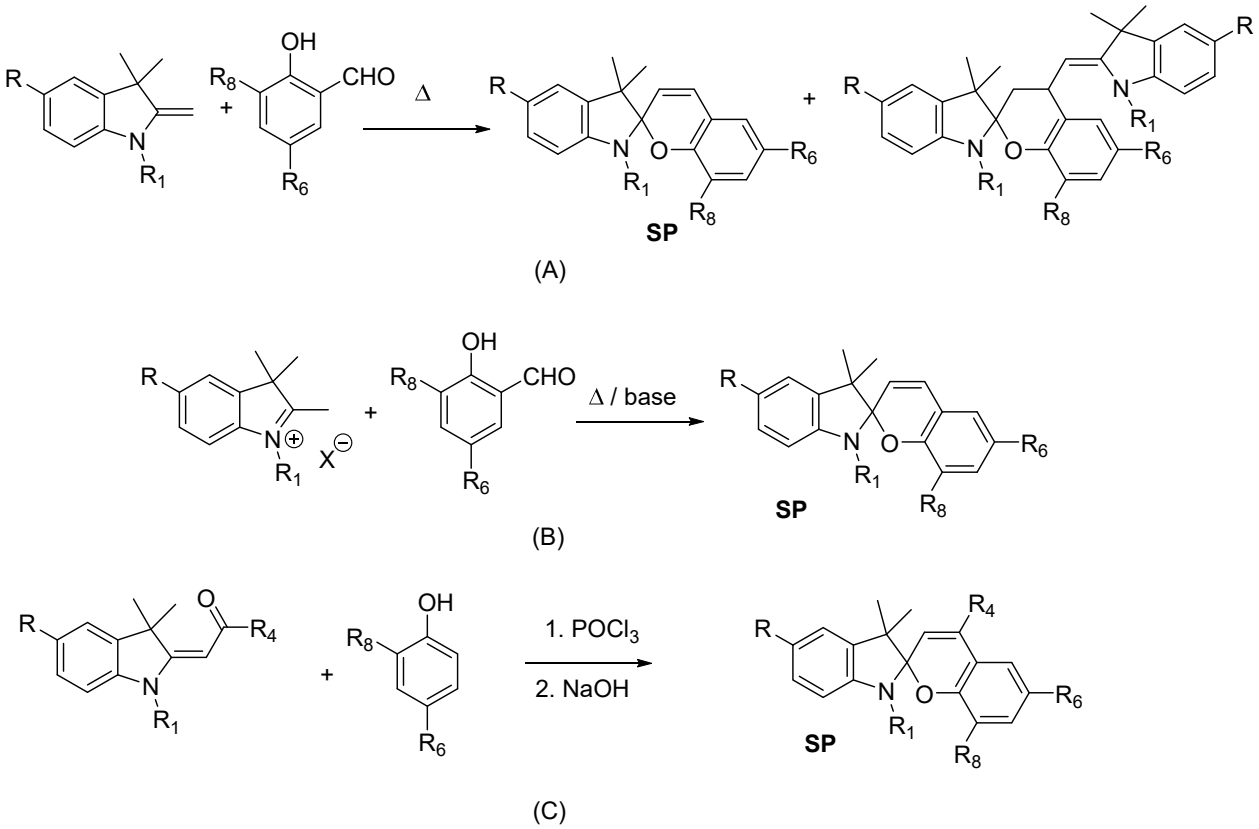

Figure 12. Classic 5′-substituted indoline spiropyran synthesis (pathway **A**; do not confuse with subfigures **A**–**C** explained below). Condensation of Fischer's base (2-methylene-1,3,3-trimethylindoline) (**A**) or their salts (**B**) with salicylaldehyde derivatives; condensation of acyl- or formyl- Fischer's base derivatives with substituted phenols (**C**).

For the synthesis of spiropyrans, the use of indolium salts is advantageous compared to directly using the corresponding 5-Fischer's bases as starting materials, because indolium salts are stable against air and moisture and as solids easy to handle. All products **SP55**, **SP56**, **SP60**, **SP61**, **SP63**, **SP64**, **SP66**, **SP67**, **SP73**–**SP75**, **SP162**–**SP164**, were isolated after crystallization from the reaction mixture. The spiropyrans bearing either bromide, iodide or hydroxy functions showed a negative photochromism on silica gel. This means that their rings have opened which leads to the zwitterionic **MC** isomer whose hydroxyl groups can interact with the silica surface by hydrogen bonding leading to severe yield losses in the purification via column chromatography. Furher functionalization of the hydroxy functions to give the corresponding trifluoromethanesulfonyl (triflat) groups was accomplished using trifluorosulfonyl anhydride as trifluorosulfonylating agent and pyridine as base in CH_2Cl_2 as the solvent [61].

To develop an organic–inorganic hybrid photomagnet, intercalation of spiropyran-5′-sulfonate anions into layered cobalt hydroxides was performed, yielding **SP159**-CoLHSP photoresponsive compound [62,63]. Target spiropyran-5′-sulfonate was synthesized from K salt **SP160**, which was prepared by condensation of Fischer's base analog (2-methylene-1,3,3-trimethylindoline-5-sulfonato potassium salt) with salicylaldehyde derivatives at reflux. After UV irradiation (313 nm), the optical and magnetic properties of CoLHSP clearly changed. Some of them demonstrate increased solubility in water and negative photochromic properties.

In similar maner, **SP161** spiropyran with isothiocyanate substituent at 5′-position was prepared from the 5-isothiocyanato-2-methylene-1,3,3-trimethylindoline [64,65].

5′-Aryl-substituted **SP20**–**SP27**, **SP263** (see Tables 1 and 4) were synthesized by standard method, but with very insignificant yields [66–68]. It is interesting to compare the

efficienty of this route with direct Wittig olefination method of the precursor **SP94** (3% vs. 62%) [50,66].

The Fischer's base moiety is readily replaced with other heterocycles, producing considerable variation in kinetics and in optical parameters of photochromism. In addition, spiropyran scaffold is in some cases sufficiently resistant to functional group transformation to modify properties or to introduce linker motifs with terminal reactive groups or "molecular address" to allow incorporation of the photochromic unit into/on different targets. Overviews of such synthetic possibilities are given in [3,5,23,24,26,69].

For further details as well as excellent overview of the progress in spiropyran dye synthesis, the reader is referred to [22]—although published over twenty years ago, it features a perspective gained in industry and also discusses the preparation and quality of indoline- and salicylaldehyde-based intermediates in depth.

At the end of this section, it is also necessary to mention the latest achievements in the field of organic synthesis, which have been successfully used to produce substituted derivatives of spiropyrans.

The solid-phase synthesis of small organic molecules has emerged as an important tool. Its use can avoid extensive workup, recrystallization, and chromatographic purification of the targeted products. It also allows for easy automation of the synthesis process and convenient handling of polar molecules throughout the synthetic protocol. Moreover, difficult or slow reactions can be facilitated by use of excess of reagents without any added complications in the ultimate purification step. Zhao et al. reports a successful application of solid-phase synthesis methods to the preparation of photochomic materials, such as spiropyran dyes. Using this SPOS method, new library of 5′-succinimide spiropyran derivatives **SP154** was synthesized on the Wang resin. Final products can be easily transformed into target 5′-succinylaminoderivatives **SP155** in high yields; the opening of the succinimide ring in spiropyran could be realized under mild conditions [70].

Because microwave irradiation-promoted reactions are typically rapid and energy efficient, and employ environmentally benign solvents, in the research [71] synthesis of stereochemically biased spiropyrans by the microwave-promoted, two-steps one-pot procedure was explored. In other work, the spiropyran synthesis using ultrasound irradiation instead of high temperatures was proposed since this type of energy offers different advantages such as reaction acceleration and less drastic operational conditions [72].

Pargaonkar reported the "greener" route for the synthesis of photo- and thermochromic spiropyrans promoted by biocompatible choline hydroxide in the water. This procedure provides several advantages such as simple workup, mild reaction conditions, short reaction time, and high yields of the products because choline hydroxide is a suitable basic catalyst in organic transformations [73].

The reversibility of condensation of 2-methyleneindolines (Fischer bases) with the most substituted salicylaldehydes in alcohol is reported in the reviews [21,22] on the basis of unpublished data of Bertelson.

The reaction goes virtually to completion only with 3,5-dinitrosalicylaldehyde because of the very low solubility of the condensation product (it is isolated in the **MC** form). So, Bertelson used the Fischer base for protection of the o-hydroxyformyl grouping in the case of chemical transformations with other substituents. Moreover, in [74], an efficient protecting method of 2-hydroxybenzaldehydes using Fischer's base has been reported; protection and deprotection of the hydroxyl and aldehyde group of 2-hydroxybenzaldehydes are also reported. The reaction of 2-hydroxybenzaldehydes with Fischer's base in ethanol under reflux produced the corresponding spiropyrans with high yield in specific conditions. The treatment of spiropyran with reagents such as $KMnO_4$ or $NaIO_4$ produced initial 2-hydroxybenzaldehyde in various solvent systems in low yield (less than 20%) as well as unidentified side products. However, when spiropyran derivative was treated with ozone at −78 °C in methanol, starting 2-hydroxybenzaldehyde was obtained with 85% yield. As a result, the hydroxyl and aldehyde group of 2-hydroxybenzaldehydes were protected at the same time by their reaction with Fischer's base in ethanol under reflux

to give the corresponding spiropyrans, the protected form of 2-hydroxybenzaldehydes. The spiropyrans were efficiently cleaved by ozonolysis to produce the corresponding 2-hydroxybenzaldehydes with high yields.

4. Chemical Properties

4.1. Classic Methods for the Modification of the Structure and Properties of 5′-Substituted Spiropyrans (Pathways A, B, C)

A wide range of behavior can be easily accessed just by altering substituents in the indolinospiropyran molecule. The following section illustrates some of these possibilities.

Some electrophilic substitution reactions in case of 1′,3′,3′-trimethyl-spiro[2*H*-1-benzopyran-2,2′-indoline] **SP1** and its 6-nitro-derivative **SP2** have been studied in the works of Gal'bershtam and co-workers and Zakhs et al. Direct chlorination, bromination, nitration, and azo-coupling with 4-nitrophenyldiazonium salt/$HgCl_2$ introduce the substituent into the 5′-position of spiropyran in 83–95% yields [23,75–77].

The spiropyrans **SP1**, **SP2** can be brominated with *N*-bromosuccinimide (NBS) in chloroform to give various substitution derivatives that are dependent upon the nature of the two parts of the molecule and NBS excess. Bromination of the unsubstituted spiropyran **SP1** occurs at first only in the indoline part to give a 77% yield of the 5′-bromocompound, then three-fold simultaneously in the indoline and chromene rings to give 60% overall yield of the 5′,7′,6,8-tetrabromocompound. To obtain the di- or tribromocompounds, it is necessary to start with 6-bromo-1′,3′,3′-trimethyl-spiro[2*H*-1-benzopyran-2,2′-indoline] or 6,8-dibromo-1′,3′,3′-trimethyl–spiro[2*H*-1-benzopyran-2,2′-indoline] [75]. Bromination of 6-nitro-1′,3′,3′-trimethylspiro [2*H*-1-benzopyran-2,2′-indoline] **SP2** with one or two equivalents of NBS takes place only in the indoline ring, giving 80 and 83% yields of 5′-bromo-6-nitro-**SP54** and 5′,7′-dibromo-6-nitro-1′,3′,3′-trimethyl-spiro[2*H*-1-benzopyran-2,2′-indoline], respectively [75]. Analogous results were reported in work [77]. Bromination of **SP2** to the 5′-bromoderivative **SP54** could be carried out with excellent yield by following reagent systems: bromine in chloroform (95%), *N*-bromosuccinimide in carbon tetrachloride (95%), cuprous bromide in acetonitrile (87%), or bromine in chloroform with boron trifluoride added (92%) (see Figure 13B). Similarly, chlorine in chloroform or cuprous chloride in acetonitrile gave the 5′-chloro compound **SP38** in very good yield (see Figure 13C).

Nitration of **SP2** in the 5′-position producing **SP127** can be carried out using nitric acid in acetic anhydride (43% yield) or concentrated sulfuric acid (60%), or better (87%), by adding sodium nitrite to the spiro compound in glacial acetic acid, followed by simply stirring in air to oxidize the initially formed nitroso compound [77] (see Figure 13E).

The reaction of 5′-bromo-substituted **SP54** with cuprous cyanide in the presence of pyridine at 150–160 °C leads to 5′-cyano-substituted **SP141.** Treatment of the **SP2** with the double salt of 4-nitrophenyldiazoniumchloride and mercuric chloride in acetone gave a 89% yield of the orange-red 5′-azosubstituted compound **SP143**, which was not photochromic (see Figure 13F) [77].

In the investigation of the chemical properties of spiropyrans, they were attempted to be used for the synthesis of derivatives that are inaccessible by the usual method of condensation (pathway **A** vs. pathways **B,C**). Compounds of this type often include an aminogroup in the 2*H*-1-benzopyran or in the indoline rings. The aminoderivatives of spiropyrans are possible key intermediates for the preparation of various derivatives via reactions with the participation of amino groups. Since the aminosalicylaldehydes necessary for their synthesis by pathway **A** are very labile and readily undergo polymerization, the possibility of the amino-substituted spiropyrans preparation by reduction of the corresponding readily accessible nitro derivatives was investigated. The reduction of **SP2** was carried out with hydrogen in the presence of Raney nickel in both a nonpolar solvent, in which the starting spiropyran exists in solution in the spiroform **A**, and in alcohol, when both forms (**A** and **MC**) are present (Figure 13C,E). However, if the reduction is carried out in alcohol, in which the **MC** form (**B**) is also present, simultaneous hydrogenation of the 3–4 double bond and the nitro group is observed.

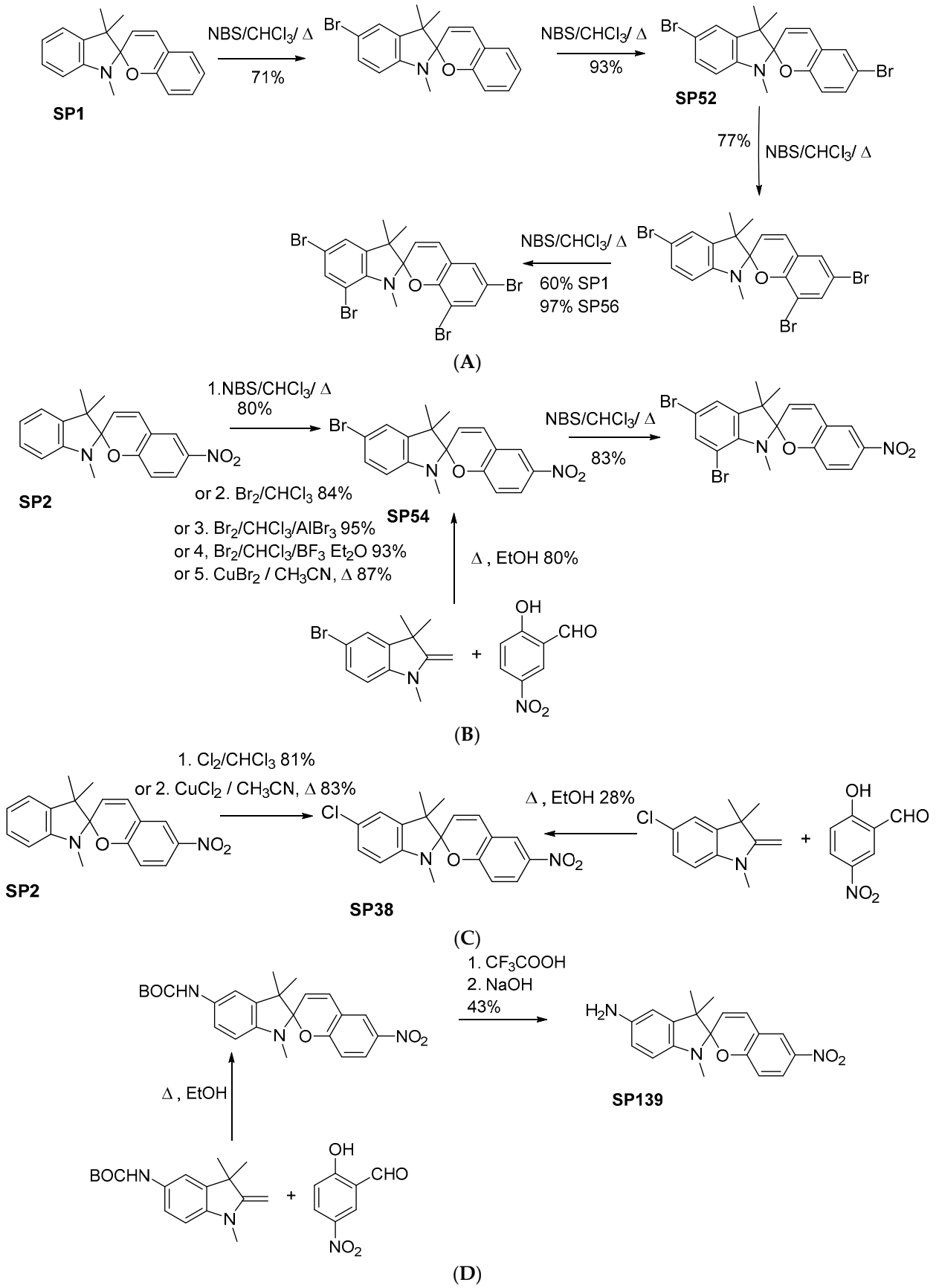

Figure 13. *Cont.*

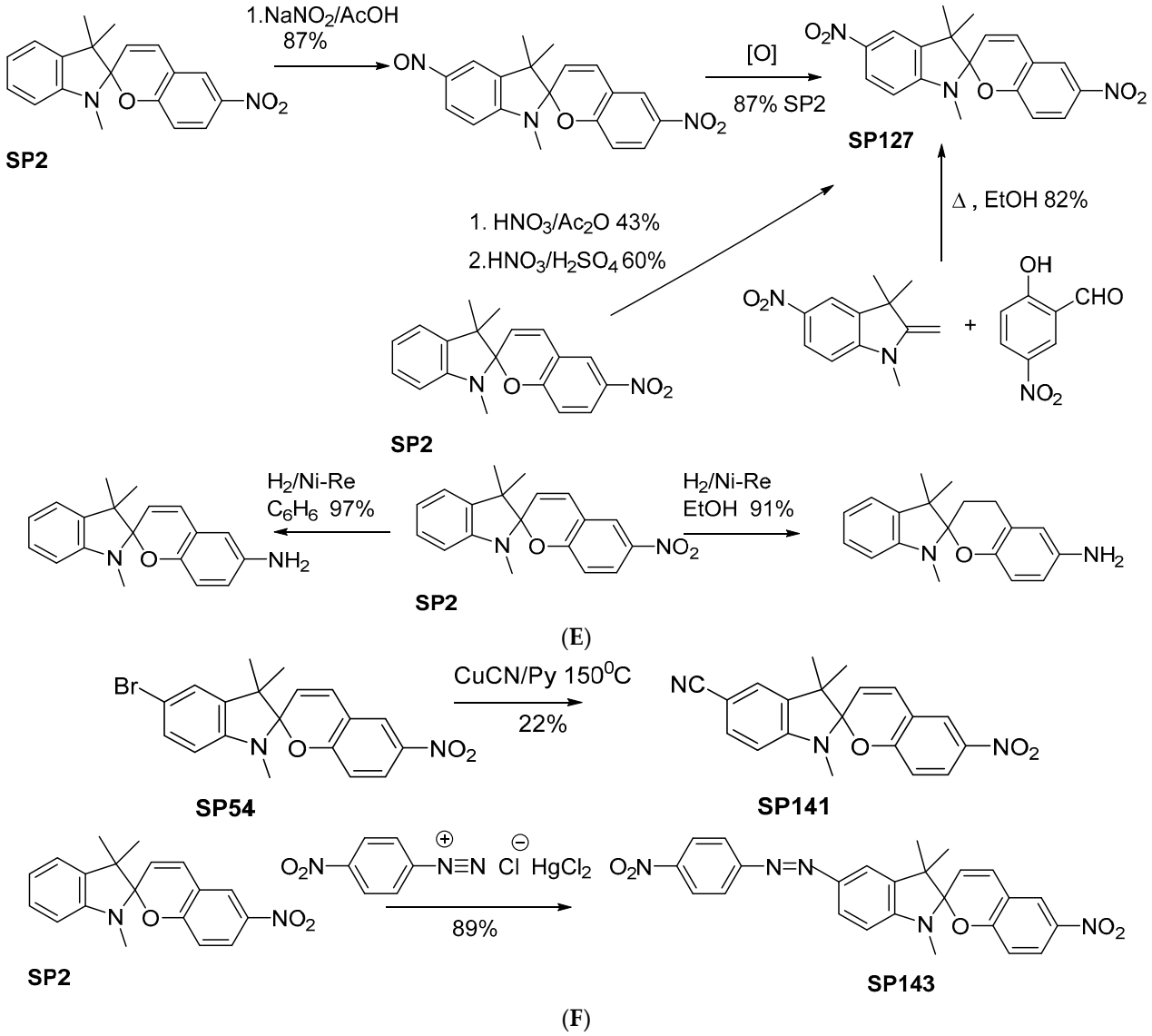

Figure 13. 5′-Substituted indoline spiropyrans synthesis (pathways **A,B,C**; do not confuse with subfigures **A**–**F** explained below). Bromination of **SP1** (**A**) and **SP2** (**B**); chlorination of **SP2** (**C**); synthesis of 5′-amino-substituted **SP139** (**D**); nitration of **SP2** (**E**); syntheses of 5′-cyano-substituted **SP141** and 5′-(4-nitrophenyl)azosubstituted **SP143** compounds (**F**).

At the same time, spiropyran derivative **SP139** with a 5′-aminogroup in the indolenine ring are readily accessible; it is formed in 43% yield in the condensation of quaternary salts or free methylene 5-BOC-amino-Fischer base with salicylaldehyde derivative, followed by removing of BOC-protection group by CF_3COOH (see Figure 13D) [78].

The promising classic 5′-substituted spiropyran precursors (**SP104** R = -COOH; **SP77** R = -OCH_3; **SP72** R = -OH) were synthesized by condensation of respectively substituted Fischer bases or its salts with 5-nitrosalicylaldehyde.

4.2. New Methods for the Modification of the Structures and Properties of Spiropyrans

We proposed 5′-substituted spiropyran derivatives as promising precursors scaffold for the synthesis of photochromic labels and probes for the different types of targets. It was necessary to modify their molecules to provide them the ability to form a covalent or non-covalent (ligand specific) interaction with different types of targets by introducing diverse reactive terminal groups or "molecular addresses" into a distinct position of the label molecules.

The choice of the target reactive group was governed by the type and nature of the target.

The following conjugation procedures were used:

(a). For the protein targets: covalent binding of a probe molecule with a target binding site by the self-recognition principle (bacteriorhodopsin). In our works [16,35,45,46,79–92], we have for the first time used photochromic derivatives of series of spiropyrans and dithienylethenes as photochromically labeled analogs of chromophore groups of a photosensitive retinal protein: the light-dependent proton translocase bacteriorhodopsin from *Halobacterium salinarum*.

(b). For the target proteins: non-covalent affine binding of a probe molecule with the target via the "molecular address" introduced into the probe molecule (photoactive thromboxane A_2 receptor inhibitors). We have previously discovered a new class of platelet aggregation inhibitors (5-substituted 3-pyridylisoxazoles) and developed new methods of their synthesis. A library of more than 120 compounds of classes of 3,5-substituted isoxazoles and their 4,5-dihydroderivatives containing 2-, 3-, and 4-pyridine moieties at the C3-position and substituents of different nature at the C5-position of the isoxazole ring was produced. To study the action mechanism of this class of human platelet aggregation inhibitors, three compounds containing the molecular address in a different spatial orientation to a fragment of a photochromic label from the series of spiropyrans were synthesized, and the process of their binding with human platelet membrane receptors was explored [85,93,94].

(c). Covalent binding of a label molecule with an inorganic nanosized target via a selective terminal reactive group. For specific binding with a target (CdSe quantum dots) various derivatives of terminal mono- and dithiols were used and different linkers for their introduction into the molecules of target photochromes were studied [35,91,95].

(d). Covalent binding of a label molecule with a target via a selective terminal reactive group. For specific binding with a target, namely, sulfhydryl groups of Cys-protein residues, a series of photochromic spiropyrans with a maleimide moiety in the molecule was synthesized [81];

(e). Covalent binding of a probe molecule with a target via a terminal reactive group. To label diverse organic molecules we have developed a complex of original synthetic methods and procedures [79,80,82,84,96].

For the first time, we have performed a sufficiently wide search for original photochromic systems with new functional capabilities and developed original effective procedures to synthesize and modify components for target photoactive label preparation. As a result of this research, we have developed a number of synthesis procedures for novel derivatives of 5′-substituted spirobenzopyrans containing the target reactive anchor groups via direct methods of introducing substituents [16,35,44–46,50,79–91,94,95].

Among the six promising scaffolds of substituted indoline spiropyrans presented in Figure 14, the most important place is occupied by 5′-formyl-6-nitro-1′,3′,3′-trimethylspiro[2*H*-1-benzopyran-2,2′-indoline] **SP94**, which is easily transformable into a whole set of key synthons for subsequent introduction of various reactive groups and/or "molecular addresses" at the 5′-position.

The formyl group is very convenient among other substituents (Br-, -OH, -NH_2, -COOH), its presence allows to implement a large number of organic reactions while preserving the rest of spiropyran molecule, for instance, to attach linkers/spacers of different nature. It should be noted that in case of formylation of spiropyrans under Vilsmeier-Haak conditions or by using the following acylation systems: Ac_2O/BF_3 Et_2O in chloroform, benzoyl chloride with $AlCl_3$ in carbon disulfide or benzoyl chloride in the dimethylaniline medium, formyl or acyl group is introduced in position 3 [97]. The analysis of available literature data shows that a direct pathway to **SP94** was not available, so that direct formylation reaction at the 5-position of indoline or at 5′-indolinospiropyran proved to fail. Previously, several unsuccessful attempts were done to carry out the indicated reactions in high yields and in a low-stage count variant. Moreover, the related efforts to find an

efficient procedure for the direct olefination of the 5′-formyl derivative under Wittig reaction conditions ended in failure, this circumstance forced Niu et al. and Gal'bershtam et al. to look for a multi-step alternative routes to the synthesis of target compounds [98,99]. Since the direct 5-formylation of indolines (or 5′-position of spiropyrans) seemed difficult and even unfeasible, they began to explore an alternative route to the desired aldehyde intermediate. A 5′-formylated indolinospiropyrane derivative **SP326** was prepared in six steps with 17.5% yield.

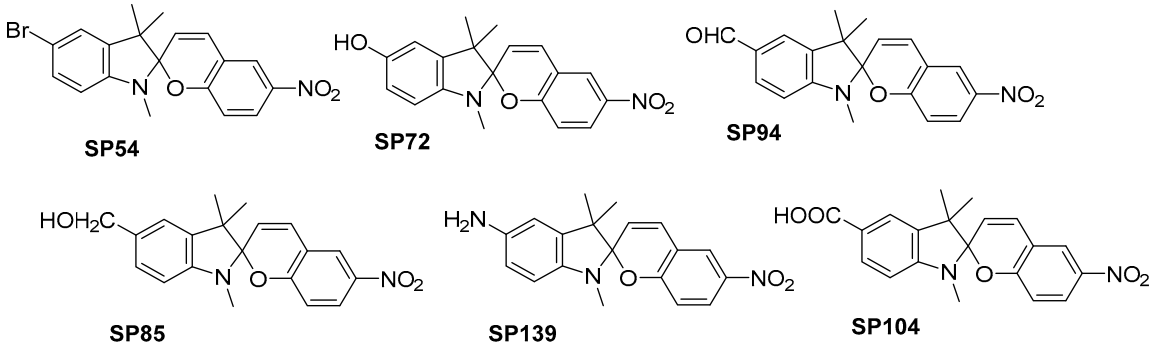

Figure 14. Key precursors in the 5′-substituted indoline spiropyran synthesis (pathways **B,C**).

Earlier, when we were searching for the synthetic route for the starting compound preparation method for carrying out the Horner-Emmons olefination in the synthesis of photochromic retinal analogs, we have investigated the formylation process of spirobenzopyrans under the Duff reaction conditions and the effect of different substituents presence in the pyran ring on its regioselectivity. At first, we investigated formylation process for unsubstituted spirobenzopyran **SP1**. Duff formylation of photochromic spiropyrans with electrone-withdrawing substituents in the pyran part of the molecule (R: H, 6-NO_2, 8-NO_2, 6-CHO, 6-CO_2Et, 6-CO_2H) was found to occur mainly at the C5′-position of the indole moiety (86–50% yeild). However, another two main regio isomers—8-formyl- and 5′,8-diformylderivatives at 1:3 ratio have been isolated upon Duff formylation reaction of 6-halogeno-substituted spiropyrans.

As a result, we developed a new one-pot synthesis of key carbonyl precursor series by direct formylation of 6-nitrospiropyran or its derivatives under the Duff reaction conditions [45,83,84,86,87,90,100]. Then we examined and considerably extended the potential of the synthetic application of 5′-formyl-6-nitro-spiropyran **SP94** for direct modification of the photochrome molecule at the C5′-position by means of a number of well-known reactions: Wittig and Horner–Emmons olefination, nucleophilic addition to the carbonyl group via reagents with active methyl or methylene groups, reductive amination, [3+2]-cycloaddition reaction, reduction with subsequent esterification, and so on (Figures 15 and 16). We have tested that synthesized **SP94** could be effectively used in the Wittig and Horner–Emmons olefination, Knoevenagel condensation reactions (olefination with CH-acids, aldol condensation-type), reduction by $NaBH_4$ into an alcohol, producing of the oximes, imines and in other processes. Thus, new photochromic labels and photosynthetic system models based on vitamin A analogs, nucleic acids fragments and porphyrins have been produced by us from this key precursor (see Figures 15–17) [16,35,44–46,50,79–91,94,95].

The reduction of the formyl group in 5′-formyl-6-nitro-spiropyran **SP94** was carried out with $NaBH_4$ in methanol at 0 °C with a yield of 46%. It was necessary to control the ratio of reagents and the temperature regime in order to avoid an additional side reaction of C3=C4 double bond reduction in the pyran ring [80,81]. The resulting alcohol **SP85** has been successfully used in a variety of esterification reactions in the creation of new probes for the modification of inorganic substrates like quantum dots and cations [95] (see Figures 15, 16A and 17E and Table 4 **SP316–SP320**).

To develop a new generation of the photochromic probes for covalent labeling of the protein targets it was necessary to combine two fragments in one molecule **SP232**: the

residue of photochrome—5′-substituted spiropyran—and the polyene chain of the retinoid conjugated with terminal formyl group. The photochromically labeled retinal **SP232** is analog of chromophoric group of the light-dependent proton translocase bacteriorhodopsin from *Halobacterium salinarum*. In this photosensitive retinal protein covalent binding of label should be implemented on the self-recognition principle with a target binding site ε-aminogroup of Lys216 [16,88] (see Figures 15, 17B and 18A and Table 4 **SP232**). For the first time, we proposed and studied a classical variant of the retinoid polyene chain extension by olefination of the initial 5′-formyl-6-nitro-spiropyran **SP94** using C_5-phosphonate anion under the conditions of Horner–Emmons reaction. The key stages of the synthesis of the photochromic analog of retinal **SP232** are shown in Figure 17B. In the first stage, we carried out the Horner–Emmons olefination of the initial **SP94** with the anion of C_5-phosphonate synthon with the terminal polar nitrile group. NaH in THF was used as the base for generating the C_5-phosphonate anion. As a result of the Horner–Emmons reaction, the newly formed C=C bond in nitrile product was shown to have an *E*-configuration, which was confirmed by the values of the spin–spin interaction constants (16.2 Hz). This was followed by a stage of reduction of the nitrile function with DIBAH at a temperature from −70 to −80 °C. Repetition of the specified sequence of operations, i.e., olefination of aldehyde **SP231** by Horner–Emmons and subsequent reduction of the nitrile function of nitrile compound, led to the synthesis of target retinoid **SP232** with a total yield of 15% relative to the initial aldehyde **SP94**.

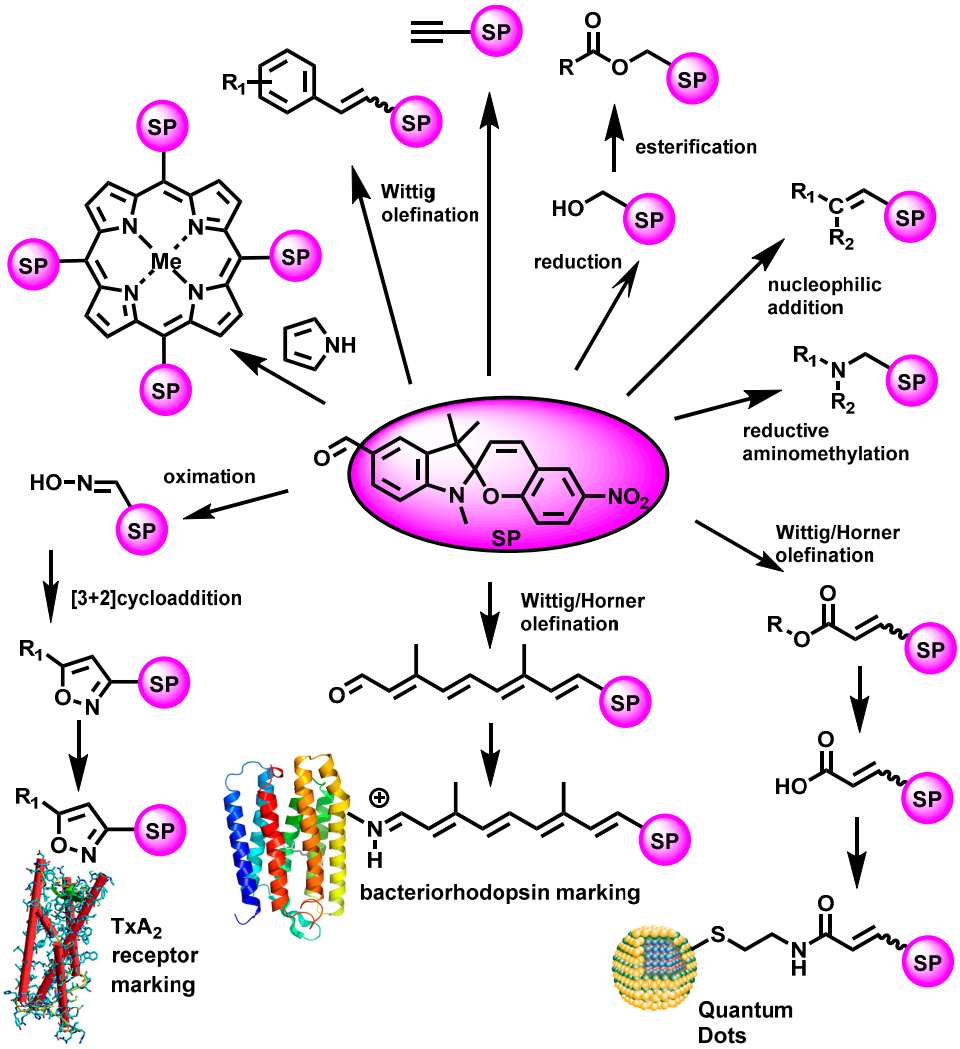

Figure 15. Basic trends in the design of photochromic probes and labels.

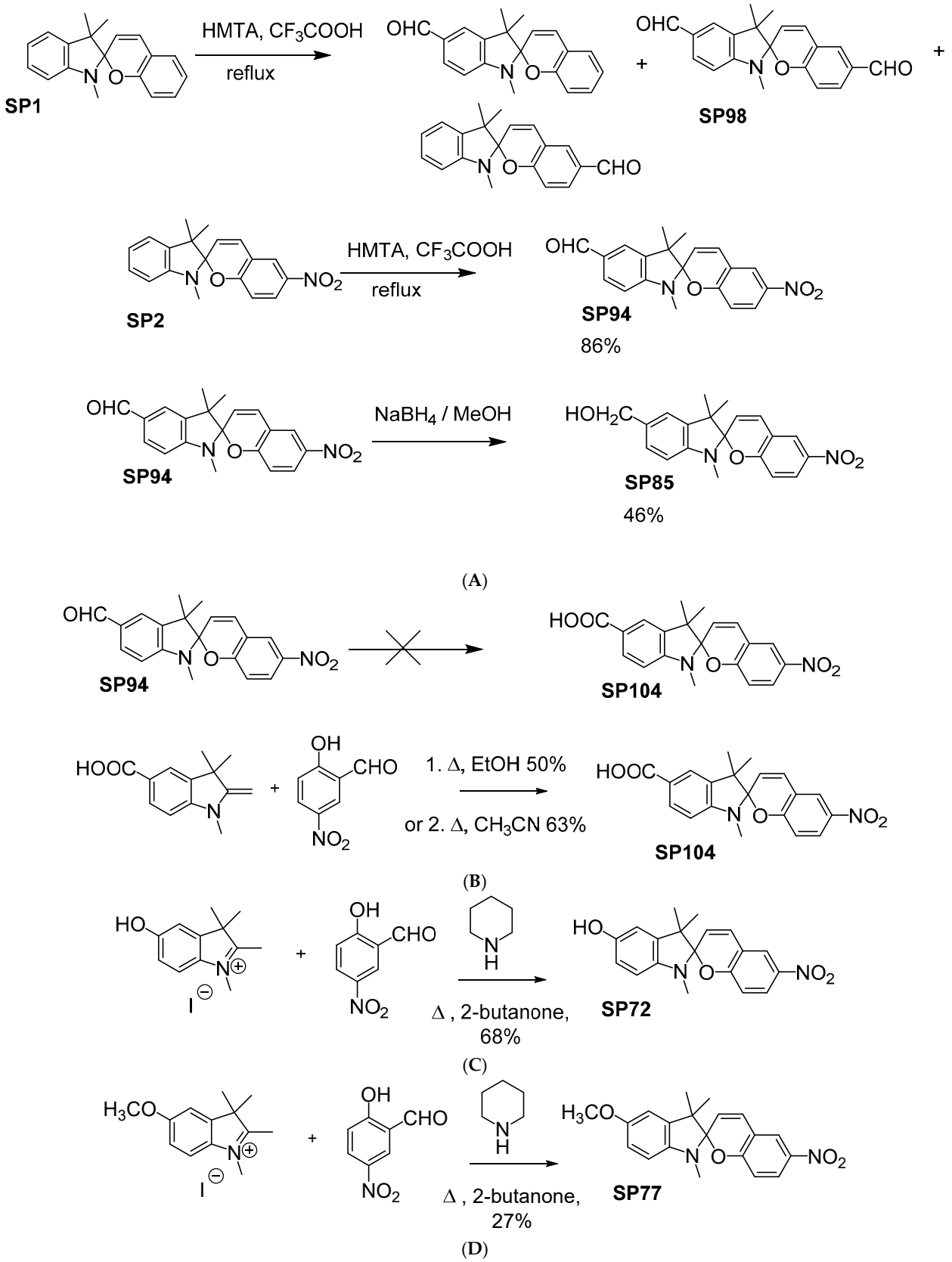

Figure 16. The variants of the key precursor synthesis for the 5′-substituted indoline spiropyran modification: 5′-formyl- **SP94** and 5′-hydroxymethyl- **SP85** (**A**); 5′-carboxy- **SP104** (**B**); 5′-hydroxy- **SP72** (**C**); 5′-methoxy- **SP77** (**D**).

Several series of carboxyl-containing spiropyran derivatives were described by Laptev et al. [82,84]. A number of unsaturated 5′-substituted spiropyrans (Figure 17C,G and Tables 1 and 4 **SP11**, **SP12**, **SP123**, **SP124**, **SP150**, **SP152**, **SP153**, **SP315**) with diverse functional groups were synthesized starting from **SP94** by the Wittig olefination or nucleophilic addition to the carbonyl group with reagents, possessing an active methyl or methylene groups [79,83,84].

Two synthesis variants of acid **SP315** were studied. Two-step procedure for **SP315** preparation by the Horner olefination of **SP94** with C_2-phosphonate followed by the saponification of intermediate ester **SP123** turned out to be more effective. One-step synthesis consisted of the Knoevenagel reaction with a low yield of 35% [35,82,84] (Figure 17A and Tables 1 and 4).

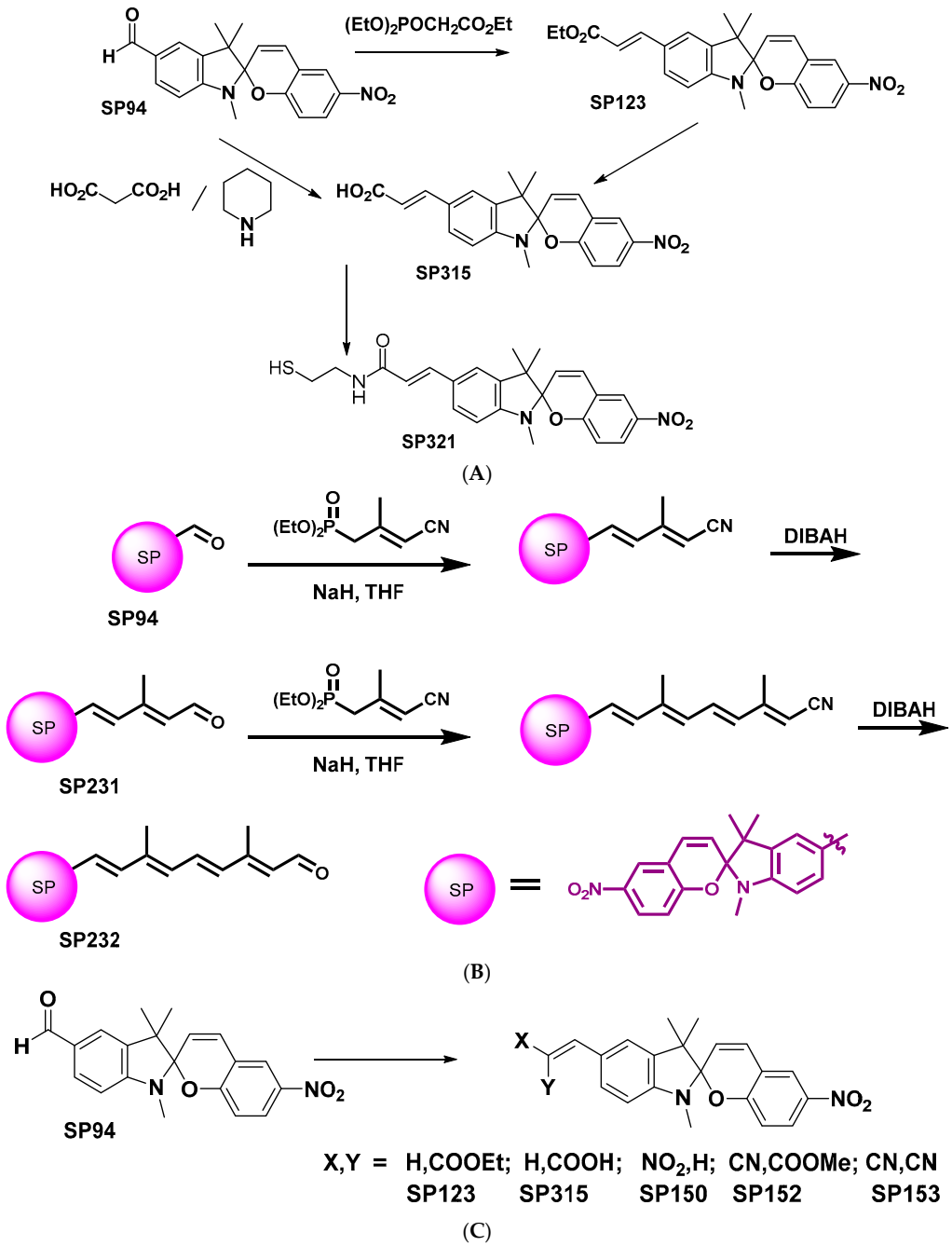

Figure 17. *Cont.*

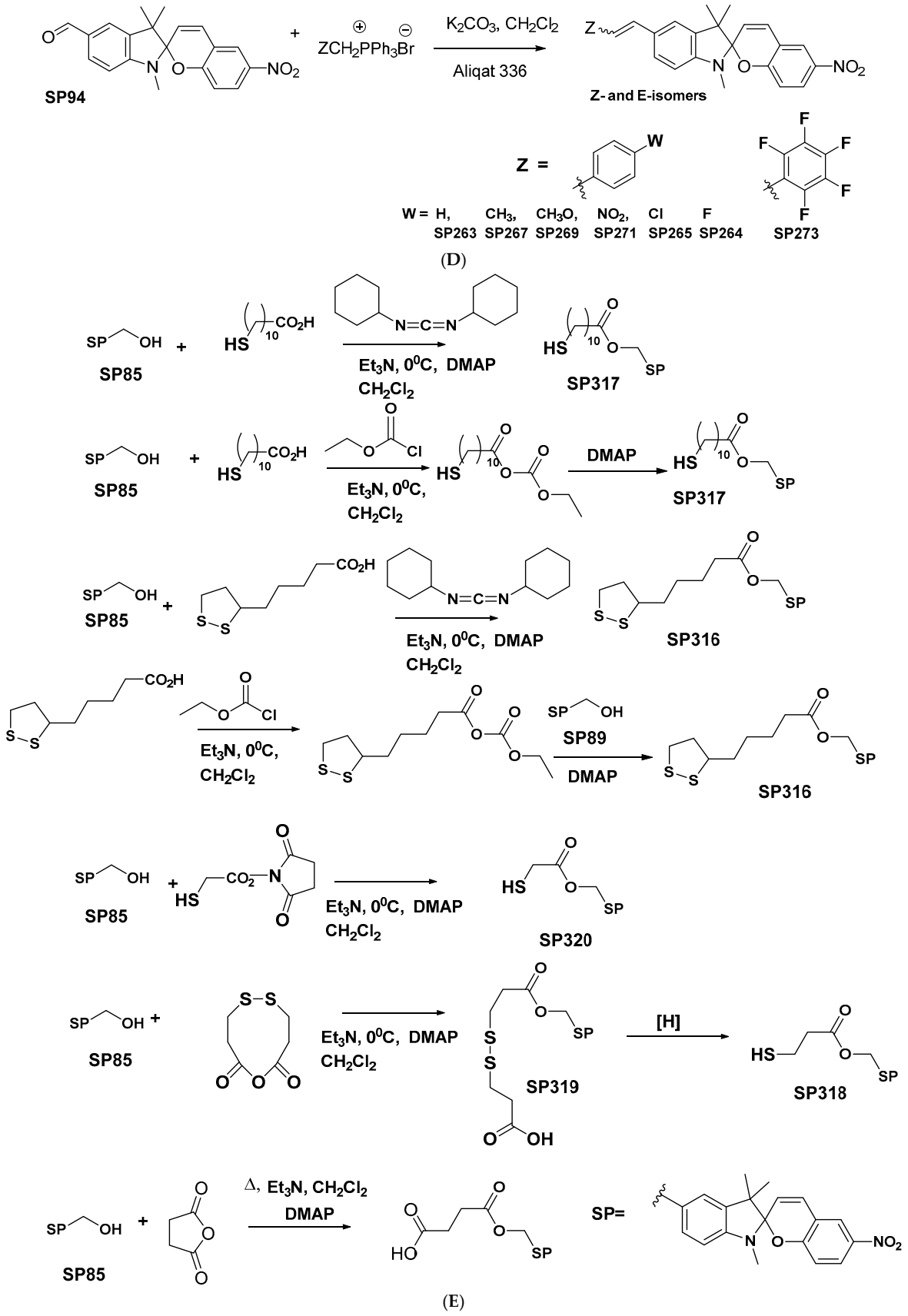

Figure 17. *Cont.*

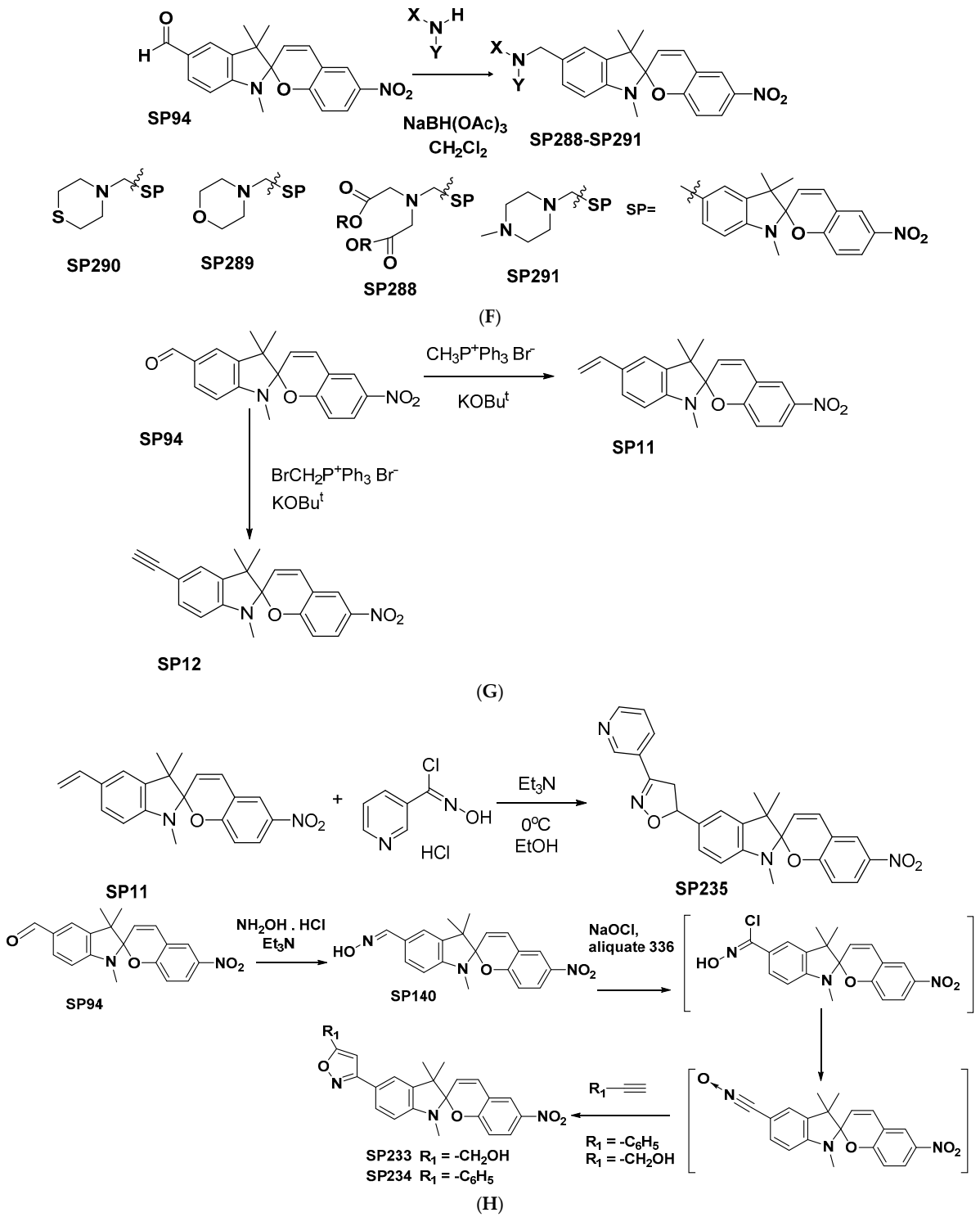

Figure 17. Examples of application of 5′-formyl-6-nitro-1′,3′,3′-trimethyl-spiro[2*H*-1-benzopyran-2,2′-indoline] **SP94** as key precursor in 5′-substituted spiropyran synthesis: **SP315** with unsaturated linker and a terminal carboxyl group and photochromic ligand **SP321** with unsaturated linker and a terminal mercapto group (**A**); photochromically labeled retinal **SP232** (**B**); series of unsaturated 5′-substituted spiropyrans with diverse functional groups (**C**); series of 5′-substituted spiropyran-stilbene containing dyads with (**D**); esterification reactions in the creation of new probes for the modification of inorganic substrates (**E**); series **SP288**–**SP291** with heterocyclic fragments or with a podand ionophoric unit attached to 5′-position through the methylene group (**F**); 5′-vinyl- **SP11** and 5′-ethynyl- **SP12** (**G**); photoactive thromboxane A_2 receptor inhibitors **SP233**–**SP235** (**H**).

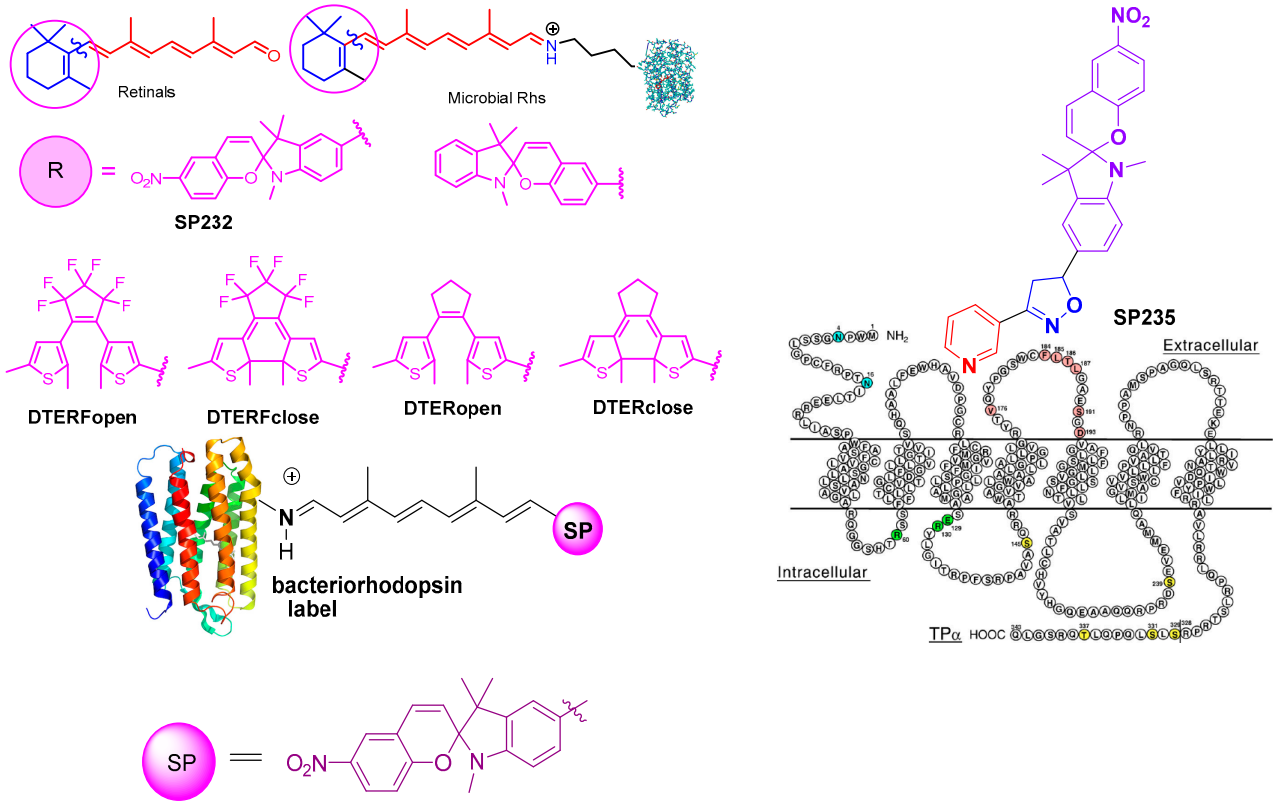

(**A**) (**B**)

Figure 18. Examples of application the photochromic probes for marking membrane proteins targets: bacteriorhodopsin (**A**) and thromboxane A_2 receptor (**B**).

To develop the photochromic labels for the non-covalent affinity binding of a probe molecule to a target through a "molecular address", it was necessary to develop a method for introducing a "molecular address" fragment into a certain position of the label molecule, as a fragment of 3,5-substituted isoxazole and their 4,5-dihydroderivative, containing 3-pyridine fragment in the C3-position, with varying orientation relative to the photochromic fragment. To study the action mechanism of this class of human platelet aggregation inhibitors, three photoactive thromboxane A_2 receptor inhibitors (compounds **SP233**–**SP235**), were synthesized starting from **SP94** by [3+2]cycloaddition reaction as key step, and the process of their binding with human platelet membrane receptors was explored (see Figures 15, 17H and 18B and Table 4 **SP233**–**SP235**) [85,93,94].

Tuktarov synthesized C60-fullerene–spiropyran hybrid dyad **SP29** by 1,3-dipolar cycloaddition of azomethine ylides, generated in situ from **SP94**/$CH_3NHCH_2CO_2H$, to fullerene C60 scaffold (Prato reaction). The photochromic properties of pyrrolidinofullerene **SP29** were found to be substantially affected by the nature of the electron-withdrawing group in the pyran ring. The physicochemical investigation of the pyrrolidinofullerene **SP29** indicated that the reversible phototransformation took place only for compound **SP29** with an NO_2 group in the pyran moiety [101]. Recently, the same group performed the synthesis of a hybrid **SP**-methanofullerene **SP28**, based on catalytic cycloaddition of diazocompounds to carbon clusters. The reaction of C60-fullerene with a diazoalkane generated in situ by oxidation of spiropyran hydrazone **SP145** with MnO_2 in the presence of three-component ($Pd(acac)_2$-$2PPh_3$-$4Et_3Al$) catalyst (20 mol%) produced methanofullerene **SP28** with 55% yield [102].

New photochromic probe **SP236** for the marking of model nucleic acid fragments, was prepared by the Sonogashira coupling with model 5-iodo-1,3-dimethyluracil. A new photochromic probe required for DNA marking was synthesized from terminal alkynes

linked to 5′-position **SP15**, **SP16** via ether bond with **SP72** or **SP85** and **SP17**–**SP19** connected through amide bond spacer with acetylenic amine derivatives from precursor **SP104** [80,103].

Potential photochromic markers for sulfhydryl groups in proteins with Cys residues—5′-maleimidomethyl **SP237** and 5′-[N-(2-maleimidoethyl)carbamoyl] **SP238** derivatives—were synthesized from 5′-hydroxymethyl precursor **SP85** by the Mitsunobu reaction or from 5′-carboxy-precursor **SP104** [81].

The series of 5′-substituted spiropyran-stilbene containing dyads **SP263**–**SP273**, with various aryl rings in stilbene fragment of the photochromic label molecule were made. They were prepared under the Wittig olefination reaction conditions from the aldehyde **SP94** by ylides, generated from substituted benzyltriphenylphosphonium salts in the phase-transfer catalysis conditions. Process was non-stereoselective, therefore, to isolate individual *Z*- and *E*-isomers from the mix, it was necessary to apply preparative HPLC. These compouds have a very low threshold of sensitivity to the traces of acids, which allows us to consider their possible use as pH sensitive elements of sensors [50] (Figures 15 and 17D and Table 4 **SP263**–**SP273**).

In the work [44], the process of reductive amination of aldehyde **SP94** was studied and its conditions were selected, as a result of which, a series of **SP288**–**SP291** was synthesized, with heterocyclic fragments or with a podand ionophoric unit attached to 5′-position of the indoline part of the molecule through the methylene group (Figures 15 and 17F and Table 4 **SP288**–**SP291**).

At the end of the review of modern methods for modifying the spiropyran molecule, we would also like to mention the widespread use of novel palladium-catalyzed cross-coupling reactions and click-chemistry strategy of late:

- Model labeling by the Sonogashira coupling of 5-iodo-1,3-dimethyluracil by terminal acetylene **SP12** with formation of target **SP236** [80].
- Catalytic cycloaddition of diazocompound to carbon clusters in **SP**-methanofullerene **SP28** synthesis [102].
- Synthesis of bis-**SP**-functionalized spiro[fluorene-9,9′-xanthene] derivative (SFX-2**SP227**). The introduction of two **SP** moieties to the SFX core included the following steps: 1. a Suzuki reaction between the di-Br-SFX and indol derivative, 2. quaternization of product by CH_3I, 3. condensation reaction of indolium salt with 2-hydroxy-5-nitrobenzaldehyde producing SFX-2**SP227** [104].
- Hybrid dyad DHA-**SP255**. The synthesis of the dyad from the precursors was carried out under Sonogashira coupling conditions. When using Pd^{+2}/CuI as catalyst system, the authors observed high conversions of the precursors, but also substantial amounts of homocoupling of the acetylenic spiropyran into a butadiyne product. Removing this resulting side product via repeated column chromatography reduced the isolated yield of DHA-**SP255** below 10%. It was nevertheless possible to suppress the homocoupling by using tris(dibenzylideneacetone)dipalladium(0) and triphenylarsine as catalyst system, and thereby DHA-**SP255** was isolated with 42% yield [105].
- Hybrid dyad **SP222**, containing a dithienylethene group between two spiropyran moieties was synthesized by the Sonogashira cross-coupling reaction between DTE-bis-alkyne and **SP61**, using $Pd(PPh_3)_4$/CuI/Et_3N as catalyst system, dissolved in toluene/THF, with yield of 60% [106].
- Suzuki coupling with thiophene-3-boronic acid, NBS bromination and Stille coupling reactions were used for the mono- and poly-thienyl **SP** conjugates **SP165**–**SP168**, **SP223** preparation [107].
- The reactions of 6-iodo and 6-bromo-spiropyrans **SP44**, **SP146**, **SP43** with phenylboronic acid under Suzuki coupling conditions (palladium acetate/Na_2CO_3 and DMF as solvent, 80 °C to give the coupling product in high isolated yield (87%). The 5′-substituents (chloro or benzoamido) and C3-C4-double bond of spiropyran **SP47** remained intact under these conditions. 6-Bromospiropyran **SP43** seemed to be less

reactive under the conditions and the reaction gave the coupling product **SP47** in 63% yield due to incomplete reaction, even in the extended reaction time [108].

- High molecular weight mechanochromic spiropyran main chain copolymer **SP356** via microwave-assisted Suzuki-Miyaura polycondensation. MW irradiation of the sample mixture of 5′,6-dibromo-**SP SP52**, boronate C_{10}-[B(pin)]$_2$ Pd_2dba_3, SPHOS in toluene with K_2CO_3 solution in water + Aliquat 336 [109].
- **SP197** precursor with two alkoxy-substituted thienyl units—monomer suitable for electropolymerization. **SP197** precursor monomer was prepared from the 5′,6-dibromo-**SP52** with thiopheneboronic acid via a double Suzuki coupling reaction. **SP351** copolymer was also described [110].
- A series of **SP256**–**SP259** was synthesized via [2+2]cycloaddition click reactions (Hagihara-Sonogashira cross-coupling reaction) [111].
- **SP**-Bodipy hybrids **SP274**–**SP276** have been designed and synthesized by [3+2]cycloaddition reaction as key step. Click chemistry of terminal alkyne with Bodipy-PEG_n-N_3, and their electrochemical, photophysical, ultrafast transient absorption, and photochromic properties have been studied [103].

In conclusion, we can recommend our novel pathways B or C as convenient one-step or multi-step methods for the functionalization of spiropyran molecule. The presence of the 5′-formyl group allows us to provide a large number of reactions with its participation, while preserving the rest part of spiropyran molecule.

5. Applications of Spiropyran Dyes

A great number of spiropyrans with diverse functional groups that have a substantial effect on the optical, physical, or chemical properties have been described. For these dyes, the effect on the spectral properties caused by changes in temperature (thermochromism), pH (acidochromism), solvent polarity (solvatochromism), redox potential (electrochromism), interaction with metal ions (ionochromism), mechanical stress (mechanochromism), and other factors have been well-studied.

Photochromic compounds, materials, and systems based on them have high potential for practical application in a number of important areas of technology, industry, and medicine. Their use is especially promising in the development of a new generation of the element base of nanoelectronics, optical molecular switches, and chemosensors. Some examples of spiropyran applications in which their exploitation has been tested are: photochromic optical lenses and eye protection glasses, materials for security printing, optoelectronics and nanophotonics (new photorecording media and materials, materials for holography, memory elements for 3D-data storage, molecular switches, elementary and integrated logic gates), sensorics (detectors for metal ions; dosimetry, photomodulation of adhesion or wettability, reaction control, mechanochromism) [5,6,15,16,35].

The main prospects for applications of spiropyrans in such fields as smart material production, molecular electronics and nanomachinery, sensorics, and photopharmacology are also discussed.

Despite active attempts to use **SP**s as elements of optical memory (3D memory prototype material **SP38** (3D-optical random access memory, 3D-ORAM) and readout system for monitoring energetic neutrons **SP**-based dosimeter), in this area, they are undoubtedly inferior to DTE derivatives [112,113].

In next sections, we only briefly describe the main aspects of the spiropyrans applications and therefore, in order to obtain the most comprehensive information for the systematic updating of their knowledge in this area, we would advise the reader to directly refer to the primary sources in the form of the latest reviews and monographs [2–19].

5.1. Photopharmacology

The design and development of efficient techniques to produce new hybrid molecular structures containing photochromic fragments as active working elements whose

characteristics substantially change upon the action of light are of special interest for nanotechnologies, in particular, for bionanophotonics and nanomedicine.

The progress in understanding and control of photophysical properties in molecular switches will increasingly stimulate development of novel materials with precise spatio-temporal control of their properties, as well as advanced tools for accurate modulation of biological systems.

Photopharmacology has undergone rapid development in the past decade. Tremendous progress has already been made, with photopharmacological agents now reported against a wide array of target classes and light-dependent results demonstrated in a range of live cell and animal models (photodynamic therapy and optogenetics). Synthetic photoswitches have been known for many years, but their usefulness in biology, pharmacology, and medicine has only recently been systematically explored [16,114–118].

The term "photochromic label" was first used by Prof. G. Likhtenshtein for the case of azobenzene derivatives in 1993. Derivatives of hybrid photochromic compounds and their components have already found application in the following areas of photopharmacology:

- To produce labeled conjugates of these photochromes with various biological substrates: polypeptides, proteins, nucleosides and nucleotides, and other physiologically active substances in order to study their behavior and mechanisms of their action in the body.
- In synthesis of a new type of photochromic labeled lipids and other natural compounds of various structures.
- In studies of process of targeted drug delivery to a selected organ.
- To develop new photo-rearrangeable forms of liposomes in studies of pharmacokinetics, metabolism and transport of drugs in vitro and in vivo.
- In the development of methods for modifying the surface of carrier polymers and films and polymer matrices (creation of photocontrolled mechanophores).
- In creating new reusable test systems in immunology and medicine.
- In tests on antitumor activity and antiviral activity assays.
- In the development of new types of photosensitizers for photodynamic therapy of tumors.

To create a novel generation of photochromic labels with the desired spectral and photochemical parameters, it is necessary to introduce an additional electron-acceptor substituent (EWG), e.g., a nitro group, to position C6 of the molecule. For the 5′-substituted spiropyrans, the functional linker fragment at the C5′-atom and the EWG group at C6-postion pyran fragment are located along one axis (uniaxially). Moreover, to ensure efficient interaction of photochromic labels with their targets, it is necessary to control the location, the nature, and length (at least C6-C10 atoms) of the spacer between the photochromic scaffold and the terminal reactive group or the "molecular address".

5.2. 5′-Substituted Spiropyran Derivatives with "Molecular Address" Designed for the Labeling of the Diverse Targets: Peptides, Proteins (Retinal-Based Proteins, GPCRs), Nucleic Acids and Their Fragments and Lipids

Combinations of molecular photoswitches with proteins and other biopolymers also resulted in interesting mechanisms of photocontrol for complex biological systems.

Below, we have presented several examples of design and development of a photochromic label scaffold and probe molecules for various types of targets based on 5′-substituted spiropyran. It was necessary to modify label molecules to provide them the ability to form a covalent or non-covalent (ligand specific) interaction with different types of targets by introducing diverse reactive terminal groups or "molecular addresses" into a distinct position of the label molecules (see Figure 17B,H and Figure 18, and in Table 4 section).

Examples of application of the photochromic probes for marking membrane proteins targets (bacteriorhodopsin and thromboxane A_2 receptor) are shown on Figure 18A,B.

SP-linked peptides (**SP242**, **SP245**–**SP247**) were prepared by the standard solid-phase peptide synthesis protocol and purified with preparative HPLC [119].

Photo-sensitive hydrogelator **SP243** with dipeptide D-Ala–D-Ala. D-Ala–D-Ala was linked to the 5′-amino group **SP** via succinic acid spacer **[120]**.

SP-Peptide **SP252** synthesis was performed by FMOC protocol on the Rink amide solid-phase resin [121].

Photochromic markers for sulfhydryl groups of Cys residues in proteins with 5′-maleimidomethyl **SP237** and 5′-[N-(2-maleimidoethyl)carbamoyl] **SP238** derivatives were synthesized [81].

New photochromic probe **SP236** for the marking of model nucleic acid fragments, was prepared by the Sonogashira coupling with model 5-iodo-1,3-dimethyluracil [80].

*5.3. **SP**-Dyads, Dimers, bis-**SP** Derivatives and poly-**SP**-Targets*

Large series of works by researchers from South Korea and other countries was devoted to the development of synthetic methods and detailed study of the properties of the resulting products based on bis-derivatives of 5′-substituted spiropyran (symmetric and non-symmetric dimers and dyads). Two identical or different fragments which are linked by 5′-5′- or by 6-6 sites are connected by linkers of various sizes and nature.

Symmetric 5′,5′-dimer **SP198 [106]** and symmetric and non-symmetric 6,6-bis-**SP**-dimers **SP199**–**SP204** [122–124] in which fragments are linked by single C-C-bond were described. **SP205** symmetric 5′,5′-dimer **SP**-CH_2-**SP** was synthesized [125]. Symmetric and non-symmetric 6,6-bis-**SP**-C≡C-**SP′ SP206-SP210** dimers were prepared via palladium-catalyzed reaction [126]. Symmetric 6,6-bis-**SP**-CO-**SP SP211** dimer [127] and symmetric and non-symmetric 6,6-bis-**SP**-S-**SP′ SP212-SP215** dimers [127,128] were made. Symmetric 5′,5′-dimers **SP**-NHCO-$(CH_2)_n$-CONH-**SP SP216a-c** and non-symmetric 5′,5′-dimers **SP**-NHCO-$(CH_2)_n$-CONH-**SP′ SP217-SP220** [129–131] were described.

Tetrakis-5′-**SP**-porphyrine **SP230** derivative [96] was produced and its spectral parameters were studied.

*5.4. 5′-**SP**-Dyads with Fluorophores, Dyes and Others*

SP222 contains a dithienylethene group between two spiropyran moieties. Similar to spiropyran, dithienylethene also performs photoisomerizaton. Upon exposure of UV, the open form of dithienylethene converts into the closed form, and reversibly turns back to the open form by visible light radiation. Unlike other photochromic materials, dithienylethene is highly stable to the thermal stimuli and does not isomerize at relatively high temperature. For **SP222** preparation, the Sonogashira cross-coupling reaction was used to connect alkyne and aromatic halide with retaining conjugation between dithienylethene and spiropyran. It was expected that **SP222** containing both spiropyran and dithienylethene moieties can be utilized for creating novel multichromic materials which exhibit metastable intermediate state other than on/off states when they are carefully combined with photo and thermal stimuli [106].

In order to use the electronic differences associated with the two isomeric forms into a materials-based switch, the spiropyran ultimately requires a covalent attachment through a conjugated pathway. A synthetic method was developed to incorporate spiropyran (**SP**) into thiophene based materials. Suzuki coupling with thiophene-3-boronic acid and Stille coupling reactions were used for the **SP**-T conjugates **SP223**, **SP165**–**SP168** preparation. A series of compounds (**SP223**, **SP165**–**SP168**) with a systematic variation of substituents was synthesized and their photochromism in both polar (methanol) and non-polar (toluene) solvents was studied. These compounds showed a cyclic variation of photochromic properties **[107]**.

Fluorescein derivative (Flu-2**SP225**) flanked by two **SP** units, was examined for fluorescence modulation in response to UV and visible-light irradiations and addition of acid. Upon addition of 2 eq. of CF_3COOH, the absorption band at 580 nm and the fluorescence

intensity at 550 nm disappeared due to the complete transformation of **MC** to **MCH⁺**. Combinational logic circuit was proposed [132].

SP-functionalized spiro[fluorene-9,9′-xanthene] derivative (SFX-2**SP227**) was synthesized. The introduction of two **SP227** moieties to the SFX core included the following steps: 1. Suzuki reaction between the di-Br-SFX and indol derivative, 2. quaternization of product by CH_3I, 3. condensation reaction of indolium salt with 2-hydroxy-5-nitrobenzaldehyde afforded SFX-2**SP227**. The SFX-2**SP227** not only preserved the isomerization property under visible light/dark and acid/base stimuli in solution but also showed high contrast emission between its ring-closed and ring-open solid states. Moreover, in a polymethyl methacrylate (PMMA) matrix, the cyan/red emission switching upon the stimulation with light and heat was achieved successfully with high reversibility due to the large free volumes caused by the orthogonally interconnected SFX moiety [104].

A tetraphenylethene derivative **SP228**−TPE−**SP228**-based solid-state photoswitch, which exhibits reversible photochromism in the solid state, was constructed. Its photoswitching characteristics of **SP228**−TPE−**SP228** in the CH_2Cl_2 and in solid state were studied [133].

Attempts to find an efficient procedure for the direct olefination of the 5′-formyl derivative **SP326** under Wittig reaction conditions ended in failure, and forced the authors of this work to look for multi-step alternative routes to the synthesis of target compounds. 5′-Functionalized **SP254, SP327** with vinylene unit as a linkage between the photochromic fragment and the ferrocene or triphenylamine moiety were produced [98].

The series of 5′-substituted spiropyran-stilbene dyads **SP263**–**SP273**, with various aryl rings in stilbene fragment of the photochromic label molecule was synthesized by the direct Wittig olefination reaction conditions of the aldehyde **SP94** by ylides, generated from substituted benzyltriphenylphosphonium salts in the phase-transfer catalysis conditions K_2CO_3/CH_2Cl_2/Aliqat 336. These compouds show a very low threshold of sensitivity to the traces of acids, which allows us to consider their possible use as pH sensitive elements of sensors [50] (Figures 15 and 17D and Table 4 **SP263**–**SP273**).

A series of **SP256**–**SP259** was synthesized via [2+2]cycloaddition click reaction (Hagihara-Sonogashira cross-coupling reaction). Its third-order nonlinear optical (NLO) properties were investigated [111].

Amide-linked **SP**-anthraquinone conjugates **SP260**–**SP261** were prepared and investigated in PC vesicles [**134**].

SP-Bodipy hybrids **SP274**–**SP276** have been designed and synthesized by [3+2]cycloaddition reaction as key step. Click chemistry of terminal alkyne with Bodipy-PEG_n-N_3, and their electrochemical, photophysical, ultrafast transient absorption, and photochromic properties have been studied [103].

SP-bonded 1,8-naphthalimide compound **SP278** is useful as photochromic and photoluminescent material [135].

From the 5′-modified **SP84**, **SP279** single-walled carbon nanotube organic thin-film transistors (OTFT) were constructed, where either alkane **SP84** or pyrene groups **SP279** are noncovalently associated with the surface of carbon nanotubes. It was shown that photochromic molecules **SP84**, **SP279** can be used to switch the conductance of a single-walled carbon nanotube transistor [**136**].

The other example of **SP**-OTFT application, for the **SP84** a facile method to make prototype of optoelectronic devices formed from organic thin-film transistors that are functionalized by photochromic spiropyran dyes in a nondestructive manner has been developed. Polydimethylsiloxane (PDMS) stamping was shown to be a nondestructive way to achieve good contact between electroactive semiconductor layer and photosensitive photochromic molecule layer. When PDMS stamps are employed, alkane-containing **SP84** can be coated simply onto the surface of organic thin films in a noninvasive manner. Upon UV irradiation, the molecules undergo isomerization from the neutral spiroform **A** to the charge-separated **MC** form, producing the local electrostatic environment. This photoinduced electrostatic environment can function as a local negative gate voltage,

thus increasing the electrical conductivity in p-type devices and decreasing the electrical conductivity in n-type devices. Further irradiation with visible light or keeping the devices in the dark can switch the device conductance back to their initial value. This method is reversible and reproducible on different devices with different thickness over a long period of time [137].

Spiropyran-fluorophore conjugates were proposed as efficient molecular optical switches. The switching performance of different fluorophore–**SP** conjugates **SP280**–**SP283** was studied. It was shown that the fluorescence of the fluorophores can be modulated by switching the **SP**. In these photochromic conjugates, **SP280**–**SP283** fluorescence emission of the fluorophore is controlled by the state of the spiropyran, which can be switched reversibly between a colorless spiroform **A** and a colored **MC** form upon irradiation with light. Thus, the efficiency of energy transfer from the fluorophore to the spiropyran can be modulated by the irradiation conditions [138].

A novel class of chiral and helical binaphthyl-substituted spiropyrans **SP226** has been synthesized and characterized. These multi-stimuli-responsive molecular switches have potential applications in not only optical data storage, anticounterfeiting, sensing, and bioimaging, but also chiral recognition and circularly polarized luminescence [139].

SP-conjugate **SP284** with rhodamine B aminoethylamide and **SP**-conjugates with rhodamine B hydrazide **SP285**–**SP287** were made [140,141].

5.5. Artificial Ion-Binding Receptors on the 5′-R-Spiropyran Basis. Photochromic Ligands for the Conjugation with Metal Cations, Nanoparticles and Quantum Dots

In the past decade, numerous efforts by researchers have been devoted to studying the phenomenon of the 5′-R-spyropyrans ionochromism. As a result, diverse photocontrolled systems with artificial ionophore receptors capable of selective complex formation with various ions were proposed and studied. The unique feature of spiropyrans is that the **MC** form is able to coordinate with metal ions and that the spiroform form (**A**) does not show such a property [6,8,11,13–15,32–40,142]. It was also found that the resulting complexes with various cations, in contrast to the original receptors, have negative or reverse photochromism.

Despite a large number of publications devoted to the methods of preparation and a detailed study of their properties, the main question related to the reasons for the selectivity of the complexation process still remains unresolved. This circumstance opens up good prospects for the development and intensification of the work in this area.

One of the most widespread types of such ionophoric systems is a covalent hybrid of a QD and a photochromic compound from the family of 5′-R-spiropyran. The optical properties of such hybrid nanosystem can be reversibly controlled by light of a given wavelength. A controllable fluorescence (photo-, bio-, or chemiluminescence) is extremely important because it opens up great prospects for practically applying these nanosystems. A lot of prototypes of smart devices were developed which were based on the new generation of hybrid photoactive systems, for which a combination of a photochromic component with inorganic fluorophores (QDs) was characteristic: molecular optical switches; photocontrollable logical modules; sensor devices for detecting ions, explosive substances and other agents, assays for estimating the proteolytic activity of enzymes; tools to visualize various nanoobjects in real time and in multiparametric (multicolored) systems; and photocontrollable means to control the structure and function of bionanoobjects (photochromic linkages, multiparametric protocols of hybridization of nucleic acids, photodriving delivery systems for biologically active compounds, etc.,) [8,13,15,35].

A number of spiropyran derivatives were selected as a starting compound for target ionophore receptors synthesis. Several examples of such photochromic systems that contain the various types of the reactive anchor group with affinity to the cations are known. Among them the diverse derivatives of crown-ethers, podands, chelates, iminodiacetates, N-heterocycles, thiols, bipyridines, and dendrimers were described. The select examples of 5′-**SP**-dyads with ionophores or chelatophores are presented in Tables 1, 2 and 4.

For effective complex formation, the presence of phenolate **MC** oxygen alone is not sufficient in most cases, and the addition of other chelating centers is necessary. In a series of works, the photochemical properties and processes of complex formation in the group of 5′,6,8-trisubstituted spiropyrans with diversified substituents at C8 were studied. The effect of the nature, size, and electronic properties of substituents at C8 and at C6 on the efficiency and selectivity of complexation with various cations were studied. The following fragments were used as additional chelators:

(a). **SP173**, **SP174** with cationic quaternized methylpyridinium moiety were synthesized. A molecular magnetic **SP174**-$CrMn(C_2O_4)_3 \bullet H_2O$, whose spiropyran cation contains a quaternized pyridine fragment in the side aliphatic chain was produced. The major effect of introducing a quaternized pyridinium fragment into the benzopyran part of the spiropyran entails a significant decrease in the rate of thermal relaxation processes [143,144];

(b). Photochromic 8-(5-(p-tolyl)-1,3,4-oxadiazol-2-yl)-substituted **SP175**, **SP176**, which are able to undergo light-controllable cation-induced isomerizations, have been prepared. Their **MC** forms contain bidentate chelating core that includes donor sites represented by the phenolate anion and the nitrogen atom of the oxadiazole ring. Introduction of electron withdrawing formyl group into 6-position of the pyran part leads to an increase in spiropyran photocoloration reaction efficiency, but decreases thermodynamical stability of **MC** form complexes. The addition of Zn^{2+}, Ni^{2+}, Cu^{2+}, Co^{2+}, Cd^{2+}, and Mn^{2+} salts to colorless or slightly colored solutions of spiropyrans causes accumulation of strongly colored products that have different position of absorption band maxima in the long-wavelength region depending on the metal ion [145,146];

(c). 8-(4,5-diphenyl-1,3-oxazol-2-yl)-substituted **SP177**–**SP179** were synthesized. They display photochromic properties in solutions. It was found that in contrast to naphthopyran analogs, the synthesized spiropyrans are characterized by significantly higher thermal stability of the **MC** isomers [147].

(d). Photochromic **SP181**–**SP183** derivatives, containing 8-(1-benzyl-4,5-diphenyl-1*H*-imidazol-2-yl)-group at the position 8 of the benzopyran fragment were synthesized [148].

(e). 8-benzoxazolyl-substituted spiropyrans **SP184**, **SP186**–**SP191** with different acceptor groups in the 5′-position of the indoline moiety have been synthesized. Novel spiropyrans exhibit photochromic properties in acetone solution at room temperature and form intensely colored complexes with heavy metal cation [149–152];

(f). 8-benzothiazolyl substituted **SP**s **SP185**, **SP192**–**SP195** were described. They demonstrate an ion driving photochromic transformations [37,151].

Symmetric 8,8-dimers **SP**-podands **SP221a**–**e** were synthesized. In podand molecule spiropyran subunits linked by a spacer of a 3-oxapentan-1,5-dioxy-group, (5′-R = MeO, ^{t}Bu, ^{i}Pr, H, Cl, Br), exhibited high selectivity to Ca^{2+} ions. Introduction of an electron-donating group to the 5′-position of each indoline ring of the podand gave rise to an increase in affinity to alkaline earth metal ions, enhancing the sensitivity [153].

Light-driven ion-binding receptor **SP224** with **MC** ionophoric fragment for Fe^{+3} ions was constructed. Two **SP** moieties at 5′-position were incorporated into perylene dye system. Spectral and electrochemical properties of the new dyad were studied. The results show the significant fluorescence enchancement due to the cooperative effect of UV-light, Fe^{+3} ions and H^+ and demonstrate for first time three input "AND" logic gate [154].

Spectral studies of dyad **SP262**-TTF, containing an electroactive TTF unit (tetrathiafulvalene), and a photochromic unit at 5′-position of **SP**, in the presence of ferric ions were conducted [155]. The electron-transfer reaction between the TTF unit (tetrathiafulvalene), and ferric ion can be photocontrolled in the presence of the **SP** unit.

The process of reductive amination of aldehyde **SP94** was studied and its conditions were selected and approved, as a result of which, a series of **SP288**–**SP291** were synthesized, with heterocyclic fragments or with a podand ionophoric unit attached to 5′-position of the indoline part of the molecule through the methylene group (Figures 15 and 17F and Table 4

SP288–**SP291**). Ion-binding receptor in **SP288** with N-iminodiacetate ionophoric fragment for the metals cations exhibited high selectivity to trivalent ions [44].

Two (**SP**)-based magnetic resonance imaging (MRI) contrast agents **SP292**–**SP293**/Gd chelates have been synthesized and evaluated for changes in relaxivity resulting from irradiation with visible light. Both electron-donating and electron-withdrawing substituents were appended to the **SP** moiety in order to study the electronic effects on the photochromic and relaxivity properties of these photoswitchable MRI contrast agents. Photoswitches lacking an electron-withdrawing substituent isomerize readily between the **MC** and spiro **A** forms, while the addition of a nitro group prevents this process [156].

A redox- and light-sensitive, magnetic resonance imaging (MRI) contrast agent **SP295**, which tethers a **spiropyran**/**MC** motif to a Gd–DO3A moiety was synthesized and characterized. When in the dark, the probe is in its **MC** form and has higher r1 relaxivity and it is triggered by either light or NADH. After irradiation with visible light or mixing with NADH, the contrast agent experiences a color change due to isomerization to spiroform **A** and r1 relaxivity decreases by 18% or 26%, respectively. The light induced isomerization is reversible, but the NADH induced process is not. This novel MRI contrast agent **SP295** may have unique potential to respond to NADH-related biochemical activities and may lead to non-invasive investigation of metabolic activities and cell signaling in vivo [157].

A series of 8-monoaza-crowned **SP**-based receptors **SP294a**–**c**, **SP296**–**SP298** and of 8-bis-aza-crowned bis-**SP**-based receptors **SP299a**,**b** for cations binding have been synthesized to investigate spectral changes induced by cations binding with perchlorates: Li^+, Na^+ and K^+ and Cs_2SO_4 [40,158–163].

5′-Methoxy-6-dimethylamino-functionalized spiropyran **SP300** was synthesized and its metal-sensing properties were investigated using UV−vis spectrophotometry. The formation of a metal complex between **SP300** and Cu^{2+} ions was associated with a color change that can be observed by the naked eye as low as ≈6 μM and the limit of detection was found to be 0.11 μM via UV−vis spectrometry [164].

Light-driven ion-binding receptor **SP301** with ionophoric fragment selective for the Zn^{+2} ions was constructed. This **SP301** was designed on the basis of 5′-carboxy-**SP** coupled with a suitable ionophore fragment of the bis(2-pyridylmethyl)amine at C8-position that is capable of complexing with a metal ions. **SP**-based Zn^{+2} sensor **SP301** is integrated into the surface of liposome [165,166].

$[Ru(bpy)_2(\mathbf{SP})](PF_6)_2$ and $[Os(bpy)_2(\mathbf{SP})](PF_6)_2$ ion-binding receptors **SP304**, **SP305**, **SP307**, **SP308**, **SP309a**,**b**, **SP310**, **SP311a**,**b** with ionophoric fragments selective for Ru, Os [38,39,167] were described.

Organic–inorganic hybrid photomagnet CoLH-O_3S-**SP** **SP313** was prepared, and the intercalation of 5′-sulfonate-substituted **SP** anions into layered cobalt hydroxides (CoLH) was performed [63].

A series of light-gated artificial transducers/Zn complex C2, C4, C6, C8, and C12 **SP314a**–**e** were synthesized, all of which exhibited relative hydrophobicity (ClogP, 4.5–10.8), which is a prerequisite for effective insertion into a hydrophobic phospholipid bilayer membrane [168].

An unsaturated linker with a terminal carboxyl group was introduced into the molecule **SP315**, which turned out to be a promising site for binding to various types of inorganic targets (cations or quantum dots) [35,82,84] (see Figures 15 and 17A and Table 4 **SP315**, **SP321**). In this work an efficient preparative method was proposed which can be used to obtain a modified photochromic ligand **SP321** containing an unsaturated linker with a terminal mercapto group on the C5′-position of a molecule indoline fragment to provide its immobilization at the surface of QDs.

The alcohol **SP85** has been successfully used in a variety of esterification reactions for the creation of new probes **SP316**–**SP320** for the modification of inorganic substrates such as quantum dots and cations [95] (see Figures 15 and 17E and Table 4).

5.6. 5′-Spiropyran Derivatives in Polymers and in Related Materials

The search, development, and study of novel smart materials that can be switched "on" and "off" or modulated in some way, are one of the main directions of development of the polymer industry and science. Such materials must possess at least two functional states that can be interconverted by an external stimulus such as heat, electric potential, or light. Of particular interest in this context is the use of an organic photochromic dye (especially spiropyrans) that can be attached to a solid support such as polymer, nanoparticles, or bulk surfaces, providing materials where surface properties such as hydrophobicity, charge, conductivity, color, molecular recognition, and material size can be easily controlled.

Spiropyrans were the primary choice for syntheses of a wide range of functional photochromic polymers (smart-polymer materials) since their switching properties are retained when incorporated either covalently or noncovalently. Additionally, a wide range of **SP**-doped polymers such as: poly(L-lactic acid) (PLLA), poly(methyl methacrylate) (PMMA), and poly(methacrylic acid) (PMAA) have been fabricated. Spiropyrans have been reported to respond to light and impact force in polymeric materials when dispersed in an amount as low as 0.5 wt%. Upon photoirradiation with light of given wavelength, these polymers reversibly change their physical and chemical properties, such as polymer chain conformation, shape of polymer gels, surface wettability, membrane potential, membrane permeability, pH, solubility, sol–gel transition temperature, and phase separation temperature of polymer blends. When photochromes are incorporated into polymer backbones or side groups, photoirradiation brings about changes in various properties of polymer both in solutions and in solids [169].

The incorporation of **SP** into main chain polymers via the 5′- and 6-positions using Suzuki polycondensation brings about significant changes to the electronic structure and stability of **SP**. However, the possibilities to access these two positions are very limited. To date, a covalent incorporation of spiropyrans to the backbones of polymers was achieved by several methods: electropolymerization [110]; introduction of an atom transfer radical polymerization (ATRP) initiator by ester condensation to a phenolic spiropyran, followed by radical polymerization [170,171]; polyurethane (PU) formation [172]; hydrosilation ring-opening polymerization (ROP) with ε-caprolactone [173]; ring-opening metathesis polymerization (ROMP) [174,175]; and polycondensation by Suzuki coupling [109,176,177]. The incorporation into polysiloxanes by hydrosilation as well as the usage of ATRP, ROP, or ROMP methods or polycondensations to form PU uses hydroxyl groups at the spiropyran. In contrast, due to a limited availability of spiropyrans with halide functions, very few examples of functionalization of spiropyrans by cross coupling have been reported [109,176,177].

The differentiating functionalization of the two halves of the molecule (indoline and pyran) with groups of different reactivity especially promises a broader variety of options for further functionalizations and thus a wider applicability of spiropyrans. Therefore, to make spiropyrans available as electrophile reagents in cross coupling reactions, a library of diversely halogenated, hydroxyl- and triflat spiropyran derivatives series **SP55**, **SP56**, **SP60**, **SP61**, **SP63**, **SP64**, **SP66**, **SP67**, **SP73**–**SP75**, **SP162**–**SP164**, was synthesized from respectively 5-substituted indolium salts and salicylaldehydes, using a versatile piperidine promoted procedure in ethanol as solvent [61].

A variety of polymer architectures have been made with covalent **SP** unit as force sensitive units, including linear homopolymers, block copolymers and networks. **SP** derivatives can be used in form of bifunctional initiators for controlled radical and ring opening polymerizations, cross-linkers for hydrosilylation, ring monomers for ring opening metathesis polymerization or bifunctional monomers for polyaddition and polycondensation reactions [172,176,178,179].

For the majority of systems, pH- and light-induced isomerizations were investigated rather than mechanically induced changes. Most structures reported to date are made by polyaddition or polycondensation techniques. Thiophene-based **SP197** monomer was prepared from **SP52** and copolymer **SP351** was made via electropolymerization [110]. **MC** units with aromatic units in 6-position show rather blue to green colors, also de-

pending on aggregation, with overall significantly bathochromic shifts in absorption compared to peak wavelength around 500 nm. Yang et al. maintained the nitro group in 6-position when preparing **SP**-containing poly-phenyleneethynylene monomer and **SP** containing polyphenyleneethynylene copolymer **SP352** via palladium-catalyzed polymerization of monomer by $Pd(PPh_3)_2Cl_2$ and CuI in a mixture of toluene and triethylamine [180]. Kadokawa et al. condensed dialdehydes of different structure with a symmetric bis-indoline to prepare main chain **SP** copolymers **SP353**–**SP354**. These polymers with very high **SP** content may be linked by an electron-deficient sulfone unit, possibly facilitating isomerization with light [181]. As the **SP**/**MC** reaction induces conformational changes of significant sterical demand, photochromism in the solid state depends on the rigidity of the matrix. This aspect is addressed by Kundu et al., who made porous, rigid organic frameworks **SP359** with a high density of **SP** units by Suzuki cross coupling. pH- and UV light-induced isomerization occurred rapidly and to a high extend, which was related to the non-hindered conformational changes within the pores of the framework. The substitution pattern of **SP** derivatives used in this study was mainly governed by the $–NO_2$ group in 6-position, with the chemistry used at the indoline side for covalent attachment not affecting or weakly affecting properties [76].

Dibrominated spiropyran **SP**Br_2, which is easily accessible, can be copolymerized with aromatic bis-boronic acid esters to obtain alternating **SP** copolymers **SP355**–**SP357** of high molecular weight [109,176,177]. The $N_{1'}$-ethyl substituent causes a slightly increased stability of **SP** compared to the commonly used methyl substituent. Komber et al. prepared main chain copolymers with alternating **SP** units and phenyl-based comonomers attached in 6-position. These copolymers could be quantitatively converted into their alternating **MCH**$^+$ form upon acidification.

Synthesis of spiropyran-functionalized dendron **SP336** and organogel was reported [182].

A number of **SP**-based liquid crystal derivatives **SP337**–**SP349** were described. They differed in the structure of the 5′-substituent, the type of anchor group, the presence, and nature of the substituent at the C6 atom [78,183–187].

The photochromic polymers are useful for various types of applications: photochromic glasses, ultraviolet (UV) sensors, optical waveguides, optical memories, holographic recording media, photogels, coatings, nonlinear optics, and so on [6,25,188–192].

But up-to-date, polymer derivatives having the 5′-substituted spiropyran as chromophore group in so-called smart-polymers are quite rare. However, in the recent times, the development in the field of polymer science related to the study of the phenomenon of mechanochromism has significantly stimulated the intensification of research in this area (see **SP334**–**SP359** Table 5). In this section of review, selected recent development carried out after 2000 is described.

5.7. Mechanochromism

Mechanochromism is a general term that comprises changes in the color of a substance during its crushing, shredding, grinding, friction (tribochromism), application of high pressure (piezochromism), or sonication, both in the solid state and in solutions [28,193].

Mechanochromic polymeric materials, which change color when force is applied, have been well studied. Spiropyran (**SP**) is one of the most promising mechanophores, which is colorless and undergoes a 6-π electrocyclic ring-opening reaction to form colored **MC** form under external force. **SP**-based mechanochromic materials can be obtained by covalent and noncovalent bonding to the matrix. The concern for noncovalently bonded systems is that **SP** has the potential to leach from the matrix, especially in the presence of solvents and this limits their practical applications.

The spiropyran (**SP**) mechanophore has been used to study mechanical forces in polymers in solution and the solid state including elastomers, glassy polymers, and crosslinked polymers. Under mechanical force, UV light, or heat, **SP** undergoes an electrocyclic ring-opening to the colored and fluorescent merocyanine (**MC**) form [194].

Craig and co-workers experimentally quantified the magnitude of the force required for the **SP** → **MC** transition (~240 pN) on the time scale of tens of milliseconds via single molecular force spectroscopy studies [174].

It has been demonstrated that **SP** mechanophore can undergo a reversible $6-\pi$ electrocyclic ring-opening reaction in response to mechanical force, heat, and light, which results in a distinct color and fluorescence change. Many factors affect the response efficiency of **SP** mechanoactivation, including **SP** types, polymeric structures, and environmental effects. Moreover, the mechanochemical activation can be realized in both solution and solid states under external force. To date, **SP** mechanophores have been successfully incorporated into various polymer architectures such as polyacrylates, polyesters, polyurethane, polystyrene, or poly(dimethylsiloxane) using different variants (initiator, cross-linker, or monomer [195].

Since 2007, spiropyrans have been used as mechanophores. Potisek et al. achieved ring opening of polymer-linked spiropyran (**SP**) in solution, marked by a change in color and fluorescence signal [170]. Davis et al. and more recently O'Bryan et al. have reported on covalently linked spiropyrans (**SP**) as highly effective color-generating mechanophores that can provide visible detection and mapping of mechanical stresses through their mechanically induced transformation to the (**MC**) conformation in glassy and elastomeric chain growth polymers. While the polymer systems explored by Davis et al. were quite successful in demonstrating a mechanochemically induced visible color change, the physical properties of these polymers were not ideal for investigation of the kinetics or thermodynamics of the mechanically induced transformations of **SP** mechanophore in bulk polymers [171,173].

Effects of **SP** substituents on the mechanochromism of **SP**-functionalized polymers were described by Sommer [192] in details. The maximum transfer of force from the polymer to the mechanophore was achieved when two polymer chains were connected to oxygen atoms at positions 5′ and 8 on the opposite sides of the spiropyran molecule, whereas minimal transfer occurred when the polymer chains were on the same side or when only one chain was attached. The most suitable attachment points for maximum force transfer are found at positions 5′ and 8, positions 1′ and 8 and positions 1′ and 6 (in Figure 19).

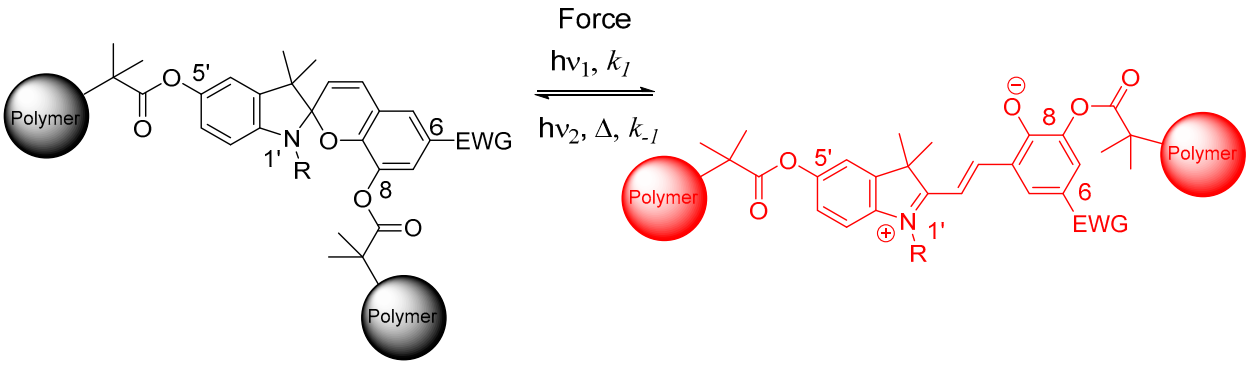

Figure 19. The diverse pathways for **SP** molecule derivatization are indicated with numbering of substituents adapted to the general numbering of the **SP** scaffold.

Gossweiler et al. has demonstrated interesting results that covalent polymer mechanochemistry provides a viable mechanism to convert the same mechanical potential energy used for actuation in soft robots into a mechanochromic, covalent chemical response. They designed, developed, and tested a soft robot prototype on the basis system formed from bis-alkene-functionalized spiropyran (**SP**) mechanophore/poly(dimethylsiloxane) (PDMS) by the methodology that exploits the platinum-catalyzed hydrosilylation of silicone elastomer. The functionalized **SP** mechanophore-based soft robots with walker and gripper functions were manufactured. This demonstration motivates the simultaneous development of new combinations of mechanophores, materials, and soft, active devices for enhanced functionality [175].

6. Conclusions

After a critical analysis of the information from available literature sources, it was found that 5′-substituted spiropyrans occupy an honorable third place among the known modifications of this photochromic scaffold, after the derivatives and analogs in the $N_{1'}$-position and the modifications in the pyran fragment molecule.

In this review the principal methods for the production of 5′-substituted spiropyrans (359 examples) and specific novel aspects of their molecule modification as well as their unusual chemical and photochromic applications were examined in detail.

We are considering the 5′-substituted spiropyran derivatives as promising precursors scaffold for the synthesis of photochromic labels and probes for different types of targets. It was necessary to modify their molecules to provide them the ability to form a covalent or non-covalent (ligand specific) interaction with different types of targets by introducing diverse reactive terminal groups or "molecular addresses" into a distinct position of the label molecule.

The apparent advantages of photochromic spiropyran-based photo-controlled systems and materials are that: (1) They possess a binary set of two different types of analytical signals (photo-induced light absorption in the range 560–600 nm and fluorescence induction in the colored merocyanine form); (2) location of the functional linker fragment at the C5′-atom and the EWG group at C6-postion pyran fragment along one axis (uniaxially).

Methods for the preparation of 5′-substituted spiropyrans, their chemical properties, and the effects of various factors on the relative stabilities of the spiropyrans and their isomeric merocyanine forms were examined and discussed.

Table 1. "Classic" 5′-R-**SP** (**SP1**–**SP168**).

No	5′-R	R_6	R_8	Synthetic Method (Yield, %)	Spectral-Kinetic Parameters	Notes and Applications	References
The substituents are numbered according to the structure: 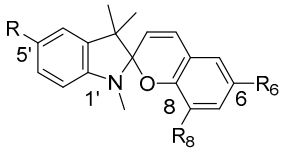					In Tables 1–5, fragment of 5′-substituted spiropyran is depicted as 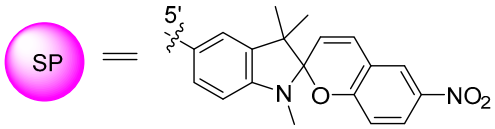		
SP1	H-	-H	-H	A	**EtOH:H_2O (1:1)**: λ^{A}_{max} 280, 310, 400, 550 nm, **EtOH**: λ^{A}_{max} 295 nm, λ^{B}_{max} 550 nm, $k_{BA}{}^{db}$ 0.36 s^{-1}		[32,196]
SP2	H-	-NO_2	-H	A (92%, in i-Pr-OH) A (89%)	**EtOH**: λ^{B}_{max} 532 nm, **Toluene**: λ^{B}_{max} 595 nm, $\lambda^{B}_{max}{}^{BH+}$ 415, 450 nm, **THF**: λ^{A}_{max} 269, 344 nm, λ^{B}_{max} 274, 309, 371, 387, 574 nm, λ^{B}_{fl} 651 nm, **EtOH:H_2O (1:1)**: λ^{A}_{max} 340, 510 nm	Treatment of **SP2** with TFA generated corresponding **MC** form, protonated at phenolate O^- atom; neutralization of TFA with an equimolar amount of Et_3N gives the starting **SP2**. Tests on antitumor activity and antiviral activity assays.	[167,196–198]
SP3	H-	-H	-NO_2	A	**EtOH**: λ^{B}_{max} 542 nm, **Toluene**: λ^{B}_{max} 598 nm		
5′-R-SP photochrome derivatives with alkyl substituents							
SP4	CH_3-	-NO_2	-H	A (83%)	λ^{B}_{fl} 610 nm	Light-triggered switch based on **SP4**/layered double hydroxide ultrathin films.	[199]
SP5	CH_3-	-CHO	-CH_3	A (63%)			[200]
SP6	CH_3-	-CHO	-OCH_3	A (58%)			[200]
SP7	CH_3-	-CH_3	-CHO	A (57%)			[200]

Table 1. *Cont.*

No	5′-R	R_6	R_8	Synthetic Method (Yield, %)	Spectral-Kinetic Parameters	Notes and Applications	References
SP8	CH_3-	-NO_2	-$COOCH_3$	A (35%)			[201]
SP9	CH_3-	-NO_2	-COOEt	A (31%)			[201]
SP10	C_6H_{13}-	R_6 = -NO_2 R_8 = -$CH_2CO_2C_{21}H_{43}$		A (93%)	λ^B_{max} 541 nm, λ^B_{max} 468 nm	H-aggregate formation of **SP10** in the bilayer.	[202]
5′-R-SP photochrome derivatives with unsaturated substituents							
SP11	H_2C=CH-	-NO_2	-H	B (75%)	**EtOH**: λ^A_{max} 277, 323sh nm, λ^B_{max} 547 nm, $\Delta D_B{}^{phot}$ 0.36, $k_{BA}{}^{db}$ 0.001 s^{-1}, $\tau_{1/2}$ * s, **Toluene**: λ^B_{max} 575sh, 615 nm, $\Delta D_B{}^{phot}$ 1.0, $k_{BA}{}^{db}$ 0.081 s^{-1}, $\tau_{1/2}$ 30 s	Precursor for functional 5′-R-6-NO_2-**SP** series (by pathway C)	[79,83]
SP12	HC≡C-	-NO_2	-H	B (50%) B (91%) B (87%) B (89%)	**CH_3CN**: λ^A_{max} 275, 331sh nm, λ^B_{max} 275, 574 nm, $\lambda^B_{max}{}^{BH+}$ 308, 409 nm, $t_{1/2BA}{}^{db}$ 31 s, λ^A_{fl} 460 nm, λ^B_{fl} 650 nm **THF**: λ^A_{max} 275 nm, λ^B_{max} 275, 598 nm	Precursor for functional 5′-R-6-NO_2-**SP** series (by pathway C) Precursor for functional 5′-R-6-NO_2-**SP** series via [2+2]cycloaddition click reactions.	[80,105,111,203]
SP13	$(CH_3)_3SiC$≡C-	-NO_2	-H	A (88%) A (77%) A (97%)	**EtOH**: λ^A_{max} 329 nm, λ^B_{max} 545 nm	Precursor for functional 5′-R-6-NO_2-**SP** series (by pathway C)	[105,111]

Table 1. *Cont.*

No	5′-R	R_6	R_8	Synthetic Method (Yield, %)	Spectral-Kinetic Parameters	Notes and Applications	References
SP14	HC≡C-	-C≡CH	-H	A (68%)	When **SP14** was irradiated with UV light, there is no detectable **MC** optical absorption (ca. 600 nm). Only limited switching to the **MCH⁺-14** (420–500 nm) was observed upon the addition of acid.	Precursor for **SP14**-functionalized Au surface electrode synthesis via a click alkyne−azide copper-catalyzed cycloaddition reaction or Sonogashira coupling	[204]
SP15	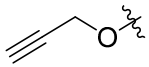	$-NO_2$	-H	B (84%)	**CH_3CN**: $k_{BA}{}^{db}$ 7.4 10^{-4} s^{-1}	Precursor for functional 5′-R-6-NO_2-**SP** series (by pathway C)	[103]
SP16	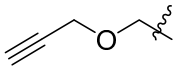	$-NO_2$	-H	B (38%)		Precursor for functional 5′-R-6-NO_2-**SP** series (by pathway C)	[80]
SP17	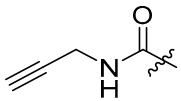	$-NO_2$	-H	B (44–46%)		Precursor for functional 5′-R-6-NO_2-**SP** series (by pathway C)	[80]
SP18	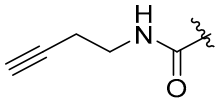	$-NO_2$	-H	B (41%)		Precursor for functional 5′-R-6-NO_2-**SP** series (by pathway C)	[80]
SP19	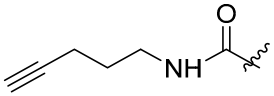	$-NO_2$	-H	B (38%)		Precursor for functional 5′-R-6-NO_2-**SP** series (by pathway C)	[80]
5′-R-SP photochrome derivatives with aryl(heteroaryl) substituents							
SP20	C_6H_5-	$-NO_2$	$-OCH_3$	A	**EtOH**: $\lambda^B{}_{max}$ 557 nm, **Toluene**: $\lambda^B{}_{max}$ 609 nm, $k_{BA}{}^{db}$ 1.52 10^2 s^{-1}, **Dioxane**: $k_{BA}{}^{db}$ 1.15 10^2 s^{-1}		[67,68]

Table 1. *Cont.*

No	5′-R	R_6	R_8	Synthetic Method (Yield, %)	Spectral-Kinetic Parameters	Notes and Applications	References
SP21	C_6H_5-	-NO_2	-H	A	**EtOH**: λ^B_{max} 534 nm, **Toluene**: λ^B_{max} 592 nm, $k_{BA}{}^{db}$ 3.25 10^2 s^{-1}, **Dioxane**: $k_{BA}{}^{db}$ 2.4 10^2 s^{-1}		[67,68]
SP22	C_6H_5-	-NO_2	-Br	A	**EtOH**: λ^B_{max} 531 nm, **Toluene**: λ^B_{max} 598 nm, $k_{BA}{}^{db}$ 3.25 10^2 s^{-1}, **Dioxane**: $k_{BA}{}^{db}$ 2.4 10^2 s^{-1}		[67,68]
SP23	4-$CH_3OC_6H_4$-	-NO_2	-OCH_3	A (12%)	**EtOH**: λ^B_{max} 563 nm, **Toluene**: λ^B_{max} 612 nm, $k_{BA}{}^{db}$ 1.65 10^2 s^{-1}, **Dioxane**: $k_{BA}{}^{db}$ 1.38 10^2 s^{-1}		[67,68]
SP24	4-$CH_3OC_6H_4$-	-NO_2	-H	A (8%)	**EtOH**: λ^B_{max} 537 nm, **Toluene**: λ^B_{max} 597 nm, $k_{BA}{}^{db}$ 5.75 10^2 s^{-1}, **Dioxane**: $k_{BA}{}^{db}$ 2.11 10^2 s^{-1}		[67,68]
SP25	4-$CH_3OC_6H_4$-	-NO_2	-Br	A (22%)	**EtOH**: λ^B_{max} 530 nm, **Toluene**: λ^B_{max} 597 nm, $k_{BA}{}^{db}$ 13.65 10^2 s^{-1}, **Dioxane**: $k_{BA}{}^{db}$ 1.38 10^2 s^{-1}		[67,68]
SP26	C_6H_5CH=CH-	-NO_2	-OCH_3	A,C (2%)	**EtOH**: λ^B_{max} 580 nm, **Toluene**: λ^B_{max} 617 nm		[66]
SP27	C_6H_5CH=CH-	-NO_2	-Br	A,C (2%)	**EtOH**: λ^B_{max} 548 nm, **Toluene**: λ^B_{max} 608 nm		[66]

Table 1. *Cont.*

No	5′-R	R_6	R_8	Synthetic Method (Yield, %)	Spectral-Kinetic Parameters	Notes and Applications	References
SP28	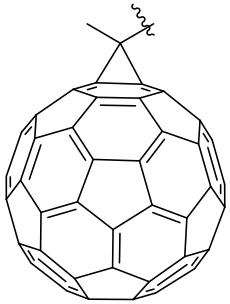	$-NO_2$	-H	A (55%)	**Toluene**: λ^A_{max} 330, 431 nm, λ^B_{max} 615 nm, $\Delta D_B{}^{phot}$ 0.4, $\tau_{1/2}$ 185 s		[102]
SP29	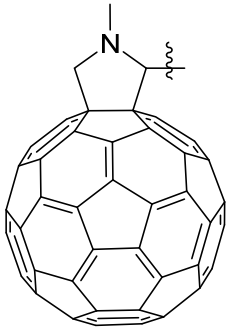	$-NO_2$	-H	A (60%)	**Toluene**: λ^A_{max} 277, 323sh nm, λ^B_{max} 320, 380sh, 580, 620 nm, $\lambda^B_{max}{}^{BH+}$ 415 nm, **$CHCl_3$**: λ^A_{max} 256, 326, 427 nm, **Toluene**: λ^A_{max} 325 nm, λ^B_{max} 610 nm, $\Delta D_B{}^{phot}$ 0.4, $k_{BA}{}^{db}$ 0.04 s^{-1}, $\tau_{1/2}$ 143 s, **$CHCl_3$**: λ^A_{max} 325 nm, λ^B_{max} 590 nm, $\Delta D_B{}^{phot}$ 0.2, $k_{BA}{}^{db}$ 0.03 s^{-1}, $\tau_{1/2}$ 57 s		[101,197]
5′-R-SP photochrome derivatives with halogenated substituents							
SP30	CF_3-	$-NO_2$	-H	A (65%) A (33%)	**EtOH**: λ^B_{max} 552 nm, **Toluene**: λ^B_{max} 600 nm		[205,206]
SP31	CF_3-	-H	$-OCH_3$	A (68%)			[162,206]

Table 1. *Cont.*

No	5′-R	R_6	R_8	Synthetic Method (Yield, %)	Spectral-Kinetic Parameters	Notes and Applications	References
SP32	CF_3-	-SO_2CF_3	-H	A (54%)	**EtOH**: λ^B_{max} 535 nm, **Toluene**: λ^B_{max} 575 nm		[205]
SP33	CF_3-	-SO_2CF_3	-NO_2	A (58%)	**EtOH**: λ^B_{max} 500 nm, **Toluene**: λ^B_{max} 570 nm		[205]
SP34	F-	-NO_2	-Br	A (41%)	**EtOH**: λ^A_{max} 380 nm, λ^B_{max} 527 nm, **Toluene**: λ^A_{max} 368 nm, λ^B_{max} 598 nm, **Dioxane**: λ^A_{max} 377 nm, λ^B_{max} 580 nm, λ^B_{max} 595 nm, $k_{BA}{}^{db}$ 1.12 10^2 s^{-1}		[207,208]
SP35	F-	-NO_2	-COOH	A (71%)			[201]
SP36	F-	-NO_2	-$COOCH_3$	A (53%)			[201]
SP37	F-	-NO_2	-COOEt	A (49%)			[201]
SP38	Cl-	-NO_2	-H	A (28%) B (81%, $Cl_2/CHCl_3$) (83%, $CuCl_2/CH_3CN$)	**CH_3OH**: λ^A_{max} 334 nm, **Solid state film**: $k_{BA}{}^{db}$ 5.1 10^{-5} s^{-1}	3D-optical random access memory (3D-ORAM) material and readout system for monitoring energetic neutrons. **SP**-based dosimeter. 3D memory prototype. Tests on antitumor activity and antiviral activity assays	[77,112,198,209–211]
SP39	Cl-	-NO_2	-Br	A (45%)	λ^B_{max} 616 nm, $k_{BA}{}^{db}$ 1.63 10^2 s^{-1}		[208]
SP40	Cl-	-NO_2	-COOH	A (66%)			[201]

Table 1. *Cont.*

No	5′-R	R_6	R_8	Synthetic Method (Yield, %)	Spectral-Kinetic Parameters	Notes and Applications	References
SP41	Cl-	$-NO_2$	$-COOCH_3$	A (41%)			[201]
SP42	Cl-	$-NO_2$	-COOEt	A (40%)			[201]
SP43	Cl-	-Br	-H	A			[108]
SP44	Cl-	-I	-H	A (89%)		Precursor for functional bis-**SP**	[108,124,126,212]
SP45	Cl-	$-CH_3$	-CHO	A (34%)	**CH_3CN**: λ^A_{max} 249, 272, 304, 361 nm, λ^B_{max} 627 nm, $k_{BA}{}^{db}$ 0.064 s^{-1}		[52]
SP46	Cl-	-C≡CH	-H	A (95%)		Precursor for functional bis-**SP**	[126]
SP47	Cl-	$-C_6H_5$	-H	B (87%) B (63%)		**SP51** was prepared by the Suzuki coupling.	[108]
SP48	Cl-	R_6 = $-C{\equiv}CC_6H_5$		B (78%)			[212]
SP49	Cl-	R_6 = $-CH{=}CHC_6H_5$		B (80%)			[212]
SP50	Cl-	$-C(CH_3)_3$	$-C(CH_3)_3$	A (31%)	**CH_3CN (−40 °C)**: λ^A_{max} 260, 320 nm, λ^A_{max} (CF_3SO_3H) 370, 400sh nm, λ^A_{max} (NaOAc) 550sh, 590, 640sh nm	**SP50** does not show significant photochromism in solution at room temperature.	[213]
SP51	Cl-	R_6 = $-CH_2OCOCH_2Cl$		A			[102]

Table 1. *Cont.*

No	5′-R	R_6	R_8	Synthetic Method (Yield, %)	Spectral-Kinetic Parameters	Notes and Applications	References
SP52	Br-	-Br	-H	A (63%) B (87%) B (93%)	**EtOH**: λ^{A}_{max} 223, 257, 307 nm	Precursor of **SP** copolymers.	[75]
SP53	Br-	-H	-Br	A		Precursor of **SP** copolymers.	
SP54	Br-	$-NO_2$	-H	A (22%) A (80%) B (77%) B (84%, $Br_2/CHCl_3$) B (95%, $Br_2/AlBr_3$) B (95%, NBS/CCl_4) (80%, NBS/$CHCl_3$) B (87%, $CuBr_2/CH_3CN$) B (93%, Br_2/BF_3 Et_2O)	**EtOH**: λ^{A}_{max} 260, 312, 340 nm, λ^{B}_{max} 545 nm, **CH_3OH**: λ^{B}_{max} 310, 360, 530 nm, **Toluene**: λ^{B}_{max} 380, 580sh, 605 nm	Precursor of PhotoPAF- (photoresponsive porous aromatic framework)	[75–77]
SP55	Br-	$-NO_2$	-Br	A (78%)	λ^{B}_{max} 595 nm, $k_{BA}{}^{db}$ 2.18 10^2 s^{-1}, **CH_3CN**: λ^{A}_{max} 315 nm, λ^{B}_{max} 556 nm		[61,208]
SP56	Br-	$-NO_2$	-I	A (50%)	**CH_3CN**: λ^{A}_{max} 306 nm, λ^{B}_{max} 559 nm		[61]

Table 1. *Cont.*

No	5′-R	R_6	R_8	Synthetic Method (Yield, %)	Spectral-Kinetic Parameters	Notes and Applications	References
SP57	Br-	$-NO_2$	-COOH	A (67%)			[201]
SP58	Br-	$-NO_2$	$-COOCH_3$	A (41%)			[201]
SP59	Br-	$-NO_2$	-COOEt	A (40%)			[201]
SP60	Br-	$-NO_2$	-OH	A (88%)	**CH_3CN**: λ^A_{max} 355 nm, λ^B_{max} 568 nm		[61]
SP61	Br-	$-NO_2$	$-OSO_2CF_3$	B (74%)	**CH_3CN**: λ^A_{max} 308 nm, λ^B_{max} 536 nm		[61]
SP62	I-	$-NO_2$	-H	A (37%)		Precursor for functional 5′-R-6-NO_2-**SP** series via Pd-catalyzed Sonogashira coupling (by pathway C)	[106]
SP63	I-	$-NO_2$	-Br	A (79%)	**CH_3CN**: λ^A_{max} 308 nm, λ^B_{max} 559 nm		[61]
SP64	I-	$-NO_2$	-I	A (62%)	**CH_3CN**: λ^A_{max} 314 nm, λ^B_{max} 561 nm		[61]
SP65	I-	R_6 = $-NO_2$ R_7 = -I		A,C (62%)	**CH_3CN**: λ^A_{max} 314 nm, λ^B_{max} 561 nm		[180]
SP66	I-	$-NO_2$	-OH	A (75%)	**CH_3CN**: λ^A_{max} 355 nm, λ^B_{max} 570 nm		[61]
SP67	I-	$-NO_2$	$-OSO_2CF_3$	B (56%)	**CH_3CN**: λ^A_{max} 311 nm, λ^B_{max} 538 nm		[61]

Table 1. *Cont.*

No	5′-R	R_6	R_8	Synthetic Method (Yield, %)	Spectral-Kinetic Parameters	Notes and Applications	References
5′-R-SP photochrome derivatives with oxygenated substituents							
SP68	HO-	-H	-H	A (49%)		Precursor for functional 5′-R-**SP** series.	[186]
SP69	HO-	-Br	-H	A (83%)		Precursor for functional 5′-R-**SP** series.	[186]
SP70	HO-	-CN	-H	A (69%)		Precursor for functional 5′-R-**SP** series.	[186]
SP71	HO-	$-CF_3$	-H	A (74%)		Precursor for functional 5′-R-**SP** series.	[186]
SP72	HO-	$-NO_2$	-H	A (68%) A (94%) A (78%) A (62%)		Precursor for functional of LC **SP** series.	[103,132,155,185,186,214,215]
SP73	HO-	$-NO_2$	-Br	A (90%)	**CH_3CN**: λ^A_{max} 320 nm, λ^B_{max} 547 nm		[61]
SP74	HO-	$-NO_2$	-I	A (83%)	**CH_3CN**: λ^A_{max} 320 nm, λ^B_{max} 549 nm		[61,216]
SP75	HO-	$-NO_2$	-OH	A (98%)			[61]
SP76	CH_3O-	-H	-H	A (44%) A (100%)	**EtOH**: λ^B_{max} 450 nm **EtOH:H_2O (1:1)**: λ^A_{max} 310, 450 nm, $k_{BA}{}^{db}$ 1.83 10^{-1} s^{-1}	Photoswitch to gadolinium chelates.	[59,196,217]

Table 1. *Cont.*

No	5′-R	R_6	R_8	Synthetic Method (Yield, %)	Spectral-Kinetic Parameters	Notes and Applications	References
SP77	CH_3O-	-NO_2	-H	A (77%) A (27%) A (54%) A (69%)	**THF**: λ^A_{max} 320 nm, λ^B_{max} 537 nm, λ^B_{max} (SP+Fe^{+3}) 424 nm, **THF**: λ^A_{max} 250, 280, 320, 350sh nm, λ^B_{max} 580 nm, λ^B_{max} (SP+Fe^{+3}) 424 nm, **THF**: λ^A_{max} 315, 340sh nm, λ^B_{max} 320, 350sh, 580 nm, λ^A_{max} (SP+Fe^{+3}) 320, 480 nm, λ^B_{max} (SP+Fe^{+3}) 310, 420 nm, **CH_3CN**: λ^A_{max} 230, 250, 270, 300, 320, 350sh nm, λ^B_{max} 560 nm, **EtOH**: λ^B_{max} 540 nm, **EtOH:H_2O (1:1)**: λ^A_{max} 310 340, 520 nm	Reference compound for ion-binding receptors with ionophoric fragment for Fe^{+3}. Photoswitch to gadolinium chelates.	[132,154,155,196, 216–218]
SP78	CH_3O-	-OCH_3	-H	A (93%)	**EtOH**: λ^A_{max} 250, 318 nm, λ^B_{max} 250, 318 nm, **EtOH:H_2O (1:1)**: λ^A_{max} 320, 580 nm, **EtOH**: λ^B_{max} 480, 600 nm, $k_{BA}{}^{db}$ 2.9 10^{-1} s^{-1}, 2.3 10^{-2} s^{-1}	Photoswitch to gadolinium chelates.	[196,217]
SP79	CH_3O-	-OCH_3	-CH_2OH	C (87%)		Precursor for preparation of (**SP**)-based magnetic resonance imaging (MRI) contrast agents	[156]
SP80	CH_3O-	-OCH_3	-CH_2I	C (66%)		Precursor for preparation of (**SP**)-based magnetic resonance imaging (MRI) contrast agents	[156]
SP81	CH_3O-	-CF_3	-H	A (67%)	**EtOH**: λ^B_{max} 550 nm	Photoswitch to gadolinium chelates.	[217]
SP82	CH_3O-	-CN	-H	A (60%)	**EtOH**: λ^B_{max} 550 nm	Photoswitch to gadolinium chelates.	[217]

Table 1. *Cont.*

No	5′-R	R_6	R_8	Synthetic Method (Yield, %)	Spectral-Kinetic Parameters	Notes and Applications	References
SP83	CH_3O-	-CHO	-OCH_3	A (84%)	**Acetone:H_2O (1:1)**: $\lambda^A{}_{max}$ 400 nm, $\lambda^B{}_{max}$ 300, 370, 546 nm		[219]
SP84	$C_{12}H_{25}O$-	-NO_2	-H	B (28%)	**CH_2Cl_2**: $\lambda^A{}_{max}$ 320 nm, $\lambda^B{}_{max}$ 320, 550 nm	Organic thin-film transistor (OTFT)	[136,137]
SP85	$HOCH_2$-	-NO_2	-H	B (46%)	**EtOH**: $\lambda^A{}_{max}$ 336 nm, $\lambda^B{}_{max}$ 537 nm, $\Delta D_B{}^{phot}$ 1.94, $k_{BA}{}^{db}$ 1.44 10^{-4} s^{-1}, 8.01 10^{-5} s^{-1}, $\tau_{1/2}$ 2700 s, λ_{fl} 650 nm **Toluene**: $\lambda^A{}_{max}$ 333 nm, $\lambda^B{}_{max}$ 604 nm, $\Delta D_B{}^{phot}$ 4.45, $k_{BA}{}^{db}$ 8.74 10^{-4} s^{-1}, $\tau_{1/2}$ 16 s, λ_{fl} 675, 505 nm	Precursor for functional 5′-R-6-NO_2-**SP** series (by pathway C)	[80,81,95]
SP86	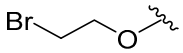	-NO_2	-H	A,C (16%)		Precursor for functional 5′-R-6-NO_2-**SP** series (by pathway C)	[214]
SP87	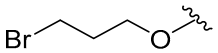	-NO_2	-H	A,C (46%)		Precursor for functional 5′-R-6-NO_2-**SP** series (by pathway C)	[182,214]
SP88	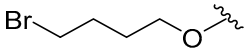	-NO_2	-H	A,C (59%)		Precursor for functional 5′-R-6-NO_2-**SP** series (by pathway C)	[214]
SP89	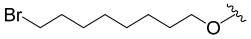	-NO_2	-H	A,C (60%)		Precursor for functional 5′-R-6-NO_2-**SP** series (by pathway C)	[214]
SP90	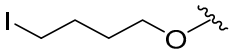	-NO_2	-H	B (25%)		Precursor for functional 5′-R-6-NO_2-**SP** series (by pathway C)	[216]
SP91	$C_{15}H_{31}COO$-	-NO_2	-H			Amphiphilic **SP91**	[220]

Table 1. *Cont.*

No	5′-R	R_6	R_8	Synthetic Method (Yield, %)	Spectral-Kinetic Parameters	Notes and Applications	References
SP92	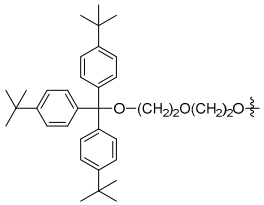	$-NO_2$	-H	A (88%)		**SP92** Langmuir Blodgett monolayers	[221]
SP93	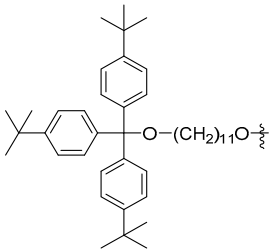	$-NO_2$	-H	A	**Hexane**: λ^{A}_{max} 316 nm, λ^{B}_{max} 316, 580, 615 nm,	**SP93** Langmuir Blodgett monolayers	[221]
SP94	OHC-	$-NO_2$	-H	B (86%)	**EtOH**: λ^{A}_{max} 328 nm, λ^{B}_{max} 567 nm, ΔD_B^{phot} 0.77, k_{BA}^{db} 0.069 s^{-1}, $\tau_{1/2}$ 44 s, **Toluene**: λ^{A}_{max} 320 nm, λ^{B}_{max} 590sh, 625 nm, ΔD_B^{phot} 1.19, k_{BA}^{db} 0.139 s^{-1}, $\tau_{1/2}$ 31 s, **Toluene**: λ^{A}_{max} 315 nm, λ^{B}_{max} 580sh, 620 nm, ΔD_B^{phot} 0.6, k_{BA}^{db} 0.1 s^{-1}, $\tau_{1/2}$ 52 s, **$CHCl_3$**: λ^{A}_{max} 320 nm, λ^{B}_{max} 595 nm, ΔD_B^{phot} 0.3, k_{BA}^{db} 0.007 s^{-1}, $\tau_{1/2}$ 21 s	Precursor for functional 5′-R-6-NO_2-**SP** series (by pathway C). Photo controlled organic field effect transistors (OFET): mixed-type or multilayer transistor from **SP94** and fullerene C60.	[35,45,83,84,86,87,90,100,101,222]

Table 1. *Cont.*

No	5′-R	R_6	R_8	Synthetic Method (Yield, %)	Spectral-Kinetic Parameters	Notes and Applications	References
SP95	OHC-	-H	-NO_2	B (79%)	**EtOH**: $\lambda^A{}_{max}$ 325 nm, $\lambda^B{}_{max}$ 580 nm, $\Delta D_B{}^{phot}$ 0.7, $k_{BA}{}^{db}$ 0.48 s^{-1}, $\tau_{1/2}$ 50 s, **Toluene**: $\lambda^A{}_{max}$ 317 nm, $\lambda^B{}_{max}$ 600sh, 640 nm, $\Delta D_B{}^{phot}$ 0.45, $k_{BA}{}^{db}$ 0.84 s^{-1}, $\tau_{1/2}$ 5 s	Precursor for functional 5′-R-**SP** series (by pathway C)	[90,100]
SP96	OHC-	-Cl	-H	B	**Toluene**: $\lambda^A{}_{max}$ 320 nm, $\lambda^B{}_{max}$ 600 nm, $\Delta D_B{}^{phot}$ 0.03, $k_{BA}{}^{db}$ 2.15 s^{-1}, $\tau_{1/2}$ 40 s, **$CHCl_3$**: $\lambda^A{}_{max}$ 325, 382 nm, $\lambda^B{}_{max}$ 505 nm, $\Delta D_B{}^{phot}$ 0.4, $k_{BA}{}^{db}$ 0.002 s^{-1}, $\tau_{1/2}$ 325 s	Precursor for functional 5′-R-**SP** series	[101]
SP97	OHC-	-F	-H	B	**Toluene**: $\lambda^A{}_{max}$ 315, 390, 580 nm, $\lambda^B{}_{max}$ 490 nm, $\Delta D_B{}^{phot}$ 0.1, $k_{BA}{}^{db}$ 0.7 s^{-1}, $\tau_{1/2}$ 75 s, **$CHCl_3$**: $\lambda^A{}_{max}$ 330, 390, 575 nm, $\lambda^B{}_{max}$ 540 nm, $\Delta D_B{}^{phot}$ 0.2, $k_{BA}{}^{db}$ 0.27 s^{-1}, $\tau_{1/2}$ 120 s	Precursor for functional 5′-R-**SP** series	[101]
SP98	OHC-	OHC-	-H	B (77%)	**EtOH**: $\lambda^A{}_{max}$ 325 nm, $\lambda^B{}_{max}$ 570 nm, $\Delta D_B{}^{phot}$ 0.9, $k_{BA}{}^{db}$ 0.39 s^{-1}, $\tau_{1/2}$ 60 s, **Toluene**: $\lambda^A{}_{max}$ 317 nm, $\lambda^B{}_{max}$ 580sh, 620 nm, $\Delta D_B{}^{phot}$ 0.23, $k_{BA}{}^{db}$ 1.64 s^{-1}, $\tau_{1/2}$ 2 s	Precursor for functional 5′-R-**SP** series (by pathway C)	[90,100]

Table 1. *Cont.*

No	5′-R	R_6	R_8	Synthetic Method (Yield, %)	Spectral-Kinetic Parameters	Notes and Applications	References
SP99		$-NO_2$	-H	A (23%)	**EtOH**: λ^A_{max} 255, 270, 301, 340 nm, λ^B_{max} 535 nm, **Toluene**: λ^B_{max} 595 nm		[60]
SP100		$-NO_2$	$-OCH_3$	A (38%)	**EtOH**: λ^A_{max} 255, 281, 301, 357 nm, λ^B_{max} 565 nm, **Toluene**: λ^B_{max} 610 nm		[60]
SP101		$-NO_2$	-Br	A (33%)	**EtOH**: λ^B_{max} 535 nm, **Toluene**: λ^B_{max} 595 nm		[60]
SP102		$-NO_2$	$-NO_2$	A (53%)	**EtOH**: λ^B_{max} 522 nm		[60]
SP103	HOOC-	-H	-H	A (51%) A,C (40% SPS) A (77% in solution) A (39%)	$\mathbf{CH_2Cl_2}$: λ^A_{max} 299 nm, λ^A_{fl} 358 nm, $\mathbf{CH_3OH}$: λ^A_{max} 296 nm, λ^A_{fl} 367 nm, $\mathbf{CH_3CN}$: λ^A_{max} 298 nm, λ^A_{fl} 359 nm, **DMSO**: λ^A_{max} 298 nm, λ^A_{fl} 359 nm	Precursor for functional 5′-R-**SP** series. **SP103** Bovine serum albumin interaction in PBS investigation. Divergent synthesis of **SP** derivatives by solid-phase approach or in solution methods.	[186,223,224]

Table 1. *Cont.*

No	5′-R	R_6	R_8	Synthetic Method (Yield, %)	Spectral-Kinetic Parameters	Notes and Applications	References
SP104	HOOC-	$-NO_2$	-H	A (45–50%) A (70%) A (72%) A (60%) A (42%) A (63%) A (99%) A (69%) A,C (45% SPS) A (76% in solution)	**CH_2Cl_2**: λ^A_{max} 290, 311 nm, λ^B_{max} 604 nm, λ^A_{fl} 480 nm, **EtOH**: λ^B_{max} 522 nm	Precursor for functional 5′-R-6-NO_2-**SP** series. Divergent synthesis of **SP** derivatives by solid-phase approach or in solution methods. **SP104** does not show photochromism in the solid state even after a very long irradiation time.	[64,82,133,138,186,216,224,225]
SP105	HOOC-	$-NO_2$	-OH	A (58%)		Precursor for functional 5′-R-**SP** series.	
SP106	HOOC-	R_6 = $-NO_2$ R_8 = $-O_2C(C{=}CH_2)-CH_3$		B (33%)		Precursor for functional 5′-R-**SP** series.	[225]
SP107	HOOC-	$-NH_2$	-H	A,C (28% SPS) A (59% in solution)		Divergent synthesis of **SP** derivatives by solid-phase approach or in solution methods.	[224]
SP108	HOOC-	-CN	-H	A (53%)		Precursor for functional 5′-R-**SP** series.	[186]
SP109	HOOC-	-Br	-H	A (46%)		Precursor for functional 5′-R-**SP** series.	[186]

Table 1. *Cont.*

No	5′-R	R_6	R_8	Synthetic Method (Yield, %)	Spectral-Kinetic Parameters	Notes and Applications	References
SP110	HOOC-	-CF_3	-H	A (45%)		Precursor for functional 5′-R-**SP** series.	[186]
SP111	HOOC-	-CH_3	-H	A,C (40% SPS) A (71% in solution)		Divergent synthesis of **SP** derivatives by solid-phase approach or in solution methods.	[224]
SP112	HOOC-	-CH_3	-CHO	A (62%)	**CH_3CN**: λ^A_{max} 228, 243, 272, 299, 357 nm, λ^B_{max} 630 nm, $k_{BA}{}^{db}$ 0.185 s^{-1}		[226]
SP113	HOOC-	-OCH_3	-CHO	A (78%)	**CH_3CN**: λ^A_{max} 230, 246, 281, 299, 379 nm, λ^B_{max} 660 nm, $k_{BA}{}^{db}$ 0.667 s^{-1}		[226]
SP114	HOOC-	-CHO	-CH_3	A (36%)	**CH_3CN**: λ^A_{max} 255, 303, 333sh nm, λ^B_{max} 582 nm, $k_{BA}{}^{db}$ 0.047 s^{-1}		[227]
SP115	HOOC-	-CHO	-OCH_3	A (74%)	**CH_3CN**: λ^A_{max} 230, 273, 301, 338sh nm, λ^B_{max} 581 nm, $k_{BA}{}^{db}$ 0.051 s^{-1}		[227]
SP116	HOOC-	-CO_2CH_3	-CHO	A (32%)	**CH_3CN**: λ^A_{max} 235, 300, 343 nm, λ^B_{max} 579 nm, $k_{BA}{}^{db}$ 0.022 s^{-1}		[226]
SP117	CH_3OOC-	-NO_2	-H	B (60%) B (85%)	**CH_2Cl_2**: λ^A_{max} 290, 311 nm, λ^B_{max} 604 nm, λ^A_{fl} 480 nm, **CH_3CN**: λ^A_{max} 220, 280sh, 300, 345sh nm, λ^B_{max} 579 nm	**SP117** does not show photochromism in the solid state even after a very long irradiation time.	[133,216]
SP118	EtOOC-	-NO_2	-H			Component of solid polymer electrolyte.	[228]

Table 1. *Cont.*

No	5′-R	R_6	R_8	Synthetic Method (Yield, %)	Spectral-Kinetic Parameters	Notes and Applications	References
SP119	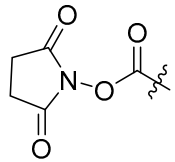	$-NO_2$	-H	B (85%)	**DMSO H_2O (5:1)**: λ^A_{max} 340 nm, λ^B_{max} 544 nm **EtOH**: λ^B_{max} 564 nm	DNA modification method via transamination with 1,6-diaminohexane and functional substituted **SP119**	[64,65]
SP120	$C_6H_5COC_6H_4OOC$-	$-NO_2$	-H	B (47%)	**CH_3CN**: λ^A_{max} 230, 250, 270, 300sh, 340sh nm, λ^B_{max} 570sh nm		[216]
SP121	$C_6H_5COC_6H_4O(CH_2)_4O$-	$-NO_2$	-H	B (25%)	**CH_3CN**: λ^A_{max} 260, 315 nm, λ^B_{max} 415sh nm		[216]
SP122	OHCCH=CH-	$-NO_2$	-H	B (60%)	**EtOH**: λ^A_{max} 364 nm, λ^B_{max} 567 nm, ΔD_B^{phot} 1.94, k_{BA}^{db} 0.02 s^{-1}, $\tau_{1/2}$ 218 s, **Toluene**: λ^A_{max} 357 nm, λ^B_{max} 590sh, 628 nm, ΔD_B^{phot} 4.45, k_{BA}^{db} 0.06 s^{-1}, $\tau_{1/2}$ 33 s		[45]
SP123	EtOOC-CH=CH-	$-NO_2$	-H	C (92%)	**EtOH**: λ^A_{max} 348 nm, λ^B_{max} 564 nm, ΔD_B^{phot} 0.54, k_{BA}^{db} 0.011 s^{-1}, $\tau_{1/2}$ 580 s, **Toluene**: λ^A_{max} 344 nm, λ^B_{max} 624, 587sh nm, ΔD_B^{phot} 0.86, k_{BA}^{db} 0.037 s^{-1}, $\tau_{1/2}$ 36 s		[82,84]
SP124	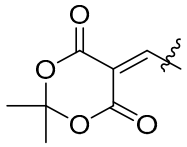	$-NO_2$	-H	B (45%)	**EtOH**: λ^A_{max} 430 nm, λ^B_{max} 575 nm, ΔD_B^{phot} 0.04, k_{BA}^{db} 0.015 s^{-1}, $\tau_{1/2}$ * s, **Toluene**: λ^A_{max} 391 nm, λ^B_{max} 637, 603sh nm, ΔD_B^{phot} 0.02, k_{BA}^{db} 0.385 s^{-1}, $\tau_{1/2}$ 50 s	functional substituted 5′-vinyl-6-NO_2- **SP** series	[79,83]

Table 1. *Cont.*

No	5′-R	R_6	R_8	Synthetic Method (Yield, %)	Spectral-Kinetic Parameters	Notes and Applications	References
5′-R-SP photochrome derivatives with nitrogen-containing fragments							
SP125	O_2N-	-H	-H	A (30%) A (63%)	**CH_3OH**: λ^A_{max} 372 nm, **EtOH**: λ^A_{max} 230, 260, 320sh, 385 nm, λ^B_{max} 230, 260, 320sh, 385 nm, **EtOH:H_2O (1:1)**: λ^A_{max} 310, 390 nm	Tests on antitumor activity and antiviral activity assays. Photoswitch to gadolinium chelates.	[196,198,217]
SP126	O_2N-	-H	-NO_2	A (72%)	λ^A_{max} 350 nm, λ^B_{max} 350 nm		[229]
SP127	O_2N-	-NO_2	-H	A (67%) A (82%) A (33%) A (75%) A (77%) A (36%) B (43%, HNO_3/Ac_2O) B (87%, $NaNO_2$/AcOH) B (60%, HNO_3/H_2SO_4)	**Toluene**: λ^B_{max} 630 nm, λ^A_{max} 350 nm, λ^B_{max} 350, 540 nm, **EtOH**: λ^A_{max} 360 nm, λ^B_{max} 360 nm, **EtOH:H_2O (1:1)**: λ^A_{max} 380 nm	Tests on antitumor activity and antiviral activity assays. Photoswitch to gadolinium chelates.	[77,196,198,206,217, 229–231]
SP128	O_2N-	-NO_2	-OCH_3	A (70%)	**CH_2Cl_2**: λ^A_{max} 362 nm, λ^B_{max} 610 nm, λ^B_{max} (**SP**+CF_3CO_2H) 420 nm	**SP128** is resistant to the TFA acid-induced spiroform C-O bond cleavage.	[231]

Table 1. *Cont.*

No	5′-R	R_6	R_8	Synthetic Method (Yield, %)	Spectral-Kinetic Parameters	Notes and Applications	References
SP129	O_2N-	-NO_2	-CH_2Cl	A (49%)		Precursor for functional ion-binding receptors.	[157]
SP130	O_2N-	-NO_2	-CH_2I	B (96%)		Precursor for functional ion-binding receptors.	[157]
SP131	O_2N-	-NO_2	-CHO	A (55%)	λ^A_{max} 360 nm, λ^B_{max} 370, 540 nm		[229]
SP132	O_2N-	-NO_2	-$COOCH_3$	A (43%)			[201]
SP133	O_2N-	-CHO	-NO_2	A (53%)	λ^A_{max} 350 nm, λ^B_{max} 320, 370, 540 nm		[229]
SP134	O_2N-	-OCH_3	-H	A (56%)	**EtOH**: λ^A_{max} 230, 260, 390 nm, λ^B_{max} 230, 260, 390 nm, **EtOH:H_2O (1:1)**: λ^A_{max} 400 nm	Photoswitch to gadolinium chelates.	[196]
SP135	O_2N-	-OCH_3	-CH_2OH	A (57%)		Precursor for preparation of (**SP**)-based magnetic resonance imaging (MRI) contrast agents	[156]
SP136	O_2N-	-OCH_3	-CH_2I	C (77%)		Precursor for preparation of (**SP**)-based magnetic resonance imaging (MRI) contrast agents	[156]
SP137	O_2N-	R_6 = -CH_2OCOCH_2Cl		A (60%)			[102]
SP138	O_2N-	R_6 = -$CH_2OCOCH_2CO_2Et$		A (65%)			[102]
SP139	H_2N-	-NO_2	-H	A (43%)		Precursor for functional 5′-R-6-NO_2-of LC **SP** series	[78]
SP140	HON=CH-	-NO_2	-H	B (77%)		Mix of *syn*- and *anti*-isomers	[85,94]
SP141	NC-	-NO_2	-H	B (22%)			[77]

Table 1. *Cont.*

No	5′-R	R_6	R_8	Synthetic Method (Yield, %)	Spectral-Kinetic Parameters	Notes and Applications	References
SP142	NC-	-CN	-H	A (43%)		**SP142** is resistant to the UV-irradiation or TFA acid-induce spiroform C-O bond cleavage.	[231]
SP143	4-O_2N-C_6H_4-N=N-	-NO_2	-H	B (89%)			[77]
SP144	$ClCH_2CONH$-	-NO_2	-H	A (47%)	**EtOH**: λ^B_{max} 546 nm		[64]
SP145	NH_2N=CH-	-NO_2	-H	B (89%)			[102]
SP146	C_6H_5-CONH-	-I	-H	A (65%)		Precursor for functional bis-**SPs**	[108,124,126]
SP147	HOOC-$(CH_2)_3$-CONH-	-NO_2	-H	C		Precursor for **SP**-self-assembled monolayers (SAMs).	[232]
SP148	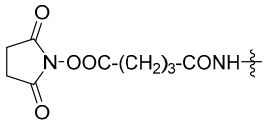	-NO_2	-H	C	**Toluene**: λ^B_{max} 611 nm	**SP**-self-assembled monolayers (SAMs).	[232]
SP149	$C_{21}H_{43}CONHCH_2$-	-NO_2	-H	A		**SP149** Langmuir–Blodgett (LB) films	[233,234]
SP150	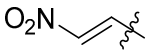	-NO_2	-H	B (65%)	**EtOH**: λ^A_{max} 404 nm, λ^B_{max} 568 nm, ΔD_B^{phot} 0.35, k_{BA}^{db} 0.043 s^{-1}, $\tau_{1/2}$ 200 s, **Toluene**: λ^A_{max} 390 nm, λ^B_{max} 628, 590sh nm, ΔD_B^{phot} 0.13, k_{BA}^{db} 0.152 s^{-1}, $\tau_{1/2}$ 18 s	Functional substituted 5′-vinyl-6-NO_2-**SP** series	[79,83]

Table 1. *Cont.*

No	5′-R	R_6	R_8	Synthetic Method (Yield, %)	Spectral-Kinetic Parameters	Notes and Applications	References
SP151	NCCH=CH-	$-NO_2$	-H	B (90%)	**EtOH**: λ^A_{max} 346 nm, λ^B_{max} 567 nm, $k_{BA}{}^{db}$ 0.003 s^{-1}, $\tau_{1/2}$ 127 s, **Toluene**: λ^A_{max} 347 nm, λ^B_{max} 628, 590sh nm, $k_{BA}{}^{db}$ 0.07 s^{-1}, $\tau_{1/2}$ 40 s		[45]
SP152	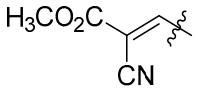	$-NO_2$	-H	B (65%)	**EtOH**: λ^A_{max} 398 nm, λ^B_{max} 576 nm, $\Delta D_B{}^{phot}$ 0.1, $k_{BA}{}^{db}$ 0.143 s^{-1}, $\tau_{1/2}$ 120 s, **Toluene**: λ^A_{max} 391 nm, λ^B_{max} 637, 603sh nm, $\Delta D_B{}^{phot}$ 0.05, $k_{BA}{}^{db}$ 0.348 s^{-1}, $\tau_{1/2}$ 30 s	Functional substituted 5′-vinyl-6-NO_2-**SP** series	[79,83]
SP153	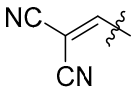	$-NO_2$	-H	B (80%)	**EtOH**: λ^A_{max} 430 nm, λ^B_{max} 575 nm, $\Delta D_B{}^{phot}$ 0.06, $k_{BA}{}^{db}$ 0.194 s^{-1}, $\tau_{1/2}$ * s, **Toluene**: λ^A_{max} 391 nm, λ^B_{max} 637, 603sh nm, $\Delta D_B{}^{phot}$ 0.01, $k_{BA}{}^{db}$ 0.83 s^{-1}, $\tau_{1/2}$ 45 s	Functional substituted 5′-vinyl-6-NO_2-**SP** series	[79,83]
SP154	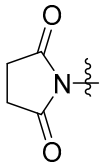	different combinations of R_6 = -H, -Br, -F, -Cl, $-NO_2$, -I, $-OCH_3$, $-CH_3$, -OH, $-C(CH_3)_3$, $-OC_2H_5$ and R_8 = -H, -Br, -Cl, -I, $-OCH_3$, -CHO, $-CH_3$, -OH, $-C(CH_3)_3$		C,A (89–100%, SPS)		Solid-phase synthesis **SP** library with bound solid-supported indoline on the high-loading Wang resin.	[70]

Table 1. *Cont.*

No	5′-R	R_6	R_8	Synthetic Method (Yield, %)	Spectral-Kinetic Parameters	Notes and Applications	References
SP155	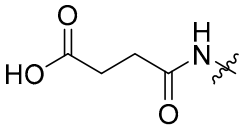	-I	-I	B (74%, SPS)		Solid-phase synthesis **SP** library with bound solid-supported indoline on the high-loading Wang resin.	[70]
SP156	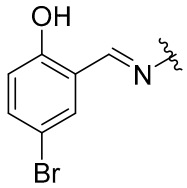	-Br	-H	A (82%)	**Toluene**: λ^{A}_{max} 390 nm, λ_{fl} 540 nm	**SP156** does not exhibit the photochromic properties.	[235,236]
SP157	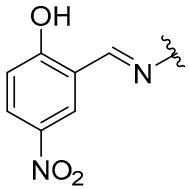	$-NO_2$	-H	A (80%)	**EtOH**: λ^{B}_{max} 550 nm, **Toluene**: λ^{A}_{max} 375, 385 nm, λ^{B}_{max} 580, 630 nm, λ_{fl} 530 nm		[235–237]
SP158	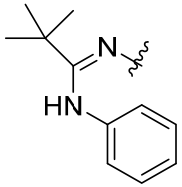	$-NO_2$	-H	A (91%)	**CH_3OH**: λ^{A}_{max} 254, 268, 316 nm, λ^{B}_{max} 267, 315, 537 nm		[238]
SP159	HO_3S-	$-NO_2$	-H	B	**CH_3OH**: λ^{A}_{max} 260, 296, 334 nm, λ^{B}_{max} 416 nm, λ_{fl} 529 nm		[62]

Table 1. *Cont.*

No	5′-R	R_6	R_8	Synthetic Method (Yield, %)	Spectral-Kinetic Parameters	Notes and Applications	References
SP160	KO_3S-	-NO_2	-H	A (37%)	**CH_3OH**: λ^B_{fl} 620 nm, **CH_3OH**: KO_3S-**SP** λ^A_{max} 261, 295, 333 nm, λ^B_{max} 537 nm, $k_{BA}{}^{db}$ 8.1 10^{-4} s^{-1}, λ_{fl} 623 nm	Precursor for organic–inorganic hybrid photomagnet by intercalation of sulfonate-substituted **SP160** anions into layered cobalt hydroxides (CoLH)	[62,63]
SP161	S=C=N-	-NO_2	-H	A (44%)	**DMSO H_2O (5:1)**: λ^A_{max} 305 nm, λ^B_{max} 542 nm, **EtOH**: λ^B_{max} 562 nm	DNA modification method via transamination with 1,6-diaminohexane and functional-substituted **SP161**	[64,65]
SP162	CF_3SO_2O-	-NO_2	-Br	B (43%)	**CH_3CN**: λ^A_{max} 331 nm, λ^B_{max} 561 nm		[61]
SP163	CF_3SO_2O-	-NO_2	-I	B (43%)	**CH_3CN**: λ^A_{max} 335 nm, λ^B_{max} 557 nm		[61]
SP164	CF_3SO_2O-	-NO_2	-OSO_2CF_3	B (89%)	**CH_3CN**: λ^A_{max} 304 nm, λ^B_{max} 537 nm		[61]
SP165	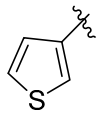	-NO_2	-H	C,A (21%)	**CH_3OH**: λ^B_{max} 280, 360sh, 540 nm, **Toluene**: λ^B_{max} 390, 580sh, 616 nm	Suzuki coupling with thiophene-3-boronic acid and Stille coupling reactions were used for the **SP**-T conjugates preparation.	[107]
SP166	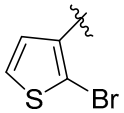	-NO_2	-H	B (99%)	**CH_3OH**: λ^B_{max} 280, 310, 360, 540 nm, **Toluene**: λ^B_{max} 390, 580sh, 616 nm	Suzuki coupling with thiophene-3-boronic acid and Stille coupling reactions were used for the **SP**-T conjugates preparation.	[107]

Table 1. *Cont.*

No	5′-R	R_6	R_8	Synthetic Method (Yield, %)	Spectral-Kinetic Parameters	Notes and Applications	References
SP167	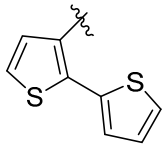	$-NO_2$	-H	B (97%)	**CH_3OH**: λ^B_{max} 280, 310, 360, 540 nm, **Toluene**: λ^B_{max} 390, 580sh, 616 nm	Suzuki coupling with thiophene-3-boronic acid and Stille coupling reactions were used for the **SP**-T conjugates preparation.	[107]
SP168	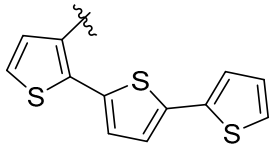	$-NO_2$	-H	B (58%)	**CH_3OH**: λ^B_{max} 280, 310, 360, 540 nm, **Toluene**: λ^B_{max} 390, 580sh, 616 nm	Suzuki coupling with thiophene-3-boronic acid and Stille coupling reactions were used for the **SP**-T conjugates preparation.	[107]

Note: λ^A_{max} and λ^B_{max} are maxima of the absorption bands of the initial and photoinduced forms, respectively; $\Delta D_B{}^{phot}$ is the maximal photoinduced change in absorbance at the absorption band maximum of the photoinduced form in the photoequilibrium state with the same value of absorbance (D 0.8) at the absorption band maximum of the initial form; is the constant of the dark bleaching reaction rate; $\tau_{1/2}$ is the time for which the maximal value of the photoinduced form optical density at the absorption band maximum reduces by half upon continuous irradiation by a nonfiltered light of Hamamatsu LC8 lamp. * was not observed upon illumination for more than 10 min. **SP** synthetic methods: (**A**) "Complete" synthesis of target derivatives by the condensation of two or more key intermediates: X + Y = **SP**. (**B**) One-step direct modification of a precursor with gived structure: **SP**-precursor → **SP**. (**C**) Production a target molecule in several stages by the progressive elaboration of the anchor group by introduction of the necessary fragments with a given set of functional groups: **SP**-precursor$_1$ → **SP**-precursor$_2$ → **SP**-precursor$_n$ → **SP**. (**D**) Modification of the final targets by the photoactive ligands with reactive terminal functions by the doping or the immobilization methods.

Table 2. Polysubstituted 5′-R-6-X-8-Y-**SP**; and others **(SP169–SP197)**.

No	Structure of Photochrome Derivatives	Synthetic Method (Yield, %)	Spectral-Kinetic Parameters	Notes and Applications	References
SP169	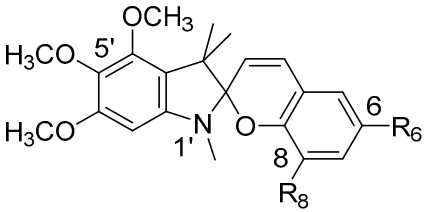 Where (a) R_6 = -NO_2, R_8=-H, (b) R_6 = -H, R_8=-H, (c) R_6 = -H, R_8=-OCH_3, (d) R_6 = -H, R_8=-OC_2H_5,	A (65–78%)	**5% DMSO/PBS buffer**: λ^A_{max} 272–296, 323–351 nm, λ^B_{max} 480–520 nm	**SP**s were tested in vitro tubulin polymerization assay.	[239]
SP170	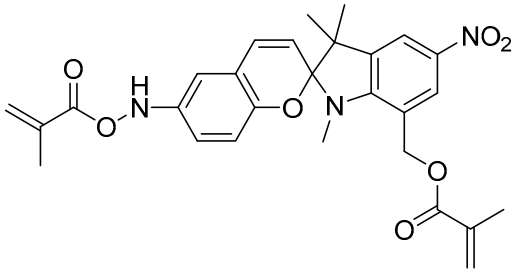	A (18%)	**CH_3OH**: λ^B_{max} 548 nm, $k_{BA}{}^{db}$ 1.58 10^{-3} s^{-1} **Benzene**: λ^B_{max} 616 nm, $k_{BA}{}^{db}$ 2.47 10^{-2} s^{-1}	**SP170**- monomer with two polymerizable groups.	[240]
SP171	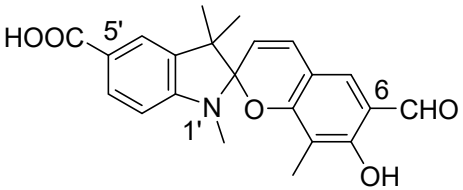	A (62%)	**CH_3CN**: λ^A_{max} 234, 253, 259, 300, 345 nm, λ^B_{max} 560 nm		[241]

Table 2. *Cont.*

No	Structure of Photochrome Derivatives	Synthetic Method (Yield, %)	Spectral-Kinetic Parameters	Notes and Applications	References
SP172	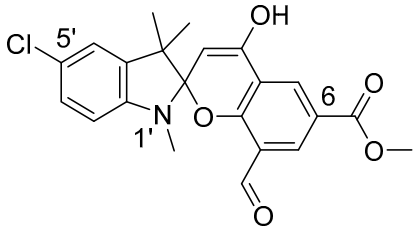	A (29%)	**CH_3CN**: λ^A_{max} 253, 299sh, 341sh nm, λ^B_{max} 402, 536 nm, λ^B_{fl} 611 nm	Regioselectivity of condensation process.	[242]
SP173	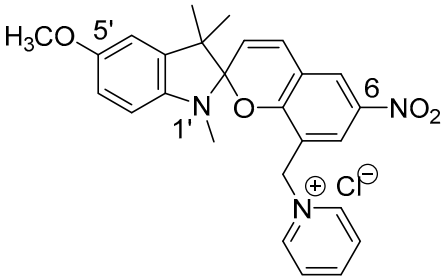	A (55%)	**CH_3CN**: λ^A_{max} 259, 317, 345sh nm, λ^B_{max} 540 nm, k_{BA}^{db} 0.8 10^{-5} s^{-1}, λ^B_{fl} 618 nm	**SP173** cationic **SP**s	[143]
SP174	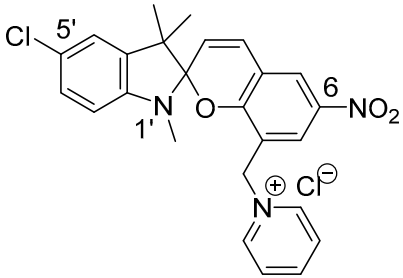	A (57%)	**CH_3CN**: λ^A_{max} 257, 311, 340sh nm, λ^B_{max} 544 nm, k_{BA}^{db} 8.9 10^{-5} s^{-1}, λ^B_{fl} 625 nm	A molecular magnetic **SP174** $CrMn(C_2O_4)_3 \bullet H_2O$ whose spiropyran cation contains a quaternized pyridine fragment in the side aliphatic chain was synthesized for the first time.	[143,144]

Table 2. *Cont.*

No	Structure of Photochrome Derivatives	Synthetic Method (Yield, %)	Spectral-Kinetic Parameters	Notes and Applications	References
SP175	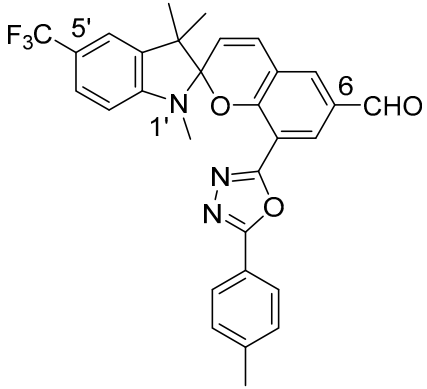	A (52%)	**Acetone**: λ^{A}_{max} 334, 351 nm, λ^{B}_{max} 583 nm, $k_{BA}{}^{db}$ 3.97 10^{-2} s^{-1}	Light-controllable cation binding	[145,146]
SP176	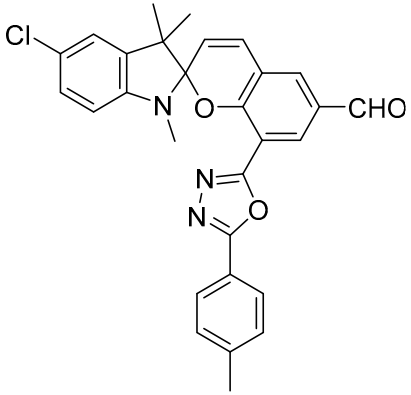	A (42%)	**Acetone**: λ^{A}_{max} 334, 352 nm, λ^{B}_{max} 580 nm, $k_{BA}{}^{db}$ 0.99 10^{-2} s^{-1}	Light-controllable cation binding	[145,146]

Table 2. *Cont.*

No	Structure of Photochrome Derivatives	Synthetic Method (Yield, %)	Spectral-Kinetic Parameters	Notes and Applications	References
SP177	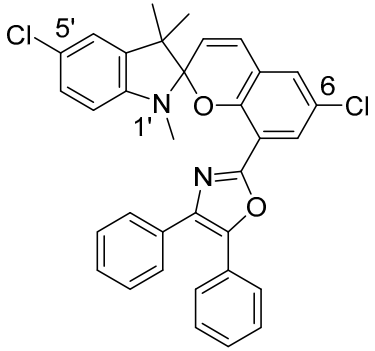	A (52%)	**Toluene**: λ^{A}_{max} 309, 358 nm, λ^{B}_{max} 470, 650 nm		[147]
SP178	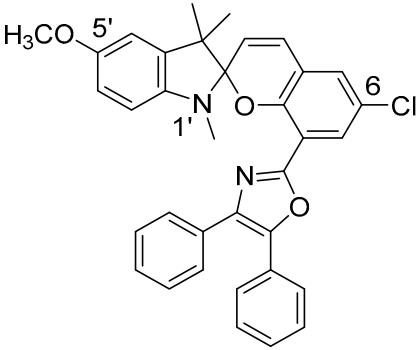	A (46%)	**Toluene**: λ^{A}_{max} 309, 358 nm, λ^{B}_{max} 470, 650 nm		[147]

Table 2. *Cont.*

No	Structure of Photochrome Derivatives	Synthetic Method (Yield, %)	Spectral-Kinetic Parameters	Notes and Applications	References
SP179	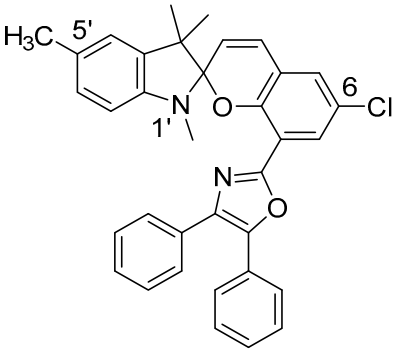	A (42%)	**Toluene**: λ^{A}_{max} 312, 358 nm, λ^{B}_{max} 440, 655 nm		[147]
SP180	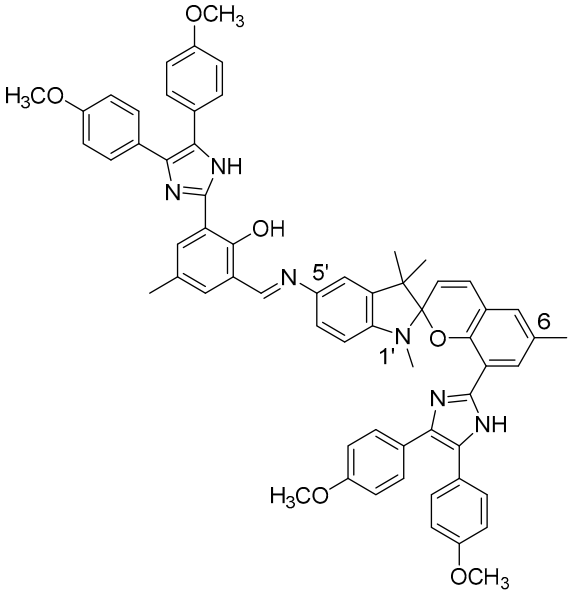	A (48%)	**EtOH**: λ_{fl} 450 nm or 520 nm, **Toluene**: λ_{fl} 500 nm	**SP180**-triarylimidazole hybrid compound.	[243]

Table 2. *Cont.*

No	Structure of Photochrome Derivatives	Synthetic Method (Yield, %)	Spectral-Kinetic Parameters	Notes and Applications	References
SP181	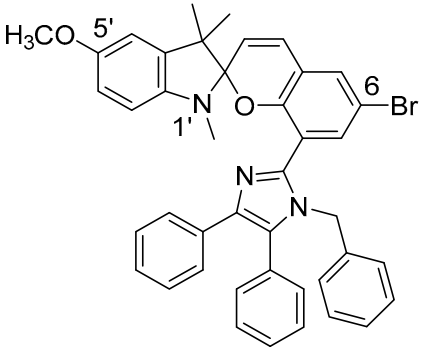	A (47%)	**Toluene**: λ^{A}_{max} 293sh, 344sh nm, λ^{B}_{max} 634 nm, $k_{BA}{}^{db}$ 0.37 s^{-1}		[148]
SP182	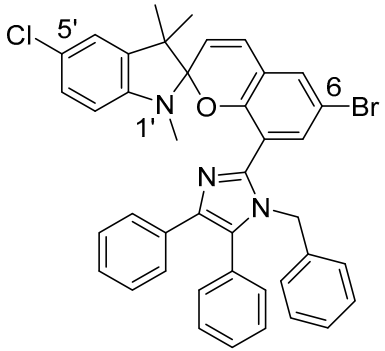	A (43%)	**Toluene**: λ^{A}_{max} 289sh, 339sh nm, λ^{B}_{max} 628 nm, $k_{BA}{}^{db}$ 0.33 s^{-1}		[148]

Table 2. *Cont.*

No	Structure of Photochrome Derivatives	Synthetic Method (Yield, %)	Spectral-Kinetic Parameters	Notes and Applications	References
SP183	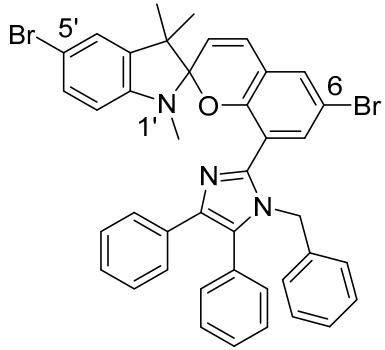	A (50%)	**Toluene**: λ^{A}_{max} 296sh, 338sh nm, λ^{B}_{max} 627 nm, $k_{BA}{}^{db}$ 0.36 s^{-1}		[148]
SP184	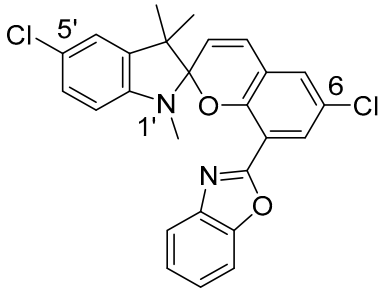	A (59%)	**Acetone**: λ^{A}_{max} 351, 367sh nm, λ^{B}_{max} 640 nm, $k_{BA}{}^{db}$ 0.02 s^{-1}, λ^{A}_{max} (Zn^{2+}) 380, 523 nm, **Toluene**: λ^{A}_{max} 298, 312, 353, 370sh nm, λ^{B}_{max} 642 nm, $k_{BA}{}^{db}$ 0.27 s^{-1}	Quantitative comparative study of the complexation of a series of **SP**, the merocyanine form of which contains bidentate chelate site.	[149–151]
SP185	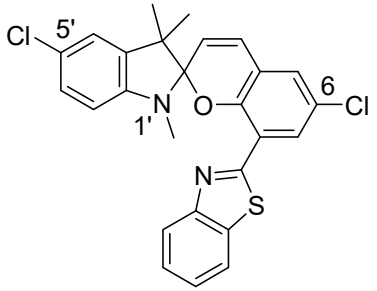	A (57%)	**Acetone**: λ^{A}_{max} 355, 370 nm, λ^{B}_{max} 648 nm, λ^{A}_{max} (Zn^{2+}) 380, 525 nm, λ^{A}_{fl} (Zn^{2+}) 640 nm		[151]

Table 2. *Cont.*

No	Structure of Photochrome Derivatives	Synthetic Method (Yield, %)	Spectral-Kinetic Parameters	Notes and Applications	References
SP186	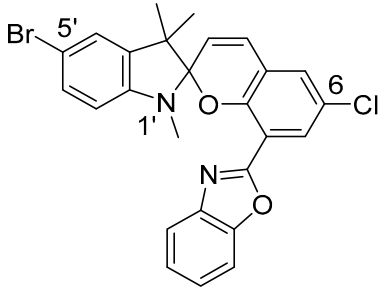	A (53%)	**Acetone**: λ^{A}_{max} 352, 367sh nm, λ^{B}_{max} 640 nm, $k_{BA}{}^{db}$ 0.02 s^{-1}, **Toluene**: λ^{A}_{max} 298, 312, 353, 370sh nm, λ^{B}_{max} 644 nm, $k_{BA}{}^{db}$ 0.29 s^{-1}	Quantitative comparative study of the complexation of a series of **SP**, the merocyanine form of which contains bidentate chelate site.	[149,150]
SP187	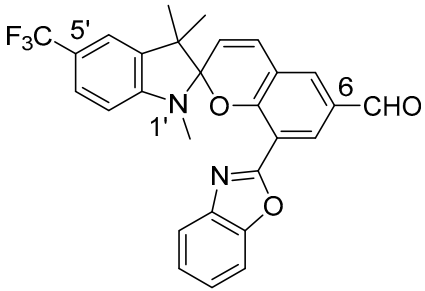	A (46%)	**Toluene**: λ^{A}_{max} 291, 341, 358 nm, λ^{B}_{max} 628 nm, $k_{BA}{}^{db}$ 10.1 10^{-2} s^{-1}, **Acetone**: λ^{A}_{max} 339, 355 nm, λ^{B}_{max} 593 nm, $k_{BA}{}^{db}$ 3.7 10^{-2} s^{-1}		[152,244]
SP188	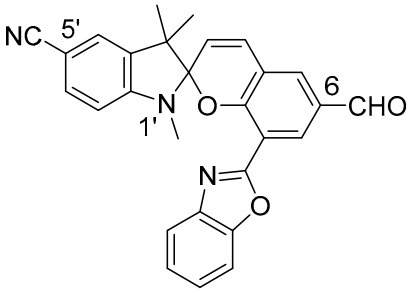	A (41%)	**Toluene**: λ^{A}_{max} 289, 339, 357 nm, λ^{B}_{max} 634 nm, $k_{BA}{}^{db}$ 21.3 10^{-2} s^{-1}, **Acetone**: λ^{A}_{max} 339, 355 nm, λ^{B}_{max} 600 nm, $k_{BA}{}^{db}$ 3.9 10^{-2} s^{-1}		[152,244]

Table 2. *Cont.*

No	Structure of Photochrome Derivatives	Synthetic Method (Yield, %)	Spectral-Kinetic Parameters	Notes and Applications	References
SP189	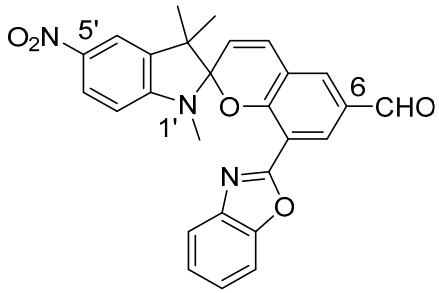	A (39%)	**Toluene**: λ^{A}_{max} 296, 344, 357 nm, λ^{B}_{max} 640 nm, $k_{BA}{}^{db}$ 58.8 10^{-2} s^{-1}, **Acetone**: λ^{A}_{max} 341, 357, 371 nm, λ^{B}_{max} 610 nm, $k_{BA}{}^{db}$ 4.8 10^{-2} s^{-1}		[152,244]
SP190	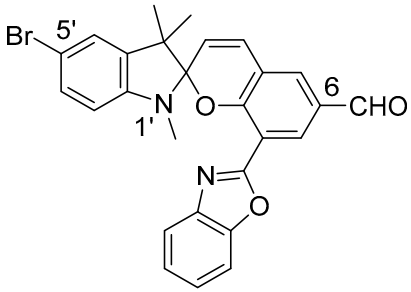	A	**Toluene**: λ^{A}_{max} 297, 342, 358 nm, λ^{B}_{max} 631 nm, $k_{BA}{}^{db}$ 4.4 10^{-2} s^{-1}, **Acetone**: λ^{A}_{max} 341, 357 nm, λ^{B}_{max} 588 nm, $k_{BA}{}^{db}$ 1.8 10^{-2} s^{-1}		[244]
SP191	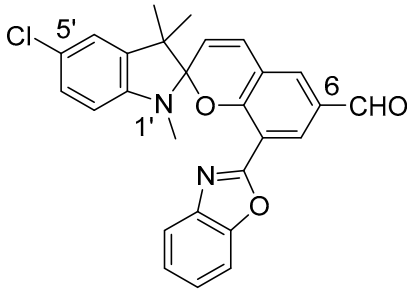	A	**Toluene**: λ^{A}_{max} 297, 342, 359 nm, λ^{B}_{max} 632 nm, $k_{BA}{}^{db}$ 6.3 10^{-2} s^{-1}, **Acetone**: λ^{A}_{max} 341, 357 nm, λ^{B}_{max} 586 nm, $k_{BA}{}^{db}$ 1.6 10^{-2} s^{-1}		[244]

Table 2. *Cont.*

No	Structure of Photochrome Derivatives	Synthetic Method (Yield, %)	Spectral-Kinetic Parameters	Notes and Applications	References
SP192	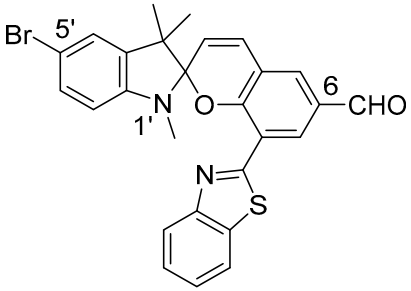	A (45%)	**Toluene**: λ^{A}_{max} 294, 321, 345, 363 nm, λ^{B}_{max} 448, 648 nm, **Acetone**: λ^{A}_{max} 345, 362 nm, λ^{B}_{max} 403, 595 nm	Benzothiazole-substituted **SP**s demonstrate ion driving photochromic transformations.	[37]
SP193	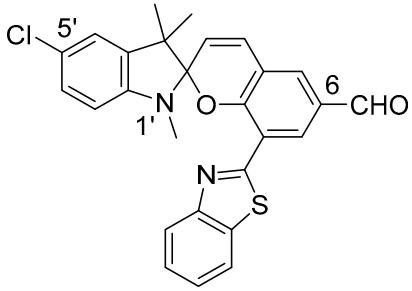	A (46%)	**Toluene**: λ^{A}_{max} 299, 321, 345, 363 nm, λ^{B}_{max} 447, 647 nm, **Acetone**: λ^{A}_{max} 345, 362 nm, λ^{B}_{max} 404, 595 nm	Benzothiazole-substituted **SP**s demonstrate ion driving photochromic transformations.	[37]
SP194	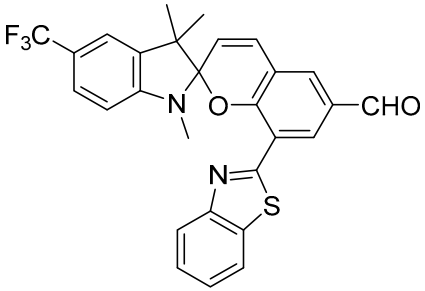	A (48%)	**Toluene**: λ^{A}_{max} 298, 320, 344, 362 nm, λ^{B}_{max} 449, 644 nm, **Acetone**: λ^{A}_{max} 344, 361 nm, λ^{B}_{max} 407, 600 nm	Benzothiazole-substituted **SP**s demonstrate ion driving photochromic transformations.	[37]

Table 2. *Cont.*

No	Structure of Photochrome Derivatives	Synthetic Method (Yield, %)	Spectral-Kinetic Parameters	Notes and Applications	References
SP195	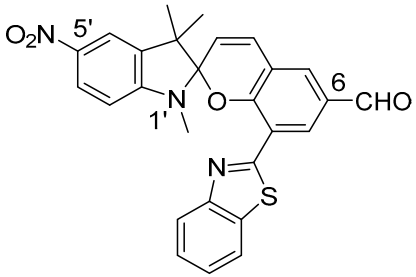	A (39%)	**Toluene**: λ^{A}_{max} 297, 305, 322, 344, 361, 373sh nm, λ^{B}_{max} 466, 655 nm, **Acetone**: λ^{A}_{max} 344, 360, 381sh nm, λ^{B}_{max} 415, 617 nm	Benzothiazole-substituted **SP**s demonstrate ion driving photochromic transformations.	[37]
SP196	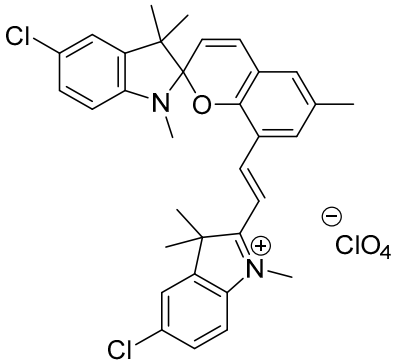	A (29%)	**CH_3CN**: λ^{A}_{max} 255, 306, 397, 459sh nm λ^{B}_{max} 255, 306, 397, 459sh nm		[52,245,246]
SP197	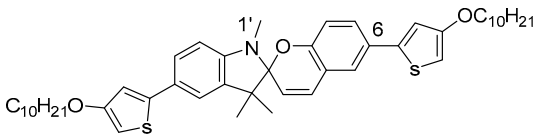	B (47%)	**CH_3OH: CH_2Cl_2 (1:1)**: λ^{A}_{max} 215, 315 nm, λ^{B}_{max} 215, 315, 490 nm, λ^{B}_{max} (**SP**+Co^{2+}) 215, 315, 490 nm	**SP197** precursor with two alkoxy-substituted thienyl units—monomer suitable for electropolymerization. **SP197** precursor monomer was prepared from the 5′,6-dibromo-**SP52** with thiopheneboronic acid via a double Suzuki coupling reaction.	[110]

Note: see remarks after Table 1.

Table 3. Dimers; bis- and poly-**SP**-substituted photochrome derivatives **(SP198–SP230)**.

No	Structure of Photochrome Derivatives	Synthetic Method (Yield, %)	Spectral-Kinetic Parameters	Notes and Applications	References
SP198	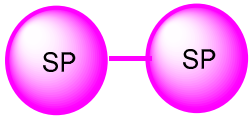	A (75%)	**EtOAc**: λ^{B}_{max} 600 nm		[106]
SP199	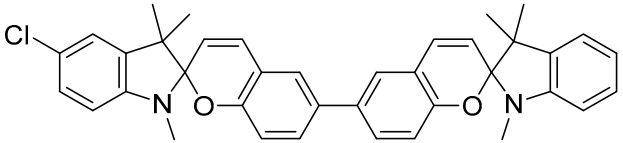	A (87%)			[122,123]
SP200	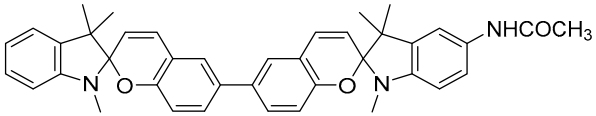	A (82%)			[122]
SP201	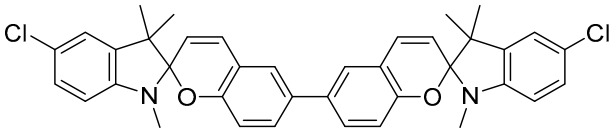	A (75%) A (25%) B (77%)	**CH_3CN (−30 °C)**: λ^{A}_{max} 270, 294 nm, λ^{B}_{max} 306, 395, 408sh, 619, 660sh nm, λ^{A}_{max} (**SP**+CF_3CO_2H) 294, 341, 385 nm		[122–124]
SP202	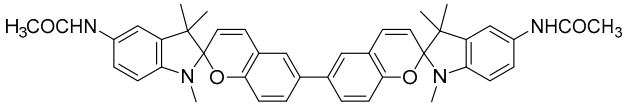	A (63%)			[122]
SP203	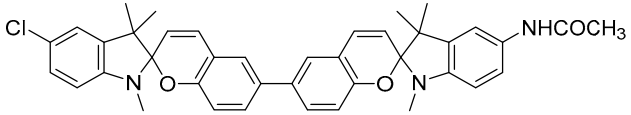	A (79%)			[122]

Table 3. *Cont.*

No	Structure of Photochrome Derivatives	Synthetic Method (Yield, %)	Spectral-Kinetic Parameters	Notes and Applications	References
SP204	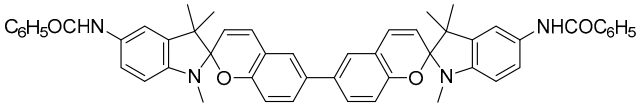	B (83%)			[124]
SP205	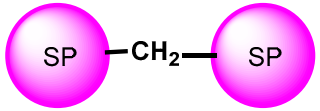	A			[125]
SP206	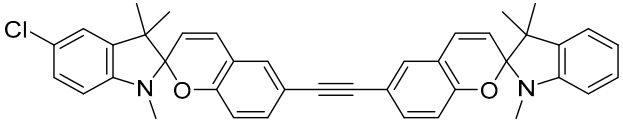	A,B (91%)	λ^{A}_{max} 305 nm	Symmetric and non-symmetric bis-sp via palladium-catalyzed reaction	[126]
SP207	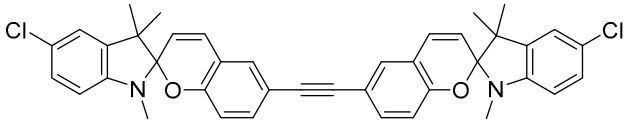	A (73%)	λ^{A}_{max} 305 nm	Symmetric and non-symmetric bis-sp via palladium-catalyzed reaction	[126]
SP208	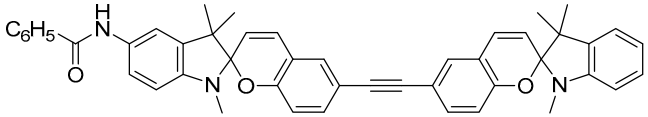	A,B (97%)	λ^{A}_{max} 310 nm	Symmetric and non-symmetric bis-sp via palladium-catalyzed reaction	[126]
SP209	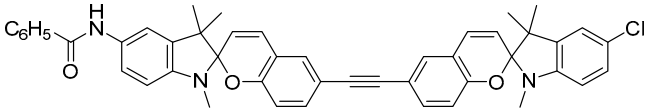	A,B (96%)	λ^{A}_{max} 308 nm	Symmetric and non-symmetric bis-sp via palladium-catalyzed reaction	[126]

Table 3. *Cont.*

No	Structure of Photochrome Derivatives	Synthetic Method (Yield, %)	Spectral-Kinetic Parameters	Notes and Applications	References
SP210	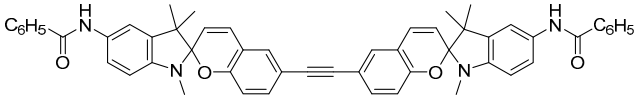	A (22%)	λ^{A}_{max} 310 nm	Symmetric and non-symmetric bis-sp via palladium-catalyzed reaction	[126]
SP211	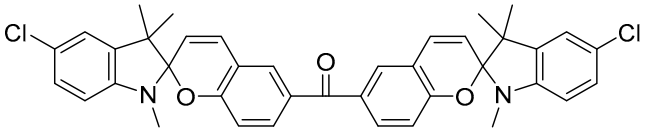	A (82%)			[127]
SP212	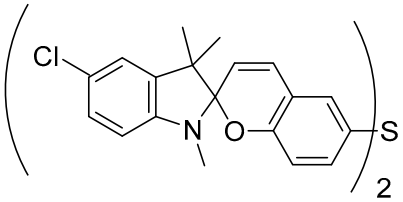	A (91%)	**EtOH**: λ^{B}_{max} 563 nm, **Toluene**: λ^{B}_{max} 625 nm		[128]
SP213	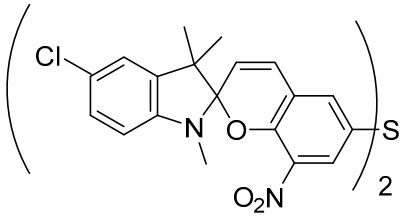	A (91%)	**EtOH**: λ^{B}_{max} 583 nm		[127]
SP214	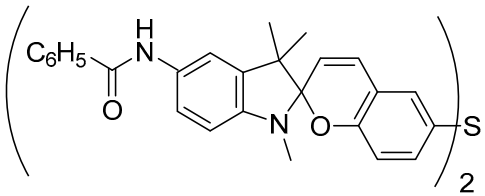	A (76%)	**EtOH**: λ^{B}_{max} 575 nm, **Toluene**: λ^{B}_{max} 598 nm		[128]

Table 3. *Cont.*

No	Structure of Photochrome Derivatives		Synthetic Method (Yield, %)	Spectral-Kinetic Parameters	Notes and Applications	References
SP215	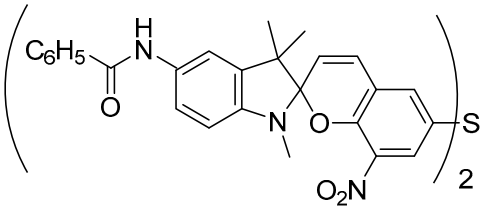		A (76%)	**EtOH**: λ^{B}_{max} 587 nm		[127]
SP216	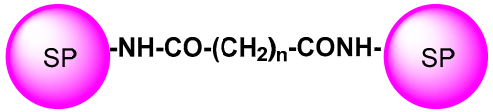	(a) $n = 3$	A (70%)	**EtOH**: λ^{B}_{max} 547 nm, **CH_2Cl_2**: λ^{B}_{max} 589 nm, **Acetone**: λ^{B}_{max} 578 nm		[129,130]
		(b) $n = 5$	A (88%)	**EtOH**: λ^{B}_{max} 547 nm, **CH_2Cl_2**: λ^{B}_{max} 586 nm, **Acetone**: λ^{B}_{max} 579 nm		
		(c) $n = 7$	A (71%)	**EtOH**: λ^{B}_{max} 548 nm, **CH_2Cl_2**: λ^{B}_{max} 588 nm, **Acetone**: λ^{B}_{max} 579 nm		
SP217	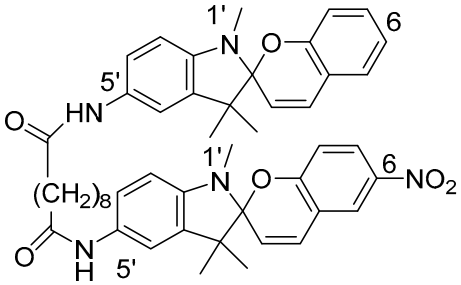		A (71%)	**Toluene**: λ^{B}_{max} 657 nm, **Acetone**: λ^{B}_{max} 623 nm, **CH_3CN**: λ^{B}_{max} 600 nm		[131]

Table 3. *Cont.*

No	Structure of Photochrome Derivatives	Synthetic Method (Yield, %)	Spectral-Kinetic Parameters	Notes and Applications	References
SP218	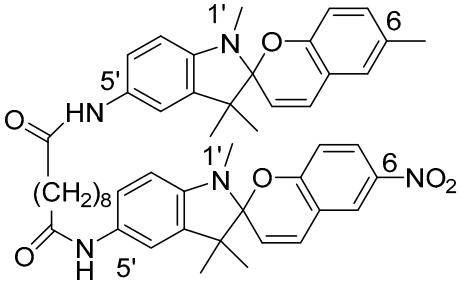	A (82%)	**Toluene**: λ^{B}_{max} 606 nm, **Acetone**: λ^{B}_{max} 576 nm, **CH_3CN**: λ^{B}_{max} 569 nm		[131]
SP219	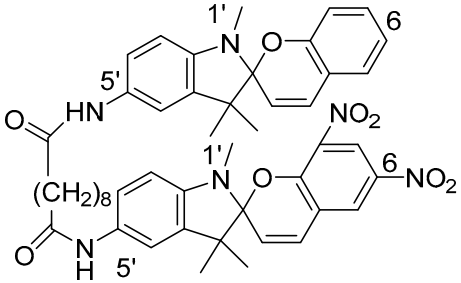	A (61%)	**Toluene**: λ^{B}_{max} 555 nm, **Acetone**: λ^{B}_{max} 540 nm, **CH_3CN**: λ^{B}_{max} 529 nm		[131]
SP220	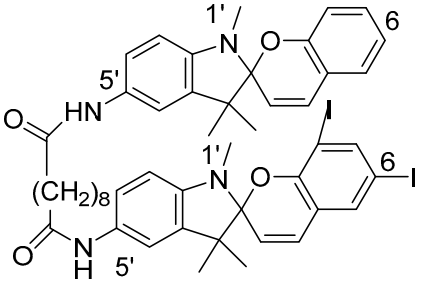	A (64%)	**Toluene**: λ^{B}_{max} 607 nm, **Acetone**: λ^{B}_{max} 577 nm, **CH_3CN**: λ^{B}_{max} 569 nm		[131]

Table 3. *Cont.*

No	Structure of Photochrome Derivatives		Synthetic Method (Yield, %)	Spectral-Kinetic Parameters	Notes and Applications	References
SP221	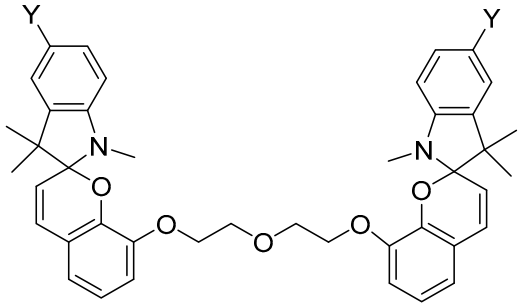	(a) Y = -OCH_3	A (43%)	**CH_3CN**: λ_{max} (SP+Me$(ClO_4)_2$ 520–550 nm	Bis-5′R-**SP** podands	[153]
		(b) Y = -Cl	A (31%)	**CH_3CN**: λ_{max} (SP+Me$(ClO_4)_2$) 530–557 nm		
		(c) Y = -Br	A (46%)	**CH_3CN**: λ_{max} (SP+Me$(ClO_4)_2$) 533–558 nm		
		(d) Y = -$CH(CH_3)_2$	A (84%)	**CH_3CN**: λ_{max} (SP+Me$(ClO_4)_2$) 519–552 nm		
		(e) Y = -$C(CH_3)_3$	A (67%)	**CH_3CN**: λ_{max} (SP+Me$(ClO_4)_2$) 519–546 nm		
SP222	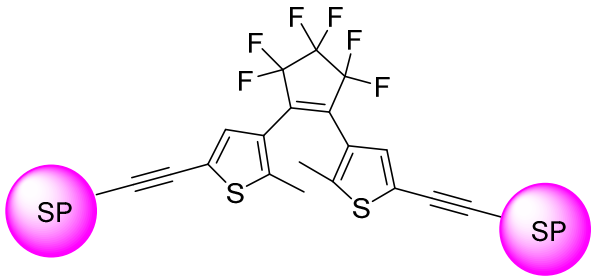		B (60%)	**EtOAc**: λ^{B}_{max} 644 nm	Sonogashira cross-coupling reaction was used.	[106]

Table 3. *Cont.*

No	Structure of Photochrome Derivatives	Synthetic Method (Yield, %)	Spectral-Kinetic Parameters	Notes and Applications	References
SP223	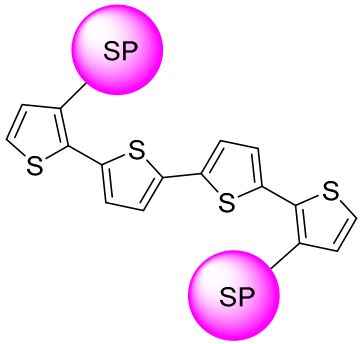	B (19%)	**CH_3OH**: λ^B_{max} 280, 310, 360, 545 nm, **Toluene**: λ^B_{max} 390, 580sh, 616 nm	Suzuki coupling with thiophene-3-boronic acid and Stille coupling reactions were used for the **SP**-T conjugates preparation.	[107]
SP224	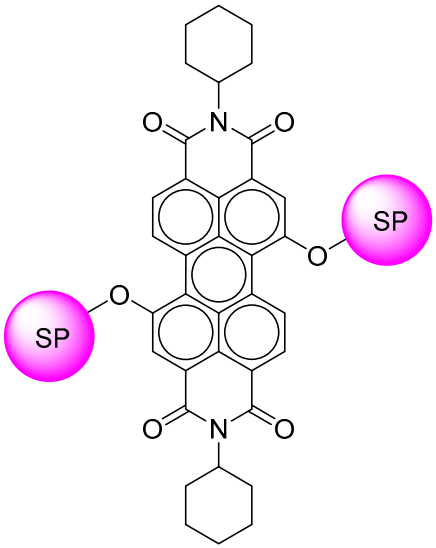	B (68%)	**THF**: λ^A_{max} 512, 550 nm, λ^B_{max} 550, 602 nm, λ^B_{max} (**SP**+Fe^{+3}) 489, 522 nm, λ^B_{fl} (SP+Fe^{+3}+ CF_3COOH) 560 nm	Light-driven ion-binding receptor with ionophoric fragment for Fe^{+3}.	[154]

Table 3. *Cont.*

No	Structure of Photochrome Derivatives	Synthetic Method (Yield, %)	Spectral-Kinetic Parameters	Notes and Applications	References
SP225	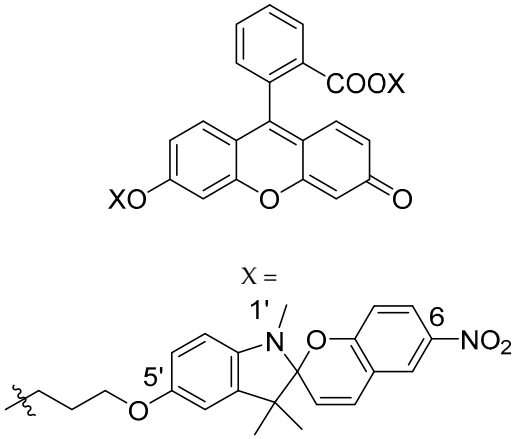	B (42%)	**THF**: λ^{A}_{max} 325, 340sh, 430, 450, 485 nm, λ^{B}_{max} 325, 340sh, 430, 450, 485, 580 nm, λ^{A}_{fl} 530, 550 nm, λ^{B}_{fl} 530, 550, 620, 660 nm, λ^{B}_{fl} (**SP**+CF_3COOH) 530, 550 nm	Fluorescein (Flu-2 **SP225**) derivative flanked by two **SP** units was examined for fluorescence modulation in response to UV and visible-light irradiations and addition of acid. Combinational logic circuit	[132]
SP226	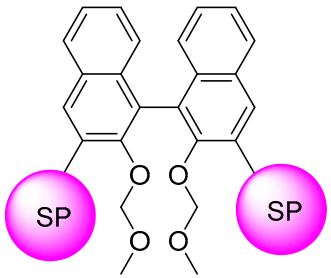	A (58%)	**CH_3CN**: λ^{B}_{max} 560 nm	BINOL-based **SP265** molecules.	[139]

Table 3. *Cont.*

No	Structure of Photochrome Derivatives	Synthetic Method (Yield, %)	Spectral-Kinetic Parameters	Notes and Applications	References
SP227	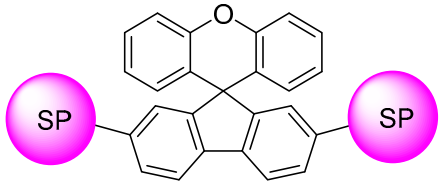	C,A (30%)	**EtOH**: λ^{A}_{max} 350 nm, λ^{B}_{max} 350, 557 nm, λ^{A}_{fl} 435 nm, λ^{B}_{fl} 435, 640 nm	**SP**-functionalized spiro[fluorene-9,9′-xanthene] derivative (SFX-2 **SP227**) was synthesized. The introduction of two **SP227** moieties to the SFX core included the following steps: 1. Suzuki reaction between the di-Br-SFX and indol derivative, 2. quaternization of product by CH_3I, 3. condensation reaction of indolium salt with 2-hydroxy-5-nitrobenzaldehyde afforded SFX-2 **SP227**.	[104]
SP228	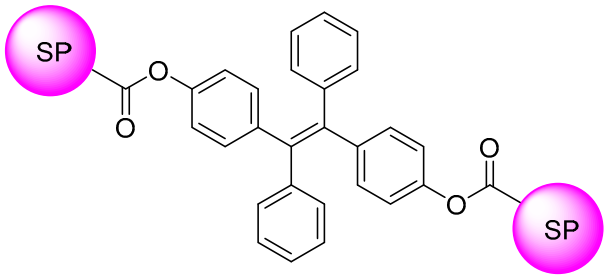	B (70%)	**CH_2Cl_2**: λ^{A}_{max} 311 nm, λ^{B}_{max} 604 nm, λ^{A}_{fl} 480 nm, **solid state**: λ^{B}_{max} 604 nm, λ^{A}_{fl} 435 nm, λ^{B}_{fl} 680 nm	Photoswitching characteristics of **SP228**−TPE−**SP228** were studied in the CH_2Cl_2 and in solid state	[133]

Table 3. *Cont.*

No	Structure of Photochrome Derivatives	Synthetic Method (Yield, %)	Spectral-Kinetic Parameters	Notes and Applications	References
SP229	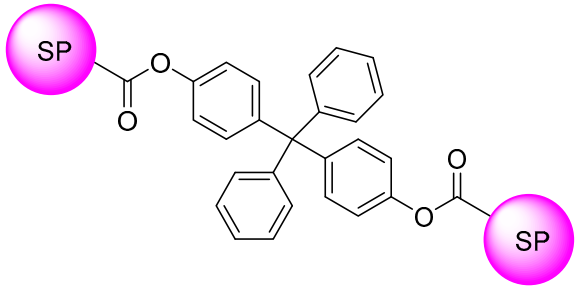	B (28%)	**CH_2Cl_2**: λ^A_{max} 311 nm, λ^B_{max} 604 nm, λ^A_{fl} 480 nm, **solid state**: λ^B_{max} 604 nm, λ^A_{fl} 435 nm, λ^B_{fl} 680 nm		[133]
SP230	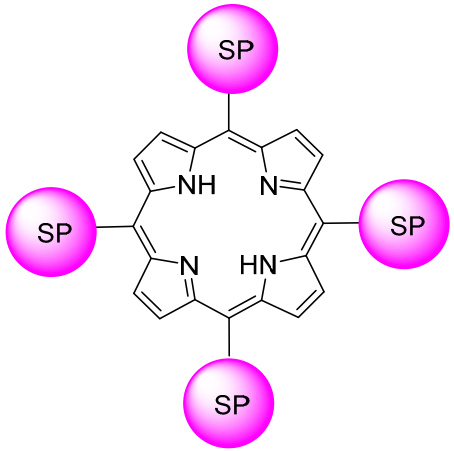	B (50%)	**EtOH**: λ^A_{max} 385 nm, λ^B_{max} 560 nm, ΔD_B^{phot} 0.1, k_{BA}^{db} 0.05 s^{-1}, $\tau_{1/2}$ * s, **Toluene**: λ^A_{max} 365 nm, λ^B_{max} 620, 585sh nm, ΔD_B^{phot} 0.5, k_{BA}^{db} 0.08 s^{-1}, $\tau_{1/2}$ 15 s		[96]

Note: see remarks after Table 1.

Table 4. Hybrid dyads of 5′-R-**SP** photochrome with various functional fragments **(SP231–SP333)**.

No	5′-R or SP Photochrome Structure	R_8	Synthetic Method (Yield, %)	Spectral-Kinetic Parameters	Notes and Applications	References
	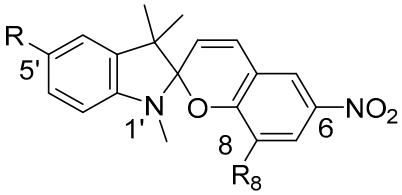					
5′-R-6-NO_2-SP photochrome derivatives with "molecular address" for the labeling of peptides, proteins (retinal-based proteins, GPCRs), nucleic acids and their fragments						
SP231	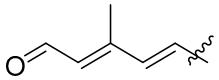	-H	B (50%)	**EtOH**: λ^{A}_{max} 385 nm, λ^{B}_{max} 563 nm, ΔD_B^{phot} 0.3, k_{BA}^{db} 0.004 s^{-1}, $\tau_{1/2}$ * s, **Toluene**: λ^{A}_{max} 377 nm, λ^{B}_{max} 630, 590sh nm, ΔD_B^{phot} 0.45, k_{BA}^{db} 0.039 s^{-1}, $\tau_{1/2}$ 35 s	Labeling of light-driven translocase bacteriorhodopsin.	[86,88,89]
SP232	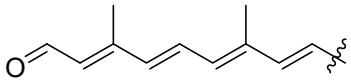	-H	B (45%)	**EtOH**: λ^{A}_{max} 330, 433 nm, λ^{B}_{max} 563 nm, ΔD_B^{phot} 0.03, k_{BA}^{db} 0.002 s^{-1}, $\tau_{1/2}$ * s, **Toluene**: λ^{A}_{max} 425 nm, λ^{B}_{max} 630, 590sh nm, ΔD_B^{phot} 0.03, k_{BA}^{db} 0.031 s^{-1}, $\tau_{1/2}$ 90 s	Labeling of light-driven translocase bacteriorhodopsin	[86,88,89]

Table 4. *Cont.*

No	5′-R or SP Photochrome Structure	R_8	Synthetic Method (Yield, %)	Spectral-Kinetic Parameters	Notes and Applications	References
SP233	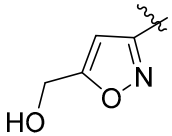	-H	C (56%)	**EtOH**: λ^{A}_{max} 277, 345sh nm, λ^{B}_{max} 555 nm, ΔD_B^{phot} 0.78, k_{BA}^{db} 9.5 10^{-3} s^{-1}, $\tau_{1/2}$ 73 s, **Toluene**: λ^{A}_{max} 320 nm, λ^{B}_{max} 617, 575sh nm, ΔD_B^{phot} 0.45, k_{BA}^{db} 0.063 s^{-1}, $\tau_{1/2}$ 11 s, **water**: **DMSO 20:1**: λ^{A}_{max} 340sh nm, λ^{B}_{max} 537 nm, ΔD_B^{phot} 0.31, $\tau_{1/2}$ * s	Labeling of TxA_2 receptor in platelets	[85,94]
SP234	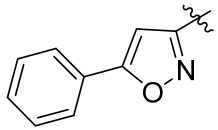	-H	C (63%)	**EtOH**: λ^{A}_{max} 273, 324sh nm, λ^{B}_{max} 556 nm, ΔD_B^{phot} 0.67, k_{BA}^{db} 7.65 10^{-3} s^{-1}, $\tau_{1/2}$ 91 s, **Toluene**: λ^{A}_{max} 320 nm, λ^{B}_{max} 617, 577sh nm, ΔD_B^{phot} 0.5, k_{BA}^{db} 0.06 s^{-1}, $\tau_{1/2}$ 12 s, **water**: **DMSO 20:1**: λ^{A}_{max} 340sh nm, λ^{B}_{max} 570 nm, ΔD_B^{phot} 0.48, k_{BA}^{db} 0.06 10^{-3} s^{-1}, $\tau_{1/2}$ 11,200 s	Labeling of TxA_2 receptor in platelets	[85,94]

Table 4. *Cont.*

No	5′-R or SP Photochrome Structure	R_8	Synthetic Method (Yield, %)	Spectral-Kinetic Parameters	Notes and Applications	References
SP235	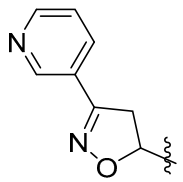	-H	C (70%)	**EtOH**: λ^{A}_{max} 265, 338sh nm, λ^{B}_{max} 545 nm, ΔD_B^{phot} 0.12, k_{BA}^{db} 2.46 10^{-3} s^{-1}, $\tau_{1/2}$ 282 s, **Toluene**: λ^{A}_{max} 320sh nm, λ^{B}_{max} 610, 572sh nm, ΔD_B^{phot} 1.1, k_{BA}^{db} 0.074 s^{-1}, $\tau_{1/2}$ 9 s, **water**: **DMSO 20:1**: λ^{A}_{max} 345 nm, λ^{B}_{max} 550 nm, ΔD_B^{phot} 0.41, k_{BA}^{db} 0.36 10^{-3} s^{-1}, $\tau_{1/2}$ 1910 s	Labeling of TxA_2 receptor in platelets	[85,94]
SP236	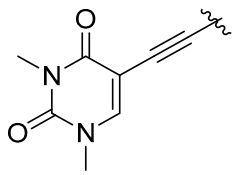	-H	B (39%)		Model Sonogashira coupling reaction with 5-iodo-1,3-dimethyluracil gave a gateway to a new procedure of nucleic acid marking with photochromic labels and probes.	[80]
SP237	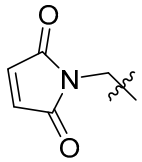	-H	B (29%)	**DMSO**: λ^{A}_{max} 260, 347 nm, λ^{B}_{max} 551 nm	5′-Maleimidomethyl **SP237** derivative was synthesized from a hydroxymethyl precursor by Mitsunobu reaction. Potential photochromic markers for sulfhydryl groups in proteins with Cys residues.	[81]

Table 4. *Cont.*

No	5′-R or SP Photochrome Structure	R_8	Synthetic Method (Yield, %)	Spectral-Kinetic Parameters	Notes and Applications	References
SP238	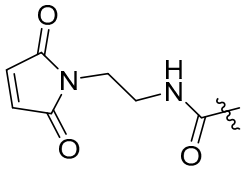	-H	B (9%)	**DMSO**: λ^{A}_{max} 277, 342 nm, λ^{B}_{max} 569 nm	**SP238** derivative was synthesized from 5′-carboxy-**SP**. Potential photochromic markers for sulfhydryl groups in proteins with Cys residues.	[81]
SP239	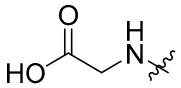	-H	B (76%)	**PBS, (80 °C)**: λ^{A}_{max} 280, 350sh nm, λ^{B}_{max} 380, 500 nm	Precursor of supramolecular hydrogels based on merocyanine-peptide conjugates.	[119]
SP240	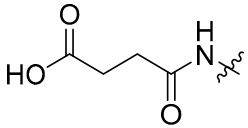	-H	A,B (76%)		Precursor of supramolecular hydrogels based on merocyanine-peptide conjugates.	[119]
SP241	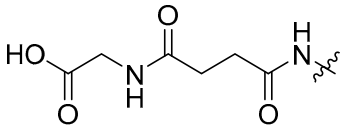	-H	A,B (76%)	**PBS, (80 °C)**: λ^{A}_{max} 280, 350sh nm, λ^{B}_{max} 380, 502 nm	Precursor of supramolecular hydrogels based on merocyanine-peptide conjugates.	[119]
SP242	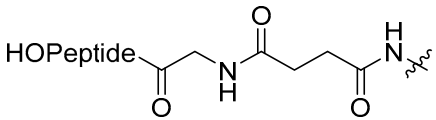 Where Peptide = tri- hepta- peptide residues	-H	C	**PBS, (80 °C)**: λ^{A}_{max} 350sh nm, λ^{B}_{max} 380, 502 nm	All spiropyran conjugated N-terminal oligopeptides were synthesized through standard solid phase peptide synthesis protocol and purified with preparative HPLC. **MC**–RGD hydrogel can be employed as an erasable photolithographic material.	[119]

Table 4. *Cont.*

No	5′-R or SP Photochrome Structure	R_8	Synthetic Method (Yield, %)	Spectral-Kinetic Parameters	Notes and Applications	References
SP243	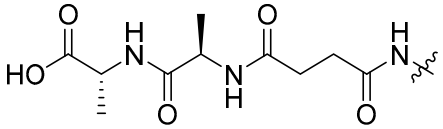	-H	A,C (66%)	**Gel**: λ^{A}_{max} 350 nm, λ^{B}_{max} 370, 510 nm	Photo-sensitive hydrogelator **SP243** with dipeptide D-Ala–D-Ala. D-Ala–D-Ala was linked to the amino group on **SP** via succinic acid.	[120]
SP244	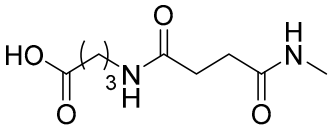	-H	C		Precursor of supramolecular hydrogels based on merocyanine-peptide conjugates.	[119]
SP245	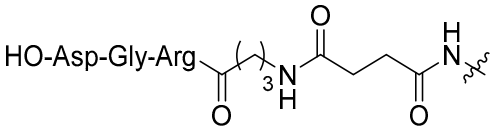	-H	C		All spiropyran conjugated N-terminal oligopeptides were synthesized through standard solid phase peptide synthesis protocol and purified with preparative HPLC.	[119]
SP246	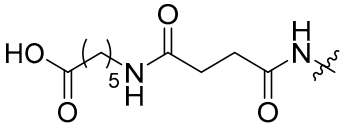	-H	C		Precursor of supramolecular hydrogels based on merocyanine-peptide conjugates.	[119]
SP247	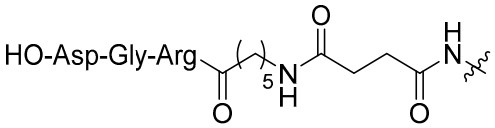	-H	C		All spiropyran conjugated N-terminal oligopeptides were synthesized through standard solid phase peptide synthesis protocol and purified with preparative HPLC.	[119]

Table 4. *Cont.*

No	5′-R or SP Photochrome Structure	R_8	Synthetic Method (Yield, %)	Spectral-Kinetic Parameters	Notes and Applications	References
SP248	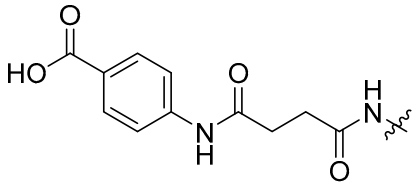	-H	C		Precursor of supramolecular hydrogels based on merocyanine-peptide conjugates.	[119]
SP249	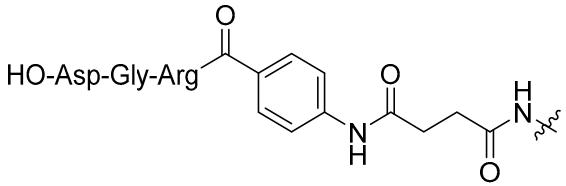	-H	C		All spiropyran conjugated N-terminal oligopeptides were synthesized through standard solid phase peptide synthesis protocol and purified with preparative HPLC.	[119]
SP250	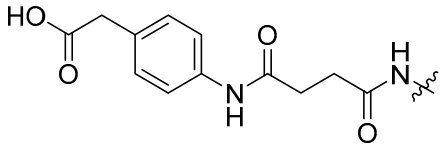	-H	C		Precursor of supramolecular hydrogels based on merocyanine-peptide conjugates.	[119]
SP251	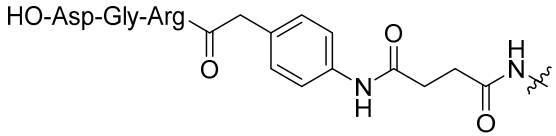	-H	B		All spiropyran conjugated N-terminal oligopeptides were synthesized through standard solid phase peptide synthesis protocol and purified with preparative HPLC.	[119]

Table 4. *Cont.*

No	5′-R or SP Photochrome Structure	R_8	Synthetic Method (Yield, %)	Spectral-Kinetic Parameters	Notes and Applications	References
SP252	Fmoc-Lys-Lys(X)-Lys-Phe-NH_2 X = 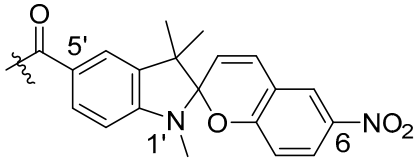		C		Peptide synthesis was performed by FMOC protocol on the Rink amide solid-phase resin.	[121]
SP253	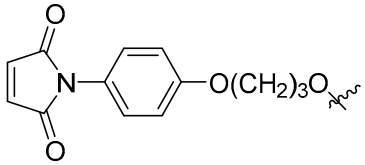	-H	C (12%)		**SP253**-DNA conjugate	[215]
		Hybrid dyads with dyes				
SP254	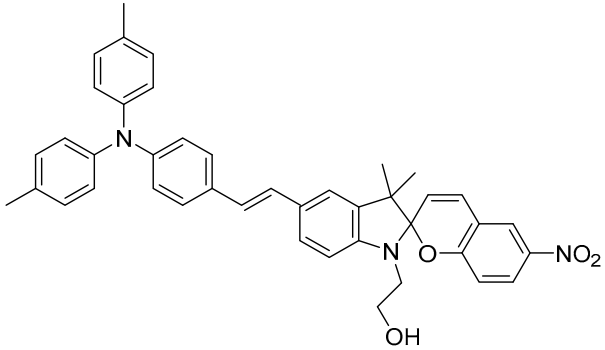		A (54%)	**CH_3CN**: λ^A_{max} 380 nm, λ^B_{max} 390, 588 nm		[98]

Table 4. *Cont.*

No	5′-R or SP Photochrome Structure	R_8	Synthetic Method (Yield, %)	Spectral-Kinetic Parameters	Notes and Applications	References
SP255	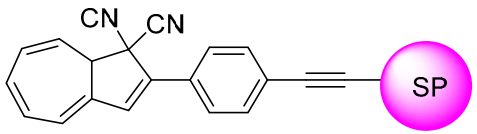 **DHA-SP**		B (42%)	**CH_3CN**: **DHA-SP** λ^A_{max} 274, 392 nm, λ^A_{fl} 660 nm, **DHA-MC** λ^B_{max} 371, 547 nm, **DHA-MCH$^+$** $\lambda^B_{max}{}^{BH+}$ 309, 410 nm, **VHF-SP** λ^A_{max} 268, 317, 473 nm, $t_{1/2BA}{}^{db}$ 138 min 40 s, **VHF-MC** λ^B_{max} 318, 437, 580 nm, $t_{1/2BA}{}^{db}$ 30 s, **VHF-MCH$^+$** $\lambda^B_{max}{}^{BH+}$ 297, 437 nm	Dyad DHA- **SP255** was synthesized under Sonogashira coupling conditions.	[105]
SP256	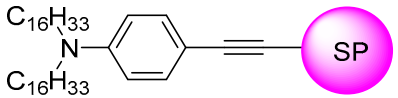		C (63%)	**CH_2Cl_2**: λ^A_{max} 264, 348 nm	Precursor for functional 5′-R-6-NO_2-**SP** series via [2+2]cycloaddition click reactions (Hagihara-Sonogashira cross-coupling reaction).	[111]
SP257	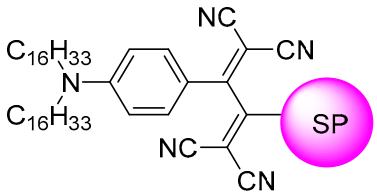		B (92%)	**CH_2Cl_2**: λ^A_{max} 264, 472 nm	Series of 5′-R-6-NO_2-**SP** was synthesized via [2+2]cycloaddition click reactions (Hagihara-Sonogashira cross-coupling reaction). The third-order nonlinear optical (NLO) properties were investigated.	[111]

Table 4. *Cont.*

No	5′-R or SP Photochrome Structure	R_8	Synthetic Method (Yield, %)	Spectral-Kinetic Parameters	Notes and Applications	References
SP258	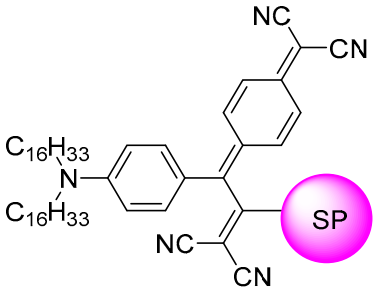		B (90%)	**CH_2Cl_2**: λ^A_{max} 420, 690 nm	Series of 5′-R-6-NO_2-**SP** was synthesized via [2+2]cycloaddition click reactions (Hagihara-Sonogashira cross-coupling reaction). The third-order nonlinear optical (NLO) properties were investigated.	[111]
SP259	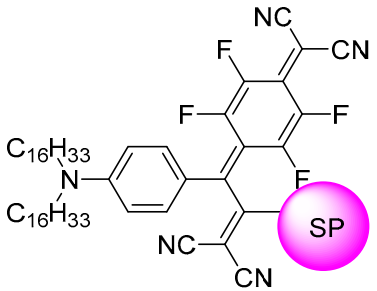		B (88%)	**CH_2Cl_2**: λ^A_{max} 420, 848 nm	Series of 5′-R-6-NO_2-**SP** was synthesized via [2+2]cycloaddition click reactions (Hagihara-Sonogashira cross-coupling reaction). The third-order nonlinear optical (NLO) properties were investigated.	[111]
SP260	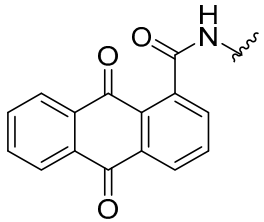	-H	A (67%)		Amide-linked **SP260**-anthraquinone (**SP**-AQ) conjugates were investigated in PC vesicles.	[134]

Table 4. *Cont.*

No	5′-R or SP Photochrome Structure	R_8	Synthetic Method (Yield, %)	Spectral-Kinetic Parameters	Notes and Applications	References
SP261	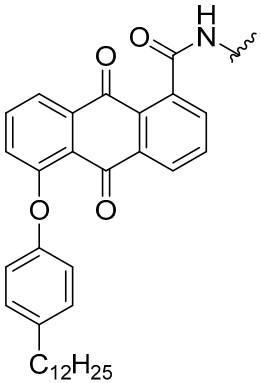	-H	A (40%)		Amide-linked **SP261**-anthraquinone (**SP**-AQ) conjugates were investigated in PC vesicles.	[134]
SP262	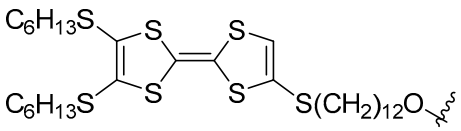	-H	B (73%)	**THF**: λ^{A}_{max} 250, 280, 315, 330 nm, λ^{B}_{max} 325, 340sh, 430, 450, 485, 580 nm, λ^{A}_{max} (**SP**+Fe^{+3}) 610 nm, λ^{B}_{max} (**SP**+Fe^{+3}) 424 nm	Spectral studies of dyad **SP262**-TTF, containing an electroactive unit (tetrathiafulvalene), and a photochromic unit **SP**, in the presence of ferric ions were conducted	[155]
Hybrid dyads with fluorophores						

Table 4. *Cont.*

No	5′-R or SP Photochrome Structure	R_8	Synthetic Method (Yield, %)	Spectral-Kinetic Parameters	Notes and Applications	References
SP263	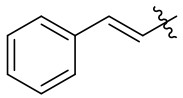 Z-isomer/E-isomer/Z- + E-isomers mix	-H	A,C (3%) B (62% mix E- + Z- isomers)	***Z*-isomer** **EtOH**: λ^{A}_{max} 315, 335sh nm, λ^{B}_{max} 400sh, 557 nm, λ^{BH+}_{max} 320sh, 338, 426 nm, ΔD_B^{phot} 0.28, k_{BA}^{db} 7.02 10^{-4} s^{-1}, 6.03 10^{-3} s^{-1}, $\tau_{1/2}$ 550 s, λ_{fl} 455sh, 478, 645 nm, **Toluene**: λ^{A}_{max} 319, 340sh, nm, λ^{B}_{max} 390sh, 590sh, 622 nm, ΔD_B^{phot} 1.33, k_{BA}^{db} 6.87 10^{-2} s^{-1}, 5.08 10^{-1} s^{-1}, $\tau_{1/2}$ 30 s, λ_{fl} 510, 685 nm, **Acetone**: λ^{A}_{max} 440sh nm, λ^{B}_{max} 405sh, 555sh, 585 nm, λ^{BH+}_{max} 445 nm, k_{BA}^{db} 8.76 10^{-3} s^{-1}, **DMSO**: λ^{A}_{max} 435sh nm, λ^{B}_{max} 580 nm, ***E*-isomer** **EtOH**: λ^{A}_{max} 320sh, 342 nm, λ^{B}_{max} 341, 395, 556 nm, ΔD_B^{phot} 0.16, k_{BA}^{db} 4.21 10^{-2} s^{-1}, 7.73 10^{-4} s^{-1}, $\tau_{1/2}$ 1500 s, λ_{fl} 485, 646 nm	Wittig olefination followed by HPLC. Z-/E-ratio 39/61	[16,50,66]

Table 4. *Cont.*

No	5′-R or SP Photochrome Structure	R_8	Synthetic Method (Yield, %)	Spectral-Kinetic Parameters	Notes and Applications	References
SP264	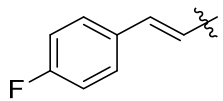 Z-isomer/E-isomer	-H	B (55% mix E- + Z-isomers)	***E*- + *Z*-isomer mix**: **EtOH**: λ^{A}_{max} 320sh, 342 nm, λ^{B}_{max} 571 nm, λ_{max}^{BH+} 478 nm, **Toluene**: λ^{A}_{max} 325 nm, λ^{B}_{max} 345, ~385sh, 585sh, 622 nm	Wittig olefination followed by HPLC. Z-/E-ratio 64/36	[16,50]
SP265	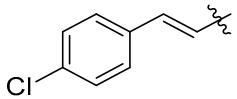 Z-isomer/E-isomer	-H	B (72% mix E- + Z- isomers)		Wittig olefination followed by HPLC. Z-/E-ratio 35/65	[16,50]
SP266	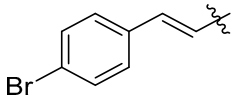 Z-isomer/E-isomer	-H	B (63% mix E- + Z- isomers)		Wittig olefination followed by HPLC. Z-/E-ratio 45/55	[16,50]
SP267	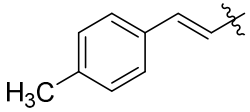 Z-isomer/E-isomer	-H	B (67% mix E- + Z- isomers)		Wittig olefination followed by HPLC. Z-/E-ratio 49/51	[16,50]

Table 4. *Cont.*

No	5′-R or SP Photochrome Structure	R_8	Synthetic Method (Yield, %)	Spectral-Kinetic Parameters	Notes and Applications	References
SP268	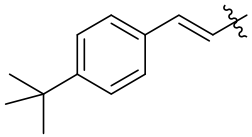 Z-isomer/E-isomer	-H	B (58% mix E- + Z- isomers)		Wittig olefination followed by HPLC. Z-/E-ratio 45/55	[16,50]
SP269	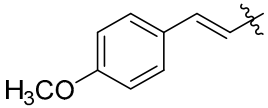 Z-isomer/E-isomer	-H	B (66% mix E- + Z- isomers)	***E*-isomer** **EtOH**: λ^{A}_{max} 265, 315sh, 339 nm, λ^{B}_{max} 265, 315sh, 339, 400sh, 558 nm, ΔD_B^{phot} 0.14,	Wittig olefination followed by HPLC. Z-/E-ratio 59/41	[16,50]
SP270	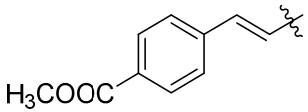 Z-isomer/E-isomer	-H	B (60% mix E- + Z- isomers)	***E*- + *Z*-isomer mix**: **EtOH**: λ^{A}_{max} 267, 364 nm, λ^{B}_{max} 267, 367, 460sh nm, ΔD_B^{phot} 0.04, **Toluene**: λ^{A}_{max} 362, 460sh nm, λ^{B}_{max} 370, 590sh, 625 nm, ΔD_B^{phot} 0.46	Wittig olefination followed by HPLC. Z-/E-ratio 21/79	[16,50]

Table 4. *Cont.*

No	5′-R or SP Photochrome Structure	R_8	Synthetic Method (Yield, %)	Spectral-Kinetic Parameters	Notes and Applications	References
SP271	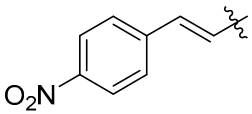 Z-isomer/E-isomer	-H	B 50% mix E- + Z- isomers)	***Z*-isomer** **EtOH**: λ^{A}_{max} 400, 294sh nm, λ^{B}_{max} 563, 405 nm, $k_{BA}{}^{db}$ 3.44 10^{-2} s^{-1}, 1.68 10^{-3} s^{-1}, $\tau_{1/2}$ 7200 s, λ_{fl} 430, 470, 654 nm **Toluene**: λ^{A}_{max} 395 nm, λ^{B}_{max} 629, 595sh nm, $k_{BA}{}^{db}$ 3.92 10^{-2} s^{-1}, $\tau_{1/2}$ 26 s, λ_{fl} 546 nm, ***E*-isomer** **EtOH**: λ^{A}_{max} 409, 294sh nm, λ^{B}_{max} 563, 405 nm, $\Delta D_B{}^{phot}$ 0.16, $k_{BA}{}^{db}$ 1.32 10^{-2} s^{-1}, 2.34 10^{-3} s^{-1}, $\tau_{1/2}$ 7200 s, λ_{fl} 654 nm, **Toluene**: λ^{A}_{max} 407 nm, λ^{B}_{max} 629, 595sh nm, $\Delta D_B{}^{phot}$ 0.56, $k_{BA}{}^{db}$ 5.47 10^{-2} s^{-1}, $\tau_{1/2}$ 28 s, λ_{fl} 546 nm	Wittig olefination followed by HPLC. Z-/E-ratio 55/45	[16,50]
SP272	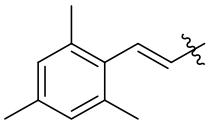 Z-isomer/E-isomer	-H	B (18% mix E- + Z- isomers)		Wittig olefination followed by HPLC. Z-/E-ratio 9/91	[16,50]

Table 4. *Cont.*

No	5′-R or SP Photochrome Structure	R_8	Synthetic Method (Yield, %)	Spectral-Kinetic Parameters	Notes and Applications	References
SP273	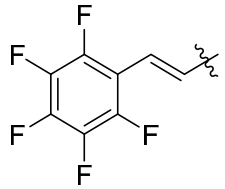 Z-isomer/E-isomer	-H	B (90% mix E- + Z- isomers)	***E*-isomer** **EtOH**: λ^{A}_{max} 260, 353 nm, λ^{B}_{max} 265, 353, 560 nm, ΔD_B^{phot} 0.23, k_{BA}^{db} 1.94 10^{-2} s^{-1}, 2.31 10^{-3} s^{-1}, $\tau_{1/2}$ 830 s, λ_{fl} 647 nm, **Toluene**: λ^{A}_{max} 354 nm, λ^{B}_{max} 405sh, 585sh, 622 nm, ΔD_B^{phot} 0.58, k_{BA}^{db} 4.72 10^{-2} s^{-1}, $\tau_{1/2}$ 42 s, λ_{fl} 558 nm	Wittig olefination followed by HPLC. Z-/E-ratio 3/97	[16,50]
SP274	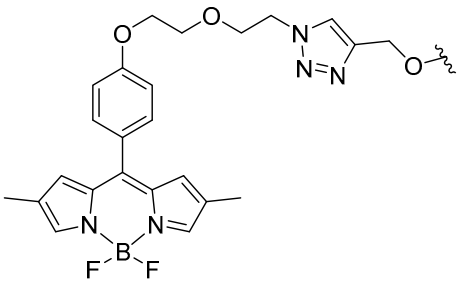	-H	C (75%)	**CH_2Cl_2**: λ^{A}_{max} 266, 357, 484, 511 nm, λ_{fl} 526 nm, φ_{fl} 0.11, **CH_3CN**: k_{BA}^{db} 5.8 10^{-4} s^{-1}	**SP274**-containing Bodipy derivatives have been designed and synthesized by CA reaction click chemistry of terminal alkyne with Bodipy-EO_n-N_3.	[103]
SP275	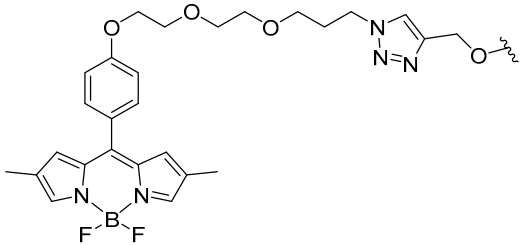	-H	C (61%)	**CH_2Cl_2**: λ^{A}_{max} 265, 357, 484, 510 nm, λ_{fl} 526 nm, φ_{fl} 0.14, **CH_3CN**: k_{BA}^{db} 6.1 10^{-4} s^{-1}	**SP275**-containing Bodipy derivatives have been designed and synthesized by CA reaction click chemistry of terminal alkyne with Bodipy-EO_n-N_3	[103]

Table 4. *Cont.*

No	5′-R or SP Photochrome Structure	R_8	Synthetic Method (Yield, %)	Spectral-Kinetic Parameters	Notes and Applications	References
SP276	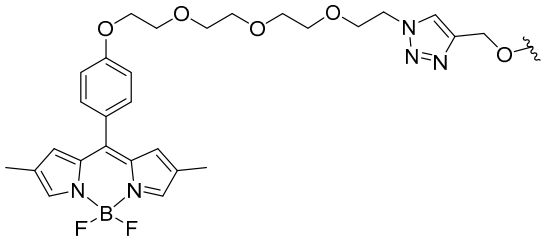	-H	C (68%)	**CH_2Cl_2**: λ^A_{max} 265, 357, 484, 510 nm, λ_{fl} 526 nm, φ_{fl} 0.16, **CH_3CN**: $k_{BA}{}^{db}$ 6.4 10^{-4} s^{-1}	**SP276**-containing Bodipy derivatives have been designed and synthesized by CA reaction click chemistry of terminal alkyne with Bodipy-EO_n-N_3.	[103]
SP277	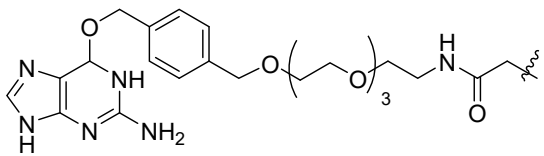	-H	C	λ_{fl} 620 nm	BG-PEG-NitroBIPS-GFP-AGT fusion protein. OLID-FRET sensor using two-photon excitation of **SP** (720 nm) to trigger the **SP**-to-**MC** transition and 543 nm to trigger the **MC**-to-**SP** transition.	[247]
SP278	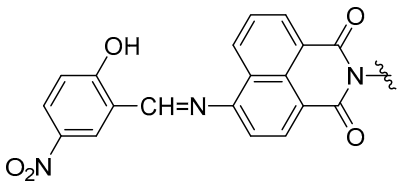	-H	A,C	λ^A_{max} 340, 432 nm, λ^B_{max} 350, 432 548 nm, λ_{fl} 650, 662 nm	**SP278** bonded 1,8-naphthalimide compound is useful as photochromic and photoluminescent material.	[135]
SP279	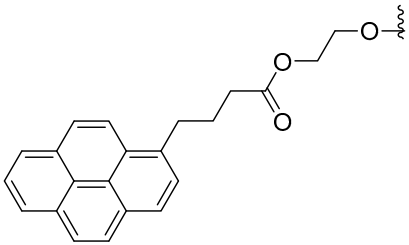	-H	B (19%)			[136]

Table 4. *Cont.*

No	5′-R or SP Photochrome Structure	R_8	Synthetic Method (Yield, %)	Spectral-Kinetic Parameters	Notes and Applications	References
SP280	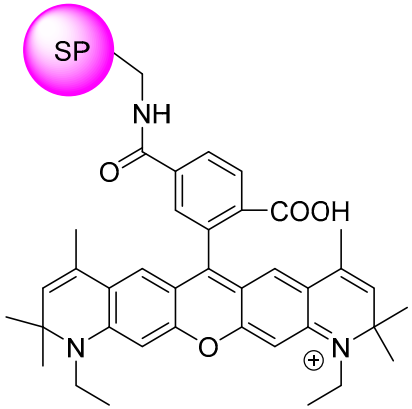		B		The switching performance of different fluorophore–**SP** conjugates was studied. It was shown that the fluorescence of the fluorophores can be modulated by switching the **SP**.	[138]
SP281	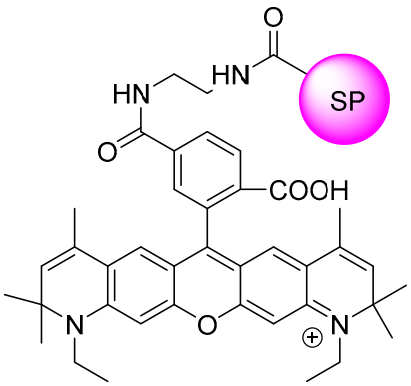		B		The switching performance of different fluorophore–**SP** conjugates was studied. It was shown that the fluorescence of the fluorophores can be modulated by switching the **SP**.	[138]

Table 4. *Cont.*

No	5′-R or SP Photochrome Structure	R_8	Synthetic Method (Yield, %)	Spectral-Kinetic Parameters	Notes and Applications	References
SP282	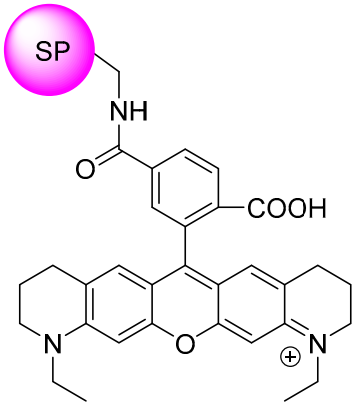		B		The switching performance of different fluorophore–**SP** conjugates was studied. It was shown that the fluorescence of the fluorophores can be modulated by switching the **SP**.	[138]
SP283	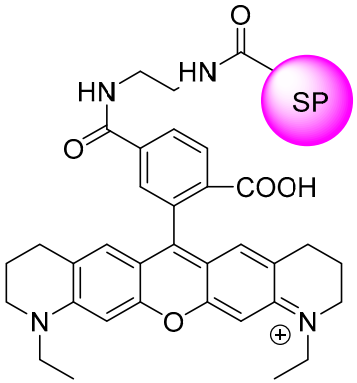		B		The switching performance of different fluorophore–**SP** conjugates was studied. It was shown that the fluorescence of the fluorophores can be modulated by switching the **SP**.	[138]

Table 4. *Cont.*

No	5′-R or SP Photochrome Structure	R_8	Synthetic Method (Yield, %)	Spectral-Kinetic Parameters	Notes and Applications	References
SP284	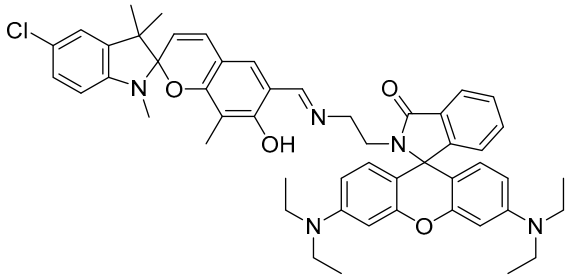		B (34%)	**Acetone**: λ^{A}_{max} 333, 420 nm, λ^{A}_{max} (+Me^{+n}) 518–555 nm	**SP284** conjugate with Rhodamine B aminoethylamide. Irradiation of solutions of the spiropyrans with UV light (365 nm) did not lead to any spectral changes.	[140]
SP285	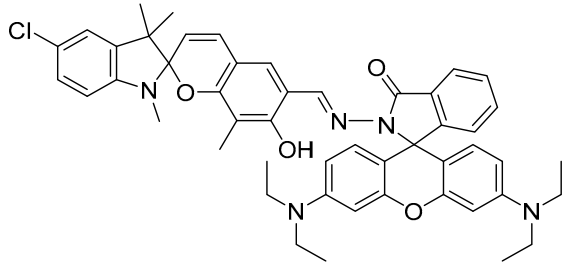		B (29%)	**Acetone**: λ^{A}_{max} 362 nm, λ^{B}_{max} 555 nm (weak), $k_{BA}{}^{db}$ 0.021 s^{-1}, **Toluene**: λ^{A}_{max} 315, 369 nm, λ^{B}_{max} 560 nm (weak), $k_{BA}{}^{db}$ 0.127 s^{-1}	**SP285** conjugate with rhodamine B hydrazide.	[141]
SP286	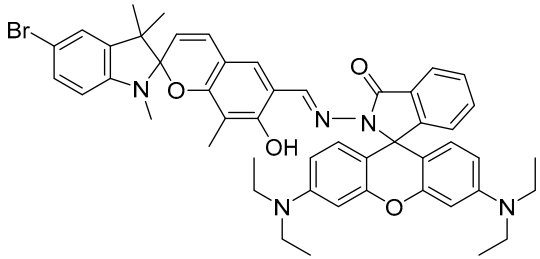		B (27%)	**Acetone**: λ^{A}_{max} 362 nm, λ^{B}_{max} 555 nm (weak), $k_{BA}{}^{db}$ 0.024 s^{-1}, **Toluene**: λ^{A}_{max} 315, 369 nm, λ^{B}_{max} 560 nm (weak), $k_{BA}{}^{db}$ 0.078 s^{-1}	**SP286** conjugate with rhodamine B hydrazide.	[141]

Table 4. *Cont.*

No	5′-R or SP Photochrome Structure	R_8	Synthetic Method (Yield, %)	Spectral-Kinetic Parameters	Notes and Applications	References
SP287	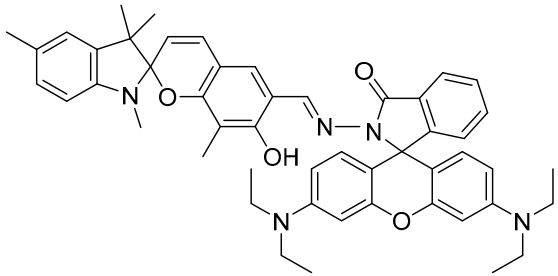		B (26%)	**Acetone**: λ^{A}_{max} 362 nm, λ^{B}_{max} 555 nm (weak), $k_{BA}{}^{db}$ 0.031 s^{-1}, **Toluene**: λ^{A}_{max} 315, 369 nm, λ^{B}_{max} 560 nm (weak), $k_{BA}{}^{db}$ 0.06 s^{-1}	**SP287** conjugate with rhodamine B hydrazide	[141]
Ion-binding receptors with ionophoric fragment						
SP288	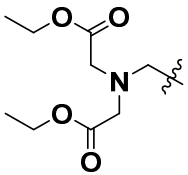	-H	B (42%)	**EtOH**: λ^{A}_{max} 337 nm, λ^{B}_{max} 538 nm, $\Delta D_B{}^{phot}$ 0.66, $k_{BA}{}^{db}$ 8.74 10^{-4} s^{-1}, $\tau_{1/2}$ 4000 s, λ_{fl} 636 nm, **Toluene**: λ^{A}_{max} 334 nm, λ^{B}_{max} 605 nm, $\Delta D_B{}^{phot}$ 3.53, $k_{BA}{}^{db}$ 0.123 s^{-1}, $\tau_{1/2}$ 28 s, λ_{fl} 666 nm **CH_3CN**: λ^{A}_{max} 336 nm, λ^{B}_{max} 561 nm, $\Delta D_B{}^{phot}$ 1.47, $k_{BA}{}^{db}$ 1.29 10^{-3} s^{-1}, $\tau_{1/2}$ 28 s, λ_{fl} 650 nm	**SP288** ion-binding receptor with ionophoric fragment for metal cations	[44]

Table 4. *Cont.*

No	5′-R or SP Photochrome Structure	R_8	Synthetic Method (Yield, %)	Spectral-Kinetic Parameters	Notes and Applications	References
SP289	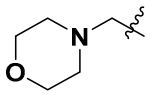	-H	B (46%)	**EtOH**: λ^{A}_{max} 338 nm, λ^{B}_{max} 538 nm, ΔD_B^{phot} 0.61, k_{BA}^{db} 1.64 10^{-3} s^{-1}, λ_{fl} 642 nm, **Toluene**: λ^{A}_{max} 334 nm, λ^{B}_{max} 607, 575sh nm, ΔD_B^{phot} 2.62, k_{BA}^{db} 1.58 10^{-2} s^{-1}, λ_{fl} 672, 530 nm	**SP289** ion-binding receptor with ionophoric fragment for metal cations	
SP290	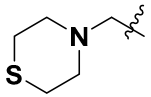	-H	B (82%)	**EtOH**: λ^{A}_{max} 342 nm, λ^{B}_{max} 538 nm, ΔD_B^{phot} 2.04, k_{BA}^{db} 1.94 10^{-4} s^{-1}, $\tau_{1/2}$ 2140 s, λ_{fl} 640 nm, **Toluene**: λ^{A}_{max} 334 nm, λ^{B}_{max} 606, 575sh nm, ΔD_B^{phot} 4.64, k_{BA}^{db} 7.84 10^{-2} s^{-1}, $\tau_{1/2}$ 20 s, λ_{fl} 680 nm	**SP290** ion-binding receptor with ionophoric fragment for the metals cations ion-binding receptor with ionophoric fragment for metal cations	
SP291	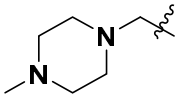	-H	B (58%)	**EtOH**: λ^{A}_{max} 321 nm, λ^{B}_{max} 540 nm, ΔD_B^{phot} 0.72, k_{BA}^{db} 4.14 10^{-2} s^{-1}, $\tau_{1/2}$ 1540 s, **Toluene**: λ^{A}_{max} 350 nm, λ^{B}_{max} 605, 575sh nm, ΔD_B^{phot} 2.08, k_{BA}^{db} 0.212 s^{-1}, $\tau_{1/2}$ 14 s	**SP291** ion-binding receptor with ionophoric fragment for the metals cations ion-binding receptor with ionophoric fragment for metal cations	

Table 4. *Cont.*

No	5′-R or SP Photochrome Structure	R_8	Synthetic Method (Yield, %)	Spectral-Kinetic Parameters	Notes and Applications	References
SP292	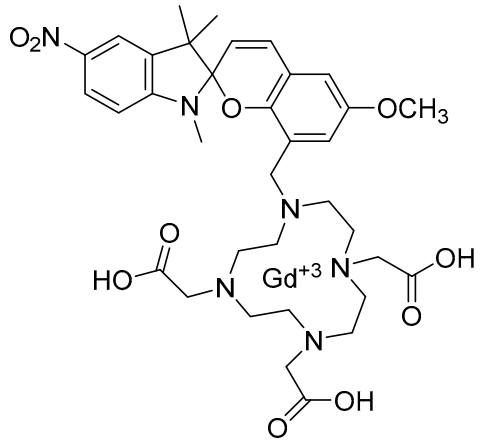		C (91%)	**water (pH = 7.4)**: complex **SP342** might not be responsive to light; furthermore, there was a minimal absorbance difference above 400 nm	(**SP292**)-based magnetic resonance imaging (MRI) contrast agents	[156]
SP293	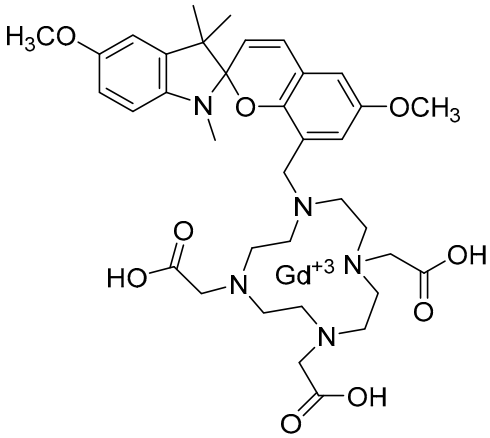		C (75%)	**water (pH = 7.4)**: λ^{A}_{max} 440 nm (without Gd^{+3}), λ^{A}_{max} 530 nm; λ^{A}_{fl} 664 nm, after visible light irradiation of sample **SP343** fluorescence and absorbance peaks decreases. After visible light irradiation of sample **SP343** a new stable absorbance peak appeared at 440 nm.	(**SP293**)-based magnetic resonance imaging (MRI) contrast agents	[156]

Table 4. *Cont.*

No	5′-R or SP Photochrome Structure	R_8	Synthetic Method (Yield, %)	Spectral-Kinetic Parameters	Notes and Applications	References
SP294	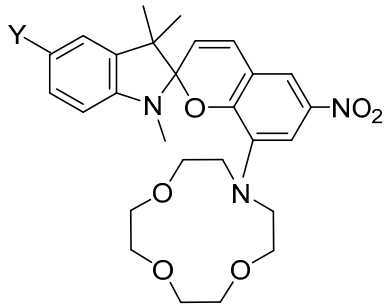 Where (a) Y = -CF_3, (b) Y = -NO_2, (c) Y = -COOH		A (90%) A (14%) C,A (18%)	**CH_3CN**: λ^B_{max} 550 nm **CH_3CN**: λ^B_{max} 550 nm **CH_3CN**: λ^A_{max} 360, 400 nm, λ^B_{max} 545 nm, λ_{fl} 627 nm	Receptor for the cations Li^+, Na^+, Ca^{2+}, Ba^{2+} and Mg^{2+}. Receptor for the cations Li^+, Na^+, Ca^{2+}, Ba^{2+} and Mg^{2+}. **SP294** with tethered aza-12-crown-4 unit was synthesized.	[40,158,159,163]
SP295	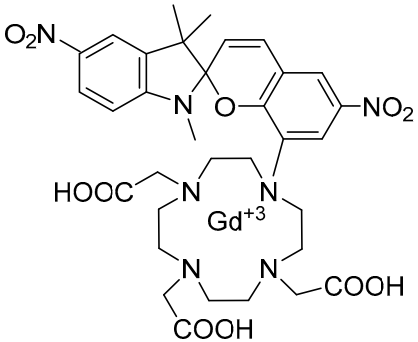		C (62% before complexation Gd^{+3}) B (79%)	**H_2O**: λ^A_{max} 502 nm, λ^B_{max} 502 nm↓, λ_{fl} 603 nm		[157]

Table 4. *Cont.*

No	5′-R or SP Photochrome Structure	R_8	Synthetic Method (Yield, %)	Spectral-Kinetic Parameters	Notes and Applications	References
SP296	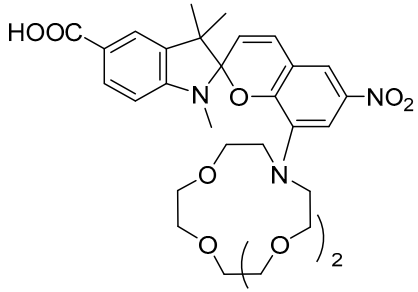		A (85%)	**CH_3CN**: λ^A_{max} 360, 400 nm, λ^B_{max} 545 nm, λ_{fl} 627 nm	**SP296** with tethered aza-15-crown-5 unit was synthesized. Spectral changes induced by cations binding with (perchlorates: Li^+, Na^+ and K^+ and Cs_2SO_4) were investigated.	[159,160,248]
SP297	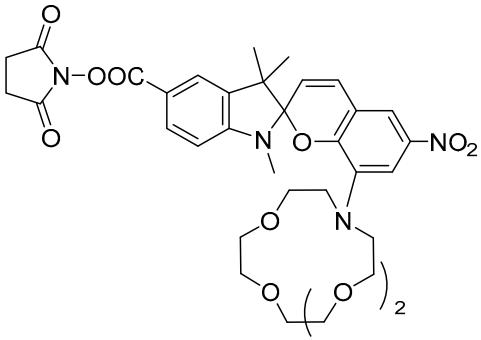		B (70%) B (36%)	**CH_3CN**: λ_{fl} 640 nm	**SP297** Li^+ ion sensor the molecular switch was developed. It was based on covalently attached **SP** to the internal surface of the microstructured optical fiber (MOF).	[160]
SP298	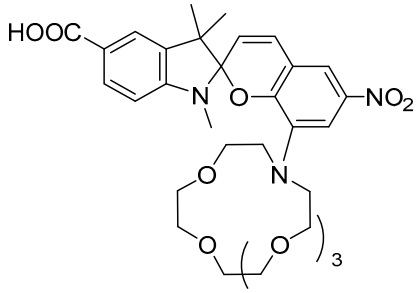		C,A (20%)	**CH_3CN**: λ^A_{max} 360 nm, λ^B_{max} 545 nm, λ_{fl} 632 nm	**SP298** with tethered aza-18-crown-6 unit was synthesized. Spectral changes induced by cations binding with (perchlorates: Li^+, Na^+ and K^+ and Cs_2SO_4) were investigated.	[159]

Table 4. *Cont.*

No	5′-R or SP Photochrome Structure	R_8	Synthetic Method (Yield, %)	Spectral-Kinetic Parameters	Notes and Applications	References
SP299	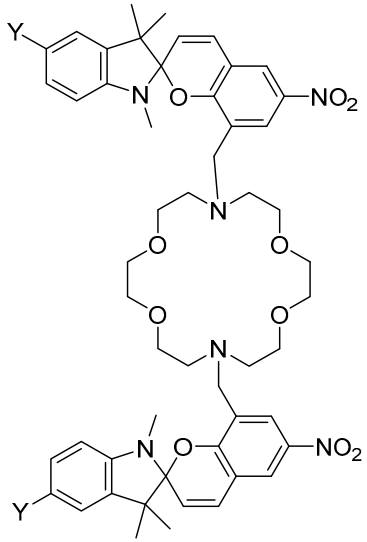	(a) Y = $-CF_3$	A (38%)		Reversible photochemical ion chelation.	[161]
		(b) Y = $-NO_2$	A (8%)			
SP300	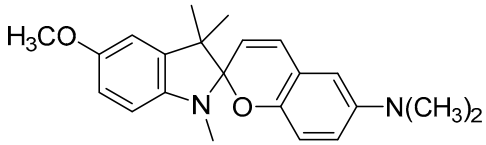		A (47%)	**EtOH**: λ^{A}_{max} 250, 320, 360 nm, λ^{B}_{max} 250, 320, 360 nm	**SP300** was synthesized. The formation of a metal complex between **SP300** and Cu^{2+} was associated with a color change. Sensor for Cu^{+2} ions.	[164]

Table 4. *Cont.*

No	5′-R or SP Photochrome Structure	R_8	Synthetic Method (Yield, %)	Spectral-Kinetic Parameters	Notes and Applications	References
SP301	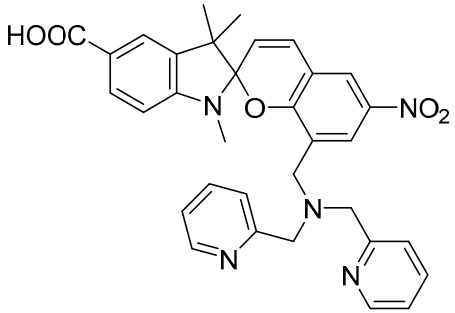		A,C (75%)	**20% CH_3CN in water**: λ_{fl} 620 nm **CH_3CN**: λ_{fl} 640 nm, **DMSO**: λ_{fl} 640 nm,	Light-driven ion-binding receptor with ionophoric fragment for Zn^{+2}.	[165,166]
SP302	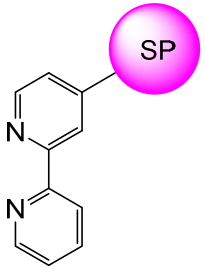		A (70%)	**THF**: λ^{A}_{max} 231, 273, 295, 328 nm λ^{B}_{max} 231, 277, 381, 590 nm, φ_{334} 0.078, λ^{B}_{fl} 660 nm	Precursor for ion-binding receptor with ionophoric fragment for Ru, Os	[38,167,249]
SP303	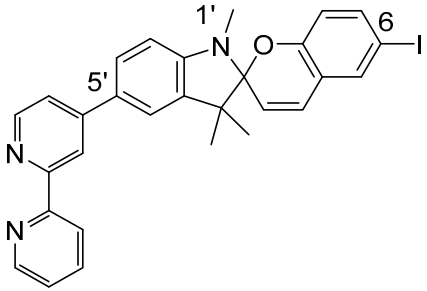		A (68%)		Precursor for ion-binding receptor with ionophoric fragment for Ru, Os	[39,249]

Table 4. *Cont.*

No	5′-R or SP Photochrome Structure	R_8	Synthetic Method (Yield, %)	Spectral-Kinetic Parameters	Notes and Applications	References
SP304	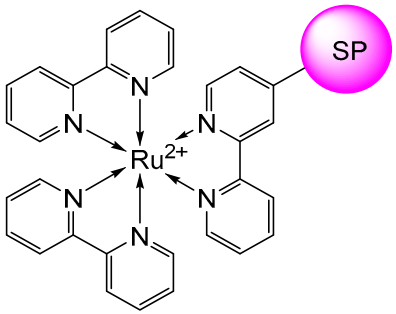		B (54%)	**THF**: λ^{A}_{max} 291, 365, 459 nm, λ^{B}_{max} 291, 391, 461, 603 nm, φ_{334} 0.0065, λ^{B}_{fl} 634 nm, λ^{B}_{fl} 655 nm	$[Ru(bpy)_2(\mathbf{SP})]$ $(PF_6)_2$, ion-binding receptor with ionophoric fragment for Ru	[38,167]
SP305	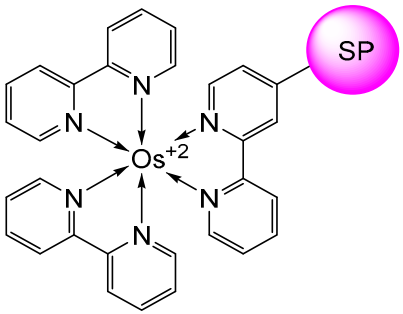		B (45%)	**THF**: λ^{A}_{max} 294, 373, 490, 591 nm, λ^{B}_{max} 294, 386, 490, 605 nm, φ_{334} 0.0049, λ^{A}_{fl} 765 nm, λ^{B}_{fl} 765 nm	$[Os(bpy)_2(\mathbf{SP})]$ $(PF_6)_2$, ion-binding receptor with ionophoric fragment for Os	[38,167]
SP306	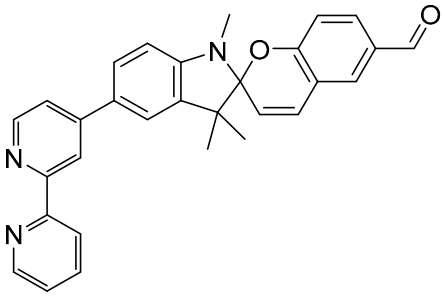		A (59%)		Precursor for ion-binding receptor with ionophoric fragment for Ru, Os	[38]

Table 4. *Cont.*

No	5′-R or SP Photochrome Structure	R_8	Synthetic Method (Yield, %)	Spectral-Kinetic Parameters	Notes and Applications	References
SP307	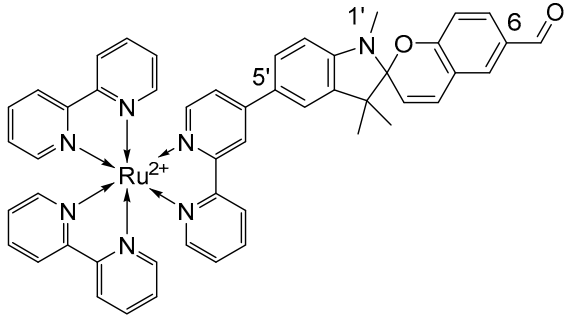		B (80%)		Precursor heterobinuclear **SP** metal complex [Ru(bpy)$_2$-4bpy-Sp-PhenIm-Os (bpy)$_2$](PF$_6$)$_4$	[38]
SP308	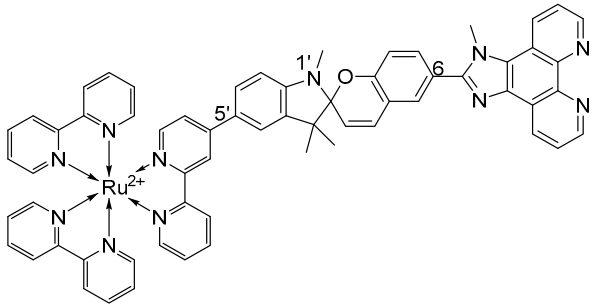		B (64%)		Precursor heterobinuclear **SP** metal complex [Ru(bpy)$_2$-4bpy-Sp-PhenIm-Os (bpy)$_2$](PF$_6$)$_4$	[38]

Table 4. *Cont.*

No	5′-R or SP Photochrome Structure	R_8	Synthetic Method (Yield, %)	Spectral-Kinetic Parameters	Notes and Applications	References
SP309	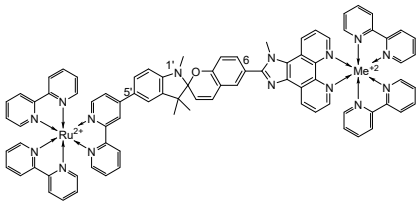	(a) Me^{+2} = Os^{+2}	B (35%)	**CH_3CN**: λ^A_{max} 288, 359, 461, 620 nm, λ^A_{fl} 619, 742 nm	**SP309(a,b)** metal complexes Ru, Os $[Ru(bpy)_2\text{-}4bpy\text{-}Sp\text{-}PhenIm\text{-}Me^{+2}(bpy)_2](PF_6)_4$. were synthesized via Suzuki coupling. Closed form of the **SP309(a)** metal complex is inactive and cannot be converted to the open form either by UV light or irradiation at 450 nm.	[38]
		(b) Me^{+2} = Ru^{+2}	B (10%)	**CH_3CN**: λ^A_{max} 287, 339, 458 nm, λ^A_{fl} 618 nm		
SP310	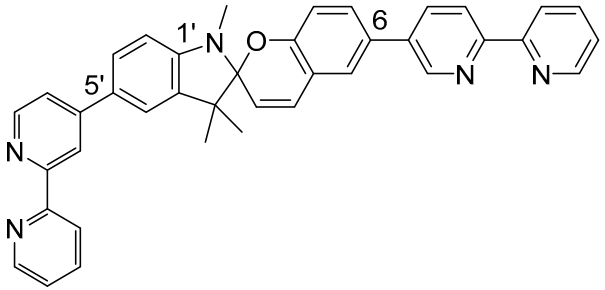		B (31%)			[39,249]

Table 4. *Cont.*

No	5′-R or SP Photochrome Structure	R_8	Synthetic Method (Yield, %)	Spectral-Kinetic Parameters	Notes and Applications	References
SP311	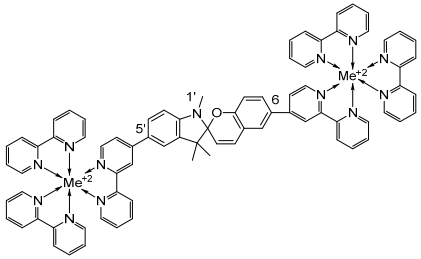 (a) Me^{+2} = Ru^{+2}		B (21%)	**CH_3CN**: λ^A_{max} 288, 338, 458 nm λ^A_{fl} 619 nm	Ion-binding receptor with ionophoric fragment for Ru, Os	[39]
	(b) Me^{+2} = Os^{+2}		B (15%)	**CH_3CN**: λ^A_{max} 291, 374, 449, 620, 825 nm λ^A_{fl} 741 nm		
SP312	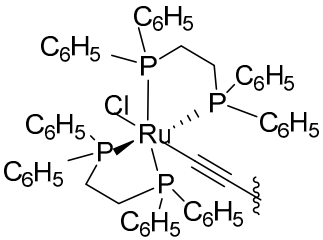	-H	B (74%)	**THF**: λ^A_{max} 270 nm, λ^B_{max} 270, 633 nm, $k_{BA}{}^{db}$ 1.61 10^{-3} s^{-1}		[203]
SP313	CoLH-O_3**SP**	-H	B	CoLH-O_3S-**SP** λ^B_{max} 564 nm	Organic–inorganic hybrid photomagnet, the intercalation of sulfonate-substituted **SP** anions into layered cobalt hydroxides (CoLH) was performed.	[63]

Table 4. *Cont.*

No	5′-R or SP Photochrome Structure		R_8	Synthetic Method (Yield, %)	Spectral-Kinetic Parameters	Notes and Applications	References
SP314	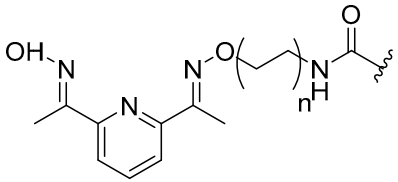	(a) n = 1	-H	C (68%)	**90% CH_3CN in water**: λ^A_{max} 342 nm/ λ^B_{max} 340, 550 nm, λ_{fl} 530 nm	**SP314** light-gated artificial transducers. Zn complex.	[168]
		(b) n = 2		C (63%)			
		(c) n = 3		C (81%)			
		(d) n = 4		C (20%)			
		(e) n = 6		C (23%)			
Photochromic ligands for the conjugation with metal cations, nanoparticles, and quantum dots							
SP315	HOOC-CH=CH-		-H	B, C (35%/ 54%)	**EtOH**: λ^A_{max} 340 nm, λ^B_{max} 555 nm, ΔD_B^{phot} 0.44, k_{BA}^{db} 0.004 s^{-1}, $\tau_{1/2}$ * s, **Toluene**: λ^A_{max} 346 nm, λ^B_{max} 622, 585 nm, ΔD_B^{phot} 0.48, k_{BA}^{db} 0.027 s^{-1}, $\tau_{1/2}$ 46 s	Two-step procedure for the preparation of **SP315** by the Horner olefination with C_2-phosphonate followed by the saponification of intermediate ester turned out to be more effective. One-step synthesis consisted in the Knoevenagel reaction with a yield of 35%.	[35,82,84]

Table 4. *Cont.*

No	5′-R or SP Photochrome Structure	R_8	Synthetic Method (Yield, %)	Spectral-Kinetic Parameters	Notes and Applications	References
SP316	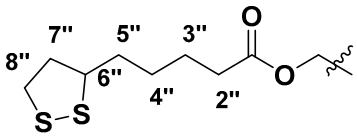	-H	B (72–42%)	**EtOH**: λ^{A}_{max} 336 nm, λ^{B}_{max} 541 nm, ΔD_B^{phot} 5.3, k_{BA}^{db} 1.94 10^{-2} s^{-1}, 6.82 10^{-4} s^{-1}, $\tau_{1/2}$ 326 s, λ_{fl} 642 nm, **Toluene**: λ^{A}_{max} 334 nm, λ^{B}_{max} 606, 580sh nm, ΔD_B^{phot} 3.63, k_{BA}^{db} 0.141 s^{-1}, 6.59 10^{-2} s^{-1}, $\tau_{1/2}$ 85 s, λ_{fl} 686 nm, **$CHCl_3$**: λ^{A}_{max} 342 nm, λ^{B}_{max} 586 nm, ΔD_B^{phot} 0.95, k_{BA}^{db} 1.21 s^{-1}, 4.96 10^{-2} s^{-1}, $\tau_{1/2}$ 4 s, λ_{fl} 663 nm, **THF**: λ^{A}_{max} 336 nm, λ^{B}_{max} 587 nm, ΔD_B^{phot} 5.3, k_{BA}^{db} 1.21 s^{-1}, 3.82 10^{-2} s^{-1}, $\tau_{1/2}$ 70 s, λ_{fl} 672 nm		[95]

Table 4. *Cont.*

No	5′-R or SP Photochrome Structure	R_8	Synthetic Method (Yield, %)	Spectral-Kinetic Parameters	Notes and Applications	References
SP317	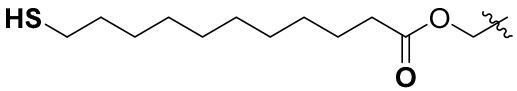	-H	B (50–55%)	**EtOH**: λ^{A}_{max} 335 nm, λ^{B}_{max} 542 nm, ΔD_{B}^{phot} 1.63, λ_{fl} 642 nm, **Toluene**: λ^{A}_{max} 333 nm, λ^{B}_{max} 604, 575sh nm, ΔD_{B}^{phot} 3.91, λ_{fl} 677 nm, **$CHCl_3$**: λ^{A}_{max} 342 nm, λ^{B}_{max} 586 nm, ΔD_{B}^{phot} 2.21, λ_{fl} 670 nm, **THF**: λ^{A}_{max} 338 nm, λ^{B}_{max} 588 nm, ΔD_{B}^{phot} 5.05		[95]
SP318	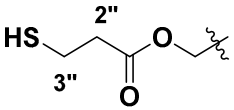	-H	C (31%)	**EtOH**: λ^{A}_{max} 336 nm, λ^{B}_{max} 390sh, 538 nm, ΔD_{B}^{phot} 1.94, λ_{fl} 638 nm		[95]
SP319	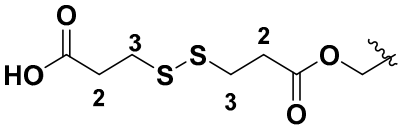	-H	B (43%)	**EtOH**: λ^{A}_{max} 302, 335 nm, λ^{B}_{max} 362, 540 nm, ΔD_{B}^{phot} 1.78, λ_{fl} 640 nm		[95]
SP320	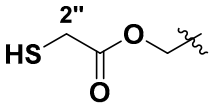	-H	B (51%)	**EtOH**: λ^{A}_{max} 330sh, 390sh nm, λ^{B}_{max} 538, 390sh nm, ΔD_{B}^{phot} 0.82, λ_{fl} 635 nm		[95]

Table 4. *Cont.*

No	5′-R or SP Photochrome Structure	R_8	Synthetic Method (Yield, %)	Spectral-Kinetic Parameters	Notes and Applications	References
SP321	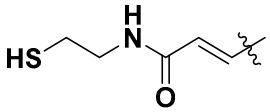	-H	C (42%)	**Toluene**: λ^{A}_{max} 341 nm, λ^{B}_{max} 620, 580sh nm, ΔD_B^{phot} 0.4, λ_{fl} 677 nm, k_{BA}^{db} 0.055 s^{-1}, $\tau_{1/2}$ 16 s, **$CHCl_3$**: λ^{A}_{max} 348 nm, λ^{B}_{max} 603, 562sh nm, ΔD_B^{phot} 0.25, λ_{fl} 670 nm, k_{BA}^{db} 0.089 s^{-1}, $\tau_{1/2}$ 2.5 s, λ_{fl} 670 nm, **THF**: λ^{A}_{max} 340 nm, λ^{B}_{max} 604, 560sh nm, ΔD_B^{phot} 0.65, k_{BA}^{db} 0.078 s^{-1}, $\tau_{1/2}$ 60 s, **CH_3CN:H_2O**: λ^{A}_{max} 224, 266, 348 nm, λ^{B}_{max} 542 nm, λ^{B}_{max} (+ graphene oxide) 432 nm, **DMSO**: λ^{A}_{max} 342 nm, λ^{B}_{max} 570 nm, ΔD_B^{phot} 0.1, k_{BA}^{db} 0.036 s^{-1}, $\tau_{1/2}$ 19 s	**SP321**-functionalized CdSe QDs	[35,91,250]

Table 4. *Cont.*

No	5′-R or SP Photochrome Structure	R_8	Synthetic Method (Yield, %)	Spectral-Kinetic Parameters	Notes and Applications	References
SP322	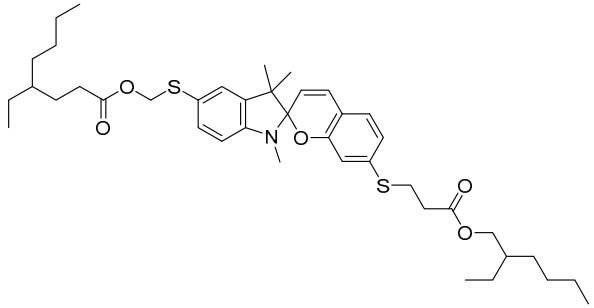		B (78%)		**SP322** was synthesized through the palladium-catalyzed coupling reaction.	[251]
SP323	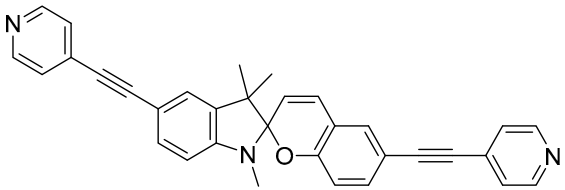		C (86%)	When **SP382** was irradiated with UV light, there is no detectable **MC** optical absorption (ca. 600 nm). λ^{B}_{max} 415 nm, **MCH**$^{+}$ form	**SP323**-functionalized Au surface electrode synthesis via Sonogashira coupling	[204]
SP324	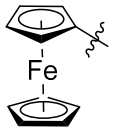	-H	A (37%)	**CH_3OH**: λ^{A}_{max} 345 nm, λ^{B}_{max} 530 nm, **CH_2Cl_2**: λ^{B}_{max} 578 nm	5′-ferrocenylspiropyran (Fc-**SP324**) was synthesized.	[252]
SP325	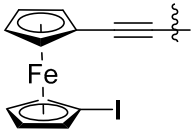	-H	A (87%)	**EtOH**: λ^{B}_{max} 565 nm, **CH_3CN**: λ^{B}_{max} 583 nm		[253]

Table 4. *Cont.*

No	5′-R or SP Photochrome Structure	R_8	Synthetic Method (Yield, %)	Spectral-Kinetic Parameters	Notes and Applications	References
SP326	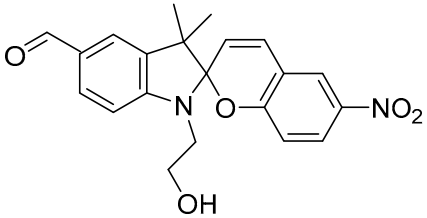		A,C (6 steps, 17.5%)		Precursor for 5′-R-6-NO_2-**SP** series synthesis	[98]
SP327	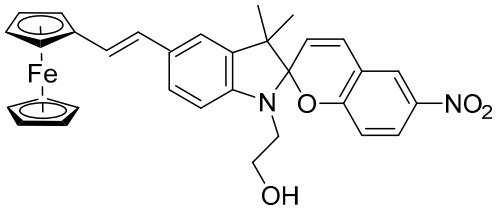		C (63%)	**CH_2Cl_2**: λ^A_{max} 334, 456 nm λ^B_{max} 334, 590 nm, **CH_3CN**: λ^A_{max} 350 nm, λ^B_{max} 334, 585 nm	5′-ferrocenylvinyl**SP** was synthesized.	[98,254]
SP328	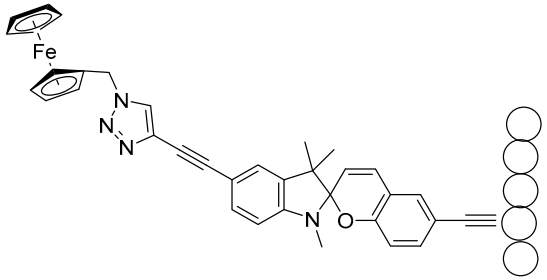				**SP328**-functionalized Au surface electrode synthesis via a click alkyne−azide copper-catalyzed cycloaddition reaction	[204]
SP329	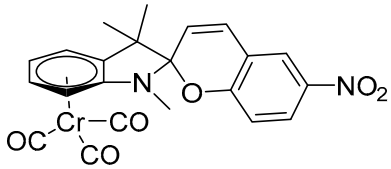		A	**Acetone**: λ^B_{max} 554 nm	Metal complexes were synthesized	[255]

Table 4. *Cont.*

No	5′-R or SP Photochrome Structure	R_8	Synthetic Method (Yield, %)	Spectral-Kinetic Parameters	Notes and Applications	References
SP330	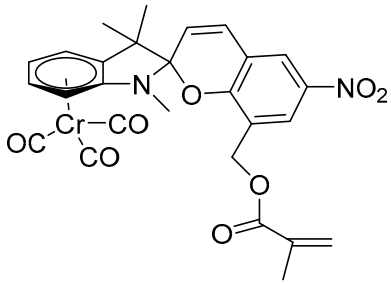		A (68%)	**Acetone**: λ^{B}_{max} 557 nm	Metal complexes were synthesized	[255]
SP331	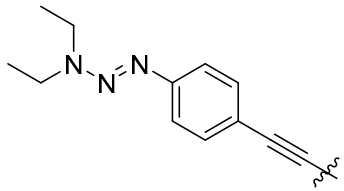	-H	B (81%)		Reversible modulation of conductance in silicon-based metal-oxide-semiconductor field-effect transistor via UV/Visible-light irradiation	[256]
SP332	X—$(CH_2)_{12}$—S—S—$(CH_2)_{12}$—X X = 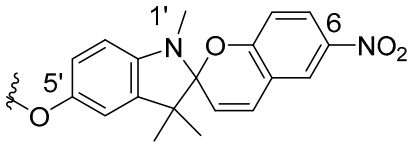		B (31%)	**THF/water (9:1)**: λ^{B}_{max} 556 nm, λ^{B}_{max} (**SP**+Zn^{+2}) 486 nm	**SP**-modified Au electrode could be reversibly modulated by UV/visible light irradiation in the presence of Zn^{2+}. A new molecular switch and an "AND" logic gates	[257]
SP333	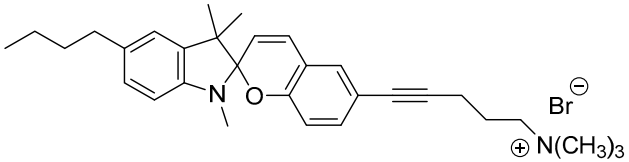		B (88%)	**H_2O, pH 7.0**: λ^{B}_{max} 380, 540 nm **H_2O, pH <7.0**: λ^{BH+}_{max} 432 nm	pH- and light-responsive Spiropyran-based surfactant	[258]

Note: see remarks after Table 1.

Table 5. Substituted **SP** derivatives in polymers, LC, and other systems **(SP334–SP432)**.

No	5′-R or SP Photochrome Structure	R_8	Synthetic Method (Yield, %)	Spectral-Kinetic Parameters	Notes and Applications	References
SP334	Cl-	-H		**in PMMA**: λ^{A}_{max} 260, 325 nm, λ^{B}_{max} 575 nm, λ^{B}_{fl} 650 nm	**SP334** in PMMA. Prototype of 3D volume memory. 3D optical random access memories (3D ORAM).	
SP335	EtOOC-	-H			**SP335** solid polymer electrolyte $LiClO_4$, poly[(ω-hydroxy) oligo(oxyethyene) methacrylate]	
SP336	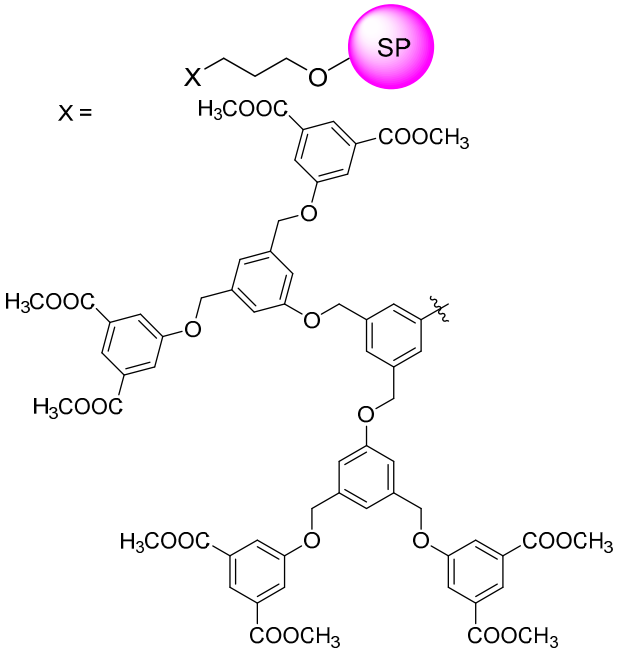		B (50%)	**Toluene**: λ^{A}_{max} 310 nm, λ^{B}_{max} 608, 570sh nm, λ^{B}_{fl} 667 nm	Synthesis of spiropyran **SP336-functionalized** dendron and organogel are reported.	[182]

Table 5. *Cont.*

No	5′-R or SP Photochrome Structure	R_8	Synthetic Method (Yield, %)	Spectral-Kinetic Parameters	Notes and Applications	References
SP337	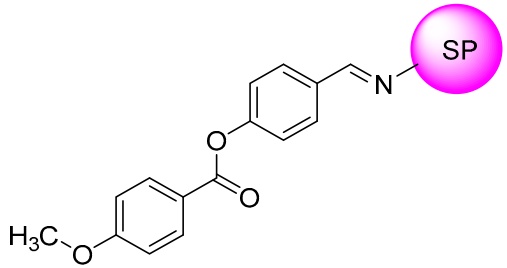		A (37%)	**Benzene**: λ^{A}_{max} 370 nm	**SP337** practically not photochromic. Precursor for synthesis.	[78]
SP338	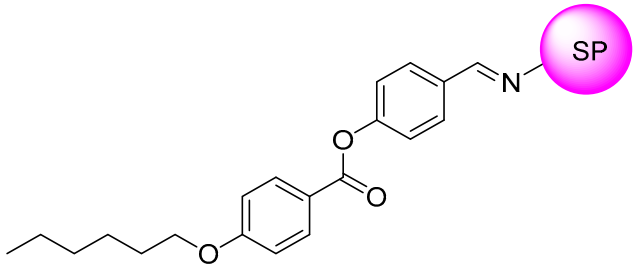		A (45%)	**Benzene**: λ^{A}_{max} 375 nm	**SP338** practically not photochromic. Precursor for synthesis.	[78]
SP339	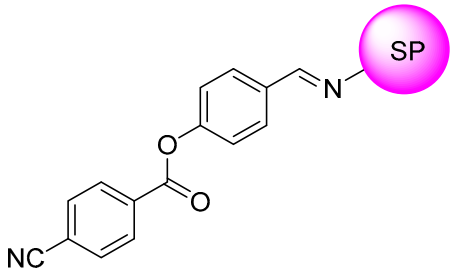		A (48%)	**Benzene**: λ^{A}_{max} 370 nm	**SP339** practically not photochromic. Precursor for synthesis.	[78]

Table 5. *Cont.*

No	5′-R or SP Photochrome Structure		R_8	Synthetic Method (Yield, %)	Spectral-Kinetic Parameters	Notes and Applications	References
SP340	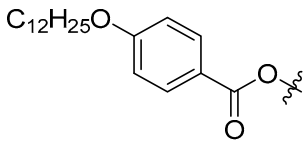		-H	B (65%)	**THF**: λ^{A}_{max} 355 nm, λ^{B}_{max} 370, 585 nm, λ^{B}_{max} (**SP**+CH_3SO_3H) 420 nm	New family of **SP** liquid crystal materials.	[187]
SP341	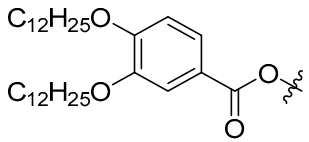		-H	B (81%)	**THF**: λ^{A}_{max} 355 nm, λ^{B}_{max} 370, 585 nm, λ^{B}_{max} (**SP**+CH_3SO_3H) 420 nm	New family of **SP** liquid crystal materials.	[187]
SP342	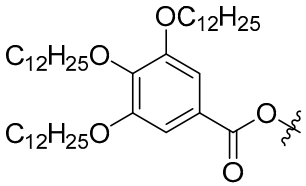		-H	B (95%)	**THF**: λ^{A}_{max} 355 nm, λ^{B}_{max} 370, 585 nm, λ^{B}_{max} (**SP**+CH_3SO_3H) 420 nm	New family of **SP** liquid crystal materials.	[187]
SP343	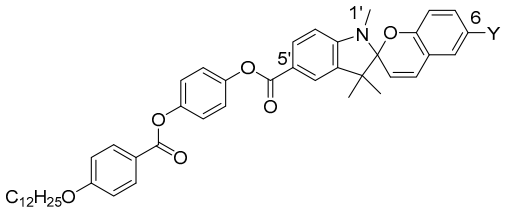	(a) Y = -H		B (77%)	**CH_2Cl_2**: λ^{A}_{max} 230, 270, 310 nm, λ^{B}_{max} 230, 270, 310, 390, 490 nm	Photochromic **SP**-based liquid crystals.	[186]
		(b) Y = -Br		B (80%)	**CH_2Cl_2**: λ^{A}_{max} 230, 270, 310 nm, λ^{B}_{max} 230, 270, 310, 380, 500 nm		
		(c) Y = $-CF_3$		B (77%)	**CH_2Cl_2**: λ^{A}_{max} 230, 270, 310 nm		

Table 5. *Cont.*

No	5′-R or SP Photochrome Structure		R_8	Synthetic Method (Yield, %)	Spectral-Kinetic Parameters	Notes and Applications	References
		(d) Y = -CN		B (45%)	**CH_2Cl_2**: λ^A_{max} 230, 270, 310 nm, λ^B_{max} 230, 270, 310, 470 nm		
		(e) Y = -NO_2		B (41%)	**CH_2Cl_2**: λ^A_{max} 230, 270, 310, 365sh nm, λ^B_{max} 230, 270, 310, 480, 600 nm		
SP344	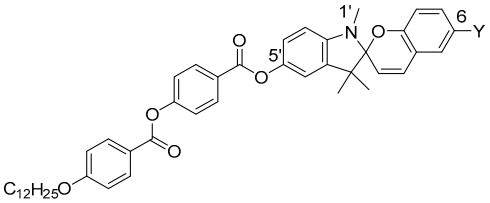	(a) Y = -H		B (59%)	**CH_2Cl_2**: λ^A_{max} 230, 270, 310 nm	Photochromic **SP**-based liquid crystals.	[186]
		(b) Y = -Br		B (82%)	**CH_2Cl_2**: λ^A_{max} 230, 270, 310 nm		
		(c) Y = -CF_3		B (28%)	**CH_2Cl_2**: λ^A_{max} 230, 270, 310 nm, λ^B_{max} 230, 270, 310, 440 nm		
		(d) Y = -CN		B (65%)	**CH_2Cl_2**: λ^A_{max} 230, 270, 310 nm		
		(e) Y = -NO_2		B (44%)	**CH_2Cl_2**: λ^A_{max} 230, 270, 310, 365sh nm, λ^B_{max} 230, 270, 310, 350sh, 440 nm		

Table 5. *Cont.*

No	5′-R or SP Photochrome Structure	R_8	Synthetic Method (Yield, %)	Spectral-Kinetic Parameters	Notes and Applications	References
SP345	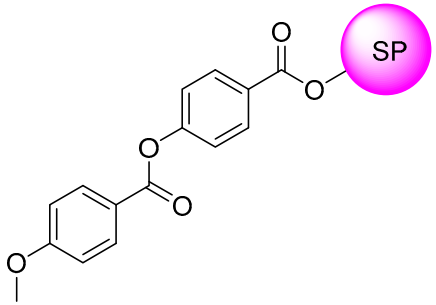		B		**SP345** QLCs	[185]
SP346	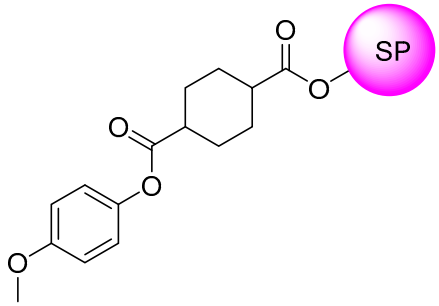		B		**SP346** QLCs	[185]
SP347	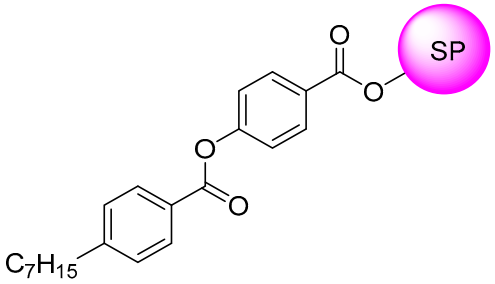		B		**SP347** QLCs	[185]

Table 5. *Cont.*

No	5′-R or SP Photochrome Structure	R_8	Synthetic Method (Yield, %)	Spectral-Kinetic Parameters	Notes and Applications	References
SP348	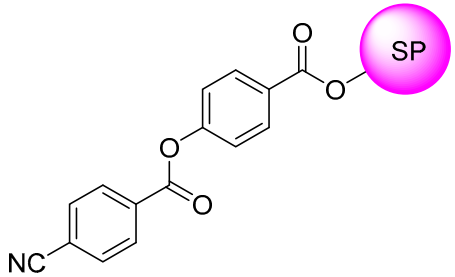		B		**SP348** QLCs	[185]
SP349	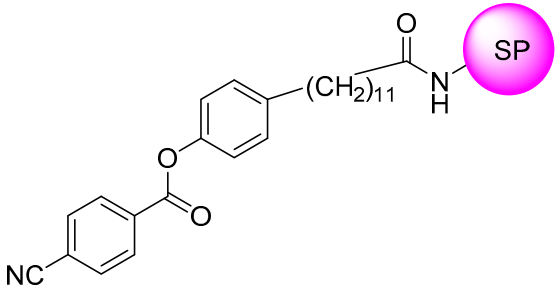		B (55%)		**SP349** QLCs	[185]
SP350	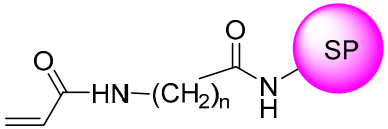	(a) $n = 2$	B (37%)		Precursors for synthesis of photochromic polyacrylates and polysiloxanes.	[183,184]
		(b) $n = 5$	B (71%)			
		(c) $n = 11$	B (43%)			

Table 5. *Cont.*

No	5′-R or SP Photochrome Structure	R_8	Synthetic Method (Yield, %)	Spectral-Kinetic Parameters	Notes and Applications	References
SP351	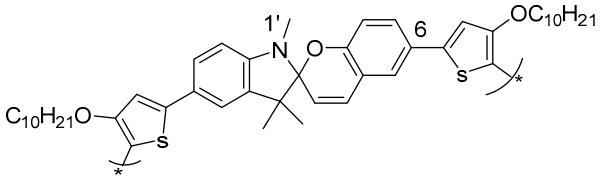		electropolymerization	**CH_3OH**: **CH_2Cl_2 (1:1) polyTMC4**: λ^A_{max} 425, 490 nm, λ^B_{max} (**SP**+Co^{2+}) 425, 517, 597, 655 nm	**SP351** with two alkoxy-substituted thienyl units furnishing a monomer suitable for electropolymerization	[110]
SP352	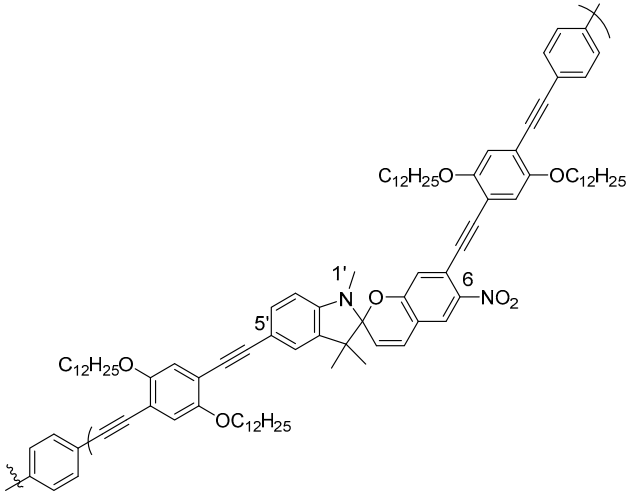		B	**$CHCl_3$**: λ^A_{max} 315, 397 nm, λ^B_{max} 309, 388, 500 nm	**SP352** containing polyphenyleneethynylene copolymer. **SP**-copolymer was prepared by palladium-catalyzed polymerization of monomer by $Pd(PPh_3)_2Cl_2$ and CuI in a mixture of toluene and triethylamine.	[180]
SP353	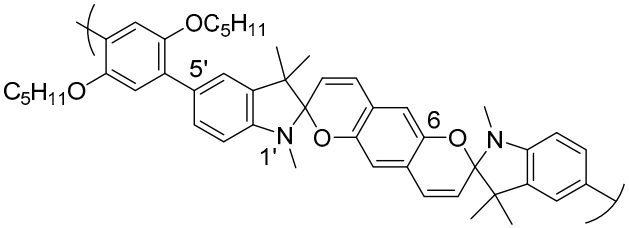				Copolymer of bis-**SP** with phenylene.	[192]

Table 5. *Cont.*

No	5′-R or SP Photochrome Structure	R_8	Synthetic Method (Yield, %)	Spectral-Kinetic Parameters	Notes and Applications	References
SP354	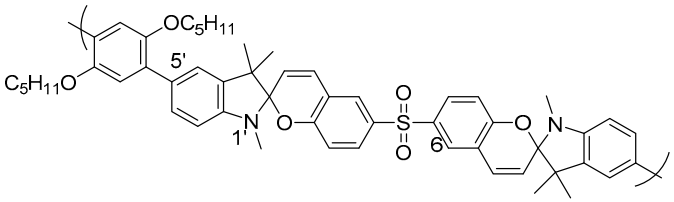				Copolymer of **SP354**-sulfone with phenylene	[192]
SP355	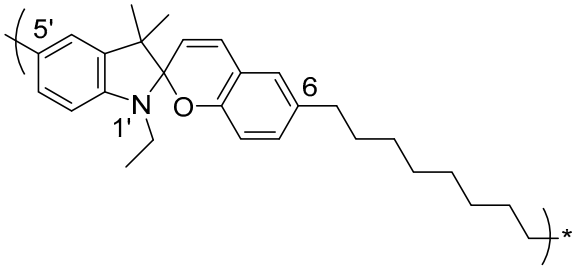				**SP** main chain copolymers prepared by Suzuki polycondensation.	[192]
SP356	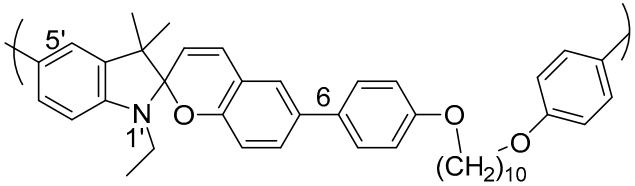				**SP** main chain copolymers prepared by MW-assisted Suzuki–Miyaura polycondensation.	[109,177]
SP357	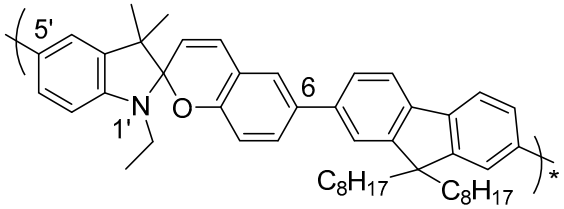				**SP** main chain copolymers based on alternating spiropyran (**SP**) and 9,9-dioctylfluorene (F8) units were synthesized via Suzuki polycondensation (SPC).	[176]

Table 5. *Cont.*

No	5′-R or SP Photochrome Structure	R_8	Synthetic Method (Yield, %)	Spectral-Kinetic Parameters	Notes and Applications	References
SP358	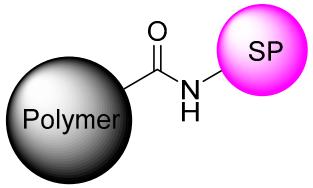		D		Synthesis of photochromic **SP**-polyacrylates and **SP**-polysiloxanes.	[184,259]
SP359	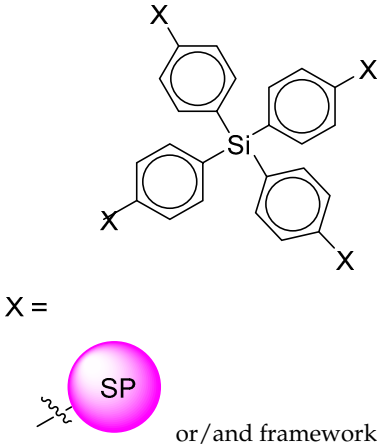		C	**Toluene**: λ^{A}_{max} 320, 340sh nm, λ^{B}_{max} 590sh, 610 nm, λ^{B}_{fl} 660 nm	PhotoPAF- (photoresponsive porous aromatic framework). 3D rigid and porous **SP** networks.	[76]

Note: see remarks after Table 1.

Author Contributions: Conceptualization, A.A.K. and V.A.B.; writing—original draft preparation, A.A.K., N.E.B., A.Y.L., A.V.L., S.D.V. and O.V.D.; writing—review and editing, A.A.K. and O.V.D. All authors have read and agreed to the published version of the manuscript.

Funding: This research received no external funding.

Institutional Review Board Statement: Not applicable.

Informed Consent Statement: Not applicable.

Data Availability Statement: Not applicable.

Conflicts of Interest: The authors declare no conflict of interest.

References

1. Barachevsky, V.A.; Lashkov, G.I.; Tsekhomskii, V.A. *Fotokhromism i Ego Primenenie (Photochromism and Its Application)*; Khimiya: Moscow, Russia, 1977.
2. Dürr, H.; Bouas-Laurent, H. (Eds.) *Photochromism: Molecules and Systems*; Elsevier B.V.: Amsterdam, The Netherlands, 2003; ISBN 978-0-444-51322-9.
3. Crano, J.C.; Guglielmetti, R.J. (Eds.) *Organic Photochromic and Thermochromic Compounds*; Topics in Applied Chemistry; Kluwer Academic/Plenum Publishers: New York, NY, USA, 1999; ISBN 978-0-306-45882-8.
4. Kozlenko, A.S.; Ozhogin, I.V.; Pugachev, A.D.; Lukyanova, M.B.; El-Sewify, I.M.; Lukyanov, B.S. A Modern Look at Spiropyrans: From Single Molecules to Smart Materials. *Top. Curr. Chem.* **2023**, *381*, 8. [CrossRef] [PubMed]
5. Towns, A. Spiropyran Dyes. *Phys. Sci. Rev.* **2021**, *6*, 341–368. [CrossRef]
6. Tian, H.; Zhang, J.; He, T. (Eds.) *Photochromic Materials: Preparation, Properties and Applications*; Wiley-VCH: Weinheim, Germany, 2016; ISBN 978-3-527-68370-3.
7. Feringa, B.L.; Browne, W.R. (Eds.) *Molecular Switches*, 2nd ed.; Wiley-VCH: Weinheim, Germany, 2011; ISBN 978-3-527-31365-5.
8. Coudret, C.; Chernyshev, A.V.; Metelitsa, A.V.; Micheau, J.C. New Trends in Spiro-Compounds Photochromic Metals Sensors: Quantitative Aspects. In *Photon-Working Switches*; Yokoyama, Y., Nakatani, K., Eds.; Springer: Tokyo, Japan, 2017; pp. 3–35. ISBN 978-4-431-56542-0.
9. Kortekaas, L.; Browne, W.R. Spiropyran—Multifaceted Chromic Compounds. In *Molecular Photoswitches*; Pianowski, Z.L., Ed.; Wiley: Hoboken, NJ, USA, 2022; pp. 131–149. ISBN 978-3-527-35104-6.
10. Kortekaas, L.; Browne, W.R. The Evolution of Spiropyran: Fundamentals and Progress of an Extraordinarily Versatile Photochrome. *Chem. Soc. Rev.* **2019**, *48*, 3406–3424. [CrossRef]
11. Barachevsky, V.A. Photochromic Spirocompounds and Chromenes for Sensing Metal Ions. *Rev. J. Chem.* **2013**, *3*, 52–94. [CrossRef]
12. Barachevsky, V.A. Negative Photochromism in Organic Systems. *Rev. J. Chem.* **2017**, *7*, 334–371. [CrossRef]
13. Paramonov, S.V.; Lokshin, V.; Fedorova, O.A. Spiropyran, Chromene or Spirooxazine Ligands: Insights into Mutual Relations between Complexing and Photochromic Properties. *J. Photochem. Photobiol. C Photochem. Rev.* **2011**, *12*, 209–236. [CrossRef]
14. Keyvan Rad, J.; Balzade, Z.; Mahdavian, A.R. Spiropyran-Based Advanced Photoswitchable Materials: A Fascinating Pathway to the Future Stimuli-Responsive Devices. *J. Photochem. Photobiol. C Photochem. Rev.* **2022**, *51*, 100487. [CrossRef]
15. Ali, A.A.; Kharbash, R.; Kim, Y. Chemo- and Biosensing Applications of Spiropyran and Its Derivatives—A Review. *Anal. Chim. Acta* **2020**, *1110*, 199–223. [CrossRef]
16. Demina, O.V.; Belikov, N.E.; Melnikova, I.A.; Lukin, A.Y.; Varfolomeev, S.D.; Khodonov, A.A. New Labels and Probes for the Application in Bionanophotonics. *Russ. J. Phys. Chem. B* **2019**, *13*, 938–941. [CrossRef]
17. Bertelson, R.C. Reminiscences about Organic Photochromics. *Mol. Cryst. Liq. Cryst. Sci. Technol. Sect. Mol. Cryst. Liq. Cryst.* **1994**, *246*, 1–8. [CrossRef]
18. Pianowski, Z.L. (Ed.) *Molecular Photoswitches: Chemistry, Properties, and Applications, 2 Volume Set*; Wiley: Hoboken, NJ, USA, 2022; ISBN 978-3-527-35104-6.
19. Dzaparidze, K.G. *Spirochromenes*; Meznierebа: Tbilisi, Georgia, 1979.
20. Fischer, E.; Hirshberg, Y. Formation of Coloured Forms of Spirans by Low-Temperature Irradiation. *J. Chem. Soc.* **1952**, 4522–4524.
21. Bertelson, R.C. Chapter 3 "Photochromic Process Involving Heterolytic Cleavage". In *Photochromism*; Brown, G.H., Ed.; Techniques of Chemistry; Wiley: London, UK, 1971; Volume III, pp. 45–431.
22. Bertelson, R.C. Spiropyrans. In *Organic Photochromic and Thermochromic Compounds*; Crano, J.C., Guglielmetti, R., Eds.; Plenum Press: New York, NY, USA, 1999; Volume I, pp. 11–83.
23. Zakhs, E.R.; Martynova, V.M.; Efros, L.S. Synthesis and Properties of Spiropyrans That Are Capable of Reversible Opening of the Pyran Ring (Review). *Chem. Heterocycl. Compd.* **1979**, *15*, 351–372. [CrossRef]
24. Lukyanov, B.S.; Lukyanova, M.B. Spiropyrans: Synthesis, Properties, and Application. (Review). *Chem. Heterocycl. Compd.* **2005**, *41*, 281–311. [CrossRef]
25. Berkovic, G.; Krongauz, V.; Weiss, V. Spiropyrans and Spirooxazines for Memories and Switches. *Chem. Rev.* **2000**, *100*, 1741–1754. [CrossRef]

26. Minkin, V.I. Photo-, Thermo-, Solvato-, and Electrochromic Spiroheterocyclic Compounds. *Chem. Rev.* **2004**, *104*, 2751–2776. [CrossRef]
27. Kozlenko, A.S.; Pugachev, A.D.; Ozhogin, I.V.; El-Sewify, I.M.; Lukyanov, B.S. Spiropyrans: Molecules in Motion. *Chem. Heterocycl. Compd.* **2021**, *57*, 984–989. [CrossRef]
28. Pugachev, A.D.; Mukhanov, E.L.; Ozhogin, I.V.; Kozlenko, A.S.; Metelitsa, A.V.; Lukyanov, B.S. Isomerization and Changes of the Properties of Spiropyrans by Mechanical Stress: Advances and Outlook. *Chem. Heterocycl. Compd.* **2021**, *57*, 122–130. [CrossRef]
29. Aiken, S.; Edgar, R.J.L.; Gabbutt, C.D.; Heron, B.M.; Hobson, P.A. Negatively Photochromic Organic Compounds: Exploring the Dark Side. *Dyes Pigments* **2018**, *149*, 92–121. [CrossRef]
30. Chibisov, A.K.; Görner, H. Photochromism of Spirobenzopyranindolines and Spironaphthopyranindolines. *Phys. Chem. Chem. Phys.* **2001**, *3*, 424–431. [CrossRef]
31. Görner, H. Photochromism of Nitrospiropyrans: Effects of Structure, Solvent and Temperature. *Phys. Chem. Chem. Phys.* **2001**, *3*, 416–423. [CrossRef]
32. Belikov, N.E.; Lukin, A.Y.; Varfolomeev, S.D.; Levina, I.I.; Petrovskaya, L.E.; Demina, O.V.; Barachevsky, V.A.; Khodonov, A.A. Spectral Study of the Structure and Properties of Complexes of Unsubstituted Indoline Spiropyran with Aluminum Ions. *Opt. Spectrosc.* **2022**, *130*, 538–546. [CrossRef]
33. Kume, S.; Nishihara, H. Photochrome-Coupled Metal Complexes: Molecular Processing of Photon Stimuli. *Dalton Trans.* **2008**, *25*, 3260–3271. [CrossRef] [PubMed]
34. Guerchais, V.; Ordronneau, L.; Le Bozec, H. Recent Developments in the Field of Metal Complexes Containing Photochromic Ligands: Modulation of Linear and Nonlinear Optical Properties. *Coord. Chem. Rev.* **2010**, *254*, 2533–2545. [CrossRef]
35. Zvezdin, K.V.; Belikov, N.E.; Laptev, A.V.; Lukin, A.Y.; Demina, O.V.; Levin, P.P.; Brichkin, S.B.; Spirin, M.G.; Razumov, V.F.; Shvets, V.I.; et al. New Hybrid Photochromic Materials with Switchable Fluorescence. *Nanotechnol. Russ.* **2012**, *7*, 308–317. [CrossRef]
36. Kume, S.; Nishihara, H. Metal-Based Photoswitches Derived from Photoisomerization. In *Photofunctional Transition Metal Complexes*; Yam, V.W.W., Ed.; Structure and Bonding; Springer: Berlin/Heidelberg, Germany, 2006; Volume 123, pp. 79–112. ISBN 978-3-540-36809-0.
37. Chernyshev, A.V.; Voloshin, N.A.; Rostovtseva, I.A.; Demidov, O.P.; Shepelenko, K.E.; Solov'eva, E.V.; Gaeva, E.B.; Metelitsa, A.V. Benzothiazolyl Substituted Spiropyrans with Ion-Driven Photochromic Transformation. *Dyes Pigments* **2020**, *178*, 108337. [CrossRef]
38. Belser, P.; De Cola, L.; Hartl, F.; Adamo, V.; Bozic, B.; Chriqui, Y.; Iyer, V.M.; Jukes, R.T.F.; Kühni, J.; Querol, M.; et al. Photochromic Switches Incorporated in Bridging Ligands: A New Tool to Modulate Energy-Transfer Processes. *Adv. Funct. Mater.* **2006**, *16*, 195–208. [CrossRef]
39. Jukes, R.T.F.; Bozic, B.; Belser, P.; De Cola, L.; Hartl, F. Photophysical and Redox Properties of Dinuclear Ru and Os Polypyridyl Complexes with Incorporated Photostable Spiropyran Bridge. *Inorg. Chem.* **2009**, *48*, 1711–1721. [CrossRef]
40. Abdullah, A.; Roxburgh, C.J.; Sammes, P.G. Photochromic Crowned Spirobenzopyrans: Quantitative Metal-Ion Chelation by UV, Competitive Selective Ion-Extraction and Metal-Ion Transportation Demonstration Studies. *Dyes Pigments* **2008**, *76*, 319–326. [CrossRef]
41. Kholmanskii, A.S.; Dyumaev, K.M. The Photochemistry and Photophysics of Spiropyrans. *Russ. Chem. Rev.* **1987**, *56*, 136–151. [CrossRef]
42. Krysanov, S.A.; Alfimov, M.V. Ultrafast Formation of Transients in Spiropyran Photochromism. *Chem. Phys. Lett.* **1982**, *91*, 77–80. [CrossRef]
43. Görner, H.; Atabekyan, L.S.; Chibisov, A.K. Photoprocesses in Spiropyran-Derived Merocyanines: Singlet versus Triplet Pathway. *Chem. Phys. Lett.* **1996**, *260*, 59–64. [CrossRef]
44. Melnikova, I.A.; Belikov, N.E.; Bakholdina, A.G.; Lukin, A.Y.; Varfolomeev, S.D.; Demina, O.V.; Khodonov, A.A. Study of the Interaction of a New Photochromic Podand with Metal Salts in Solutions of Organic Solvents. In Proceedings of the XIX Annual International Youth Conference IBCP RAS-Universities "Biochemical Physics", Moscow, Russia, 28–30 October 2019; pp. 152–155.
45. Demina, O.V.; Levin, P.P.; Belikov, N.E.; Laptev, A.V.; Lukin, A.Y.; Barachevsky, V.A.; Shvets, V.I.; Varfolomeev, S.D.; Khodonov, A.A. Synthesis and Photochromic Reaction Kinetics of Unsaturated Spiropyran Derivatives. *J. Photochem. Photobiol. Chem.* **2013**, *270*, 60–66. [CrossRef]
46. Levin, P.P.; Tatikolov, A.S.; Laptev, A.V.; Lukin, A.Y.; Belikov, N.E.; Demina, O.V.; Khodonov, A.A.; Shvets, V.I.; Varfolomeev, S.D. The Investigation of the Intermediates of Spiropyran Retinal Analogs by Laser Flash Photolysis Techniques with Different Excitation Wavelengths. *J. Photochem. Photobiol. Chem.* **2012**, *231*, 41–44. [CrossRef]
47. Tamai, N.; Miyasaka, H. Ultrafast Dynamics of Photochromic Systems. *Chem. Rev.* **2000**, *100*, 1875–1890. [CrossRef] [PubMed]
48. Murin, V.A.; Mandjikov, V.F.; Barachevskii, V.A. Study of Triplet-Triplet Absorption of Photochromic Spiropyran by Laser Photoexcitation. *Opt. Spectrosc.* **1976**, *40*, 1084–1086.
49. Murin, V.A.; Mandjikov, V.F.; Barachevskii, V.A. Study of Photochromism of Methoxysubstituted Indolenine Spiropyrans by Laser Nanosecond Spectroscopy. *Opt. Spectrosc.* **1977**, *41*, 79–81.
50. Melnikova, I.A.; Lukin, A.Y.; Belikov, N.E.; Demina, O.V.; Levin, P.P.; Varfolomeev, S.D.; Khodonov, A.A. Synthesis and Study of the Spectral Properties of a Series of Stilbenes Containing, as One of the Aryl Fragments, a Molecule of a Photochromic Label of the Spiropyran Series. In Proceedings of the XIV Annual International Youth Conference IBCP RAS-Universities "Biochemical Physics", Moscow, Russia, 28–30 October 2014; pp. 128–133.

51. Feuerstein, T.J.; Müller, R.; Barner-Kowollik, C.; Roesky, P.W. Investigating the Photochemistry of Spiropyran Metal Complexes with Online LED-NMR. *Inorg. Chem.* **2019**, *58*, 15479–15486. [CrossRef]
52. Pugachev, A.D.; Ozhogin, I.V.; Lukyanova, M.B.; Lukyanov, B.S.; Kozlenko, A.S.; Rostovtseva, I.A.; Makarova, N.I.; Tkachev, V.V.; Aldoshin, S.M.; Metelitsa, A.V. Synthesis, Structure and Photochromic Properties of Indoline Spiropyrans with Electron-Withdrawing Substituents. *J. Mol. Struct.* **2021**, *1229*, 129615. [CrossRef]
53. Ren, J.; Tian, H. Thermally Stable Merocyanine Form of Photochromic Spiropyran with Aluminum Ion as a Reversible Photo-Driven Sensor in Aqueous Solution. *Sensors* **2007**, *7*, 3166–3178. [CrossRef]
54. Tian, W.; Tian, J. An Insight into the Solvent Effect on Photo-, Solvato-Chromism of Spiropyran through the Perspective of Intermolecular Interactions. *Dyes Pigments* **2014**, *105*, 66–74. [CrossRef]
55. Zhou, J.; Li, Y.; Tang, Y.; Zhao, F.; Song, X.; Li, E. Detailed Investigation on a Negative Photochromic Spiropyran. *J. Photochem. Photobiol. Chem.* **1995**, *90*, 117–123. [CrossRef]
56. Song, X.; Zhou, J.; Li, Y.; Tang, Y. Correlations between Solvatochromism, Lewis Acid-Base Equilibrium and Photochromism of an Indoline Spiropyran. *J. Photochem. Photobiol. Chem.* **1995**, *92*, 99–103. [CrossRef]
57. Seiler, V.K.; Robeyns, K.; Tumanov, N.; Cinčić, D.; Wouters, J.; Champagne, B.; Leyssens, T. A Coloring Tool for Spiropyrans: Solid State Metal–Organic Complexation versus Salification. *CrystEngComm* **2019**, *21*, 4925–4933. [CrossRef]
58. Keum, S.-R.; Ku, B.-S.; Shin, J.-T.; Ko, J.J.; Buncel, E. Stereoselective Formation of Dicondensed Spiropyran Product Obtained from the Reaction of Excess Fischer Base with Salicylaldehydes: First Full Characterization by X-Ray Crystal Structure Analysis of a DC·acetone Crystal. *Tetrahedron* **2005**, *61*, 6720–6725. [CrossRef]
59. Wizinger, R.; Wenning, H. Über Intramolekulare Ionisation. *Helv. Chim. Acta* **1940**, *23*, 247–271. [CrossRef]
60. Gal'bershtam, M.A.; Bondarenko, E.M.; Khrolova, O.R.; Bolyleva, G.K.; Pod'yachev, Y.B.; Przhiyalgovskaya, N.M.; Suvorov, N.N. Synthesis and Photochromic Properties of 5-Acetyl-Substituted Indolinospirochromenes. *Chem. Heterocycl. Compd.* **1979**, *15*, 1329–1333. [CrossRef]
61. Schulz-Senft, M.; Gates, P.J.; Sönnichsen, F.D.; Staubitz, A. Diversely Halogenated Spiropyrans—Useful Synthetic Building Blocks for a Versatile Class of Molecular Switches. *Dyes Pigments* **2017**, *136*, 292–301. [CrossRef]
62. Sugahara, A.; Tanaka, N.; Okazawa, A.; Matsushita, N.; Kojima, N. Photochromic Property of Anionic Spiropyran with Sulfonate-Substituted Indoline Moiety. *Chem. Lett.* **2014**, *43*, 281–283. [CrossRef]
63. Tanaka, N.; Okazawa, A.; Sugahara, A.; Kojima, N. Development of a Photoresponsive Organic–Inorganic Hybrid Magnet: Layered Cobalt Hydroxides Intercalated with Spiropyran Anions. *Bull. Chem. Soc. Jpn.* **2015**, *88*, 1150–1155. [CrossRef]
64. Zhang, P.; Meng, J.; Li, X.; Wang, Y.; Matsuura, T. Synthesis and Photochromism of Photochromic Spiro Compounds Having a Reactive Pendant Group. *J. Heterocycl. Chem.* **2002**, *39*, 179–184. [CrossRef]
65. Zhang, P.; Meng, J.B.; Matsuura, T.; Wang, Y.M. DNA Modification with Photochromic Spiro Compounds. *Chin. Chem. Lett.* **2002**, *13*, 299–302.
66. Gal'bershtam, M.A.; Lazarenko, I.B.; Bobyleva, G.K.; Pod'yachev, Y.B.; Przhiyalgovskaya, N.M.; Suvorov, N.N. Photochromic 5-Styryl-Substituted Indolinospirochromenes. *Chem. Heterocycl. Compd.* **1984**, *20*, 1222–1225. [CrossRef]
67. Gal'bershtam, M.A.; Przhiyalgovskaya, N.M.; Lazarenko, I.B.; Kononova, V.S.; Suvorov, N.N. Synthesis and Spectral Characteristics of Photochromic 5′-Aryl-1′,3′,3′-trimethyl-6-nitro-2H-chromene-2-spiro-2′-indolines. *Chem. Heterocycl. Compd.* **1976**, *12*, 417–419. [CrossRef]
68. Gal'bershtam, M.A.; Przhiyalgovskaya, N.M.; Samoilova, N.P.; Braude, E.V.; Lazarenko, I.B.; Suvorov, N.N. Effect of Aryl Substituents on the Rate of Dark Decolorization of Photochromic Spirochromenes of the Indoline Series. *Chem. Heterocycl. Compd.* **1977**, *13*, 67–69. [CrossRef]
69. Samat, A.; De Keukeleire, D.; Guglielmetti, R. Synthesis and Spectrokinetic Properties of Photochromic Spiropyrans. *Bull. Sociétés Chim. Belg.* **2010**, *100*, 679–700. [CrossRef]
70. Zhao, W.; Carreira, E.M. Solid-Phase Synthesis of Photochromic Spiropyrans. *Org. Lett.* **2005**, *7*, 1609–1612. [CrossRef]
71. Perry, A.; Davis, K.; West, L. Synthesis of Stereochemically-Biased Spiropyrans by Microwave-Promoted, One-Pot Alkylation–Condensation. *Org. Biomol. Chem.* **2018**, *16*, 7245–7254. [CrossRef]
72. Silvia, T.R.; Ana, V.S.L.; González, E.A.S. Novel Syntheses of Spiropyran Photochromatic Compounds Using Ultrasound. *Synth. Commun.* **1995**, *25*, 105–110. [CrossRef]
73. Pargaonkar, J.G.; Patil, S.K.; Vajekar, S.N. Greener Route for the Synthesis of Photo- and Thermochromic Spiropyrans Using a Highly Efficient, Reusable, and Biocompatible Choline Hydroxide in an Aqueous Medium. *Synth. Commun.* **2018**, *48*, 208–215. [CrossRef]
74. Cho, Y.J.; Lee, S.H.; Bae, J.W.; Pyun, H.-J.; Yoon, C.M. Fischer's Base as a Protecting Group: Protection and Deprotection of 2-Hydroxybenzaldehydes. *Tetrahedron Lett.* **2000**, *41*, 3915–3917. [CrossRef]
75. Zakhs, E.R.; Zvenigorodskaya, L.A.; Leshenyuk, N.G.; Martynova, V.P. Bromination of Spiropyrans and Reduction of Their Nitro Derivatives. *Chem. Heterocycl. Compd.* **1977**, *13*, 1055–1061. [CrossRef]
76. Kundu, P.K.; Olsen, G.L.; Kiss, V.; Klajn, R. Nanoporous Frameworks Exhibiting Multiple Stimuli Responsiveness. *Nat. Commun.* **2014**, *5*, 3588. [CrossRef]
77. Samoilova, N.P.; Gal'bershtam, M.A. Some Substitution Reactions in a Number of Photochromic Indolinespirochromenes. *Chem. Heterocycl. Compd.* **1977**, *13*, 855–858. [CrossRef]

78. Shvartsman, F.P.; Krongauz, V.A. Quasi-Liquid Crystals of Thermochromic Spiropyrans. A Material Intermediate between Supercooled Liquids and Mesophases. *J. Phys. Chem.* **1984**, *88*, 6448–6453. [CrossRef]
79. Laptev, A.V.; Lukin, A.J.; Belikov, N.E.; Fomin, M.A.; Demina, O.V.; Shvets, V.I.; Khodonov, A.A. Photochromic 5′-Vinyl-6-nitro-spirobenzopyran Derivatives and Production Method Thereof. Patent RU2458927C1, 20 August 2012.
80. Laptev, A.V.; Lukin, A.Y.; Belikov, N.E.; Barachevskii, V.A.; Demina, O.V.; Khodonov, A.A.; Varfolomeev, S.D.; Shvets, V.I. Ethynyl-Equipped Spirobenzopyrans as Promising Photochromic Markers for Nucleic Acid Fragments. *Mendeleev Commun.* **2013**, *23*, 145–146. [CrossRef]
81. Laptev, A.V.; Lukin, A.Y.; Belikov, N.E.; Demina, O.V.; Khodonov, A.A.; Shvets, V.I. New Maleimide Spirobenzopyran Derivatives as Photochromic Labels for Macromolecules with Sulfhydryl Groups. *Mendeleev Commun.* **2014**, *24*, 245–246. [CrossRef]
82. Laptev, A.V.; Lukin, A.Y.; Belikov, N.E.; Zvezdin, K.V.; Demina, O.V.; Barachevsky, V.A.; Varfolomeev, S.D.; Khodonov, A.A.; Shvets, V.I. Synthesis and Studies of Photochromic Properties of Spirobenzopyran Carboxy Derivatives and Their Model Compounds as Potential Markers. *Russ. Chem. Bull.* **2014**, *63*, 2026–2035. [CrossRef]
83. Laptev, A.V.; Lukin, A.Y.; Belikov, N.V.; Demina, O.V.; Varfolomeev, S.D.; Barachevsky, V.A.; Khodonov, A.A.; Shvets, V.I. Synthesis and Study of the Photochromic Behavior of Substituted 6′-Nitro-1,3,3-trimethyl-5-vinylspiro(indolino-2,2′-[2H]chromenes). *Vestn. MITHT* **2013**, *8*, 18–25.
84. Laptev, A.V.; Lukin, A.Y.; Belikov, N.E.; Zemtsov, R.V.; Shvets, V.I.; Demina, O.V.; Varfolomeev, S.D.; Barachevskii, V.A.; Khodonov, A.A. Synthesis and Study of the Photochromic Behavior of 3-[6′-Nitro-1,3,3-trimethylspiro(indolino-2,2′-[2H]-chromen-5-yl)]Propenoic Acid and Its Ethyl Ester. *High Energy Chem.* **2010**, *44*, 211–215. [CrossRef]
85. Khodonov, A.A.; Demina, O.V.; Laptev, A.V.; Belikov, N.E.; Lukin, A.Y.; Fomin, M.A.; Shvets, V.I.; Varfolomeev, S.D. Synthesis and Study of Spectral Properties of Labelled Isoxazole Derivatives. In Proceedings of the Materials of Russian-French Joint Symposium on Organic Photochromes "Phenics in Russia", Chernogolovka, Russia, 6–8 October 2011; p. 50.
86. Laptev, A.; Lukin, A.; Belikov, N.; Fomin, M.; Zvezdin, K.; Demina, O.; Barachevsky, V.; Varfolomeev, S.; Shvets, V.; Khodonov, A. Polyenic Spirobenzopyrans: Synthesis and Study of Photochromic Properties. *J. Photochem. Photobiol. Chem.* **2011**, *222*, 16–24. [CrossRef]
87. Laptev, A.V.; Lukin, A.J.; Belikov, N.E.; Shvets, V.I.; Demina, O.V.; Barachevskij, V.A.; Khodonov, A.A. 5-Formyl-Substituted Indoline Spirobenzopyrans and Method of Producing Them. Patent RU2358977C1, 20 June 2009.
88. Laptev, A.V.; Belikov, N.E.; Lukin, A.Y.; Barachevskii, V.A.; Alfimov, M.V.; Demina, O.V.; Varfolomeev, S.D.; Shvets, V.I.; Khodonov, A.A. Spiropyran Analogs of Retinal: Synthesis and Study of Their Photochromic Properties. *High Energy Chem.* **2008**, *42*, 601–603. [CrossRef]
89. Barachevsky, V.A.; Khodonov, A.A.; Belikov, N.E.; Laptev, A.V.; Lukin, A.Y.; Demina, O.V.; Luyksaar, S.I.; Krayushkin, M.M. Properties of Photochromic Retinals. *Dyes Pigments* **2012**, *92*, 831–837. [CrossRef]
90. Laptev, A.V.; Lukin, A.Y.; Belikov, N.E.; Fomin, M.A.; Demina, O.V.; Shvets, V.I.; Khodonov, A.A. Study of Substituted Spirobenzopyrans Formylation Process. In Proceedings of the Materials of the 17th European Symposium on Organic Chemistry (ESOC-17), Crete, Greece, 10–15 July 2011; p. P2.041.
91. Barachevskii, V.A.; Kobeleva, O.I.; Valova, T.M.; Ait, A.O.; Kol'tsova, L.S.; Shienok, A.I.; Zaichenko, N.L.; Laptev, A.V.; Khodonov, A.A.; Kuznetsova, O.Y.; et al. Spectral Indications of Interaction of Functionalized Photochromic Compounds with Ag and Au Nanoparticles. *Theor. Exp. Chem.* **2012**, *48*, 14–20. [CrossRef]
92. Belikov, N.; Lukin, A.; Laptev, A.; Shvets, V.; Barachevsky, V.; Strokach, Y.; Valova, T.; Krayushkin, M.; Demina, O.; Varfolomeev, S.; et al. Photochromic Behavior of Retinal Analogs. *J. Photochem. Photobiol. Chem.* **2008**, *196*, 262–267. [CrossRef]
93. Demina, O.V.; Belikov, N.E.; Varfolomeev, S.D.; Khodonov, A.A. 3-Pyridylisoxazoles as Prototypes of Antiaggregatory Agents. *Russ. Chem. Bull.* **2018**, *67*, 866–877. [CrossRef]
94. Demina, O.V.; Belikov, N.E.; Varfolomeev, S.D.; Khodonov, A.A. Synthesis of Isoxazoles with Photochromic Label. In Proceedings of the Book of Abstracts of XV International Conference on Heterocycles in Bioorganic Chemistry (Bio-Heterocycles-2013), Riga, Latvia, 27–30 May 2013; p. 68.
95. Khodonov, A.A.; Belikov, N.E.; Lukin, A.Y.; Levin, P.P.; Varfolomeev, S.D.; Demina, O.V. Photochromic Derivatives of 5′-Hydroxymethyl-6-nitro-1′,3′,3′-trimethylspiro [2H 1-benzopyran-2,2′-indoline]. Patent RU2694904C1, 18 July 2019.
96. Laptev, A.V.; Pugachev, D.E.; Lukin, A.Y.; Nechaev, A.V.; Belikov, N.E.; Demina, O.V.; Levin, P.P.; Khodonov, A.A.; Mironov, A.F.; Varfolomeev, S.D.; et al. Synthesis of 5,10,15,20-Tetra [6′-nitro-1,3,3-trimethylspiro-(indolino-2,2′-2H-chromen-5-yl)]porphyrin and Its Metal Complexes. *Mendeleev Commun.* **2013**, *23*, 199–201. [CrossRef]
97. Gal'bershtam, M.A.; Artamonova, N.N.; Samoilova, N.P. Synthesis of 3′-Acyl-Substituted Indoline Spiropyrans. *Chem. Heterocycl. Compd.* **1975**, *11*, 167–172. [CrossRef]
98. Niu, C.; Song, Y.; Yang, L. Synthesis of 5′-Functionalized Indolinospiropyrans with Vinylene Unit as Linker. *Chin. J. Chem.* **2009**, *27*, 2001–2006. [CrossRef]
99. Braude, E.V.; Gal'bershtam, M.A. Styryl-Substituted Spirochromenes of the Indoline Series. *Chem. Heterocycl. Compd.* **1979**, *15*, 173–179. [CrossRef]
100. Demina, O.V.; Laptev, A.V.; Lukin, A.Y.; Belikov, N.E.; Fomin, M.A.; Shvets, V.I.; Khodonov, A.A. Study of Substituted Spirobenzopyran Formylation Process. In Proceedings of the Materials of the 23rd International Congress on Heterocyclic Chemistry, Glasgow, UK, 31 July–4 August 2011; p. 273.

101. Tuktarov, A.R.; Khuzin, A.A.; Tulyabaev, A.R.; Venidictova, O.V.; Valova, T.M.; Barachevsky, V.A.; Khalilov, L.M.; Dzhemilev, U.M. Synthesis, Structure and Photochromic Properties of Hybrid Molecules Based on Fullerene C60 and Spiropyrans. *RSC Adv.* **2016**, *6*, 71151–71155. [CrossRef]
102. Khuzin, A.A.; Tuktarov, A.R.; Barachevsky, V.A.; Valova, T.M.; Tulyabaev, A.R.; Dzhemilev, U.M. Synthesis, Photo and Acidochromic Properties of Spiropyran-Containing Methanofullerenes. *RSC Adv.* **2020**, *10*, 15888–15892. [CrossRef] [PubMed]
103. Kong, L.; Wong, H.-L.; Tam, A.Y.-Y.; Lam, W.H.; Wu, L.; Yam, V.W.-W. Synthesis, Characterization, and Photophysical Properties of Bodipy-Spirooxazine and -Spiropyran Conjugates: Modulation of Fluorescence Resonance Energy Transfer Behavior via Acidochromic and Photochromic Switching. *ACS Appl. Mater. Interfaces* **2014**, *6*, 1550–1562. [CrossRef] [PubMed]
104. Wang, L.; Xiong, W.; Tang, H.; Cao, D. A Multistimuli-Responsive Fluorescent Switch in the Solution and Solid States Based on Spiro[fluorene-9,9′-xanthene]-spiropyran. *J. Mater. Chem. C* **2019**, *7*, 9102–9111. [CrossRef]
105. Dowds, M.; Stenspil, S.G.; de Souza, J.H.; Laursen, B.W.; Cacciarini, M.; Nielsen, M.B. Orthogonal- and Path-Dependent Photo/Acidoswitching in an Eight-State Dihydroazulene-Spiropyran Dyad. *ChemPhotoChem* **2022**, *6*, e202200152:1–e202200152:9. [CrossRef]
106. Lee, S.; Ji, S.; Kang, Y. Synthesis and Characterizations of Bis-Spiropyran Derivatives. *Bull. Korean Chem. Soc.* **2012**, *33*, 3740–3744. [CrossRef]
107. Dissanayake, D.S.; McCandless, G.T.; Stefan, M.C.; Biewer, M.C. Systematic Variation of Thiophene Substituents in Photochromic Spiropyrans. *Photochem. Photobiol. Sci.* **2017**, *16*, 1057–1062. [CrossRef]
108. Lee, J.H.; Park, E.S.; Yoon, C.M. Suzuki Coupling Reaction of 6-Iodo- or 6,8-Diiodospiropyran: Synthesis of Spiropyran Analogs. *Tetrahedron Lett.* **2001**, *42*, 8311–8314. [CrossRef]
109. Metzler, L.; Reichenbach, T.; Brügner, O.; Komber, H.; Lombeck, F.; Müllers, S.; Hanselmann, R.; Hillebrecht, H.; Walter, M.; Sommer, M. High Molecular Weight Mechanochromic Spiropyran Main Chain Copolymers via Reproducible Microwave-Assisted Suzuki Polycondensation. *Polym. Chem.* **2015**, *6*, 3694–3707. [CrossRef]
110. Wagner, K.; Zanoni, M.; Elliott, A.B.S.; Wagner, P.; Byrne, R.; Florea, L.E.; Diamond, D.; Gordon, K.C.; Wallace, G.G.; Officer, D.L. A Merocyanine-Based Conductive Polymer. *J. Mater. Chem. C* **2013**, *1*, 3913. [CrossRef]
111. Zhao, P.; Wang, D.; Gao, H.; Zhang, J.; Xing, Y.; Yang, Z.; Cao, H.; He, W. Third-Order Nonlinear Optical Properties of the "Clicked" Closed-Ring Spiropyrans. *Dyes Pigments* **2019**, *162*, 451–458. [CrossRef]
112. Dvornikov, A.S.; Malkin, J.; Rentzepis, P.M. Spectroscopy and Kinetics of Photochromic Materials for 3D Optical Memory Devices. *J. Phys. Chem.* **1994**, *98*, 6746–6752. [CrossRef]
113. Irie, M. Diarylethenes for Memories and Switches. *Chem. Rev.* **2000**, *100*, 1685–1716. [CrossRef]
114. Velema, W.A.; Szymanski, W.; Feringa, B.L. Photopharmacology: Beyond Proof of Principle. *J. Am. Chem. Soc.* **2014**, *136*, 2178–2191. [CrossRef] [PubMed]
115. Szymański, W.; Beierle, J.M.; Kistemaker, H.A.V.; Velema, W.A.; Feringa, B.L. Reversible Photocontrol of Biological Systems by the Incorporation of Molecular Photoswitches. *Chem. Rev.* **2013**, *113*, 6114–6178. [CrossRef] [PubMed]
116. Fuchter, M.J. On the Promise of Photopharmacology Using Photoswitches: A Medicinal Chemist's Perspective. *J. Med. Chem.* **2020**, *63*, 11436–11447. [CrossRef]
117. Hüll, K.; Morstein, J.; Trauner, D. In Vivo Photopharmacology. *Chem. Rev.* **2018**, *118*, 10710–10747. [CrossRef] [PubMed]
118. Lerch, M.M.; Hansen, M.J.; van Dam, G.M.; Szymanski, W.; Feringa, B.L. Emerging Targets in Photopharmacology. *Angew. Chem. Int. Ed.* **2016**, *55*, 10978–10999. [CrossRef] [PubMed]
119. Wang, W.; Hu, J.; Zheng, M.; Zheng, L.; Wang, H.; Zhang, Y. Multi-Responsive Supramolecular Hydrogels Based on Merocyanine–Peptide Conjugates. *Org. Biomol. Chem.* **2015**, *13*, 11492–11498. [CrossRef] [PubMed]
120. Qiu, Z.; Yu, H.; Li, J.; Wang, Y.; Zhang, Y. Spiropyran-Linked Dipeptide Forms Supramolecular Hydrogel with Dual Responses to Light and to Ligand–Receptor Interaction. *Chem. Commun.* **2009**, 3342–3344. [CrossRef]
121. Liu, M.; Creemer, C.N.; Reardon, T.J.; Parquette, J.R. Light-Driven Dissipative Self-Assembly of a Peptide Hydrogel. *Chem. Commun.* **2021**, *57*, 13776–13779. [CrossRef]
122. Keum, S.-R.; Choi, Y.-K.; Kim, S.-H.; Yoon, C.-M. Symmetric and Unsymmetric Indolinobenzospiropyran Dimers: Synthesis and Characterization. *Dyes Pigments* **1999**, *41*, 41–47. [CrossRef]
123. Kortekaas, L.; Steen, J.D.; Duijnstee, D.R.; Jacquemin, D.; Browne, W.R. Noncommutative Switching of Double Spiropyrans. *J. Phys. Chem. A* **2020**, *124*, 6458–6467. [CrossRef]
124. Chang, Y.M.; Lee, S.H.; Cho, M.Y.; Yoo, B.W.; Rhee, H.J.; Lee, S.H.; Yoon, C.M. Homocoupling of Aryl Iodides and Bromides Using a Palladium/Indium Bimetallic System. *Synth. Commun.* **2005**, *35*, 1851–1857. [CrossRef]
125. Flerova, A.N.; Prokhoda, A.L.; Zaitseva, E.L.; Krongauz, V.A. Synthesis and Properties of Photochromic Bisindolinospiropyrans. *Chem. Heterocycl. Compd.* **1973**, *9*, 1476–1482. [CrossRef]
126. Cho, Y.J.; Rho, K.Y.; Kim, S.H.; Keum, S.R.; Yoon, C.M. Synthesis and Characterization of Symmetric and Non-Symmetric Bis-Spiropyranylethyne. *Dyes Pigments* **1999**, *44*, 19–25. [CrossRef]
127. Keum, S.-R.; Choi, Y.-K.; Lee, M.-J.; Kim, S.-H. Synthesis and Properties of Thermo- and Photochromic Bisindolinobenzospiropyrans Linked by Thio- and Carbonyl Groups. *Dyes Pigments* **2001**, *50*, 171–176. [CrossRef]
128. Keum, S.-R.; Ku, B.-S.; Kim, S.-E.; Choi, Y.-K.; Kim, S.-H.; Koh, K.-N. Solvatokinetic and Solvatochromic Behavior of Bis(indolinobenzospiropyranyl) Sulfide Derivatives in Various Solvents. *Bull. Korean Chem. Soc.* **2004**, *25*, 1361–1365. [CrossRef]

129. Keum, S.-R.; Lee, J.-H.; Seok, M.-K.; Yoon, C.-M. A Simple and Convenient Synthetic Route to the Bis-Indolinospirobenzopyrans. *Bull. Korean Chem. Soc.* **1994**, *15*, 275–277. [CrossRef]
130. Keum, S.-R.; Lee, J.-H.; Seok, M.-K. Synthesis and Characterization of Bis-Indolinospirobenzopyrans, New Photo- and Thermochromic Dyes. *Dyes Pigments* **1994**, *25*, 21–29. [CrossRef]
131. Keum, S.-R.; Lim, S.-S.; Min, B.-H.; Kazmaier, P.M.; Buncel, E. Synthesis and Characterization of Unsymmetrical Bis-Indolinospirobenzopyrans, a New Class of Thermo- and Photo-Chromic Dyes. *Dyes Pigments* **1996**, *30*, 225–234. [CrossRef]
132. Guo, X.; Zhang, D.; Zhou, Y.; Zhu, D. Synthesis and Spectral Investigations of a New Dyad with Spiropyran and Fluorescein Units: Toward Information Processing at the Single Molecular Level. *J. Org. Chem.* **2003**, *68*, 5681–5687. [CrossRef] [PubMed]
133. Wu, Z.; Pan, K.; Mo, S.; Wang, B.; Zhao, X.; Yin, M. Tetraphenylethene-Induced Free Volumes for the Isomerization of Spiropyran toward Multifunctional Materials in the Solid State. *ACS Appl. Mater. Interfaces* **2018**, *10*, 30879–30886. [CrossRef] [PubMed]
134. Zhu, L.; Khairutdinov, R.F.; Cape, J.L.; Hurst, J.K. Photoregulated Transmembrane Charge Separation by Linked Spiropyran−Anthraquinone Molecules. *J. Am. Chem. Soc.* **2006**, *128*, 825–835. [CrossRef] [PubMed]
135. Yang, S.; Liu, Y.; Lin, X.; Sun, W. Preparation of Spiropyran Bonded 1,8-Naphthalimide Compound Useful as Photochromic and Photoluminescent Material. Patent CN201510863463A, 4 May 2016.
136. Guo, X.; Huang, L.; O'Brien, S.; Kim, P.; Nuckolls, C. Directing and Sensing Changes in Molecular Conformation on Individual Carbon Nanotube Field Effect Transistors. *J. Am. Chem. Soc.* **2005**, *127*, 15045–15047. [CrossRef]
137. Shen, Q.; Cao, Y.; Liu, S.; Steigerwald, M.L.; Guo, X. Conformation-Induced Electrostatic Gating of the Conduction of Spiropyran-Coated Organic Thin-Film Transistors. *J. Phys. Chem. C* **2009**, *113*, 10807–10812. [CrossRef]
138. Seefeldt, B.; Kasper, R.; Beining, M.; Mattay, J.; Arden-Jacob, J.; Kemnitzer, N.; Drexhage, K.H.; Heilemann, M.; Sauer, M. Spiropyrans as Molecular Optical Switches. *Photochem. Photobiol. Sci.* **2010**, *9*, 213–220. [CrossRef]
139. Qu, L.; Xu, X.; Song, J.; Wu, D.; Wang, L.; Zhou, W.; Zhou, X.; Xiang, H. Solid-State Photochromic Molecular Switches Based on Axially Chiral and Helical Spiropyrans. *Dyes Pigments* **2020**, *181*, 108597. [CrossRef]
140. Solovyova, E.V.; Rostovtseva, I.A.; Shepelenko, K.E.; Voloshin, N.A.; Chernyshev, A.V.; Borodkin, G.S.; Metelitsa, A.V.; Minkin, V.I. Synthesis and Complex Formation of Spirobenzopyranindolines Containing Rhodamine Fragment. *Russ. J. Gen. Chem.* **2017**, *87*, 1007–1014. [CrossRef]
141. Solov'eva, E.V.; Rostovtseva, I.A.; Shepelenko, K.E.; Voloshin, N.A.; Chernyshev, A.V.; Borodkin, G.S.; Trofimova, N.S.; Metelitsa, A.V.; Minkin, V.I. Synthesis and Complex Formation of Rhodamine-Substituted Spirobenzopyranindolines. *Russ. J. Gen. Chem.* **2018**, *88*, 968–972. [CrossRef]
142. Sahoo, P.R.; Prakash, K.; Kumar, S. Light Controlled Receptors for Heavy Metal Ions. *Coord. Chem. Rev.* **2018**, *357*, 18–49. [CrossRef]
143. Voloshin, N.A.; Bezugliy, S.O.; Solov'eva, E.V.; Metelitsa, A.V.; Minkin, V.I. Photo- and Thermochromic Spiranes. 31. Photochromic Cationic Spiropyrans with a Pyridinium Fragment in the Aliphatic Side Chain. *Chem. Heterocycl. Compd.* **2008**, *44*, 1229–1237. [CrossRef]
144. Aldoshin, S.M.; Sanina, N.A.; Nadtochenko, V.A.; Yur'eva, E.A.; Minkin, V.I.; Voloshin, N.A.; Ikorskii, V.N.; Ovcharenko, V.I. Specific Spectral Properties of a Photochromic Ferromagnetic $(C_{25}H_{23}N_3O_3Cl)CrMn(C_2O_4)_3{\cdot}H_2O$. *Russ. Chem. Bull.* **2007**, *56*, 1095–1102. [CrossRef]
145. Chernyshev, A.V.; Voloshin, N.A.; Sletova, V.V.; Metelitsa, A.V. Chromogenic Spiroindolinobenzopyrans of the Oxadiazole Series with Photodriven Ionochromic Properties. *Dokl. Chem.* **2018**, *481*, 145–149. [CrossRef]
146. Chernyshev, A.V.; Voloshin, N.A.; Solov'eva, E.V.; Gaeva, E.B.; Zubavichus, Y.V.; Lazarenko, V.A.; Vlasenko, V.G.; Khrustalev, V.N.; Metelitsa, A.V. Ion-Depended Photochromism of Oxadiazole Containing Spiropyrans. *J. Photochem. Photobiol. Chem.* **2019**, *378*, 201–210. [CrossRef]
147. Voloshin, N.A.; Gaeva, E.B.; Chernyshev, A.V.; Metelitsa, A.V.; Minkin, V.I. Spiropyrans and Spirooxazines 5. Synthesis of Photochromic 8-(4,5-Diphenyl-1,3-oxazol-2-yl)-Substituted Spiro[indoline-benzopyrans]. *Russ. Chem. Bull.* **2009**, *58*, 156–161. [CrossRef]
148. Solov'eva, E.V.; Chernyshev, A.V.; Voloshin, N.A.; Metelitsa, A.V.; Minkin, V.I. Photo- and Thermochromic Spirans. 38. New (1-Alkyl-4,5-diphenyl)imidazolyl-Substituted Spirobenzopyrans. *Chem. Heterocycl. Compd.* **2013**, *48*, 1533–1538. [CrossRef]
149. Rostovtseva, I.A.; Solov'eva, E.V.; Chernyshev, A.V.; Voloshin, N.A.; Trofimova, N.S.; Metelitsa, A.V. Photo- and Thermochromic Spiropyrans 43. Spectral Kinetic Study of New Benzoxazolyl-Substituted Spirobenzopyrans. *Chem. Heterocycl. Compd.* **2015**, *51*, 223–228. [CrossRef]
150. Chernyshev, A.V.; Metelitsa, A.V.; Rostovtseva, I.A.; Voloshin, N.A.; Solov'eva, E.V.; Gaeva, E.B.; Minkin, V.I. Chromogenic Systems Based on 8-(1,3-Benzoxazol-2-yl) Substituted Spirobenzopyrans Undergoing Ion Modulated Photochromic Rearrangements. *J. Photochem. Photobiol. Chem.* **2018**, *360*, 174–180. [CrossRef]
151. Chernyshev, A.V.; Guda, A.A.; Cannizzo, A.; Solov'eva, E.V.; Voloshin, N.A.; Rusalev, Y.; Shapovalov, V.V.; Smolentsev, G.; Soldatov, A.V.; Metelitsa, A.V. Operando XAS and UV–Vis Characterization of the Photodynamic Spiropyran–Zinc Complexes. *J. Phys. Chem. B* **2019**, *123*, 1324–1331. [CrossRef]
152. Rostovtseva, I.A.; Voloshin, N.A.; Solov'eva, E.V.; Shepelenko, K.E.; Chernyshev, A.V.; Metelitsa, A.V.; Minkin, V.I. Photo- and Ionochromism of Benzoxazolyl-Substituted Spirobenzopyrans. *Dokl. Chem.* **2018**, *478*, 26–30. [CrossRef]
153. Yagi, S.; Nakamura, S.; Watanabe, D.; Nakazumi, H. Colorimetric Sensing of Metal Ions by Bis(Spiropyran) Podands: Towards Naked-Eye Detection of Alkaline Earth Metal Ions. *Dyes Pigments* **2009**, *80*, 98–105. [CrossRef]

154. Guo, X.; Zhang, D.; Zhu, D. Logic Control of the Fluorescence of a New Dyad, Spiropyran-Perylene Diimide-Spiropyran, with Light, Ferric Ion, and Proton: Construction of a New Three-Input "AND" Logic Gate. *Adv. Mater.* **2004**, *16*, 125–130. [CrossRef]
155. Guo, X.; Zhang, D.; Zhu, D. Photocontrolled Electron Transfer Reaction between a New Dyad, Tetrathiafulvalene−Photochromic Spiropyran, and Ferric Ion. *J. Phys. Chem. B* **2004**, *108*, 212–217. [CrossRef]
156. Gao, M.; Shen, B.; Zhou, J.; Kapre, R.; Louie, A.Y.; Shaw, J.T. Synthesis and Comparative Evaluation of Photoswitchable Magnetic Resonance Imaging Contrast Agents. *ACS Omega* **2020**, *5*, 14759–14766. [CrossRef] [PubMed]
157. Tu, C.; Osborne, E.A.; Louie, A.Y. Synthesis and Characterization of a Redox- and Light-Sensitive MRI Contrast Agent. *Tetrahedron* **2009**, *65*, 1241–1246. [CrossRef] [PubMed]
158. Roxburgh, C.J.; Sammes, P.G. Substituent Tuning of Photoreversible Lithium Chelating Agents. *Dyes Pigments* **1995**, *28*, 317–325. [CrossRef]
159. Stubing, D.B.; Heng, S.; Abell, A.D. Crowned Spiropyran Fluoroionophores with a Carboxyl Moiety for the Selective Detection of Lithium Ions. *Org. Biomol. Chem.* **2016**, *14*, 3752–3757. [CrossRef]
160. Heng, S.; Nguyen, M.-C.; Kostecki, R.; Monro, T.M.; Abell, A.D. Nanoliter-Scale, Regenerable Ion Sensor: Sensing with a Surface Functionalized Microstructured Optical Fibre. *RSC Adv.* **2013**, *3*, 8308. [CrossRef]
161. Roxburgh, C.J.; Sammes, P.G. Synthesis of Some New Substituted Photochromic N,N′-Bis(spiro [1-benzopyran-2,2′-indolyl])diazacrown Systems with Substituent Control over Ion Chelation. *Eur. J. Org. Chem.* **2006**, *2006*, 1050–1056. [CrossRef]
162. Roxburgh, C.J.; Sammes, P.G.; Abdullah, A. Photoreversible Zn^{2+} Ion Transportation Across an Interface Using Ion-Chelating Substituted Photochromic 3,3′-Indolospirobenzopyrans: Steric and Electronic Controlling Effects. *Eur. J. Inorg. Chem.* **2008**, *2008*, 4951–4960. [CrossRef]
163. Li, S.; Li, M.; Chen, L.; Yang, J.; Wang, Z.; Yang, F.; He, L.; Li, X. Engineering Highly Efficient Li^{+} Responsive Nanochannels via Host–Guest Interaction and Photochemistry Regulation. *J. Colloid Interface Sci.* **2022**, *615*, 674–684. [CrossRef]
164. Trevino, K.M.; Tautges, B.K.; Kapre, R.; Franco, F.C., Jr.; Or, V.W.; Balmond, E.I.; Shaw, J.T.; Garcia, J.; Louie, A.Y. Highly Sensitive and Selective Spiropyran-Based Sensor for Copper(II) Quantification. *ACS Omega* **2021**, *6*, 10776–10789. [CrossRef] [PubMed]
165. Heng, S.; McDevitt, C.A.; Stubing, D.B.; Whittall, J.J.; Thompson, J.G.; Engler, T.K.; Abell, A.D.; Monro, T.M. Microstructured Optical Fibers and Live Cells: A Water-Soluble, Photochromic Zinc Sensor. *Biomacromolecules* **2013**, *14*, 3376–3379. [CrossRef] [PubMed]
166. Stubing, D.B.; Heng, S.; Monro, T.M.; Abell, A.D. A Comparative Study of the Fluorescence and Photostability of Common Photoswitches in Microstructured Optical Fibre. *Sens. Actuators B Chem.* **2017**, *239*, 474–480. [CrossRef]
167. Jukes, R.T.F.; Bozic, B.; Hartl, F.; Belser, P.; De Cola, L. Synthesis, Photophysical, Photochemical, and Redox Properties of Nitrospiropyrans Substituted with Ru or Os Tris(bipyridine) Complexes. *Inorg. Chem.* **2006**, *45*, 8326–8341. [CrossRef]
168. Yang, H.; Du, S.; Ye, Z.; Wang, X.; Yan, Z.; Lian, C.; Bao, C.; Zhu, L. A System for Artificial Light Signal Transduction via Molecular Translocation in a Lipid Membrane. *Chem. Sci.* **2022**, *13*, 2487–2494. [CrossRef]
169. Colaco, R.; Shree, S.; Siebert, L.; Appiah, C.; Dowds, M.; Schultzke, S.; Adelung, R.; Staubitz, A. Mechanochromic Microfibers Stabilized by Polymer Blending. *ACS Appl. Polym. Mater.* **2020**, *2*, 2055–2062. [CrossRef]
170. Potisek, S.L.; Davis, D.A.; Sottos, N.R.; White, S.R.; Moore, J.S. Mechanophore-Linked Addition Polymers. *J. Am. Chem. Soc.* **2007**, *129*, 13808–13809. [CrossRef]
171. Davis, D.A.; Hamilton, A.; Yang, J.; Cremar, L.D.; Van Gough, D.; Potisek, S.L.; Ong, M.T.; Braun, P.V.; Martínez, T.J.; White, S.R.; et al. Force-Induced Activation of Covalent Bonds in Mechanoresponsive Polymeric Materials. *Nature* **2009**, *459*, 68–72. [CrossRef]
172. Lee, C.K.; Davis, D.A.; White, S.R.; Moore, J.S.; Sottos, N.R.; Braun, P.V. Force-Induced Redistribution of a Chemical Equilibrium. *J. Am. Chem. Soc.* **2010**, *132*, 16107–16111. [CrossRef]
173. O'Bryan, G.; Wong, B.M.; McElhanon, J.R. Stress Sensing in Polycaprolactone Films via an Embedded Photochromic Compound. *ACS Appl. Mater. Interfaces* **2010**, *2*, 1594–1600. [CrossRef]
174. Gossweiler, G.R.; Kouznetsova, T.B.; Craig, S.L. Force-Rate Characterization of Two Spiropyran-Based Molecular Force Probes. *J. Am. Chem. Soc.* **2015**, *137*, 6148–6151. [CrossRef]
175. Gossweiler, G.R.; Brown, C.L.; Hewage, G.B.; Sapiro-Gheiler, E.; Trautman, W.J.; Welshofer, G.W.; Craig, S.L. Mechanochemically Active Soft Robots. *ACS Appl. Mater. Interfaces* **2015**, *7*, 22431–22435. [CrossRef]
176. Sommer, M.; Komber, H. Spiropyran Main-Chain Conjugated Polymers. *Macromol. Rapid Commun.* **2013**, *34*, 57–62. [CrossRef]
177. Komber, H.; Müllers, S.; Lombeck, F.; Held, A.; Walter, M.; Sommer, M. Soluble and Stable Alternating Main-Chain Merocyanine Copolymers through Quantitative Spiropyran–Merocyanine Conversion. *Polym. Chem.* **2014**, *5*, 443–453. [CrossRef]
178. Kempe, F.; Brügner, O.; Buchheit, H.; Momm, S.N.; Riehle, F.; Hameury, S.; Walter, M.; Sommer, M. A Simply Synthesized, Tough Polyarylene with Transient Mechanochromic Response. *Angew. Chem. Int. Ed.* **2018**, *57*, 997–1000. [CrossRef]
179. Vidavsky, Y.; Yang, S.J.; Abel, B.A.; Agami, I.; Diesendruck, C.E.; Coates, G.W.; Silberstein, M.N. Enabling Room-Temperature Mechanochromic Activation in a Glassy Polymer: Synthesis and Characterization of Spiropyran Polycarbonate. *J. Am. Chem. Soc.* **2019**, *141*, 10060–10067. [CrossRef] [PubMed]
180. Yang, J.; Ng, M.-K. Synthesis of a Photochromic Conjugated Polymer Incorporating Spirobenzopyran in the Backbone. *Synthesis* **2006**, *2006*, 3075–3079. [CrossRef]

181. Kadokawa, J.; Tanaka, Y.; Yamashita, Y.; Yamamoto, K. Synthesis of Poly(Spiropyran)s by Polycondensation and Their Photoisomerization Behaviors. *Eur. Polym. J.* **2012**, *48*, 549–559. [CrossRef]
182. Chen, Q.; Feng, Y.; Zhang, D.; Zhang, G.; Fan, Q.; Sun, S.; Zhu, D. Light-Triggered Self-Assembly of a Spiropyran-Functionalized Dendron into Nano-/Micrometer-Sized Particles and Photoresponsive Organogel with Switchable Fluorescence. *Adv. Funct. Mater.* **2010**, *20*, 36–42. [CrossRef]
183. Cabrera, I.; Krongauz, V. Physical Crosslinking of Mesomorphic Polymers Containing Spiropyran Groups. *Macromolecules* **1987**, *20*, 2713–2717. [CrossRef]
184. Cabrera, I.; Krongauz, V.; Ringsdorf, H. Photo- and Thermo-Chromic Liquid Crystal Polymers with Spiropyran Groups. *Mol. Cryst. Liq. Cryst. Inc. Nonlinear Opt.* **1988**, *155*, 221–230. [CrossRef]
185. Shragina, L.; Buchholtz, F.; Yitzchaik, S.; Krongauz, V. Searching for Photochromic Liquid Crystals Spironaphthoxazine Substituted with a Mesogenic Group. *Liq. Cryst.* **1990**, *7*, 643–655. [CrossRef]
186. Malinčík, J.; Kohout, M.; Svoboda, J.; Stulov, S.; Pociecha, D.; Böhmová, Z.; Novotná, V. Photochromic Spiropyran-Based Liquid Crystals. *J. Mol. Liq.* **2022**, *346*, 117842. [CrossRef]
187. Tan, B.-H.; Yoshio, M.; Kato, T. Induction of Columnar and Smectic Phases for Spiropyran Derivatives: Effects of Acidichromism and Photochromism. *Chem.-Asian J.* **2008**, *3*, 534–541. [CrossRef]
188. Abdollahi, A.; Roghani-Mamaqani, H.; Razavi, B. Stimuli-Chromism of Photoswitches in Smart Polymers: Recent Advances and Applications as Chemosensors. *Prog. Polym. Sci.* **2019**, *98*, 101149. [CrossRef]
189. Li, M.; Zhang, Q.; Zhou, Y.-N.; Zhu, S. Let Spiropyran Help Polymers Feel Force! *Prog. Polym. Sci.* **2018**, *79*, 26–39. [CrossRef]
190. Shibaev, V.; Bobrovsky, A.; Boiko, N. Photoactive Liquid Crystalline Polymer Systems with Light-Controllable Structure and Optical Properties. *Prog. Polym. Sci.* **2003**, *28*, 729–836. [CrossRef]
191. Qiu, W.; Scofield, J.M.P.; Gurr, P.A.; Qiao, G.G. Mechanochromophore-Linked Polymeric Materials with Visible Color Changes. *Macromol. Rapid Commun.* **2022**, *43*, 2100866. [CrossRef]
192. Sommer, M. Substituent Effects Control Spiropyran–Merocyanine Equilibria and Mechanochromic Utility. *Macromol. Rapid Commun.* **2021**, *42*, 2000597. [CrossRef]
193. Caruso, M.M.; Davis, D.A.; Shen, Q.; Odom, S.A.; Sottos, N.R.; White, S.R.; Moore, J.S. Mechanically-Induced Chemical Changes in Polymeric Materials. *Chem. Rev.* **2009**, *109*, 5755–5798. [CrossRef]
194. Lee, C.K.; Diesendruck, C.E.; Lu, E.; Pickett, A.N.; May, P.A.; Moore, J.S.; Braun, P.V. Solvent Swelling Activation of a Mechanophore in a Polymer Network. *Macromolecules* **2014**, *47*, 2690–2694. [CrossRef]
195. Cao, Z. Highly Stretchable Tough Elastomers Crosslinked by Spiropyran Mechanophores for Strain-Induced Colorimetric Sensing. *Macromol. Chem. Phys.* **2020**, *221*, 2000190. [CrossRef]
196. Garcia, J.; Addison, J.B.; Liu, S.Z.; Lu, S.; Faulkner, A.L.; Hodur, B.M.; Balmond, E.I.; Or, V.W.; Yun, J.H.; Trevino, K.; et al. Antioxidant Sensing by Spiropyrans: Substituent Effects and NMR Spectroscopic Studies. *J. Phys. Chem. B* **2019**, *123*, 6799–6809. [CrossRef]
197. Tuktarov, A.R.; Khuzin, A.A.; Dzhemilev, U.M. Acid-Base Isomerization of Hybrid Molecules Based on Fullerene C60 and Spiropyrans. *Mendeleev Commun.* **2019**, *29*, 229–231. [CrossRef]
198. Raic-Malic, S.; Tomaskovic, L.; Mrvos-Sermek, D.; Prugovecki, B.; Cetina, M.; Grdiša, M.; Pavelić, K.; Mannschreck, A.; Balzarini, J.; De Clercq, E.; et al. Spirobipyridopyrans, Spirobinaphthopyrans, Indolinospiropyridopyrans, Indolinospironaphthopyrans and Indolinospironaphtho-1,4-oxazines: Synthesis, Study of X-Ray Crystal Structure, Antitumoral and Antiviral Evaluation. *Bioorg. Med. Chem.* **2004**, *12*, 1037–1045. [CrossRef]
199. Li, Z.; Wan, S.; Shi, W.; Wei, M.; Yin, M.; Yang, W.; Evans, D.G.; Duan, X. A Light-Triggered Switch Based on Spiropyran/Layered Double Hydroxide Ultrathin Films. *J. Phys. Chem. C* **2015**, *119*, 7428–7435. [CrossRef]
200. Voloshin, N.A.; Volbushko, N.V.; Voloshina, E.N.; Shelepin, N.E.; Minkin, V.I. New Formyl-Substituted Spiropyrans of the Indoline Series. *Chem. Heterocycl. Compd.* **1996**, *32*, 1427–1428. [CrossRef]
201. Pantsyrnyi, V.I.; Gal'bershtam, M.A. Preparation of Spiropyrans from 3-Formylsalicylic Acid Derivatives. *Chem. Heterocycl. Compd.* **1971**, *7*, 134–135. [CrossRef]
202. Seki, T.; Ichimura, K. Formation of Head-to-Tail and Side-by-Side Aggregates of Photochromic Spiropyrans in Bilayer Membrane. *J. Phys. Chem.* **1990**, *94*, 3769–3775. [CrossRef]
203. Walkey, M.C.; Byrne, L.T.; Piggott, M.J.; Low, P.J.; Koutsantonis, G.A. Enhanced Bi-Stability in a Ruthenium Alkynyl Spiropyran Complex. *Dalton Trans.* **2015**, *44*, 8812–8815. [CrossRef] [PubMed]
204. Walkey, M.C.; Peiris, C.R.; Ciampi, S.; Aragonès, A.; Domínguez-Espíndola, R.B.; Jago, D.; Pulbrook, T.; Skelton, B.W.; Sobolev, A.N.; Díez Pérez, I.; et al. Chemically and Mechanically Controlled Single-Molecule Switches Using Spiropyrans. *ACS Appl. Mater. Interfaces* **2019**, *11*, 36886–36894. [CrossRef] [PubMed]
205. Yagupolskii, L.M.; Pasenok, S.V.; Gal'bershtam, M.A.; Bobyleva, G.K.; Popov, V.I.; Kondratenko, N.V. Synthesis and Photochromic Properties of Perfluoroalkyl and Trifluoromethylsulphonyl Substituted Indoline Spirochromenes. *Dyes Pigments* **1981**, *2*, 205–213. [CrossRef]
206. Roxburgh, C.J.; Sammes, P.G.; Abdullah, A. Steric and Electronically Biasing Substituent Effects on the Photoreversibility of Novel, 3′-, 5′- and 3-Substituted Indolospirobenzopyrans. Thermal Evaluation Using ^{1}H NMR Spectroscopy and Overhauser Enhancement Studies. *Dyes Pigments* **2009**, *83*, 31–50. [CrossRef]

207. Gal'bershtam, M.A.; Mikheeva, L.M.; Samoilova, N.P. Electronic Absorption Spectra of Merocyanine Forms of Spiropyrans. *Chem. Heterocycl. Compd.* **1972**, *8*, 1386–1389. [CrossRef]
208. Gordin, M.B.; Gal'bershtam, M.A. Existence of a Photodecolorization Reaction of the Colored Form of Spiropyrans under the Influence of Initiating UV Irradiation. *Chem. Heterocycl. Compd.* **1971**, *7*, 1089–1091. [CrossRef]
209. Cullum, B.M.; Mobley, J.; Bogard, J.S.; Moscovitch, M.; Phillips, G.W.; Vo-Dinh, T. Three-Dimensional Optical Random Access Memory Materials for Use as Radiation Dosimeters. *Anal. Chem.* **2000**, *72*, 5612–5617. [CrossRef]
210. Parthenopoulos, D.A.; Rentzepis, P.M. Three-Dimensional Optical Storage Memory. *Science* **1989**, *245*, 843–845. [CrossRef]
211. Moscovitch, M.; Phillips, G.W. Radiation Dosimetry Using Three-Dimensional Optical Random Access Memories. *Nucl. Instrum. Methods Phys. Res. Sect. B Beam Interact. Mater. At.* **2001**, *184*, 207–218. [CrossRef]
212. Cho, Y.J.; Rho, K.Y.; Rok Keum, S.; Kim, S.H.; Yoon, C.M. Synthesis of Conjugated Spiropyran Dyes via Palladium-Catalyzed Coupling Reaction. *Synth. Commun.* **1999**, *29*, 2061–2068. [CrossRef]
213. Steen, J.D.; Duijnstee, D.R.; Sardjan, A.S.; Martinelli, J.; Kortekaas, L.; Jacquemin, D.; Browne, W.R. Electrochemical Ring-Opening and -Closing of a Spiropyran. *J. Phys. Chem. A* **2021**, *125*, 3355–3361. [CrossRef] [PubMed]
214. Zhang, L.; Deng, Y.; Tang, Z.; Zheng, N.; Zhang, C.; Xie, C.; Wu, Z. One-Pot Synthesis of Spiropyrans. *Asian J. Org. Chem.* **2019**, *8*, 1866–1869. [CrossRef]
215. Liu, H.; Zhou, Y.; Yang, Y.; Wang, W.; Qu, L.; Chen, C.; Liu, D.; Zhang, D.; Zhu, D. Photo-pH Dually Modulated Fluorescence Switch Based on DNA Spatial Nanodevice. *J. Phys. Chem. B* **2008**, *112*, 6893–6896. [CrossRef] [PubMed]
216. Tomasulo, M.; Kaanumal, S.L.; Sortino, S.; Raymo, F.M. Synthesis and Properties of Benzophenone−Spiropyran and Naphthalene−Spiropyran Conjugates. *J. Org. Chem.* **2007**, *72*, 595–605. [CrossRef]
217. Balmond, E.I.; Tautges, B.K.; Faulkner, A.L.; Or, V.W.; Hodur, B.M.; Shaw, J.T.; Louie, A.Y. Comparative Evaluation of Substituent Effect on the Photochromic Properties of Spiropyrans and Spirooxazines. *J. Org. Chem.* **2016**, *81*, 8744–8758. [CrossRef] [PubMed]
218. Guo, X.; Zhang, D.; Zhang, G.; Zhu, D. Monomolecular Logic: "Half-Adder" Based on Multistate/Multifunctional Photochromic Spiropyrans. *J. Phys. Chem. B* **2004**, *108*, 11942–11945. [CrossRef]
219. Chernyshev, A.V.; Chernov'yants, M.S.; Voloshina, E.N.; Voloshin, N.A. To Estimation of PKa for Spiropyrans of the Indoline Series. *Russ. J. Gen. Chem.* **2002**, *72*, 1468–1472. [CrossRef]
220. Khairutdinov, R.F.; Hurst, J.K. Photocontrol of Ion Permeation through Bilayer Membranes Using an Amphiphilic Spiropyran. *Langmuir* **2001**, *17*, 6881–6886. [CrossRef]
221. Collier, C.P.; Ma, B.; Wong, E.W.; Heath, J.R.; Wudl, F. Photochemical Response of Electronically Reconfigurable Molecule-Based Switching Tunnel Junctions. *ChemPhysChem* **2002**, *3*, 458. [CrossRef]
222. Tuktarov, A.R.; Salikhov, R.B.; Khuzin, A.A.; Safargalin, I.N.; Mullagaliev, I.N.; Venidiktova, O.V.; Valova, T.M.; Barachevsky, V.A.; Dzhemilev, U.M. Optically Controlled Field Effect Transistors Based on Photochromic Spiropyran and Fullerene C60 Films. *Mendeleev Commun.* **2019**, *29*, 160–162. [CrossRef]
223. da Costa Duarte, R.; da Silveira Santos, F.; Bercini de Araújo, B.; Cercena, R.; Brondani, D.; Zapp, E.; Fernando Bruno Gonçalves, P.; Severo Rodembusch, F.; Gonçalves Dal-Bó, A. Synthesis of a 5-Carboxy Indole-Based Spiropyran Fluorophore: Thermal, Electrochemical, Photophysical and Bovine Serum Albumin Interaction Investigations. *Chemosensors* **2020**, *8*, 31. [CrossRef]
224. Kollarigowda, R.H.; Braun, P.V. Direct and Divergent Solid-Phase Synthesis of Azobenzene and Spiropyran Derivatives. *J. Org. Chem.* **2021**, *86*, 4391–4397. [CrossRef] [PubMed]
225. Grady, M.E.; Birrenkott, C.M.; May, P.A.; White, S.R.; Moore, J.S.; Sottos, N.R. Localization of Spiropyran Activation. *Langmuir* **2020**, *36*, 5847–5854. [CrossRef]
226. Ozhogin, I.V.; Chernyavina, V.V.; Lukyanov, B.S.; Malay, V.I.; Rostovtseva, I.A.; Makarova, N.I.; Tkachev, V.V.; Lukyanova, M.B.; Metelitsa, A.V.; Aldoshin, S.M. Synthesis and Study of New Photochromic Spiropyrans Modified with Carboxylic and Aldehyde Substituents. *J. Mol. Struct.* **2019**, *1196*, 409–416. [CrossRef]
227. Ozhogin, I.V.; Chernyshev, A.V.; Butova, V.V.; Lukyanov, B.S.; Radchenko, E.A.; Mukhanov, E.L.; Soldatov, A.V. Structure and Photochromic Properties of New Spiropyrans of Indoline Series Containing Free Carboxylic Groups. *J. Surf. Investig. X-ray Synchrotron Neutron Tech.* **2020**, *14*, 534–539. [CrossRef]
228. Kubo, N.; Yoshii, T.; Kobayashi, N.; Ikeda, K.; Hirohashi, R. Photoresponse in Ionic Conductivity for Poly[(ω-hydroxy)oligo (oxyethylene) methacrylate-co-butyl methacrylate] Doped with Spiropyran Derivative and $LiClO_4$. *Polym. Adv. Technol.* **1993**, *4*, 119–123. [CrossRef]
229. Sepehr, Z.; Nasr-Isfahani, H.; Mahdavian, A.R.; Amin, A.H. Synthesis, Characterization, and UV–Visible Study of Some New Photochromic Formyl-Containing 1′,3′,3′-Trimethylspiro[chromene-2,2′-indoline] Derivatives. *J. Iran. Chem. Soc.* **2021**, *18*, 3061–3067. [CrossRef]
230. Arsenov, V.D.; Manakova, I.V.; Przhiyalgovskaya, N.M.; Suvorov, N.N. Thermal and Photostability of 5′,7′-Dialkoxy-5,6′-dinitro-1,3,3-trimethylspiro(indolin-2,2′-[2H]chromenes). *Chem. Heterocycl. Compd.* **1987**, *23*, 961–964. [CrossRef]
231. Darwish, N.; Aragonès, A.C.; Darwish, T.; Ciampi, S.; Díez-Pérez, I. Multi-Responsive Photo- and Chemo-Electrical Single-Molecule Switches. *Nano Lett.* **2014**, *14*, 7064–7070. [CrossRef]
232. Patel, K.; Castillo-Muzquiz, A.; Biewer, M.C. Studying Monolayer/Solvent Interactions with a Photochromic Compound in a Self-Assembled Monolayer. *Tetrahedron Lett.* **2002**, *43*, 5933–5935. [CrossRef]
233. McArdle, C.B.; Blair, H.; Barraud, A.; Ruaudel-Teixier, A. Positive and Negative Photochromism in Thin Organic Langmuir-Blodgett Films. *Thin Solid Films* **1983**, *99*, 181–188. [CrossRef]

234. Blair, H.S.; McArdle, C.B. Photoresponsive Polymeric Systems: 1. Mixed Monomolecular Films of Some Synthetic Polymers and Indolinospiropyrans. *Polymer* **1984**, *25*, 999–1005. [CrossRef]
235. Mardaleishvili, I.R.; Kol'tsova, L.S.; Zaichenko, N.L.; Sister, V.G.; Shienok, A.I.; Levin, P.P.; Tatikolov, A.S. Spectral and Luminescent Properties of Hydroxyazomethines of Indoline Spiropyrans. *High Energy Chem.* **2012**, *46*, 160–165. [CrossRef]
236. Shienok, A.I.; Ivashina, N.A.; Kol'tsova, L.S.; Zaichenko, N.L. One-Step Synthesis of Novel Photochemically Bifunctional Compounds of the Spiropyran Class. *Russ. Chem. Bull.* **2008**, *57*, 2437–2439. [CrossRef]
237. Mardaleishvili, I.R.; Kol'tsova, L.S.; Zaichenko, N.L.; Shienok, A.I.; Levin, P.P.; Tatikolov, A.S. Peculiarities of Photochromism and Luminescence of Dinitrosubstituted Hydroxyazomethinespiropyran. *High Energy Chem.* **2015**, *49*, 30–35. [CrossRef]
238. Andrews, M.C.; Peng, P.; Rajput, A.; Cozzolino, A.F. Modulation of the Carboxamidine Redox Potential through Photoinduced Spiropyran or Fulgimide Isomerisation. *Photochem. Photobiol. Sci.* **2018**, *17*, 432–441. [CrossRef]
239. Rastogi, S.K.; Zhao, Z.; Gildner, M.B.; Shoulders, B.A.; Velasquez, T.L.; Blumenthal, M.O.; Wang, L.; Li, X.; Hudnall, T.W.; Betancourt, T.; et al. Synthesis, Optical Properties and in Vitro Cell Viability of Novel Spiropyrans and Their Photostationary States. *Tetrahedron* **2021**, *80*, 131854. [CrossRef]
240. Lyubimov, A.V.; Zaichenko, N.L.; Marevtsev, V.S.; Cherkashin, M.I. Indolinospiropyrans with Two Polymerizable Groups. *Bull. Acad. Sci. USSR Div. Chem. Sci.* **1982**, *31*, 585–587. [CrossRef]
241. Ozhogin, I.V.; Tkachev, V.V.; Mukhanov, E.L.; Lukyanov, B.S.; Chernyshev, A.V.; Lukyanova, M.B.; Aldoshin, S.M. Studies of Structure and Photochromic Properties of Spiropyrans Based on 4,6-Diformyl-2-methylresorcinol. *Russ. Chem. Bull.* **2015**, *64*, 672–676. [CrossRef]
242. Ozhogin, I.V.; Pugachev, A.D.; Kozlenko, A.S.; Rostovtseva, I.A.; Makarova, N.I.; Borodkin, G.S.; El-Sewify, I.M.; Metelitsa, A.V.; Lukyanov, B.S. Methyl 5′-Chloro-8-formyl-5-hydroxy-1′,3′,3′-trimethyl-spiro-[chromene-2,2′-indoline]-6-carboxylate. *Molbank* **2023**, *2023*, M1549. [CrossRef]
243. Zaichenko, N.L.; Shienok, A.I.; Kol'tsova, L.S.; Lyubimov, A.V.; Mardaleishvili, I.R.; Retivov, V.M.; Belus', S.K.; Ait, A.O. Synthesis of Triarylimidazole Hybrid Compound with Switchable Luminescence. *Russ. J. Gen. Chem.* **2016**, *86*, 1022–1027. [CrossRef]
244. Chernyshev, A.V.; Voloshin, N.A.; Rostovtseva, I.A.; Solov'eva, E.V.; Gaeva, E.B.; Metelitsa, A.V. Polychromogenic Molecular Systems Based on Photo- and Ionochromic Spiropyrans. *Dyes Pigments* **2018**, *158*, 506–516. [CrossRef]
245. Pugachev, A.D.; Lukyanova, M.B.; Lukyanov, B.S.; Ozhogin, I.V.; Kozlenko, A.S.; Tkachev, V.V.; Chepurnoi, P.B.; Shilov, G.V.; Minkin, V.I.; Aldosin, S.M. Replacement of the Hetarene Moiety of Molecule in the Synthesis of Indoline Spiropyran with Cationic Fragment. *Dokl. Chem.* **2020**, *492*, 76–83. [CrossRef]
246. Pugachev, A.D.; Kozlenko, A.S.; Luk'yanova, M.B.; Luk'yanov, B.S.; Tkachev, V.V.; Shilov, G.V.; Demidov, O.P.; Minkin, V.I.; Aldoshin, S.M. One-Pot Synthesis and Structure Study of a New Indoline Spiropyran with Cationic Substituent. *Dokl. Chem.* **2019**, *488*, 252–256. [CrossRef]
247. Mao, S.; Benninger, R.K.P.; Yan, Y.; Petchprayoon, C.; Jackson, D.; Easley, C.J.; Piston, D.W.; Marriott, G. Optical Lock-In Detection of FRET Using Synthetic and Genetically Encoded Optical Switches. *Biophys. J.* **2008**, *94*, 4515–4524. [CrossRef]
248. Heng, S.; Nguyen, M.-C.; Kostecki, R.; Monro, T.M.; Abell, A.D. Nanoliter-Scale, Regenerable Ion Sensor: Sensing with Surface Functionalized Microstructured Optical Fiber. *Proc. SPIE* **2013**, *8774*, 877403. [CrossRef]
249. Querol, M.; Bozic, B.; Salluce, N.; Belser, P. Synthesis, Metal Complex Formation, and Switching Properties of Spiropyrans Linked to Chelating Sites. *Polyhedron* **2003**, *22*, 655–664. [CrossRef]
250. Venidiktova, O.V.; Gorelik, A.M.; Barachevsky, V.A.; Khuzin, A.A.; Tuktarov, A.R. Study of the Possibility of Functionalization of Graphene Oxide Nanoplatelets with Photochromic Chromene and Spiropyrans in Solutions. *Russ. J. Gen. Chem.* **2021**, *91*, 2640–2646. [CrossRef]
251. Tamaki, T.; Minode, K.; Numai, Y.; Ohto, T.; Yamada, R.; Masai, H.; Tada, H.; Terao, J. Mechanical Switching of Current–Voltage Characteristics in Spiropyran Single-Molecule Junctions. *Nanoscale* **2020**, *12*, 7527–7531. [CrossRef]
252. Nagashima, S.; Murata, M.; Nishihara, H. A Ferrocenylspiropyran That Functions as a Molecular Photomemory with Controllable Depth. *Angew. Chem. Int. Ed.* **2006**, *45*, 4298–4301. [CrossRef]
253. Takase, M.; Inouye, M. Synthesis and Photochromic Properties of Ferrocene-Modified Bis(spirobenzopyran)s. *Mol. Cryst. Liq. Cryst. Sci. Technol. Sect. Mol. Cryst. Liq. Cryst.* **2000**, *344*, 313–318. [CrossRef]
254. Ma, Y.; Niu, C.; Wen, Y.; Li, G.; Wang, J.; Li, H.; Du, S.; Yang, L.; Gao, H.; Song, Y. Stable and Reversible Optoelectrical Dual-Mode Data Storage Based on a Ferrocenylspiropyran Molecule. *Appl. Phys. Lett.* **2009**, *95*, 183307. [CrossRef]
255. Miyashita, A.; Iwamoto, A.; Kuwayama, T.; Shitara, H.; Aoki, Y.; Hirano, M.; Nohira, H. Synthesis and Diastereoselective Structural Change of a Photochromic Transition Metal Complex, (H6-Spirobenzopyran)(tricarbonyl)chromium. *Chem. Lett.* **1997**, *26*, 965–966. [CrossRef]
256. He, T.; Lu, M.; Yao, J.; He, J.; Chen, B.; Di Spigna, N.H.; Nackashi, D.P.; Franzon, P.D.; Tour, J.M. Reversible Modulation of Conductance in Silicon Devices via UV/Visible-Light Irradiation. *Adv. Mater.* **2008**, *20*, 4541–4546. [CrossRef]
257. Wen, G.; Yan, J.; Zhou, Y.; Zhang, D.; Mao, L.; Zhu, D. Photomodulation of the Electrode Potential of a Photochromic Spiropyran-Modified Au Electrode in the Presence of Zn^{2+}: A New Molecular Switch Based on the Electronic Transduction of the Optical Signals. *Chem. Commun.* **2006**, 3016. [CrossRef]

258. Reifarth, M.; Bekir, M.; Bapolisi, A.M.; Titov, E.; Nußhardt, F.; Nowaczyk, J.; Grigoriev, D.; Sharma, A.; Saalfrank, P.; Santer, S.; et al. A Dual PH- and Light-Responsive Spiropyran-Based Surfactant: Investigations on Its Switching Behavior and Remote Control over Emulsion Stability. *Angew. Chem. Int. Ed.* **2022**, *61*, e202114687:1–e202114687:9. [CrossRef]
259. Cabrera, I.; Krongauz, V.; Ringsdorf, H. Photo- and Thermochromic Liquid Crystal Polysiloxanes. *Angew. Chem. Int. Ed. Engl.* **1987**, *26*, 1178–1180. [CrossRef]